A Thesis for the Degree of Doctor of Philosophy in Pharmacology

Neuroprotection of active principles from the *Cudrania tricuspidata* in *in vitro* models of Parkinson's disease: Effect on the ubiquitin-proteasome system and Nrf2-ARE pathway

꾸지뽕나무로부터 분리한 유효성분물질의 파킨슨병 세포모델에서의 신경보호효과: Ubiquitin-proteasome system 및 Nrf2-ARE 관련 기전에 관한 효과연구

August, 2017

By

Dong-Woo Kim

Natural Products Science Major, College of Pharmacy

Doctor Course in the Graduate School

Seoul National University

Abstract

Neuroprotection of active principles from the *Cudrania tricuspidata* in *in vitro* models of Parkinson's disease: Effect on the ubiquitin-proteasome system and Nrf2- ARE pathway

Dong-Woo Kim

Natural Products Science Major

College of Pharmacy

Doctor Course in the Graduate School

Seoul National University

Parkinson's disease (PD) is characterized by severe motor deficits, cogwheel rigidity, bradykinesia, and the loss of dopaminergic neurons. The aetiology of PD has not been clearly identified; however, oxidative stress is thought to be a common factor that leads to cellular dysfunction and neurodegeneration. In particular, the pathological events that occur in PD have been suggested to be linked to protein oxidation caused by oxidative stress, and excessive intracellular ROS induce apoptosis that is characterized by the cleavage of caspase-3, caspase-9 and poly

ADP-ribose polymerase (PARP). The neurotoxin 6-hydroxydopamine (6-OHDA), Carbonyl cyanide 3-chlorophenylhydrazone (CCCP) destroys dopaminergic and noradrenergic neurons in the brain by inducing excessive ROS such as superoxide radicals, which leads to protein oxidation and neuronal cell death. Also, ubiquitin-proteasome system play a key role in the etiology of PD. The proteasome selective degrades oxidized proteins via ubiquitin-mediated processes, and its role is essential for cellular protein maintenance. However, dysfunctions in the ubiquitination machinery or in the proteolytic activities of the proteasome induce the accumulation of polyubiquitinated misfolded proteins and oxidized proteins. Subsequently, this induces protein aggregation, further inhibits proteasome activity, generates additional cellular stress, and ultimately leads to neuronal cell death. Additionally, mitophagy play a major role in the etiology of PD. Mitophagy, a specialized autophagy pathway that mediates the clearance of damaged mitochondria by lysosomes, is important for mitochondrial quality control. Defective mitochondria, if left uncleared, can be a source of oxidative stress and compromise the health of the entire mitochondrial network. The several lines of evidence propose that mitochondrial dysfunction is central to the disease. PD-associated mutations in PINK1 or parkin impair parkin recruitment, mitochondrial ubiquitination, and/or mitophagy. In the context of the inherently high mitochondrial oxidative stress in substantia nigra dopamine neurons, loss of parkin-mediated mitophagy could explain the greater susceptibility of substantia nigra

neurons to neurodegeneration. Thus, promoting mitophagy and enhancing mitochondrial quality control could benefit dopaminergic neurons. The current therapeutic drugs are based on prohibiting the progress of PD through treatment of dopamine agonist or dopamine precursor. New therapies in development are aimed at protecting dopaminergic neurons. In this study, the effects of natural products on 6-OHDA, CCCP-mediated signaling in SH-SY5Y neuroblastoma cell were investigated to discover new lead compounds for the treatment of PD.

Cudrania tricuspidata (Moraceae) is a subtropical tree that is widely distributed in Korea, China, and Japan. The fruits of *C. tricuspidata* are used in jams, juices, and a fermented alcoholic beverage with sugar, and they are commercially produced as food in Korea. Also, the cortex and root bark of *C. tricuspidata* have been used as a traditional medicine for inflammation and tumors. A recent study demonstrated that the extracts of *C. tricuspidata* protect neurons against oxidative stress-induced cytotoxicity and inhibitory effects on nitric oxide synthase (NOS). The compounds isolated from *C. tricuspidata* are primarily xanthones and flavones in addition to some alkaloids, lignins, coumarins, polysaccharides, and chromones. The isoflavones and chromones from *C. tricuspidata* have been reported to exert protective effects against 6-OHDA-induced neurotoxicity and to have inhibitory effects against IgE-mediated allergic and inflammatory responses.

In first chapter, it was investigated that 5,7-dihydroxychromone (DHC) isolated from the roots of *C. tricuspidata* for its neuronal cell protection and inhibition of

the generation of ROS in 6-OHDA-induced SH-SY5Y cells. Flow cytometric analysis revealed that DHC protected against the 6-OHDA-induced generation of ROS and protected against neuronal cell death. Additionally, DHC increased the nuclear translocation of Nrf2 and the binding of Nrf2 to ARE, which subsequently resulted in the up-regulation of the expression of Nrf2-dependent antioxidant genes, including heme oxygenase 1 (HO-1), NAD(P)H quinone oxidoreductase 1 (NQO1) and glutamate-cysteine ligase, catalytic subunit (GCLc). DHC inhibited the expression of cleaved caspase-3 and caspase-9 and PARP in 6-OHDA-induced SH-SY5Y cells. The addition of Nrf2 siRNA abolished the neuroprotective effect of DHC against 6-OHDA-induced cell death and the expression of Nrf2-mediated antioxidant genes. These findings suggest that the neuroprotective effect of DHC against 6-OHDA-induced toxicity is partly due to the induction of Nrf2-mediated antioxidant gene expression via the activation of the Nrf2-ARE signaling pathway in SH-SY5Y cells.

In the second chapter, the effects of ethanol extract from the fruits of *C. tricuspidata* (CTE) and it active compounds were studied. Among the nine isolates from a 50% ethanol extract from *C. tricuspidata* fruits (CTE50), orobol (OB), 6-prenylorobol (POB), and 6,8-diprenylorobol (DPOB) showed neuroprotective effects in 6-OHDA-induced SH-SY5Y cell death. In addition, CTE50 and the three orobol derivatives (OB, POB, and DPOB) attenuated the cleavage of caspase-3, caspase-9, and PARP and inhibited the excessive generation of ROS. Furthermore,

it enhanced the 6-OHDA-induced dysfunction of proteasome activity and reduced the accumulation of ubiquitin conjugated-proteins and the polyubiquitination of α-synuclein and synphilin-1. The proteasome inhibitor MG132 blocked the neuroprotective effects and the enhanced proteasome activity produced by CTE50 and the three orobol derivatives. These results demonstrate that CTE50 and three orobol derivatives protect against 6-OHDA-induced neurotoxicity by enhancing the ubiquitin/proteasome-dependent degradation of α-synuclein and synphilin-1, suggesting that they might be possible candidates for the treatment of neurodegenerative diseases.

In the third chapter, the effects of active compounds from the *C. tricuspidata* extracts on deubiquitinating enzymes were studied. TH3-125-4 (TH20) isolated from the root barks of the *C. tricuspidata* protected against CCCP-induced neuronal cell death in Parkin K.D. SH-SY5Y cells. Also, TH20 significantly inhibited USP30 enzyme activity and disassembly of polyubiquitin chain in *in vitro* assay. Additionally, TH20 decreased protein expression of USP30. Based on the results, it was suggested that TH20 might be promising candidates for the therapy of familiar PD via restoring Parkin-mediated mitophagy.

Keywords : *Cudrania tricuspidata*, oxidative stress, 6-OHDA, neuroprotection, 5,7-Dihydroxychromone, Nrf2/ARE pathway, orobol derivatives, proteasome activity, ubiquitination, deubiquitinating enzyme, PINK1, Parkin, mitophagy

Student number **:** 2012-21566

Table of Contents

Abstract · · ·

2.6 Measurement of intracellular ROS by Flow cytometry · · · · · · · · · · · ·13

2.7 Nuclear and cytosolic lysate preparations ·13

2.8 Electrophoretic mobility shift assay (EMSA)· · · · · · · · · · · · · · · · · · · 14

2.9 Nrf2 knockout via the transfection of small interfering RNA (siRNA)·

· · · · · · · · · · · · · · · · · · · ·

SH-SY5Y cells · · ·

3.5 Effects of CTE50 and three orobol derivatives on proteasome subunit mRNA expression · · ·

3.2 Effect of TH3-125-4 (TH20) on ubiquitin chain disassembly · · · · · · 123

3.3 The protective effects of TH3-125-4 (TH20) against CCCP-induced neuronal cell death in parkin knock down SH-SY5Y cells · · · · · · · · · · · 125

3.4 Inhibitory effect of TH3-125-4 (TH20) on USP30 protein expression in SH-SY5Y cells· · · · · · · · · · · ·

List of Figures

Figure 13. Effects of DHC on the mRNA expressions of NQO1 in SH-SY5Y cells· · · ·

Figure 23. Inhibitory effects of CTE50 and three orobol derivatives against 6-OHDA-induced apoptotic markers · 77

Figure 24. Protective effects of CTE50 and three orobol derivatives (OB, POB, and DPOB) against 6-OHDA-induced dysfunction of proteasome activities in SH-SY5Y cells ·80

Figure 25. Effects of CTE50 and three orobol derivatives (OB, POB, and DPOB) on mRNA expression of proteasome subunits in SH-SY5Y cells · · · · · · ·83

Figure 26. Inhibitory effects of CTE50 and three orobol derivatives against 6-OHDA-induced ubiquitin-conjugated proteins · · · · · · · · · · · · · · · · · · ·85

Figure 27. Inhibitory effects of CTE50 and three orobol derivatives against 6-OHDA-induced polyubiquitination of α-synuclein · 87

Figure 28. Inhibitory effects of CTE50 and three orobol derivatives against 6-OHDA-induced polyubiquitination of synphilin-1· · · · · · · · · · · · · · · · · · · ·88

Figure 29. Inhibitory effects of MG132 on the protective effects of CTE50 and three orobol derivatives against 6-OHDA-induced neuronal cell death · · · · 90

Figure 30. Inhibitory effects of MG132 on the protective effects of CTE50 and three orobol derivatives against 6-OHDA-induced proteasome dysfunction · · · · · · · · · · · · · · · · · · ·

neuronal cell death in parkin knock down SH-SY5Y cells · · · · · · · ·128

Figure 42. Inhibitory effect of TH3-125-4 (TH20) on USP30 protein expression in SH-SY5Y cells · · · · · · ·

List of Tables

Chapter 1

Neuroprotection against 6-OHDA-induced oxidative stress and apoptosis in SH-SY5Y cells by 5,7-Dihydroxychromone

: Activation of the Nrf2/ARE pathway

1. Introduction

The incidence of neurodegenerative diseases is increasing with the continuous growth of the elderly population. Although the causes of neurodegenerative diseases have not been clearly elucidated, recent studies have demonstrated that reactive oxygen species (ROS) might be one of the important factors in the neurotoxicity that occurs in neurodegenerative diseases (Farooqui and Farooqui, 2011). Cells exposed to environment fortified with oxygen constantly generate oxygen free radicals. ROS includes oxygen-related free radicals and reactive species, and they are produced as a result of aerobic metabolism. Formation of ROS can occur in two ways: enzymatic and non-enzymatic responses. Enzymatic responses generating free radicals include those involved in the mitochondrial respiratory chain, phagocytosis, prostaglandin synthesis and the cytochrome P450 system. The non-enzymatic process can also occur through oxidative phosphorylation (*i.e.* aerobic respiration) in the mitochondria. ROS is generated from either endogenous or exogenous sources. Endogenous free radicals are generated from immune cell activation, inflammation, mental stress, excessive exercise, ischemia, infection, cancer and aging. Exogenous ROS result from air and water

pollution, cigarette smoke, alcohol, heavy or transition metals (Cd, Hg, Pb, Fe, As), certain drugs (cyclosporine, tacrolimus, gentamycin, bleomycin), industrial solvents, cooking (smoked meat, used oil, fat) and radiation. After penetrated into the body by different ways, these exogenous agents are decomposed or metabolized into free radicals (Chen et al., 2012). Increased ROS production causes impairment to cell organelles. Many studies have confirmed the benefits of antioxidants in reducing oxidative stress in neurons and protecting against neurodegenerative diseases (Alfieri et al., 2011). In response to excessive ROS, the cellular expressions and bioactivity of numerous antioxidant enzymes are changed via initiating the upstream factor NF-E2-related factor 2 (Nrf2)/antioxidant response elements (AREs) complex (Leutner et al., 2000).

The Nrf2/ARE signal has an important effect on the induction of antioxidant gene expression, and it has been reported that the activation of Nrf2 is an important signal which can neutralize oxidative stress (Sun et al., 2010). Nrf2 activity is regulated partly by Keap1 protein, which was initially proposed to act by binding and tethering the transcription factor in the cytoplasm. Activation of Nrf2 in response to stress signals was thought to result from a interruption of this association, releasing Nrf2 for translocation into the nucleus to affect its transcriptional activity. Independently, Nrf2 has been

found to be a highly unstable protein, subject to proteolytic degradation catalyzed by the proteasome via the ubiquitin-dependent pathway. In this case, activation of Nrf2 was suggested to be dependent on mechanisms that increase its stability, leading to its accumulation in the cell. The unstable nature of the Nrf2 protein and its regulation through this dynamic mechanism suggest that Nrf2 is unlikely to be joined in a passive complex in the cytoplasm. This was supported by a number of studies demonstrating a more active role of Keap1 in its repression of Nrf2 activity. Keap1 appears to promote Nrf2 ubiquitylation in a constitutive manner through the cullin-3-dependent pathway. That Nrf2 is constantly degraded in non-stressed cells implies that Keap1 is a constitutively active protein and that it promotes Nrf2 ubiquitylation in an unregulated manner. This is supported by the observation that overexpression of Keap1 leads to increased levels of ubiquitin-conjugated forms of Nrf2 in cells, indicating that Keap1 is expressed as a functionally active protein. Thus, interaction between the two proteins is more likely a transient encounter rather than a sustained association. Given that the steady-state level of Nrf2 in the cell is maintained in part through its constitutive expression, requiring *de novo* gene transcription and protein synthesis, the pathway through which Nrf2 activity is regulated, from synthesis to degradation, requires examination in further detail (Nguyen et al., 2009). In

summary, under normal state, Nrf2 is localized in the cytoplasm and is subject to ubiquitination and proteasomal degradation. However, antioxidant agents block the elimination of Nrf2 from the cytosolic Nrf2 complex, which induces nuclear translocation of Nrf2 and subsequently makes the Nrf2/ARE complex to mediate the induction of many antioxidant enzyme genes, such as heme oxygenase 1 (HO-1), NAD(P)H: quinone oxidoreductase (NQO1), and glutamate-cysteine ligase catalytic subunit (GCLc) (Zhang et al., 2013).

The heme-heme oxygenase (HO) system is a controller of endothelial cell integrity and oxidative stress. HO-1 and HO-2, two isoforms of HO, are viewed as having a major role in the construction of carbon monoxide (CO) and bilirubin and in heme breakdown. The fact that HO-1 is strongly induced by oxidant stress and its substrate heme, in conjunction with the ability of HO-1, to protect against oxidative insult suggests a countervailing system to oxidative stress damage. The antioxidant effects of HO-1 arise from its capacity to increase reduced glutathione levels and to degrade heme, as well as from the elaboration of biliverdin and bilirubin, which have potent antioxidant properties. CO, a product of HO, is not an antioxidant, but it does have an antiapoptotic effect. Furthermore, CO is a vasodilator that has been shown to enhance endothelial function and plays an important role in regulating basal and constrictor-induced vascular tone (Turkseven et al., 2005).

NQO1 has multiple protective roles that include and extend beyond its catalytic function. It is a widely-distributed FAD-dependent flavoprotein that catalyzes the reduction of quinones, quinoneimines, nitroaromatics, and azo dyes. NQO1 was discovered and named DT-diaphorase in the late 1950s, and shown to be identical to the dicoumarol-inhibited vitamin K reductase described. The classical direct antioxidant role of NQO1 is characteristic in its catalytic mechanism: the obligatory two-electron reduction of a wide array of quinones to their corresponding hydroquinones by using either NADPH or NADH as the hydride donor. In doing so, NQO1 diverts quinone electrophiles from participating in reactions that could lead to either sulfhydryl depletion, or to one-electron reductions that can produce semiquinones and various reactive oxygen intermediates as a result of redox cycling. In addition, the hydroquinone products of the NQO1 reaction can be further metabolized to glucuronide and sulfate conjugates, thereby facilitating their excretion. Remarkably, quinone reductases have been found in a wide range of eukaryotic organisms ranging from yeast to mammals. Although in many systems much remains to be learned about the complicated details of the function and regulation of these enzymes, it is clear that in all cases quinone reductases are at the forefront of the cellular defense by providing multiple layers of protection (Dinkova-Kostova and Talalay, 2010).

Glutathione (GSH) is considered the most abundant molecule among endogenous antioxidants. GSH is a reduced peptide consisting of three-residues (γ-l-glutamyl-l-cysteinyl glycine) which can donate an electron with the consequence that two electrons donating GSH molecules form oxidized GSSG. In humans, GSH is almost uniquely present in a quite high concentration (1–10 mM) which allows to scavenge ROS either directly or indirectly. It can directly react with O^{2-} and some other ROS, but its indirect ROS-scavenging functions, such as revitalizing other antioxidants, are likely more important; e.g. it can reduce dehydroascorbic acid which is formed in the reconversion of α-tocopheroxyl radical to α-tocopherol, a lipophilic chain breaking antioxidant, which interacts with the polyunsaturated acyl groups of lipids, stabilizes membranes and scavenges various reactive oxygen species and lipid oxy-radicals. As an antioxidant it reacts with ROS, RNS and radicals produced in association with electron transport, xenobiotic metabolism and inflammatory responses. GSH is synthesized from its constituent amino acids forming a tripeptide thiol and this synthesis requires two ATP-dependent steps. The first and limiting synthesis is catalyzed by γ-glutamyl-cysteine ligase (GCL) and the second step mediated by GSH synthetase (GS). GCL is a heterodimeric enzyme composed by a heavy subunit, GCLc with catalytic activity and a smaller one, GCLm that has a regulatory role on the other

subunit. GSH homeostasis in the cell is not only regulated by its de novo synthesis, but also by other factors such as utilization, recycling and cellular export. This redox cycle is known as the GSH cycle and incorporates other important antioxidant, redox-related enzymes. Nearly every eukaryotic cell, from plants to yeast to humans, expresses a form of the GCL protein for the purpose of synthesizing GSH. To further highlight the critical nature of this enzyme, genetic knockdown of GCL results in embryonic lethality. Furthermore, dysregulation of GCL enzymatic function and activity is known to be involved in the vast majority of human diseases, such as diabetes, Parkinson's disease, Alzheimer's disease, COPD, HIV/AIDS, and cancer. This typically involves impaired function leading to decreased GSH biosynthesis, reduced cellular antioxidant capacity, and the induction of oxidative stress (Espinosa-Diez et al., 2015). Numerous research results reported that Nrf2 and Nrf2 dependent antioxidant genes are potent factors for developing the therapy of neurodegenerative diseases due to its abilities to regulate the excessive oxidative stress and inflammation. A recent study demonstrated that the extracts of *Cudrania tricuspidata* protect neurons against oxidative stress-induced cytotoxicity (Jeong et al., 2010) and have inhibitory effects on nitric oxide synthase (NOS) (Kang et al., 2002). It was also reported that 5,7-Dihydroxychromone (DHC), from *Cudrania*

tricuspidata, has an antioxidant activity (Qiu et al., 2012). However, neuroprotective effects of DHC and the related mechanisms of neuroprotection were poorly elucidated.

In this study, it was demonstrated that neuroprotective effects of DHC against 6-OHDA-induced neurotoxicity via the induction of the Nrf2/ARE-mediated signal.

2. Materials and methods

2.1. Chemicals and reagents

Propidium iodide (PI), 6-hydroxydopamine (6-OHDA), and 2',7'-dichlorfluorescein-diacetate (DCFH-DA) were purchased from Sigma-Aldrich (St. Louis, MO, USA). Dulbecco's modified Eagle's medium (DMEM) and fetal bovine serum (FBS) were purchased from Gibco BRL (Rockville, MD, USA). Hybond-polyvinylidene difluoride (PVDF) membranes were purchased from Amersham Pharmacia Biotechnology. (Piscataway, NJ, USA). Easy-Blue® total RNA extraction solution, PRO-PREP protein extraction solution and WEST-ZOL® ECL solution were purchased from iNtRON Biotech. (Kyunggi, Korea). SuPrimeScript RT premix®, and SYBRs HS Prime qPCR premix® were purchased from Genet Bio (Daejeon, Korea). Nrf2 siRNA, scrambled siRNA, Nrf2, HO-1, NQO1, GCLc, LaminB1, α-tubulin, β-actin, caspase-3, caspase-9, PARP, secondary antibody and FITC-conjugated secondary antibody were purchased from Santa Cruz Biotechnology. (Santa Cruz, CA, USA)

2.2. Preparation of 5,7-dihydroxychromone (DHC)

Cudrania tricuspidata was stored at the Korea Forest Research Institute at Southern Forest Research Center (Jinju, Korea) in September 2008. A voucher specimen (accession number KH1-4-090814) was kept at the Department of Biosystems and Biotechnology at Korea University (Seoul, Korea). 5,7-Dihydroxychromone (DHC) was isolated from the roots of *Cudrania tricuspidata* and the structure of DHC was determined by spectroscopic methods, and the purity was more than 98.5% (Wei and Yu, 2008). DHC was dissolved in DMSO and diluted with PBS to obtain the proper concentration of DHC. Final concentration of DMSO was less than 0.1% and it didn't influence the performed assays.

2.3. Cell cultures

The human neuroblastoma cell line SH-SY5Y (ATCC No. CRL-2266) was purchased from the American Type Culture Collection (Manassas, VA, USA) and cultured in DMEM supplemented with 10 % heat-inactivated FBS and 1 % penicillin/streptomycin at 37 ºC in a humidified 5 % CO_2 atmosphere.

2.4. Measurement of cell viability

SH-SY5Y cells were seeded at a density of 1×10^5 cells/200 μL/well in 96-well plates for 24 h, and the cells were pre-treated with DHC (0.4, 2, or 10 μM) for 24 h followed by subsequent treatment with 6-OHDA (100 μM) for an additional 24 h. To evaluate the effect of Nrf2, cells were transfected with scrambled siRNA or Nrf2 siRNA for 48 h and its final concentration was 50 nM. After transfected cells were treated with DHC (10 μM) and 6-OHDA (100 μM),-cell viability was determined using a MTT (3-(4,5-Dimethylthiazol-2-yl)-2,5-Diphenyltetrazolium Bromide) and measured by ELISA (Koo et al., 2011).

2.5. Measurement of cell necrosis by propidium iodide staining

SH-SY5Y cells were seeded at a density of 2×10^5 cells/2 mL/well in 6-well plates for 24 h, and the cells were pre-treated with DHC (0.4, 2, or 10 μM) for 24 h followed by subsequent treatment with 6-OHDA (100 μM) for an additional 24 h. To evaluate the effect of Nrf2, cells were transfected with scrambled siRNA or Nrf2 siRNA for 48 h and its final concentration was 50 nM. After transfected cells were treated with DHC (10 μM) and 6-OHDA (100

μM),-cell viability was determined using a propidium iodide (PI) staining and measured by flow cytometry (BD FACSCalibur ^{TM}) (Koo et al., 2011).

2.6. Measurement of intracellular ROS by Flow cytometry

ROS levels in cells were measured with the 2',7'-dichlorofluorescein diacetate (DCFH-DA) method (Munch et al., 1998a). Briefly, the cells were washed with PBS, and then incubated with 4 μM of DCFH-DA for 30 min at 37 ºC in the dark. The cells were then washed with PBS. The fluorescence intensities were measured by flow cytometry (BD FACSCalibur ^{TM} San Jose, CA, USA).

2.7. Nuclear and cytosolic lysate preparations

The nuclear and cytosolic proteins were extracted with a commercial kit (Nuclear Extract Kit) according to the manufacturer's procedure (Active Motif, Carlsbad, CA). Briefly, the cells were incubated in hypotonic buffer on ice for 15 min, homogenized with detergent, and centrifuged for 30 sec at 14,000 x g in a microcentrifuge at 4 ºC. The supernatant was used as the cytosolic proteins. The nuclear pellets were washed with cold PBS, extracted completely with lysis buffer for 30 min on ice and centrifuged for 10 min at 14,000 x g in a microcentrifuge at 4 ºC. The supernatant was used as the nuclear proteins.

2.8. Electrophoretic mobility shift assay (EMSA)

To determine the Nrf2-ARE binding activity, an electrophoretic mobility shift assay (EMSA) was accomplished as previously described (Meyer et al., 1998). Briefly, the nuclear proteins from the SH-SY5Y cells were reacted with ^{32}P-end-labeled 22-mer double-stranded oligonucleotide containing the Nrf2 sequence for 30 min at 37 ºC. The DNA-protein complexes were electrophoresed and gels were dried. The binding signals were visualized by BAS-1500 (Fuji, Tokyo, Japan).

2.9. Nrf2 knockout via the transfection of small interfering RNA (siRNA)

The transfection with scrambled siRNA or Nrf2 siRNA were progressed at final concentrations of 50 nM for 48 h by Lipofectamine 2000 (Invitrogen, Carlsbad, CA) prior to treatment with DHC (10 μM) and 6-OHDA (100 μM) as recommended by the manufacturer's guidelines.

2.10. Measurement of mRNA expression

After treatments, total RNA was isolated from SH-SY5Y cells by easy-BLUE® and cDNA was synthesized by using SuPrimeScript RT premix® according to the manufacturer's procedure. The synthesized cDNA was used for PCR and the primer pair sequence were listed as follows:

HO-1 5-TGCTCGCATGAACACTCTG-3 (Sense) and

5- TCCTCTGTCAGCAGTGCC-3 (antisense);

NQO1 5-AGCCCAGATATTGTGGCTGA-3 (Sense) and

5-AAGCCACAGAAATGCAGAATG-3 (antisense);

GCLc 5-AGGCCAACATGCGAAAC-3 (Sense) and

5-CGGATATTTCTTGTTAAGGTACTGG-3 (antisense);

GAPDH 5-CTCTGCTCCTCCTGTTCGAC-3 (Sense) and

5-ACGACCAAATCCGTTGACTC-3 (antisense). The cycle condition was as follow; 94℃ for 20s, 56℃ for 20s, 72℃ for 30s and 40 cycles. PCR were performed by using SYBRs HS Prime qPCR premix® in an ABI 7300 real-time PCR (Applied Bio systems, CA, USA). Ct (threshold cycle) values were obtained using the Sequence Detection Software version1.2.3 (Applied Bio systems, CA, USA). To evaluate quantification of the changes in target gene expression, we used the $2^{-\triangle\triangle Ct}$ method (Tucker and Munchus, 1998). Fold change=$2^{-\triangle\triangle Ct}$, $\triangle\triangle Ct = (Ct_{\text{target gene}} - Ct_{GAPDH}) - (Ct_{\text{control}} - Ct_{GAPDH})$

2.11. Measurement of protein expression

The SH-SY5Y cells were collected, washed with PBS and lysed with a PRO-PREP protein extraction solution at -20 ºC for 20 min. After centrifugation at 13,000 x g for 30 min, the supernatant was used as the total protein extracts. Western blot analysis was accomplished as previously described method (Ham et al., 2013).

2.12. Nuclear translocation of Nrf2 using fluorescence microscope

The culture dish was coated with 0.2 % gelatin at 37 °C for 30 min and dried at RT on a clean bench. The SH-SY5Y cells were plated at a density of 5×10^4 cells/200 μL/well in coated dishes for 24 h and incubated with DHC (0.4, 2, or 10 μM) for 6 h. After treatment with DHC, the cells were washed with 1x PBS/Tween-20 buffer (pH 7.4) (PBST) once. The cells were fixed with 4 % paraformaldehyde for 30 min at room temperature (RT). After washing with PBST, the blocking steps were performed with 1 % BSA in PBST. Next, the cells were incubated with the primary antibody at 4 °C overnight. The next day, the cells were washed with PBST 3 times and incubated with FITC-conjugated secondary antibody for 1 h at RT. After 1 h, the cells were washed with PBST 3 times, and DAPI staining was performed for 5 min at RT. Lastly, the PBST washing and mounting steps were conducted.

2.13. Statistical analysis

All experimental data are expressed as mean value ± standard deviation. Statistical significance between multiple groups was determined by one-way ANOVA (PRISM Graph Pad, San Diego, CA, USA). When ANOVA had a significant difference, *post hoc* Bonferroni's multiple comparison tests was conducted. *P* value less than 0.05 was regarded to be statistically significant.

3. Results

3.1. Protective effect of DHC against 6-OHDA-induced neuronal cell death.

The protective effects of DHC (Fig. 2) on SH-SY5Y cells were evaluated to determine the non-cytotoxic dose range (data not shown). The percentage of cell necrosis was evaluated with PI staining. As shown in Fig. 3, the percentage of PI-stained dead cells induced by 6-OHDA increased to 44.5 % compared to the vehicle-treated group (8.7 %). In contrast, 6-OHDA-induced cell death was dose-dependently prevented by DHC treatments at concentrations of 0.4, 2 and 10 μM within the non-toxic dose range. DHC (10 μM) treatment elicited its neuroprotective effects against 6-OHDA by decreasing the percentage of PI-positive cells to 13.8 %, whereas treatment with Nrf2 siRNA and DHC (10 μM) reduced the neuroprotective effect by increasing the percentage of PI-positive cells to 50.1 %. Also, the neuroprotective effect of DHC was evaluated by MTT assay (Fig. 4). The result of MTT assay was correlated with PI staining assay.

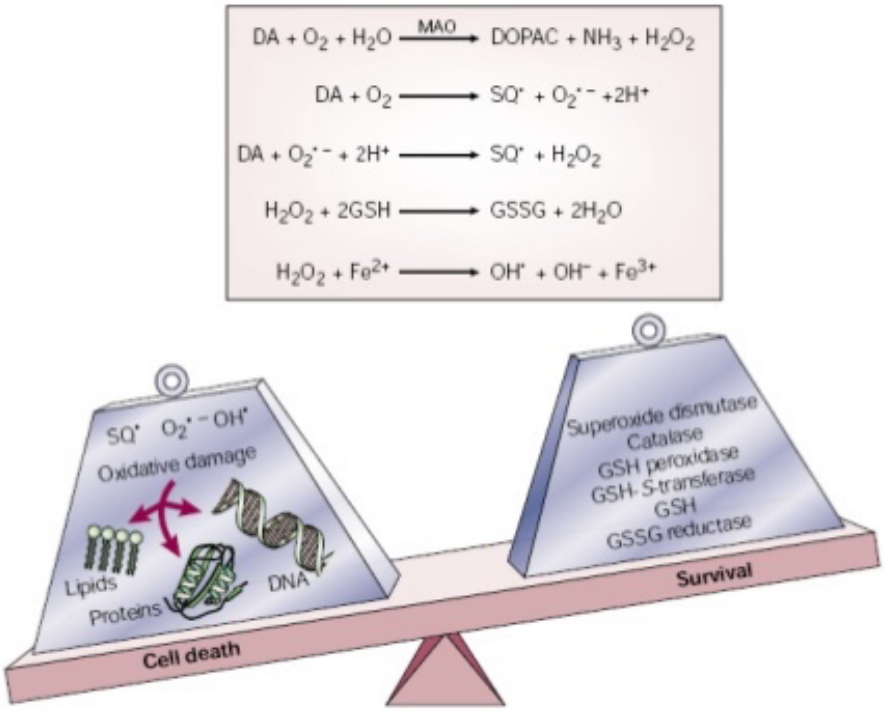

Figure 1. Scheme of oxidative stress and antioxidant enzymes in neuronal cell.

Table 1. The protective effect of isolated compounds from *Cudrania tricuspidata* root barks against 6-OHDA-induced neuronal cell death.

No.	Sample	6-OHDA-induced neuronal cell death MTT EC_{50} (μM)
1	**JY1-13-2**	**12.9**
2	**JY1-14-1**	**7.2**
3	JY1-15-1	>40
4	JY1-19-1	>40
5	JY1-19-2	>40
6	JY1-29-2	>40
7	JY1-30-1	>40
8	**JY1-36-1**	**9.5**
9	**JY1-37-2**	**9.2**
10	**JY1-53-2**	**15.5**
11	JY1-54-1	>40
12	JY1-54-3	>40
13	**JY1-56-2**	**9.1**
14	JY1-59-2	>40
15	JY1-64-2	>40
16	JY1-69-3	>40
17	**JY1-88-2**	**30.2**
18	JY1-88-3	>40
19	**JY1-89-7**	**8**
20	JY1-89-9	>40
21	JY1-89-11	>40

22	JY1-89-12	>40

Table 1. Continued

No.	Sample	6-OHDA-induced neuronal cell death MTT EC_{50} (μM)
23	JY1-91-7	>40
24	JY1-97-1	>40
25	JY1-62-1	>40
26	JY1-64-4	>40
27	JY1-64-5	>40
28	JY1-64-7	>40
29	JY1-88-13	>40
30	JY1-89-8	>40
31	JY1-99-1	>40
32	JY1-99-2	>40
33	JY1-101-1	>40
34	JY1-101-4	>40
35	JY1-102-4	>40
36	JY1-104-3	>40
37	JY1-120-3	>40
38	JY1-146-1	>40
39	JY1-153-2	>40
40	JY1-154-2	>40
41	JY1-158-2	>40
42	JY1-162-1	>40
43	JY1-164-4	>40

44	JY1-164-5	>40
45	JY1-165-8	>40

Table 1. Continued

No.	Sample	6-OHDA-induced neuronal cell death MTT EC_{50} (μM)
46	JY1-166-3	>40
47	JY1-167-6	>40
48	JY1-168-6	>40
49	JY1-170-5	>40
50	JY1-170-6	>40
51	JY1-172-2	>40
52	JY1-173-1	>40
53	JY1-179-6	>40
54	JY1-179-8	>40
55	JY1-179-9	>40
56	**JY1-180-4 (5,7-Dihydroxychromone ;DHC)**	**1.9**

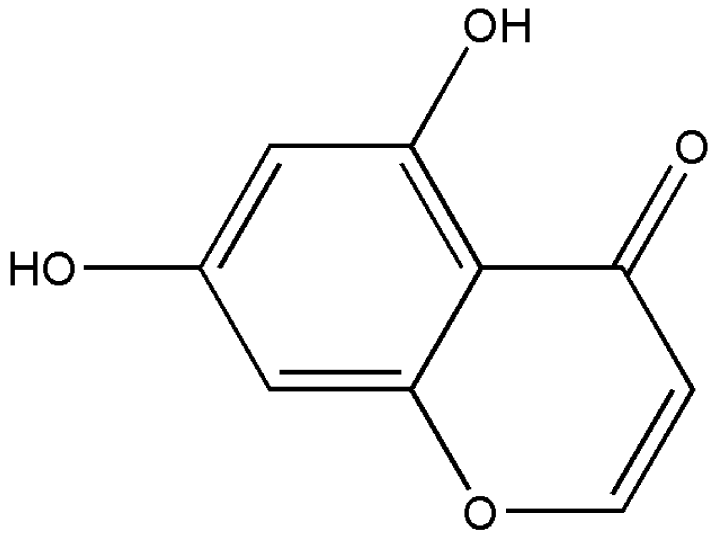

Figure 2. Chemical structure of 5,7-Dihydroxychromone (DHC).

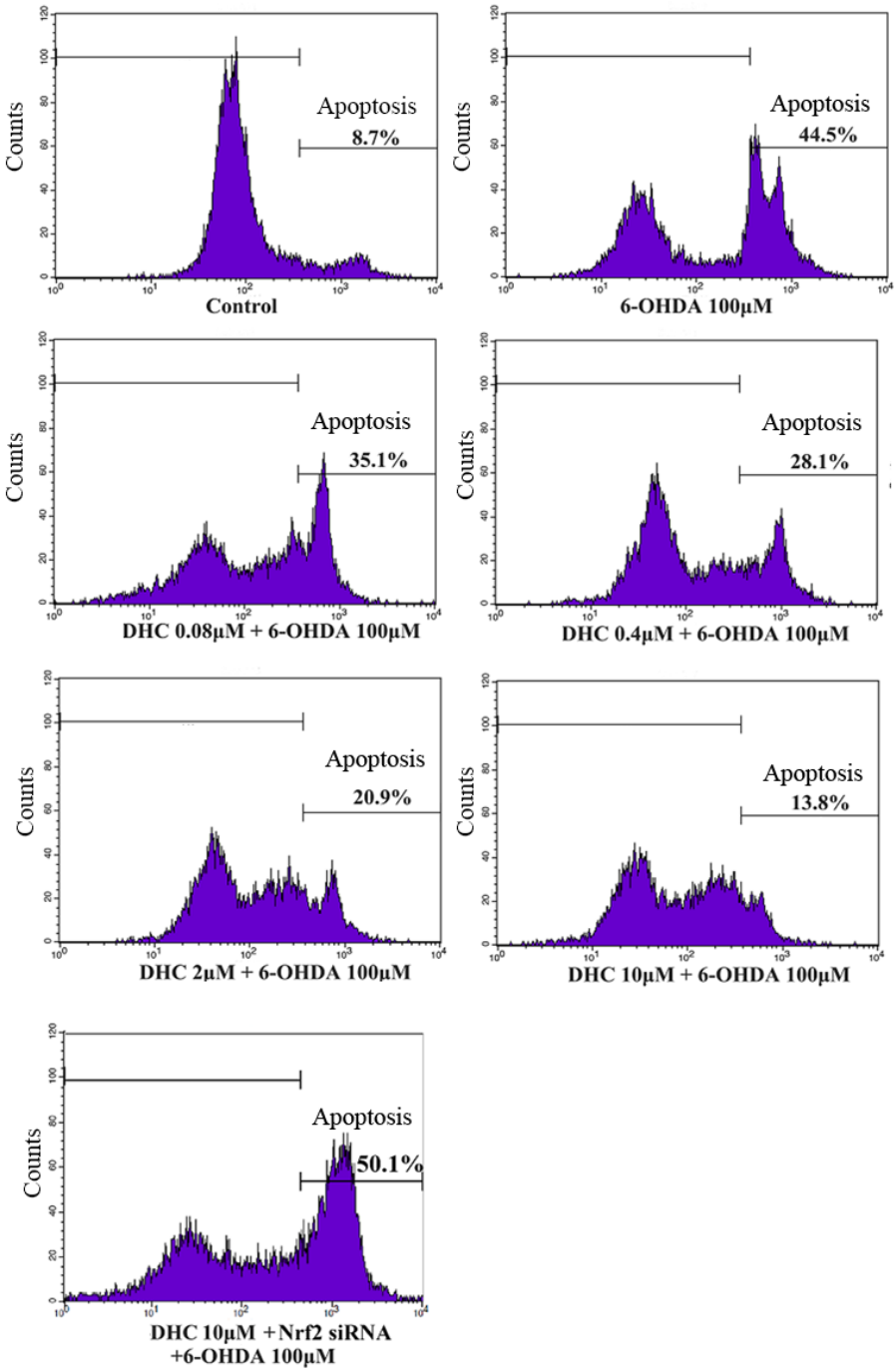
Counts
Apoptosis
8.7%
Control
Apoptosis
44.5%
6-OHDA 100μM
Apoptosis
35.1%
DHC 0.08μM + 6-OHDA 100μM
Apoptosis
28.1%
DHC 0.4μM + 6-OHDA 100μM
Apoptosis
20.9%
DHC 2μM + 6-OHDA 100μM
Apoptosis
13.8%
DHC 10μM + 6-OHDA 100μM
Apoptosis
50.1%
DHC 10μM +Nrf2 siRNA
+6-OHDA 100μM

Figure 3. Effects of DHC against 6-OHDA-induced cell necrosis in SH-SY5Y cells.

The cells were pre-treated with different concentrations of DHC (0.08 - 10 μM) for 24 h and subsequently treated with 6-OHDA (100 μM) for another 24 h. The cells were transfected with Nrf2 siRNA (50 nM) for 48 h before the treatment with DHC (10 μM). The cells were stained with PI dyes for 30 min and determined by FACS analysis using FL-2 channel. The values of fluorescence intensity were obtained from histogram statistic of CellQuest software.

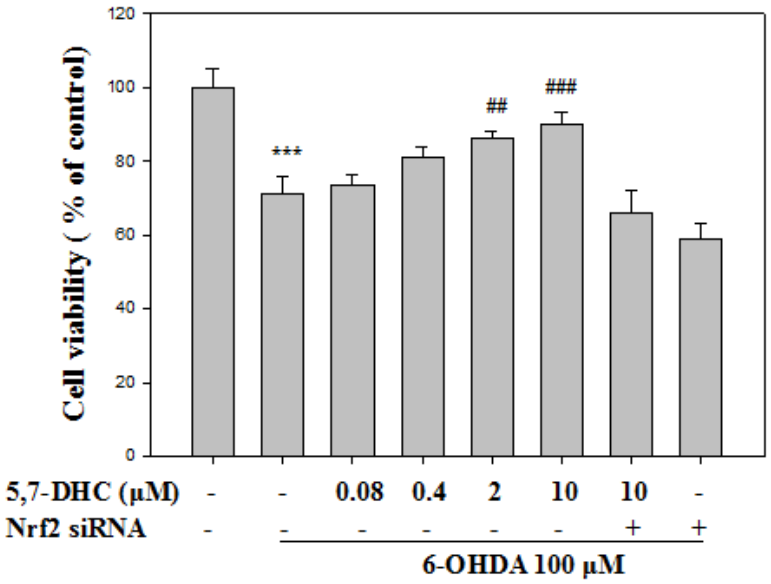

Figure 4. Effects of DHC against 6-OHDA-induced cell death in SH-SY5Y cells.

The cells were pre-treated with different concentrations of DHC (0.08 - 10 μM) for 24 h and subsequently treated with 6-OHDA (100 μM) for another 24 h. The cells were transfected with Nrf2 siRNA (50 nM) for 48 h before the treatment with DHC (10 μM). The cell viability was determined by MTT assay. ($^{***}p<0.001$ versus control group, $^{\#\#}p<0.01$ and $^{\#\#\#}p<0.001$ versus 6-OHDA-induced group)

3.2. Inhibitory effect of DHC against 6-OHDA-induced intracellular ROS generation.

Intracellular ROS were detected by DCFH-DA dye, which can be diffused to the cell membrane and deacetylated by esterase to the 2',7'-dichlorodihydrofluorescin (DCFH), which is swiftly converted into the dichlorofluorescein (DCF) emitting fluorescence by ROS. As shown in Fig. 5, the 6-OHDA-induced cells exhibited higher DCF fluorescence intensities than the vehicle-treated cells. The amount of ROS generation was decreased in a dose-dependent manner when the 6-OHDA-induced cells were treated with different concentrations of DHC (0.4 - 10 μM). The 6-OHDA-induced group generated approximately 5-fold greater amount of ROS than that of the vehicle-treated group. When the DHC (10 μM)-treated cells were treated with 6-OHDA, the ROS level was approximately 2-fold greater than that of the vehicle-treated group. However, the inhibitory effect of DHC (10 μM) on intracellular ROS generation disappeared upon treatment with Nrf2 siRNA, and the combined treatment with Nrf2 siRNA and DHC (10 μM) produced the similar ROS generation compared to the 6-OHDA-treated group.

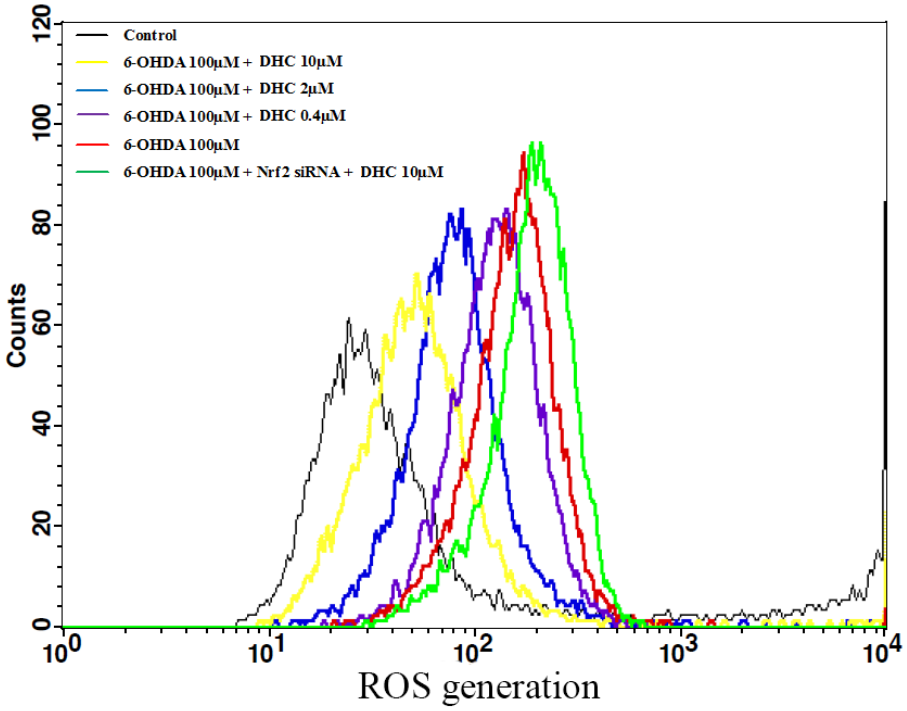

Figure 5. Effects of DHC against 6-OHDA-induced intracellular ROS generation in SH-SY5Y cells.

The cells were pre-treated with different concentrations of DHC (0.4 - 10 μM) for 24 h and subsequently treated with 6-OHDA (100 μM) for another 24 h. The cells were transfected with Nrf2 siRNA (50 nM) for 48 h before the treatment with DHC (10 μM). The cells were stained with DCFH-DA dyes for 30 min and determined by FACS analysis using FL-1 channel. The values of fluorescence intensity were obtained from histogram statistic of CellQuest software.

3.3. Effects of DHC on induction of the nuclear Nrf2 and binding affinity of Nrf2/ARE in SH-SY5Y cells

Nrf2 in nucleus has a binding affinity to the ARE region and Nrf2/ARE complex induces the transcription of ARE-mediated antioxidant genes. DHC increased the induction of nuclear Nrf2 with a peak effect that occurred at 6 h. As shown in Fig. 6, the nuclear Nrf2 was dose-dependently increased by DHC treatment (0.08 - 10 μM) at 6 h (Fig. 7). The increase of nuclear Nrf2 by DHC was visualized by immunocytochemistry in Fig. 8. To elucidate the binding activity between Nrf2 and ARE, an electrophoretic mobility gel-shift assay (EMSA) was performed. As shown in Fig. 9, DHC (2 μM) drastically increased Nrf2-ARE binding activity and the maximum binding activity was observed at 12 h.

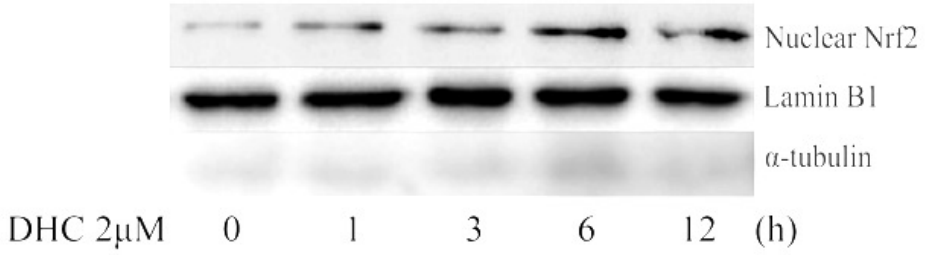

Figure 6. Effects of DHC on the nuclear translocation of Nrf2 in SH-SY5Y cells.

The cells were treated with DHC (2 μM) for different durations (0 - 12 h). The nuclear protein was extracted. Lamin B1 was used for nuclear marker and α-tubulin was used for cytosol marker. The protein expression levels of Nrf2, Lamin B1, and α-tubulin were determined by western blot analysis. Representative data from three independent experiments are shown.

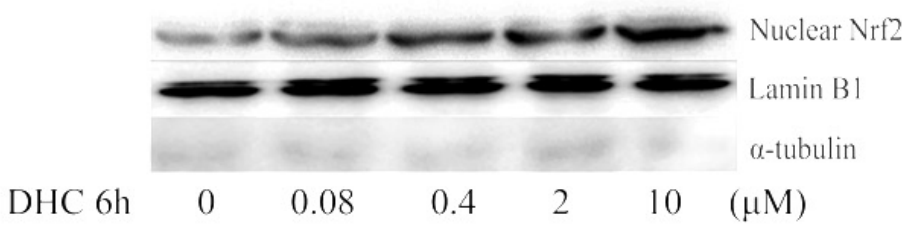

Figure 7. Effects of DHC on the nuclear translocation of Nrf2 in SH-SY5Y cells.

The cells were treated with different concentrations of DHC (0.4 - 10 μM) for 6 h. The nuclear protein was extracted. Lamin B1 was used for nuclear marker and α-tubulin was used for cytosol marker. The protein expression levels of Nrf2, Lamin B1, and α-tubulin were determined by western blot analysis. Representative data from three independent experiments are shown.

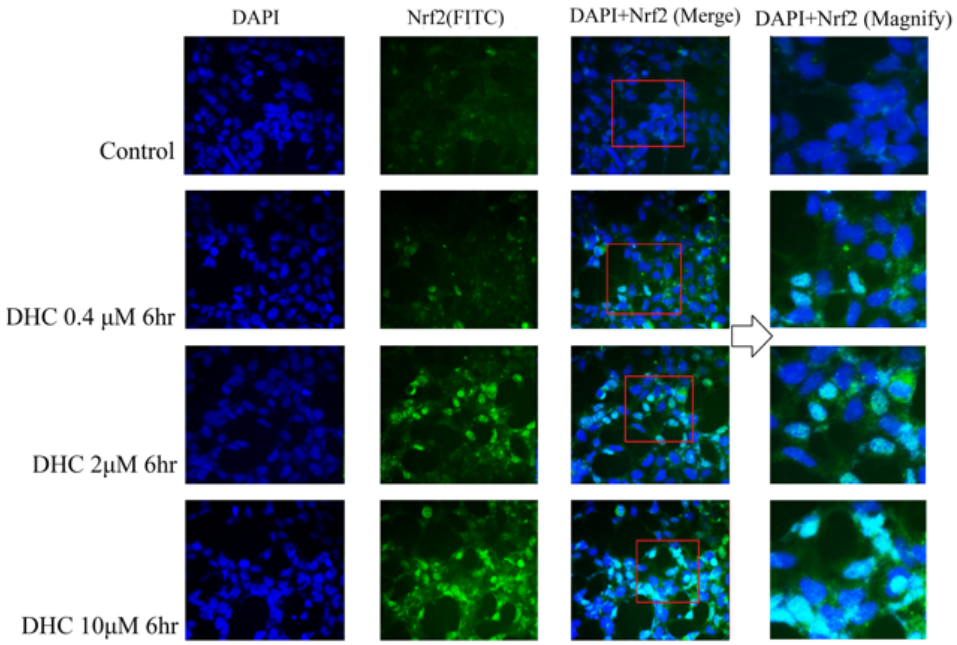

Figure 8. Effects of DHC on the nuclear translocation of Nrf2 in SH-SY5Y cells.

The cells were treated with DHC (0.4 - 10 μM) for 6 h. Cells were fixed and the nuclei were visualized with DAPI staining. Nrf2 was detected with FITC-conjugated antibodies. Cellular morphologies were visualized with a fluorescence microscope (×400). Representative images from three independent experiments are shown.

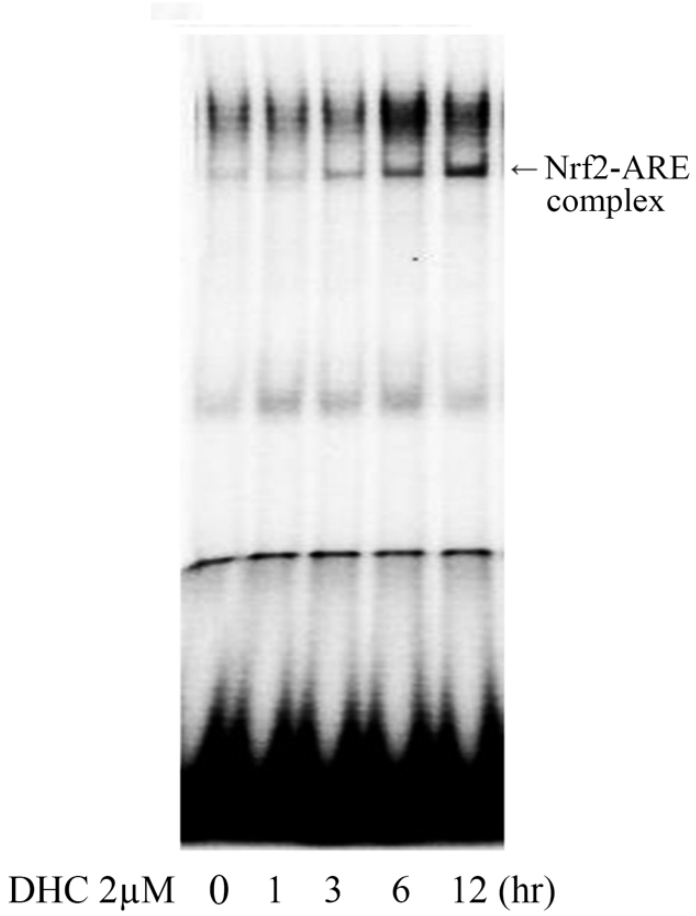

Figure 9. Effects of DHC on the binding activity of Nrf2-ARE.

The cells were treated with DHC (2 μM) for different durations (0 - 12 h), and the nuclear extracts were incubated with [γ-^{32}P]-labeled oligonucleotides harboring an ARE consensus sequence. Nrf2-ARE binding activity was measured via an electrophoretic mobility gel-shift assay (EMSA).

3.4. Effects of DHC on HO-1, NQO1 and GCLc protein expression in SH-SY5Y cells.

The protein levels of HO-1, NQO1, and GCLc, which are reported as a major phase II antioxidant enzymes that are transcribed upon Nrf2/ARE binding, were measured in the SH-SY5Y cells. As shown in Fig. 10, HO-1, NQO1, and GCLc protein expression levels were increased in a time- and dose-dependent manner by DHC treatment. As shown in Fig. 10 (B), HO-1, NQO1, and GCLc protein expression levels at 24 h were gradually increased by DHC treatment (0.08 - 10 μM). Upon Nrf2 siRNA treatment, the increased protein expression levels of HO-1, NQO1, and GCLc induced by DHC treatment (10 μM) were drastically reduced to a near-baseline level (Fig. 11). These results revealed that Nrf2/ARE binding is a key step in the transcriptions of HO-1, NQO1, and GCLc proteins.

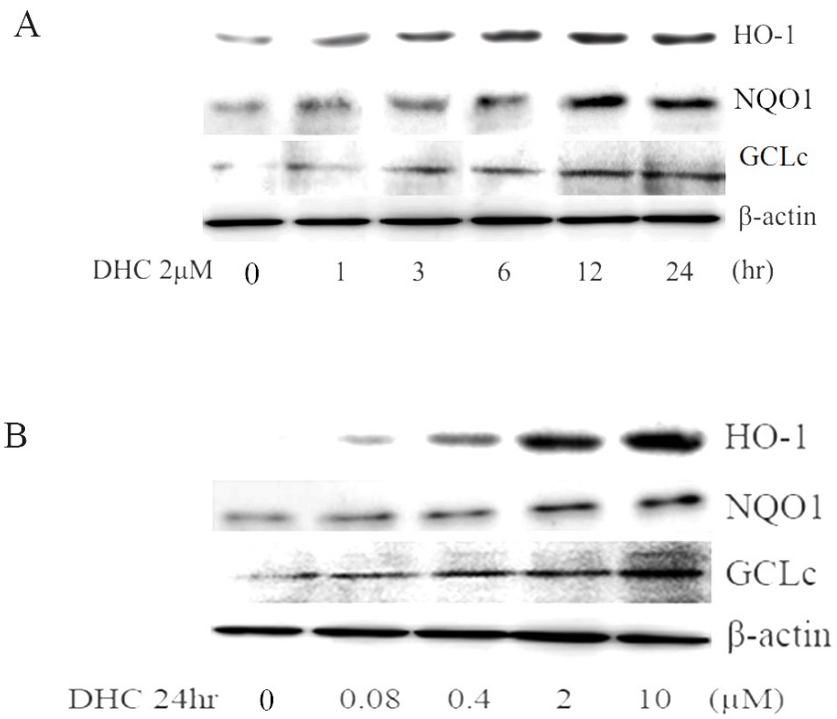

Figure 10. Effects of DHC on the expressions of the HO-1, NQO1, and GCLc proteins in the SH-SY5Y cells.

The cells were treated with DHC (2 μM) for different durations (0 - 24 h) **(A)**. The cells were treated with different concentrations of DHC (0.08 - 10 μM) for 24 h **(B)**. After treatment, the total protein was extracted and determined protein expression level by western blot assay. Representative data from three independent experiments are shown.

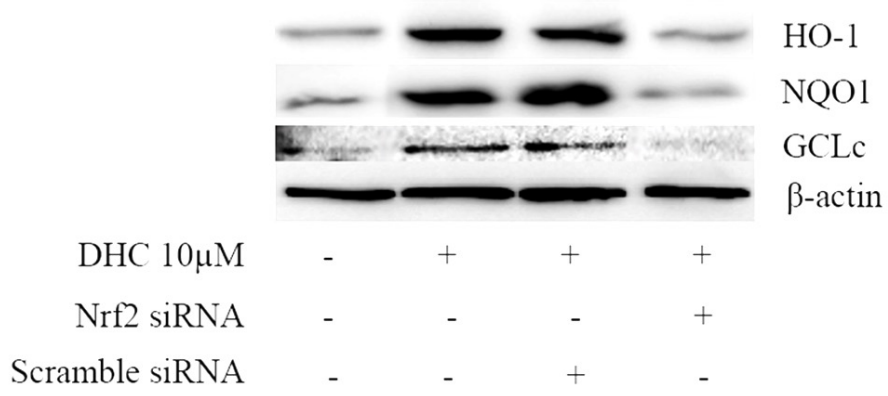

Figure 11. Effects of DHC on the expressions of the HO-1, NQO1, and GCLc proteins in Nrf2 siRNA treated SH-SY5Y cells.

The cells were transfected with Nrf2 siRNA (50 nM) or scrambled siRNA (50 nM) prior to treatment with DHC (10 μM) for 48 h. After DHC treatment, the total protein was extracted and evaluated HO-1, NQO1, and GCLc protein expression level by western blot assay. Representative data from three independent experiments are shown.

3.5. Effects of DHC on HO-1, NQO1 and GCLc mRNA expression in SH-SY5Y cells

The mRNA levels of HO-1, NQO1, and GCLc, which are reported as a major phase II antioxidant enzymes that are transcribed upon Nrf2/ARE binding, were measured in the SH-SY5Y cells. As shown in Fig. 12 - 14, HO-1, NQO1, and GCLc mRNA expression levels were increased in concentration-dependent manner by DHC treatment. HO-1, NQO1, and GCLc mRNA expression levels at 24 h were gradually increased by DHC treatment (0.08 - 10 μM). These results revealed that Nrf2/ARE binding is a key step in the transcriptions of HO-1, NQO1, and GCLc mRNA.

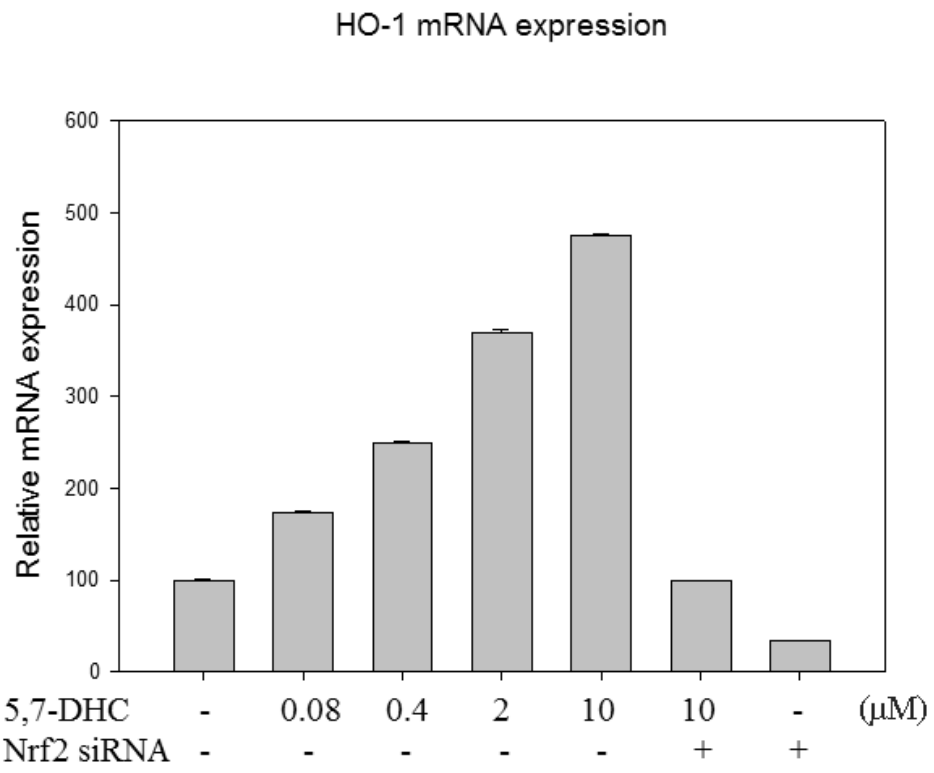

Figure 12. Effects of DHC on the mRNA expressions of HO-1 in SH-SY5Y cells.

The cells were transfected with Nrf2 siRNA (50 nM) or scrambled siRNA (50 nM) for 48 h prior to treatment with DHC (0.08 - 10 μM). After DHC treatment for 24h, the total RNA was extracted. The mRNA expression levels of HO-1 was determined by qRT-PCR analysis. Data represent the mean ± SD of three independent experiments.

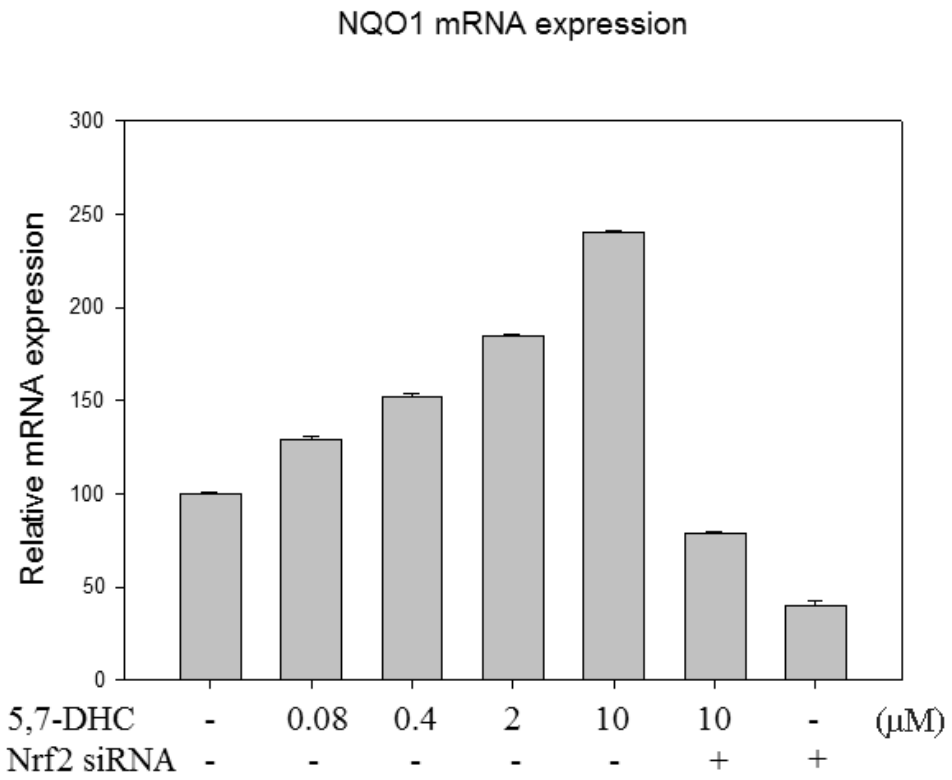

Figure 13. Effects of DHC on the mRNA expressions of NQO1 in SH-SY5Y cells.

The cells were transfected with Nrf2 siRNA (50 nM) or scrambled siRNA (50 nM) for 48 h prior to treatment with DHC (0.08 - 10 μM). After DHC treatment for 24h, the total RNA was extracted. The mRNA expression levels of NQO1 was determined by qRT-PCR analysis. Data represent the mean ± SD of three independent experiments.

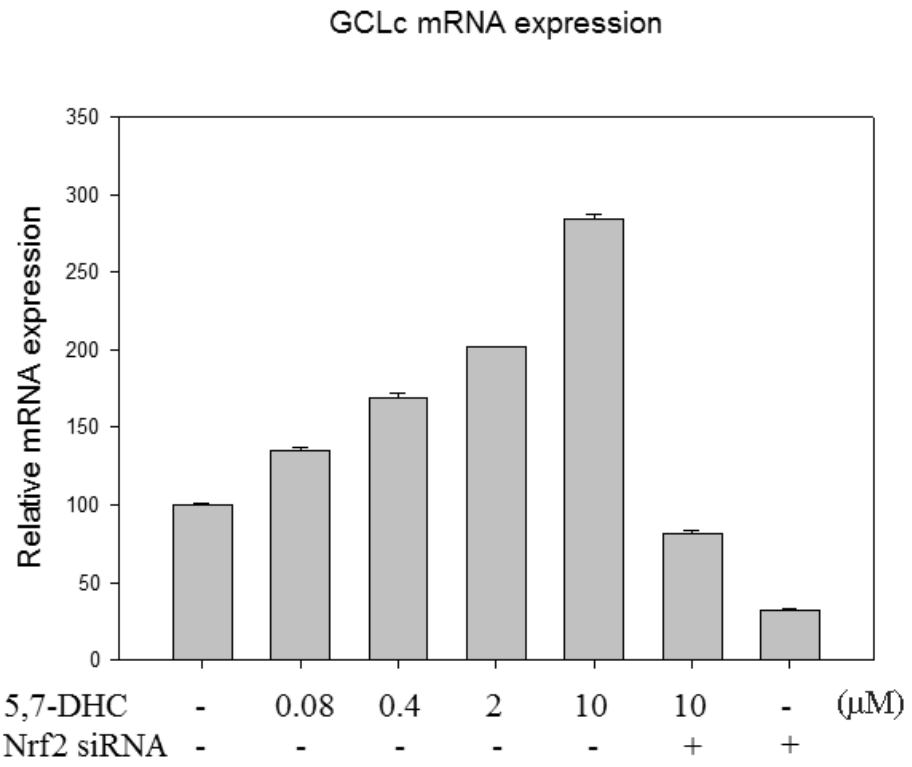

Figure 14. Effects of DHC on the mRNA expressions of GCLc in SH-SY5Y cells.

The cells were transfected with Nrf2 siRNA (50 nM) or scrambled siRNA (50 nM) for 48 h prior to treatment with DHC (0.08 - 10 μM). After DHC treatment for 24h, the total RNA was extracted. The mRNA expression levels of GCLc was determined by qRT-PCR analysis. Data represent the mean ± SD of three independent experiments.

3.6. The inhibitory effects of DHC on the 6-OHDA-induced apoptotic signal.

The inhibitory effects of DHC on the expressions of cleaved caspase-9, caspase-3, and PARP during the process of apoptosis were evaluated. ROS accumulation is known to activate caspase-9 and caspase-3, and activated caspase-3 cleaves PARP. As shown in Fig. 15, the cleaved caspase-9, caspase-3, and PARP were over-expressed when the SH-SY5Y cells were induced by 6-OHDA. However, the over-expression of these cleaved proteins was concentration-dependently inhibited by DHC treatment (0.08 - 10 μM).

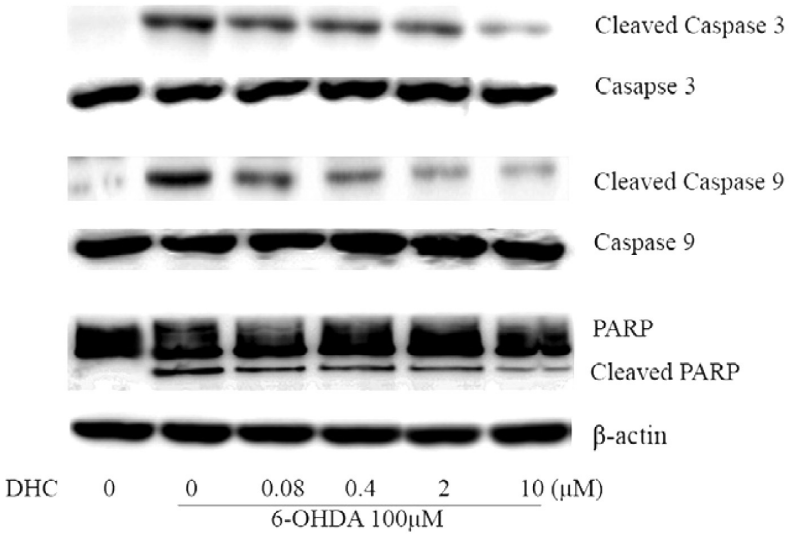

Figure 15. Inhibitory effects of DHC on the expressions of cleaved caspase-9, caspase-3 and PARP protein.

The cells were pre-treated with different concentrations of DHC (0.08 - 10 μM) for 24 h and subsequently treated with 6-OHDA (100 μM) for another 24 h. Then, each cell lysate was subjected to western blot analysis. Representative data from three independent experiments are shown.

4. Discussion

Neurodegenerative diseases may occur without obvious causes or be the result of numerous circumstances that cause the impairment of cellular performance in neuron and ultimately cell death. Due to the rapid aging of the populations of societies across the world, the number of patients suffering from the neurodegenerative disease is also increasing. Although the causes of these diseases have not been clearly elucidated, recent studies have revealed that ROS is composed of their pathogenesis (Farooqui and Farooqui, 2011). Because of their abundant iron contents and relatively deficient antioxidant defense system, neuronal cells are vulnerable to excessive ROS and electrophile related stress. It has been suggested that ROS is highly involved in the neurotoxicity of neurodegenerative disease (Munch et al., 1998b). Over the past decade, many studies of antioxidant enzymes have resulted in progress in the treatment and prevention of diseases (Rahman, 2007). In this context, it has been suggested that the coordinated expression of phase II antioxidant enzymes via the induction of nuclear Nrf2 could be a promising strategy for protection against oxidative stress-related neurodegenerative diseases.

The effects of DHC (Fig. 2) have not been thoroughly examined, particularly in relation to protection against neuronal cell death. In this report, DHC was found to protect against neuronal cell death and the ROS generation in 6-OHDA-induced SH-SY5Y cells. It was reported that caspase-9 could be cleaved by the ROS generation (Zuo et al., 2009). Cleaved caspase-9 induces activation of caspase-3 by making cleaved form of caspase-3, which is the important caspase involved in the apoptotic process and neuronal cell death caused by 6-OHDA (Dodel et al., 1999; Kuida et al., 1998). PARP is cleaved by active form of caspase-3, and this cleaved PARP loses the ability to participate in DNA repair, which results in apoptosis. PARP cleavage by active form of caspase-3 is a reliable indicator of apoptosis (Kaufmann et al., 1993). In our results, DHC prevented the 6-OHDA-induced cleavages of caspase-3, caspase-9, and PARP, which inhibited the activation of the apoptotic cascade in the SH-SY5Y cells. Moreover, DHC down-regulated the ROS level, which was increased by treatment with 6-OHDA. Based on its results, we suggest that this anti-apoptotic effect of DHC is associated with the down-regulation of ROS.

The effects of the Nrf2/ARE signaling pathway on the ROS generation were also evaluated. Our results revealed that treatment with DHC inhibited the generation of 6-OHDA-induced ROS, which affect the early and late stages

of apoptosis. The ability of DHC to inhibit ROS generation seems to be an important factor in neuronal cell protection. DHC also increased the induction of nuclear Nrf2, which has a binding affinity to ARE and activates ARE-driven phase II antioxidant enzymes; NQO1, HO-1, and GCLc. Nrf2 is regarded as a key regulator of antioxidant defensive responses and a sensor of cellular redox status (Kang et al., 2005). Many lines of research have proven the importance of Nrf2-related antioxidant enzymes in neuroprotection (Park et al., 2010). It has been also reported that the levels of antioxidant genes are considerably decreased in Nrf2-K.O. mice and the expression levels of antioxidant enzymes were eliminated by Nrf2-siRNA in *in vitro* models (Ramos-Gomez et al., 2001). NQO1, HO-1, and GCLc are representative antioxidant enzymes whose expressions are increased by diverse environmental stimulus including ROS and thiol-reactive substances (Rizzardini et al., 1993; Su et al., 2013; Fraser et al., 2002). NQO1 has been reported to be a potentially attractive therapeutic target for protecting cells from oxidative damage because it makes stable form of hydroquinone by catalyzing quinone (Lim et al., 2008). Moreover, it has been reported that HO-1 catalyzes heme to carbon monoxide, biliverdin and iron, which exerts potent antioxidant effects (Farooqui and Farooqui, 2011). CGLc participates in glutathione synthesis and prevents the impairment of cellular function from

the excessive ROS (Pompella et al., 2003). Many studies have shown that these antioxidant enzymes have powerful antioxidant effects, and it has been suggested that the regulation of antioxidant enzymes might be a key factor in the prevention of age-related disease (Uttara et al., 2009). Our results revealed that DHC treatment induced the nuclear translocation of Nrf2, which resulted in the increases in NQO1, HO-1, and CGLc at the level of protein expression, suggesting that the neuroprotective effects of DHC against 6-OHDA-induced cell death are involved in the inhibition of ROS generation. Based on our research, we expect that one of the neuroprotective effects exerted by DHC is the increased induction of the Nrf2/ARE signal. When the cells were transfected with Nrf2 siRNA, the protective effects of DHC against 6-OHDA-induced neurotoxicity and ROS generation were inhibited. Moreover, the increased protein expression levels of NQO1, HO-1, and GCLc by DHC treatment (10 μM) were also drastically reduced to basal levels by treatment with Nrf2 siRNA. The results revealed that the neuroprotective effects of DHC are due to the activation of Nrf2/ARE signal pathways and the subsequent inhibition of ROS generation.

5. Conclusion

The present study demonstrated that DHC prevented 6-OHDA-induced neurotoxicity via the induction of Nrf2/ARE signal, which subsequently led to the overexpression of antioxidant enzymes, including NQO1, HO-1, and CGLc. As a result of these effects, DHC inhibited the generation of ROS and neuronal cell death in 6-OHDA-induced SH-SY5Y cells. Our study suggests that DHC can be a promising neuroprotective candidate in the therapy of neurodegenerative diseases such as Parkinson's disease.

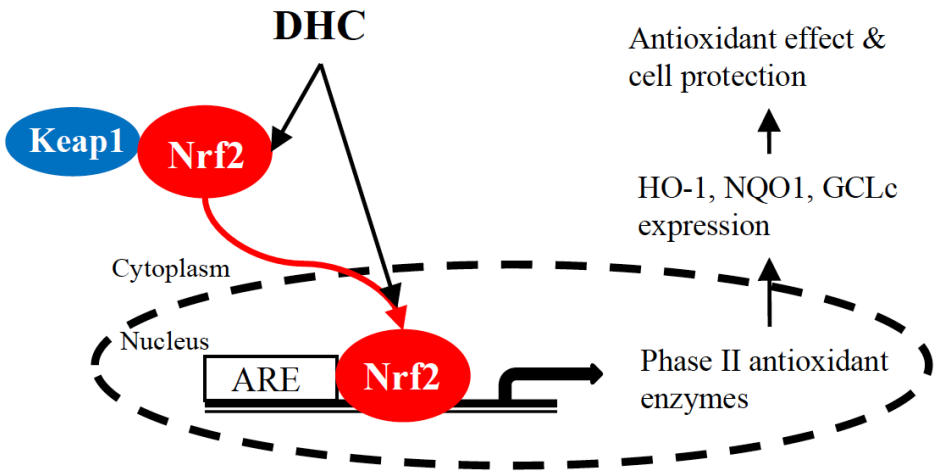

Figure 16. A scheme of protective effects of DHC on 6-OHDA-induced neuronal cell death via activation of Nrf2/ARE signal.

DHC protected 6-OHDA-induced neurotoxicity via the induction of Nrf2/ARE signal, which subsequently led to the overexpression of antioxidant enzymes, including NQO1, HO-1, and CGLc. As a result of these effects, DHC inhibited the generation of ROS and neuronal cell death in 6-OHDA-induced SH-SY5Y cells.

Chapter 2

Orobol derivatives and extracts from *Cudrania tricuspidata* fruits protect against 6-hydroxydopamine-induced neuronal cell death by enhancing proteasome activity and the ubiquitin/proteasome-dependent degradation of α-synuclein and synphilin-1

1. Introduction

Cudrania tricuspidata (Moraceae) is a subtropical tree that is widely distributed in Korea, China, and Japan. The fruits of *C. tricuspidata* are used in jams, juices, and a fermented alcoholic beverage with sugar, and they are commercially produced as food in Korea. In addition, the root, stem, leaf, and fruits of this plant have been reported to have anti-atherosclerotic, anti-inflammatory and antioxidant activities (Lee et al., 2012; Park, KH et al., 2006; Jeong et al., 2010). Recent studies have demonstrated that the fruit of *C. tricuspidata* inhibited pancreatic lipase (Jeong et al., 2014), protected neuronal cells against oxidative stress-induced toxicity (Jeong et al., 2010), and inhibited IgE-mediated allergic and inflammatory responses (Lee et al., 2015). The compounds isolated from *C. tricuspidata* are primarily xanthones and flavones in addition to some alkaloids, lignins, coumarins, polysaccharides, and chromones (Hano et al., 1991; Lee et al., 1996; Seo et al., 2001; Fujimoto et al., 1984; Hiep et al., 2015). The isoflavones from the fruits of *C. tricuspidata* have been reported to exert protective effects against 6-hydroxydopamine (6-OHDA)-induced neurotoxicity (Hiep et al., 2015) and to have inhibitory effects against IgE-mediated allergic and inflammatory

responses (Lee et al., 2015). Orobol (OB), 6-prenylorobol (POB) and 6,8-diprenylorobol (DPOB) are prenylated isoflavones. It was reported that OB increases cisplatin sensitivity in human ovarian carcinoma (Shiotsuka and Isonishi, 2001) and that DPOB shows anti-estrogenic activity (Okamoto et al., 2006) and inhibits lipofuscin fluorophore-mediated photo oxidation (Uddin et al., 2011).

Parkinson's disease (PD) is characterized by severe motor deficits, cogwheel rigidity, bradykinesia, and the loss of dopaminergic neurons. The aetiology of PD has not been clearly identified; however, oxidative stress is thought to be a common factor that leads to cellular dysfunction and neurodegeneration. Reactive oxygen species (ROS) are mainly produced as a by-product of cellular metabolism and oxidative phosphorylation. Non-neutralized ROS produce oxidative stress in cellular organisms and lead to abnormal molecular activities (Bochkov et al., 2010). In particular, the pathological events that occur in PD have been suggested to be linked to protein oxidation caused by oxidative stress (Butterfield and Kanski, 2001), and excessive intracellular ROS induce apoptosis that is characterized by the cleavage of caspase-3, caspase-9 and poly ADP-ribose polymerase (PARP) (Klovekorn and Munch, 1998). The neurotoxin 6-OHDA destroys dopaminergic and noradrenergic neurons in the brain by inducing excessive ROS such as superoxide radicals,

which leads to protein oxidation and neuronal cell death (Kanthasamy et al., 2010).

The proteasome plays a key role in the selective degradation of oxidized proteins via ubiquitin-mediated processes, and its role is essential for cellular protein maintenance (Tai and Schuman, 2008; Jung and Grune, 2013). The ubiquitin-proteasome system (UPS) is responsible for the degradation of many cellular proteins, except membrane and extracellular proteins, which after endocytosis are degraded within the lysosomes. In addition, misfolded, mutant, and oxidatively damaged proteins are also degraded by the UPS. Proteins to be degraded are first marked by covalent attachment of a polyubiqutin chain to a lysine residue on the substrate. The polyubiquitinated protein is then degraded by a large proteolytic complex, the 26S proteasome. Monoubiquitinylation, on the other hand, regulates transcription, translation, protein trafficking, DNA repair, and numerous other cellular functions. Polyubiquitination of a target protein is accomplished through a series of enzyme-mediated reactions that are required to ensure specificity and activate the ubiquitinmoiety. First, activated ubiquitin is generated by ubiquitin-activating enzyme (E1), which forms a thiol ester linkage between a cysteine residue and carboxy-terminalglycine in ubiquitin in an ATP-dependent manner. The activated ubiquitin is transferred to one of the several

ubiquitin carrier proteins or ubiquitin conjugating enzymes (E2s) via the formation of another thiol linkage. Finally, ubiquitin is ligated to the lysine residue of the protein substrate that is specifically bound to an E3 ligase. Parkin, involved in familial PD, is an example of such an E3 ligase. Additional activated ubiquitin moieties can be attached to internal lysine residues within the ubiquitin to form polyubiquitin linkages, which then act as the degradation sign that is recognized by the 26S proteasome complex (Dahlmann, 2007). A minimum of four ubiquitin moieties is required for efficient targeting to the proteasome. Selectivity of ubiquitination and recognition of substrates are largely mediated by E3s. There are more E2s than E1s, and more E3s than E2s so at each step the number of proteins that can possibly be involved increases, as does the specificity of binding to the next component. It is the E3, either alone or in combination with its bound E2, that determines the specificity of substrate recognition (Betarbet et al., 2005).

Proteasomes are existing in the cytoplasm, perinuclear regions, and nuclei of all eukaryotic cells. Their relative abundance within these compartments is extremely variable. In the cytoplasm, proteasomes are associated with centrosomes, cytoskeletal networks, and the outer surface of the endoplasmic reticulum. In the nucleus, proteasomes are present throughout the nucleoplasm but not in the nucleoli. Impairment of

the proteolytic pathway results in accumulation of proteasomes in these locations, forming organized aggregates. Aggregates located in the pericentrosomal areas have been termed “aggresomes”. Aggresomes are known to damage proteasomal function and promote apoptosis (Wojcik and DeMartino, 2003).

The 26S proteasome consists of a catalytic core—the 20S proteasome. The 20S proteasome is made up of 28 subunits assembled as two outer and two inner heptameric rings stacked axially to form a hollow cylindrical structure wherein proteolysis occurs (Doskeland and Flatmark, 2002). The two inner rings of the 20S proteasome are composed of seven different β-subunits each. The three different catalytic sites (chymotrypsin-like, trypsin-like, and caspase-like-peptide hydrolytic sites) of the proteasome reside on the inner surface of the inner rings, thereby preventing indiscriminate degradation of proteins (Huang and Figueiredo-Pereira, 2010). The noncatalytic outer rings, comprising of seven different α-subunits, serve as an anchor for the 19S (PA700) multisubunit ATPase containing proteasome activator or regulator. The 19S complex determines substrate specificity and consists of at least six ATPases and more than 15 additional subunits that lack the capacity to bind to ATP. The 19S regulatory complex serves at least three ATP-dependent functions: it selectively opens the channel through the 20S proteasome,

unfolds ubiquitinated proteins to allow entry into the catalytic core, and cleaves off the polyubiquitinated chain from the substrate. The degradation products of proteasomal catalysis are small peptides and amino acids that can be recycled to produce new proteins. At the same time, polyubiquitin chains, released from targeted proteins, are then disassembled by ubiquitin carboxy-terminal hydrolases to produce monomeric ubiquitin molecules that can be reused. Recent research has suggested that oxidative stress-induced proteasome dysfunction might play a key role in neurodegenerative diseases and that rescuing the decrease in proteasome activity could be a new therapeutic strategy (Seo et al., 2007). Additionally, dysfunction in proteasome activity was observed in the substantia nigra of PD patients, suggesting that the impairment of the UPS is involved in the formation of Lewy bodies and in dopaminergic neuronal cell death in PD (McNaught and Jenner, 2001). Lewy bodies are characteristic hallmarks of PD and are composed of primarily α-synuclein and synphilin-1 along with ubiquitin and other fibrils. α-synuclein, a small acidic protein composed of 140 amino acids, is abundant in the human brain; is also found in the heart, muscles, and other tissues; and is a naturally unfolded protein with the ability to self-aggregate. The aggregation process of α-synuclein results in potential cell damage, leading to dopaminergic neuronal loss in Parkinson's disease (Cookson, 2005).

α-synuclein also associates with other protein partners in the cell, including a significant interaction with synphilin-1. It has been reported that synphilin-1 is a presynaptic protein that could be a modulator of UPS, and the overexpression of synphilin-1 promotes the formation of inclusions under conditions of proteasome inhibition. Additionally, synphilin-1 inhibits the degradation of α-synuclein by the proteasome, thus increasing its half-life (Alvarez-Castelao and Castano, 2011). Therefore, it is possible that the inhibition Lewy body-associated protein accumulation through the protection against proteasome dysfunction could be a key aspect of PD treatment.

In our previous reports, we investigated the neuroprotective effect of different extracts (0 – 100% ethanol ratio) containing isoflavones from *C. tricuspidata* fruits (Hiep et al., 2015). Here, nine isolates obtained from 50% ethanol extract from *C. tricuspidata* fruits (CTE50) were evaluated for their neuroprotective potential against 6-OHDA-induced cell death in SH-SY5Y human neuroblastoma cells. The study focused on the potential effects on apoptosis, intracellular ROS generation, proteasome activities, polyubiquitination of Lewy body-associated α-synuclein and synphilin-1 against 6-OHDA-induced SH-SY5Y cells.

2. Materials and methods

2.1. Chemicals and reagents

6-Hydroxydopamine (6-OHDA), and 2',7'-dichlorfluorescein-diacetate (DCFH-DA) were purchased from Sigma-Aldrich (St. Louis, MO, USA). MG132 was purchased from Enzo Life Sciences (Farmingdale, NY, USA). Dulbecco's modified Eagle's medium (DMEM) and foetal bovine serum (FBS) were purchased from Hyclone™ Thermo Scientific (Wyman Street Waltham, MA, USA). Hybond®-Polyvinylidene difluoride (PVDF) membranes were purchased from Amersham Pharmacia Biotechnology Inc. (Piscataway, NJ, USA). PRO-PREP protein extraction solution and WEST-ZOL® ECL solution were purchased from iNtRON Biotech Inc. (Kyunggi, Korea). Antibodies against ubiquitin, α-synuclein, synphilin-1, β-actin, caspase-3, cleaved caspase-3, caspase-9, cleaved caspase-9, PARP, and A/G Plus-Agarose and secondary antibodies were purchased from Santa Cruz Biotechnology, Inc. (CA, U.S.A.)

2.2. Preparation of ethanol extracts from the fruits of *C. tricuspidata* (CTE)

The fruits of *C. tricuspidata* were collected from the Korea Forest Research Institute, Southern Forest Research Center (Jinju, Korea). A voucher specimen (accession no. KH1-5-090904) was deposited at the Department of Biosystems and Biotechnology, Korea University (Seoul, Korea). The dry fruit of *C. tricuspidata* (3.4 kg) was ground into powder form and sifted through a 120-mesh sieve. The dry powder (7 g) was refluxed three times for 1 h each by means of a heating mantle with 250 mL of 0, 30, 50 70, or 100% ethanol in round 500-mL flasks. The combined extracts were filtered and concentrated in vacuo to yield 2.85 g, 2.71 g, 2.57 g, 2.67 g, and 2.1 g, respectively.

2.3. Ultra performance liquid chromatography (UPLC) analysis of CTE50

The CTE50 was analysed using an Acquity UPLC system (Waters, Millford, MA, USA) with an Acquity UPLC BEH C18 column (1.7 μm, 2.1 × 150 mm i.d.). The mobile phase consisted of solvent A (0.05% formic acid in water) and solvent B (acetonitrile), which flowed at rate of 0.3 mL/min. The starting eluent was 40% B at 0 min, and the proportion of B was increased linearly to 100% from 0 to 10 min, held constant at 100% for 11.5 min, and then returned to the initial condition over the course of 1.5 min to re-equilibrate the column.

The sample injection volume was 4 μL for extract and 2 μL for compounds (CTE50: 3 mg/mL, OB, POB, and DPOB: 0.2 mg/mL). The column and sample managers were maintained at 35 and 15 °C, respectively, and the UV detection wavelength was monitored at 265 nm.

2.4. Isolation and identification of compounds from CTE50

Nine isoflavones, namely, orobol (**1**, 0.0021%), 6-prenylorobol (**2**, 0.0100%), 6,8-diprenylorobol (**3**, 0.0015%), millewanins H and G (**4** and **5**, 0.0029 and 0.0045%), alpinumisoflavone (**6**, 0.0762%), 4′-*O*-methylalpinumisoflavone (**7**, 0.0046%), erysenegalensein E (**8**, 0.0181%), and 6,8-diprenylgenistein (**9**, 0.0055%), were isolated from the fruits of *C. tricuspidata*. The chemical structures were determined by interpretation of spectroscopic data, including MS and NMR spectra, as compared to the previously reported literature (supplementary data 1). The detailed isolation procedures are included in the supplementary materials and methods. The purity of each compound was more than 95%.

2.5. Cell cultures

The human neuroblastoma cell line SH-SY5Y (ATCC No. CRL-2266) was purchased from the American Type Culture Collection (Manassas, VA, USA)

and cultured in DMEM supplemented with 10% heat-inactivated FBS and 1% penicillin/streptomycin at 37 ºC in a humidified 5% CO_2 atmosphere. Test samples were dissolved in 10% DMSO, and the cells were treated within non-cytotoxic concentration ranges of test samples at a final concentration of 0.1% DMSO.

2.6. Measurement of cell viability

SH-SY5Y cells were plated at a density of 1×10^5 cells/200 μL/well in 96-well plates for 24 h, and the cells were simultaneously treated with 6-OHDA and test samples (0.16 – 20 μg/mL of 0 – 100% CTE; 0.2 – 25 μM of nine isolates) for 48 h. After treatment, cell viability was evaluated using the MTT assay as previously described (Koo et al., 2011). Briefly, the medium was removed, and the cells were incubated with fresh medium containing 0.5 mg/mL MTT for 4 h at 37 ºC, after which the medium was gently removed. Formazan crystals were dissolved in 100 μL DMSO, and absorbance was measured at 540 nm using a microplate reader (SpectraMax M5, Molecular Devices, USA).

2.7. Measurement of intracellular ROS by flow cytometry

Intracellular ROS levels were measured by the 2',7'-dichlorofluorescein diacetate (DCFH-DA) method as described previously (Kim, D-W et al.,

2015). Briefly, SH-SY5Y cells were plated at a density of 1×10^6 cells/1 mL/well in 12-well plates for 24 h, simultaneously treated with 6-OHDA (75 μM) and test samples (0.16 – 20 μg/mL of 0 – 100% CTE, 0.2 – 25 μM of isolates) for 48 h, and washed three times with PBS. DCFH-DA (4 μM/mL in PBS) was then added, and afterwards, the cells were incubated for 30 min at 37 ºC in the dark. The cells were then washed 3 times with PBS, and the fluorescence intensities of a total of 10,000 events were measured by the FL-1 channel of a flow cytometer (BD FACS Calibur™).

2.8. Measurement of proteasome activity

Proteasome activity was determined using SH-SY5Y cells as previously described (Kim, B-H et al., 2015). Briefly, cells (1.0×10^5 cells/300 μL/well) were plated in 48-well plates for 24 h and then simultaneously treated with 6-OHDA (75 μM) and samples (0.16 – 20 μg/mL of CTE50, 0.2 – 25 μM of nine isolates) for 48 h. After washing twice with PBS, cells were lysed by freeze-thawing 3 times (between -70 ºC and 37 ºC, 5 min each) and scraped into PBS buffer. Supernatants were collected by centrifugation at 15,000 rpm (15 min, 4 ºC), and the total protein concentration was determined by the Bradford method (Bradford, 1976). The proteolytic activity of the proteasomes was evaluated with a 20S proteasome activity kit (APT 280;

Millipore, USA). In brief, supernatants (40 μg) were incubated for 2 h at 37 °C in the provided buffer with fluorophore-linked peptide substrates. Suc-LLVY-AMC (40 μM), Boc-LRR-AMC (40 μM), and Z-LLE-MCA (80 μM) were used as the substrates for chymotrypsin-, trypsin- and caspase-like protease activities, respectively. Reaction mixtures without cell lysates were used as negative controls, and aminomethylcoumarin (AMC) or methylcoumarylamide (MCA) fluorescence was measured at excitation/emission wavelengths of 380/460 and 380/440 nm, respectively, using a microplate reader (SpectraMax M5, Molecular Devices, USA).

2.9. Measurement of mRNA expression

After treatments, total RNA was isolated from SH-SY5Y cells by easy-BLUE® and cDNA was synthesized by using SuPrimeScript RT premix® according to the manufacturer's procedure. The synthesized cDNA was used for PCR and the primer pair sequence were listed as follows:

Chymotrypsin-like proteasome subunit (PSMB-8)

5-GTTCCAGCATGGAGTGATTG-3 (sense) and

5- TGTTCACCCGTAAGGCACTA-3 (antisense);

Trypsin-like proteasome subunit (PSMB-7)

5-ATGGCTGTACCACGAAACAA-3 (sense) and

5-AGGGATCCTTCAGTTTCTTCAGT-3 (antisense);

Caspase-like proteasome subunit (PSMB-6)

5-TCGATTTGATACCTTTGATAGCC-3 (sense) and

5-CCAGGGTCAATGGGTGAC-3 (antisense);

GAPDH

5-CTCTGCTCCTCCTGTTCGAC-3 (sense) and

5-ACGACCAAATCCGTTGACTC-3 (antisense). The cycle condition was as follow; 94℃ for 20s, 56℃ for 20s, 72℃ for 30s and 40 cycles. PCR were performed by using SYBRs HS Prime qPCR premix® in an ABI 7300 real-time PCR (Applied Bio systems, CA, USA). Ct (threshold cycle) values were obtained using the Sequence Detection Software version1.2.3 (Applied Bio systems, CA, USA). To evaluate quantification of the changes in target gene expression, we used the $2^{-\triangle\triangle Ct}$ method (Tucker and Munchus, 1998). Fold change=$2^{-\triangle\triangle Ct}$, $\triangle\triangle Ct = (Ct_{\text{target gene}} - Ct_{GAPDH}) - (Ct_{\text{control}} - Ct_{GAPDH})$

2.10. Measurement of protein expression

SH-SY5Y cells were plated at a density of 2×10^6 cells/4 mL in 60-mm dishes for 24 h. The cells were then simultaneously treated with 6-OHDA (75 μM) and samples (0.16 – 20 μg/mL of CTE50, 0.2 – 25 μM of three orobol

derivatives) for 48 h, washed three times with PBS, and lysed with a PRO-PREP protein extraction solution at -20 ºC for 20 min. After centrifugation at 13,000 rpm for 30 min, the supernatant was used as the total protein extract. Western blot analysis was accomplished as previously described (Ham et al., 2013). Briefly, protein extracts were separated by electrophoresis on a SDS-PAGE gel and then transferred to PVDF membranes. Then, the PVDF membranes were incubated overnight at 4 ºC with primary antibodies followed by a 1-h incubation at RT with the secondary antibody. The blots were developed using WEST-Queen® ECL solution and analysed using LAS4000 (GE Healthcare, UK)

2.11. Immunoprecipitation assay

Immunoprecipitation was performed as previously described with slight modifications (Chen et al., 2014). Briefly, SH-SY5Y cells were plated at a density of 2×10^6 cells/4 mL in 100-mm dishes for 24 h. The cells were then simultaneously treated with 6-OHDA (75 μM) and samples (0.8 – 20 μg/mL of CTE50, 1 – 25 μM of three orobol derivatives) for 48 h and washed three times with PBS. SH-SY5Y cells were homogenized and lysed in cold-lysis buffer (50 mM Tris, 1 mM PMSF, 150 mM NaCl, 50 mM NaF, 1% Nonidet P-40, 0.25% sodium deoxycholate, 10 mM sodium pyrophosphate) and

centrifuged at 14,000 × g (10 min, 4 °C), and the supernatant was transferred to a new ep-tube and incubated with 2 μg of α-synuclein or synphilin-1 antibody overnight at 4 °C. The next day, A/G plus agarose beads were added and incubated overnight at 4 °C followed by 3 washes in cold-lysis buffer. The loading samples were adjusted to total volume of 30 μL with lysis buffer, and the immune-complexes were eluted at 95 °C on a heating block for 5 min, vortexed, and spun down by centrifugation at 15,000 × g for 10 min.

2.12. Statistical analysis

All experimental data are expressed as the mean ± standard deviation. Statistical significance between multiple groups was determined by one-way ANOVA (PRISM Graph Pad, San Diego, CA, USA). When the ANOVA showed a significant difference, Bonferroni's multiple comparison *post hoc* tests were conducted. A *P* value less than 0.05 was considered statistically significant.

3. Results

3.1. Protective effects against 6-OHDA-induced neuronal cell death in SH-SY5Y cell

Ethanol is often used to extract bioactive compounds from plant materials, and the bioactivity of plant extracts depends on the ratio of water to ethanol used in the extraction process (Ganora, 2009). We evaluated the neuroprotective effects within non-cytotoxic concentration ranges from different CTE extracts (0, 30, 50, 70, and 100% ethanol) and nine isolates. As shown in Table 2, CTE50 showed the most potent protective effects with an EC_{50} value of 3.3 μg/mL. The constituents of CTE50 were identified using UPLC, and nine isolates were obtained (Figs. 17 and 18). Among the nine isolates, three orobol derivatives (OB, POB, and DPOB) significantly attenuated 6-OHDA-induced neurotoxicity with EC_{50} values of 6.4 μM, 4.5 μM, and 10.1 μM, respectively (Table. 2). As shown in Fig. 20, 6-OHDA-induced neuronal cell death was observed by the morphology of cells: 6-OHDA resulted in cellular morphological changes including cell shrinkage and rounding. However, treatment with CTE50 (20 μg/mL) or the three orobol derivatives (25 μM)

ameliorated the 6-OHDA-induced morphological changes to almost normal levels. As shown in Fig. 19, the 6-OHDA-induced group showed a significant decrease in cell viability compared to the vehicle-treated group. However, CTE50 (0.16 – 20 μg/mL) or the three orobol derivatives (0.2 – 25 μM) protected 6-OHDA-induced neuronal cell death in a concentration-dependent manner. Additionally, it was examined that the comparison of neuroprotective effect of CTE50 and three orobol derivatives against 6-OHDA-induced neurotoxicity by pre-, co-, and post treatment. Among three groups, co-treatment group exerted potent neuroprotective effects (Fig. 31).

Table 2. Inhibitory effects of ethanol extracts and isolates from the fruits of *C. tricuspidata* against 6-OHDA-induced cell death and ROS generation in SH-SY5Y cells

Extract / Compound	Neuroprotective effect against 6-OHDA-induced cell death (EC_{50} value)	Inhibitory effect against 6-OHDA-induced ROS generation (IC_{50} value)
0% ethanol extract of *C.tricuspidata* fruit	>20 μg/mL	>20 μg/mL
30% ethanol extract of *C.tricuspidata* fruit	5.4 ± 0.8 μg/mL	10.2 ± 1.2 μg/mL
50% ethanol extract of *C.tricuspidata* fruit	3.3 ± 0.3 μg/mL	6.7 ± 0.7 μg/mL
70% ethanol extract of *C.tricuspidata* fruit	7.8 ± 0.9 μg/mL	14.2± 1.1 μg/mL
100% ethanol extract of *C.tricuspidata* fruit	>20 μg/mL	>20 μg/mL
(**1**) orobol	6.4 ± 0.5 μM	7.2 ± 0.6 μM
(**2**) 6-prenylorobol	4.5 ± 0.3 μM	5.9 ± 0.4 μM
(**3**) 6,8-diprenylorobol	10.1 ± 0.8 μM	17.3 ± 1.0 μM
(**4**) millewanin H	15.2 ± 1.3 μM	19.2 ± 1.5 μM
(**5**) millewanin G	18.5 ± 2.1 μM	22.4 ± 2.4 μM
(**6**) alpinumisoflavone	>25 μM	>25 μM
(**7**) 4'-*O*-methylalpinumisoflavone	>25 μM	>25 μM
(**8**) erysenegalensein E	>25 μM	>25 μM
(**9**) 6,8-diprenylgenistein	>25 μM	>25 μM

The EC_{50} & IC_{50} values were determined in a semi-logarithmic graph with 4 different concentrations.
The values are presented as the mean ± standard deviation of three independent experiments

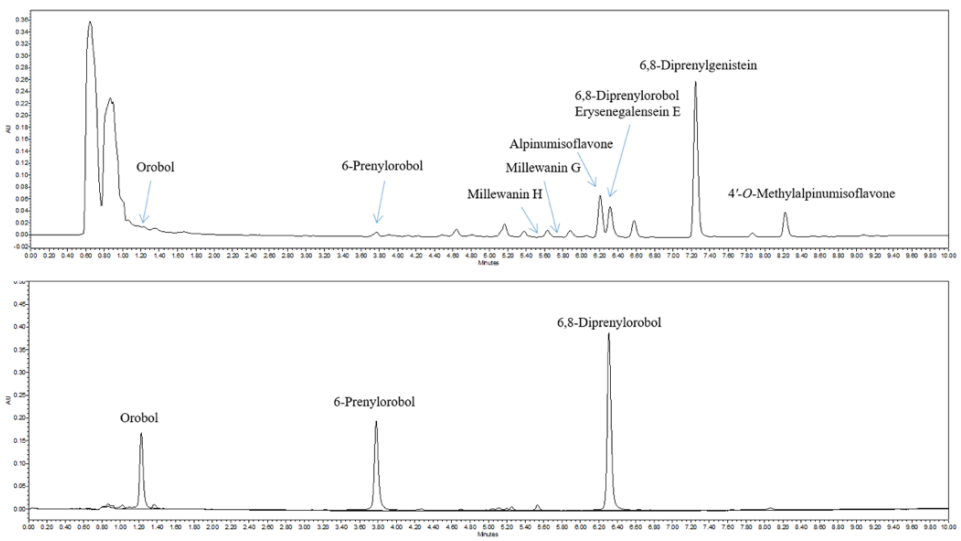

Figure 17. UPLC chromatograms and structures of isolates from CTE50.

UPLC chromatogram of CTE50 and isolates from CTE50. Nine compounds were isolated from CTE50. Among nine isolates, orobol, 6-prenylorobol, and 6,8-diprenylorobol were selected for further study. The selected three orobol derivatives were confirmed the elution time for identification.

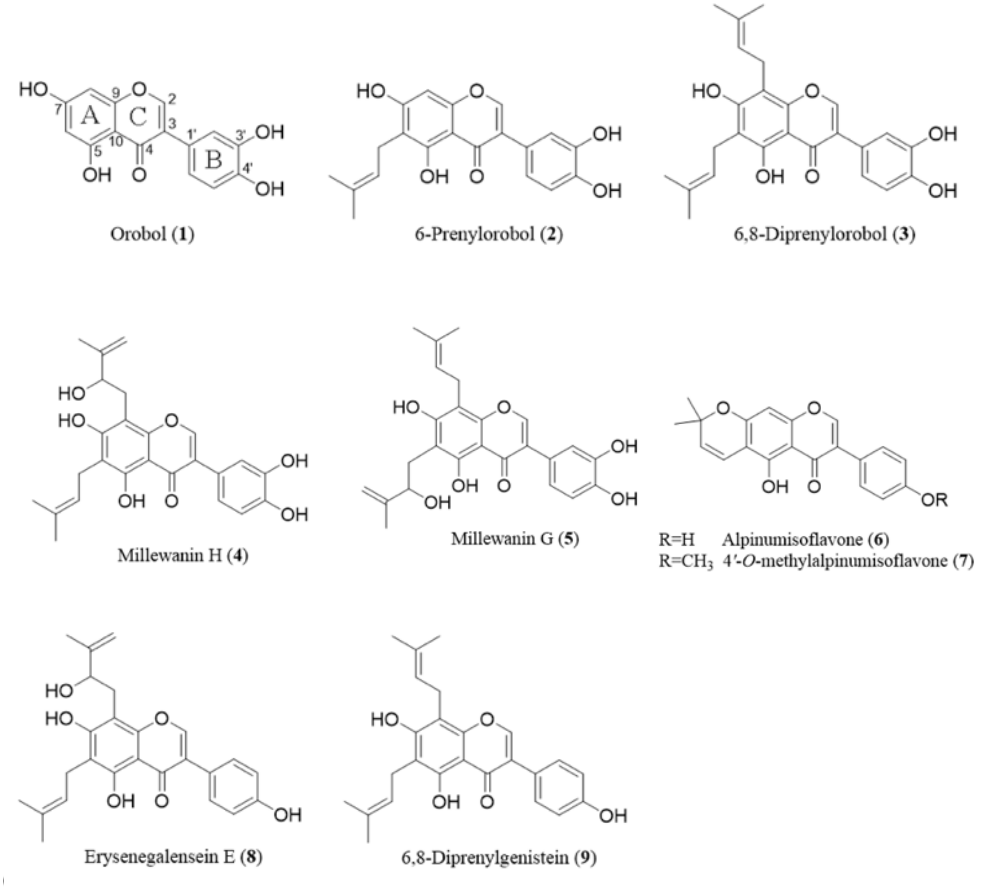

Figure 18. Chemical structures of the isolates from CTE50.

The isolated compounds are orobol (**1**), 6-prenylorobol (**2**), 6,8-diprenylorobol (**3**), millewanin H (**4**), millewanin G (**5**), alpinumisoflavone (**6**), 4′-O-methylalpinumisoflavone (**7**), erysenegalensein E (**8**), and 6,8-diprenylgenistein (**9**).

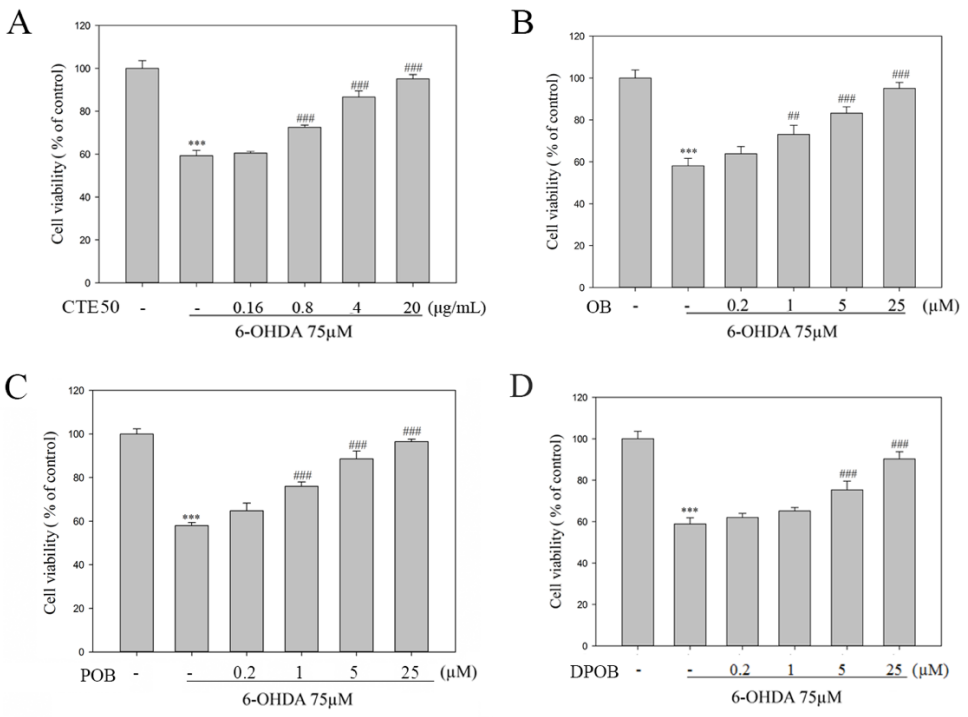

Figure 19. Inhibitory effects of CTE50 and three orobol derivatives (OB, POB, and DPOB) against 6-OHDA-induced neurotoxicity.

Cells were cultured in 96-well plate for 24 h, and CTE50 or orobol derivatives were simultaneously treated with 6-OHDA (75 μM) for 48 h. Cell viability were measured by MTT reduction assay (A – D). Data represent the mean ± SD of three independent experiments. (***$p<0.001$ versus control group, $^{\#\#}p<0.01$ and $^{\#\#\#}p<0.001$ versus 6-OHDA-induced group)

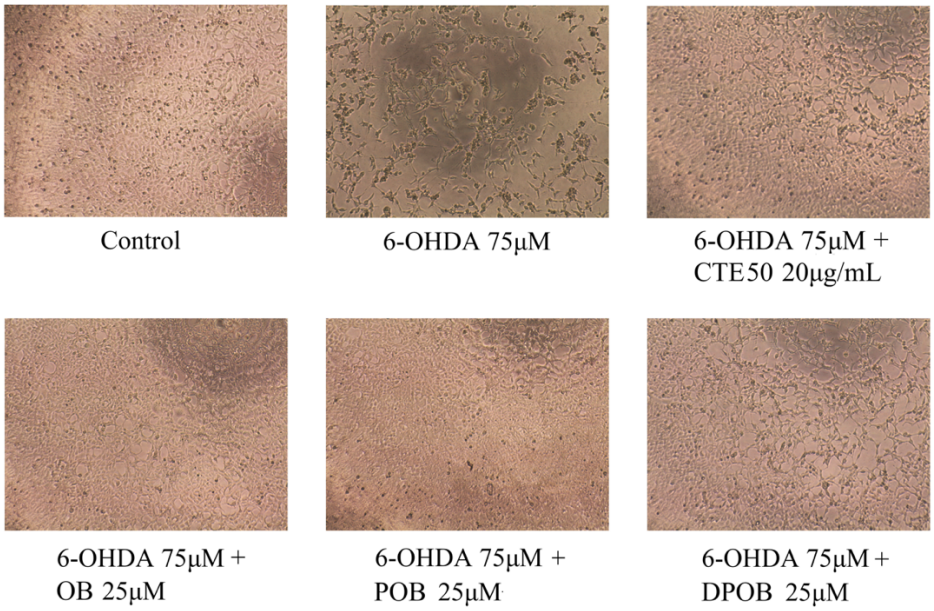

Figure 20. Neuroprotective effects of CTE50 and the three orobol derivatives (OB, POB, and DPOB) against 6-OHDA-induced neurotoxicity in SH-SY5Y cells.

Cells were cultured in 96-well plate for 24h, and CTE50 or three orobol derivatives were simultaneously treated with 6-OHDA (75 μM) for 48 h. The morphological change of cell was observed by inverted phase-contrast microscopy. Representative images were captured at 100× magnification.

3.2. Inhibition of 6-OHDA-induced intracellular ROS generation

Excessive intracellular ROS induce cellular stress and neuronal cell death, and it has been reported that ROS play important roles in the pathogenesis of neurodegenerative diseases. As shown in Table 2, CTE50 showed the most potent inhibition of 6-OHDA-induced ROS generation with an IC_{50} value of 6.7 μg/mL. Among the nine compounds derived from CTE50, the three orobol derivatives showed a significant inhibitory effect against 6-OHDA-induced intracellular ROS generation with IC_{50} values of 7.2 μM (OB), 5.9 μM (POB), and 17.3 μM (DPOB). As shown in Fig. 21 and 22, 6-OHDA-treated cells showed strong DCF fluorescence intensities compared to vehicle-treated cells. The amount of intracellular ROS was decreased in a concentration-dependent manner when cells were treated with CTE50 (0.8 – 20 μg/mL) or the three orobol derivatives (1 – 25 μM).

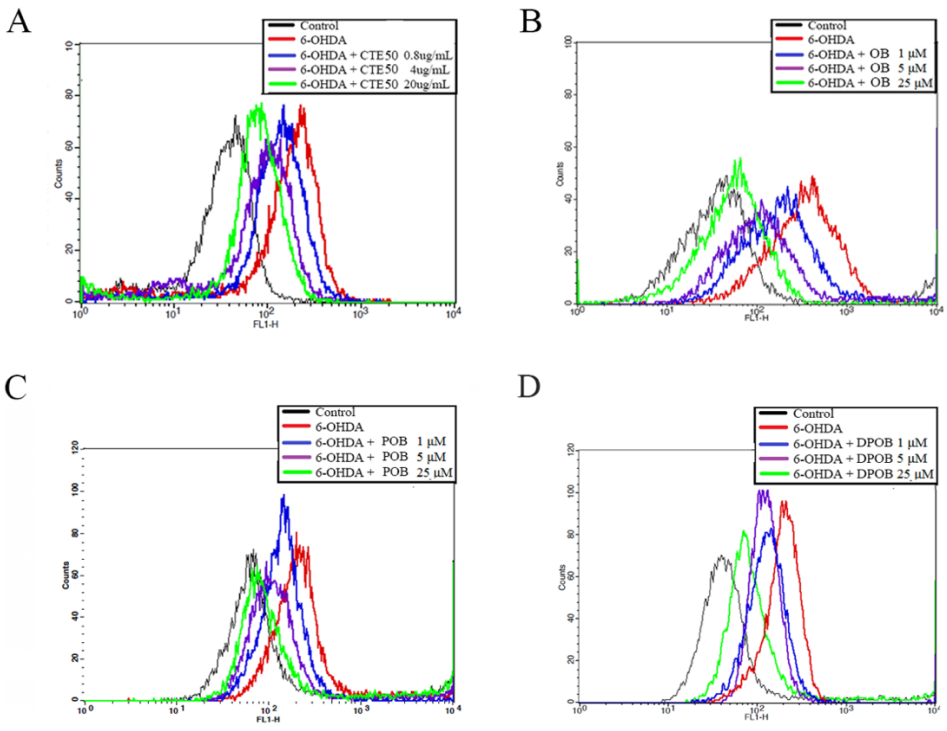

Figure 21. Inhibitory effects of CTE50 and three orobol derivatives (OB, POB, and DPOB) against 6-OHDA-induced ROS generation.

Cells were cultured in 12-well plate for 24h, and CTE50 or three orobol derivatives were simultaneously treated with 6-OHDA (75 μM) for 48 h (A – D). The cells were stained with DCFH-DA dyes for 30 min and determined by FACS analysis using FL-1 channel. The values of fluorescence intensity were obtained from histogram statistic of CellQuest software.

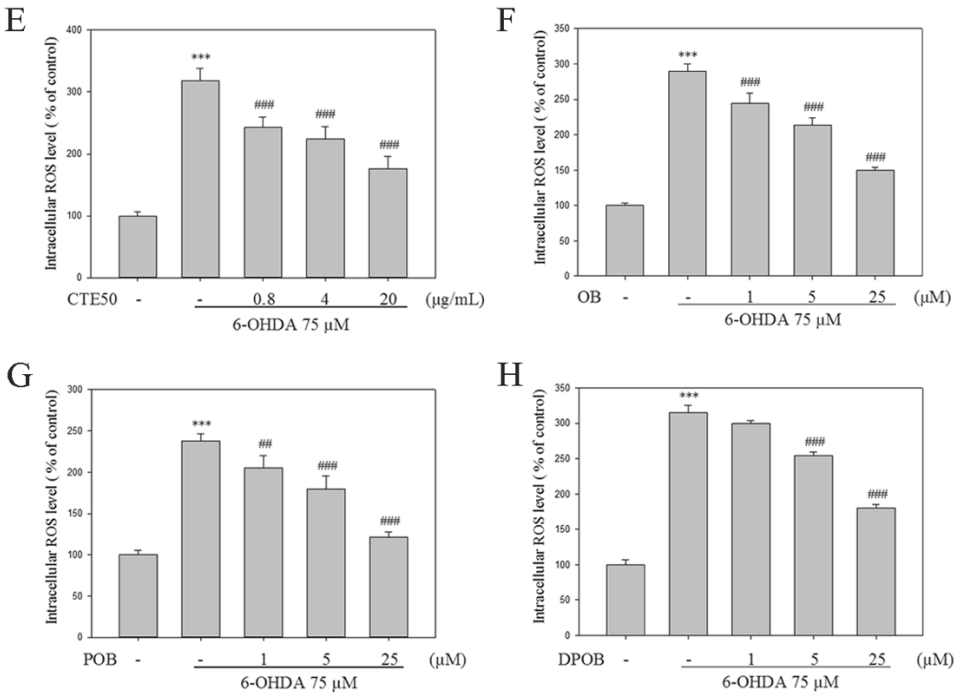

Figure 22. Inhibitory effects of CTE50 and three orobol derivatives (OB, POB, and DPOB) against 6-OHDA-induced ROS generation.

Cells were cultured in 96-well plate for 24h, and CTE50 or three orobol derivatives were simultaneously treated with 6-OHDA (75 μM) for 48 h (E – H). The cells were stained with DCFH-DA dyes for 30 min and fluorescence intensity was measured by multi-plate reader. Data represent the mean ± SD of three independent experiments. (***$p<0.001$ versus control group, $^{\#\#}p<0.01$ and $^{\#\#\#}p<0.001$ versus 6-OHDA-induced group)

3.3. Neuroprotective effects against 6-OHDA-induced apoptosis

It has been reported that 6-OHDA induces ROS-dependent apoptosis, which is characterized by the cleavage of caspase-9, caspase-3 and PARP**.** Excessive ROS accumulation results in the activation of the caspases (caspase-9 and caspase-3), and activated caspase-3 cleaves the DNA repair protein PARP**;** cleaved, activated PARP is final apoptotic marker. To investigate the inhibitory effects of CTE50 and three orobol derivatives on the levels of cleaved caspase-9, caspase-3, and PARP protein, we performed a western blot assay. As shown in Fig. 23, the cleavage levels of caspase-9, caspase-3, and PARP were increased when the SH-SY5Y cells were exposed to 6-OHDA. However, CTE50 (0.16 – 20 μg/mL) or the three orobol derivatives (0.2 – 25μM) inhibited the cleavage of caspase-9, caspase-3, and PARP protein in a concentration-dependent manner in 6-OHDA-induced SH-SY5Y cells.

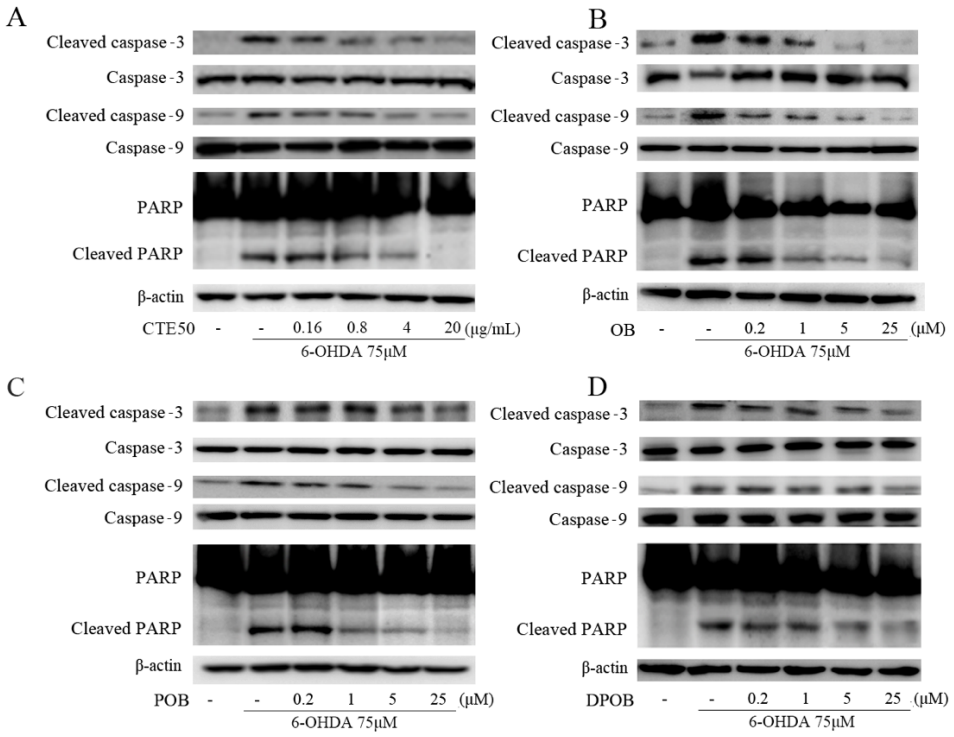

Figure 23. Inhibitory effects of CTE50 and three orobol derivatives against 6-OHDA-induced apoptotic markers.

Cells were simultaneously treated with 6-OHDA (75 μM) and (A) CTE50-or (B – D) three orobol derivatives for 48 h. The levels of cleaved caspase-9, caspase-3 and PARP were assessed by western blot; β-actin was used as a housekeeping protein. Representative data from three independent experiments are shown.

3.4. Protective effects against 6-OHDA-induced dysfunction of proteasome activity

Proteasome function is essential for cellular physiology and protein degradation. To evaluate the effects of CTE50 and the nine isolates against the dysfunction of proteasome activity induced by 6-OHDA in SH-SY5Y cells, we measured the activities of chymotrypsin-, trypsin- and caspase-like proteases. As shown in Table 3 and Fig. 24, 6-OHDA significantly inhibited all three different types of proteasome activities; however, CTE50 most potently attenuated the 6-OHDA-induced dysfunction of proteasome activities from extracts (0 – 100%) with an EC_{50} value of 1.2 μg/mL (chymotrypsin-like), 1.5 μg/mL (trypsin-like), and 6.7 μg/mL (caspase-like). The three orobol derivatives at the concentration of 25 μM prominently protected against 6-OHDA-induced dysfunction of the proteasome and almost restored the activities to normal levels. (Fig. 24B – 24D).

Table 3. The protective effects of ethanol extracts and isolates from the fruits of *C. tricuspidata* against 6-OHDA-induced proteasome dysfunction in SH-SY5Y cells

Extract / Compound	Protective effect against 6-OHDA-induced dysfunction of proteasome activities		
	Chymotrypsin-like (EC_{50} value)	Trypsin-like (EC_{50} value)	Caspase-like (EC_{50} value)
0% ethanol extract of *C.tricuspidata* fruit	>20 μg/mL	>20 μg/mL	>20 μg/mL
30% ethanol extract of *C.tricuspidata* fruit	5.4 ± 0.4 μg/mL	9.5 ± 0.6 μg/mL	18.5 ± 1.5 μg/mL
50% ethanol extract of *C.tricuspidata* fruit	1.2 ± 0.3 μg/mL	1.5 ± 0.4 μg/mL	6.7 ± 0.8 μg/mL
70% ethanol extract of *C.tricuspidata* fruit	7.8 ± 0.7 μg/mL	13.2 ± 1.2 μg/mL	>20 μg/mL
100% ethanol extract of *C.tricuspidata* fruit	>20 μg/mL	>20 μg/mL	>20 μg/mL
(1) orobol	7.4 ± 0.3 μM	3.7 ± 0.3 μM	2.9 ± 0.2 μM
(2) 6-prenylorobol	6.8 ± 0.7 μM	3.9 ± 0.4 μM	1.3 ± 0.2 μM
(3) 6,8-diprenylorobol	7.9 ± 0.4 μM	4.2 ± 0.4 μM	1.8 ± 0.1 μM
(4) millewanin H	22.1 ± 2.0 μM	24.4 ± 2.1 μM	6.8 ± 0.4 μM
(5) millewanin G	24.4 ± 1.5 μM	5.9 ± 0.3 μM	1.2 ± 0.3 μM
(6) alpinumisoflavone	>25 μM	>25 μM	>25 μM
(7) 4'-*O*-methylalpinumisoflavone	>25 μM	>25 μM	>25 μM
(8) erysenegalensein E	>25 μM	>25 μM	>25 μM
(9) 6,8-diprenylgenistein	>25 μM	>25 μM	>25 μM

The EC_{50} values were determined in a semi-logarithmic graph with 4 different concentrations.

The values are presented as the mean ± standard deviation of three independent experiments

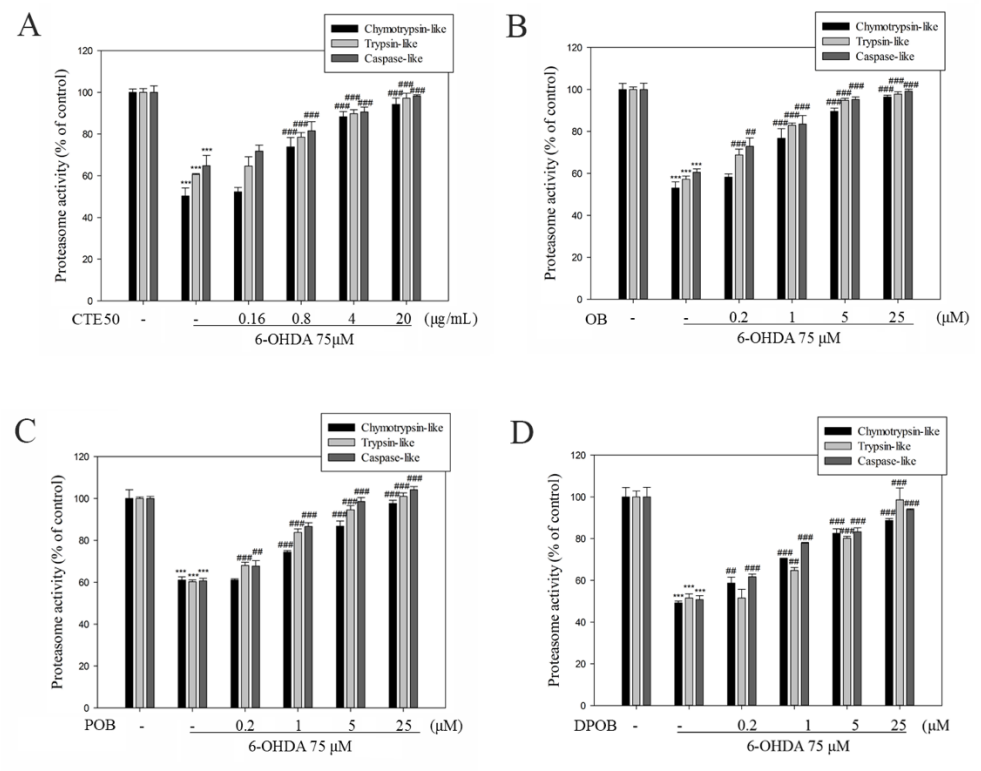

Figure 24. Protective effects of CTE50 and three orobol derivatives (OB, POB, and DPOB) against 6-OHDA-induced dysfunction of proteasome activities in SH-SY5Y cells.

Cells were cultured in 48-well plate for 24h, and (A) CTE50 or (B – D) three orobol derivatives were treated with 6-OHDA (75 μM) for 48 h. Chymotrypsin-, trypsin-, and caspase-like proteasome activities were measured by multiplate reader with fluorophore-linked peptide substrates. The relative fluorescence intensity was indicated. Data represent the mean ± SD

of three independent experiments. (***$p<0.001$ versus control group, $^{\#\#}p<0.01$ and $^{\#\#\#}p<0.001$ versus 6-OHDA-induced group)

3.5. Effects of CTE50 and three orobol derivatives on proteasome subunit mRNA expression

Proteasome function is essential for cellular physiology and protein degradation. Proteasome is composed of subunit and each subunit correlates chymotrypsin-like, trypsin-like, caspase-like proteasome activities. To evaluate the effects of CTE50 and three orobol derivatives on proteasome subunit mRNA expression, we measured the mRNA expression of chymotrypsin-, trypsin- and caspase-like proteases. As shown in Fig. 25, CTE50 significantly increase all three different types of proteasome subunit mRNA expressions; Also, three orobol derivatives increased three types of proteasome subunit mRNA expression at a concentration dependent manner. However, the increased mRNA expression of each proteasome subunits was not correlated the results about the protective effect of 6-OHDA-induced proteasome activities.

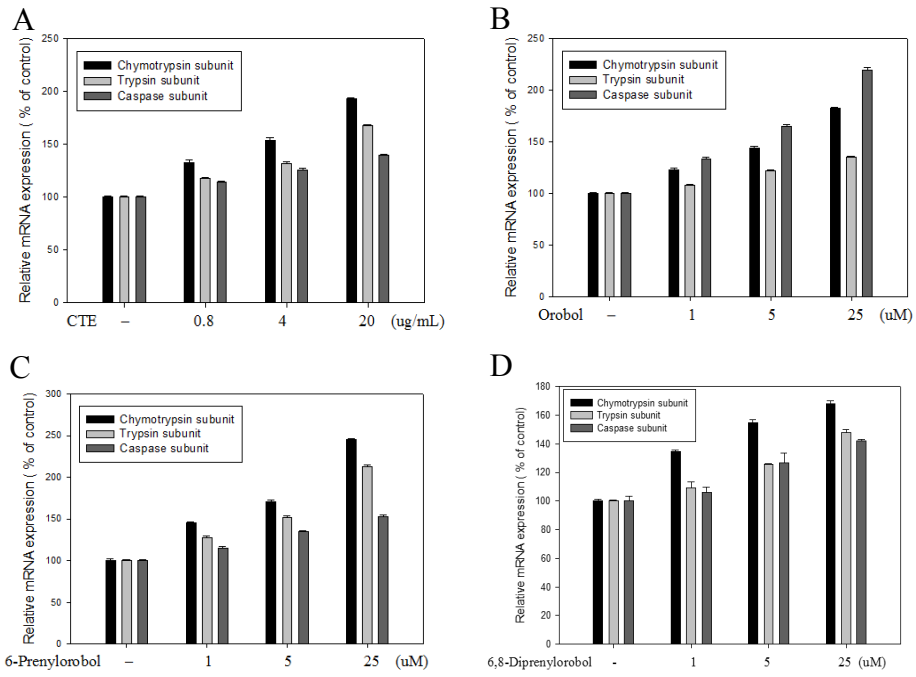

Figure 25. Effects of CTE50 and three orobol derivatives (OB, POB, and DPOB) on mRNA expression of proteasome subunits in SH-SY5Y cells.

Cells were cultured in 12-well plate for 24h, and (A) CTE50 or (B – D) three orobol derivatives were treated for 24 h. The mRNA expression of Chymotrypsin-, trypsin-, and caspase-like proteasome subunit were measured by qRT-PCR analysis. Data represent the mean ± SD of three independent experiments.

3.6. Inhibition of 6-OHDA-induced ubiquitin-conjugated proteins

Proteasome dysfunction causes a reduction in the degradation of misfolded proteins, consequently resulting in the accumulation of polyubiquitinated proteins. To investigate the inhibitory effects of CTE50 and the three orobol derivatives against 6-OHDA-induced ubiquitin conjugated-protein formation, we performed western blot analysis. As shown in Fig. 26, 6-OHDA increased the levels of high molecular ubiquitin-conjugated proteins. When cells were treated with different concentrations of CTE50 (0.16 – 20 μg/mL) (Fig. 26A) or the three orobol derivatives (0.2 – 25 μM) (Fig. 26B – 26D), the levels of ubiquitin-conjugated proteins were decreased to normal in a concentration-dependent manner. CTE50 (20 μg/mL) and the three orobol derivatives (25 μM) restored the ubiquitin-conjugated proteins to almost normal levels.

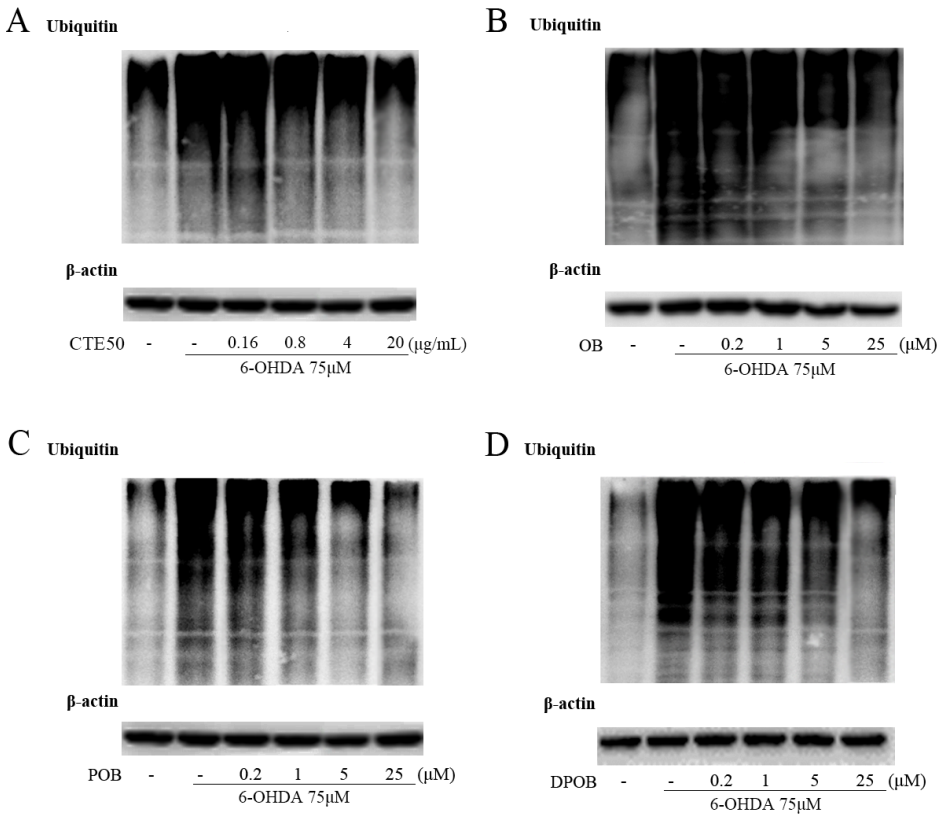

Figure 26. Inhibitory effects of CTE50 and three orobol derivatives against 6-OHDA-induced ubiquitin-conjugated proteins.

Cells were simultaneously treated with 6-OHDA (75 μM) and (A) CTE50 or (B – D) three orobol derivatives for 48 h. The levels of ubiquitin-conjugated proteins were determined by western blot; β-actin was used as a housekeeping protein. Representative data from three independent experiments are shown.

3.7. Inhibition of 6-OHDA-induced poly-ubiquitination of α-synuclein, and synphilin-1

Physiologically, polyubiquitinated proteins are normally rapidly degraded by the proteasome. However, dysfunction in proteasome activity increases the polyubiquitination of α-synuclein and synphilin-1, inducing neurotoxicity. As shown in Fig. 27, 6-OHDA increased the polyubiquitination of α-synuclein. When the cells were treated with different concentrations of CTE50 (0.8 – 20 μg/mL) or the three orobol derivatives (1 – 25 μM), the polyubiquitination of α-synuclein was restored to almost normal levels in a concentration-dependent manner (Fig. 27A – 27D). Additionally, as shown in Fig. 28, 6-OHDA increased the polyubiquitination of synphilin-1; however, CTE50 (0.8 – 20 μg/mL) and the three orobol derivatives (1 – 25 μM) reduced the polyubiquitinated synphilin-1 to almost normal levels in a concentration-dependent manner (Fig. 28E – 28H).

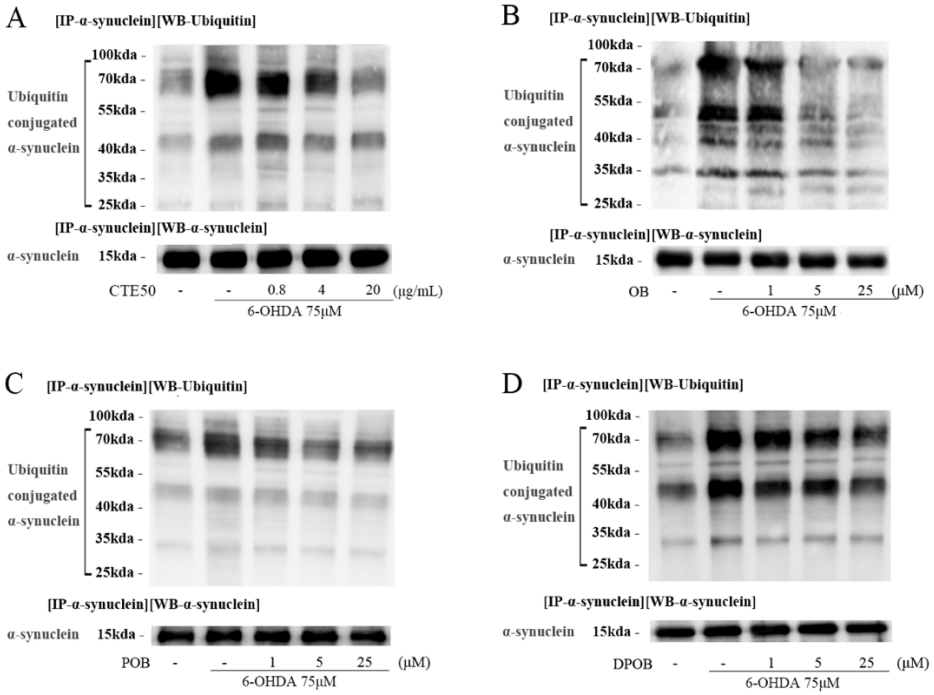

Figure 27. Inhibitory effects of CTE50 and three orobol derivatives against 6-OHDA-induced polyubiquitination of α-synuclein.

Cells were simultaneously treated with 6-OHDA (75 μM) and (A) CTE50 or (B – D) three orobol derivatives for 48 h. The polyubiquitination of α-synuclein was determined by immunoprecipitation and western blot analysis. Representative data from three independent experiments are shown.

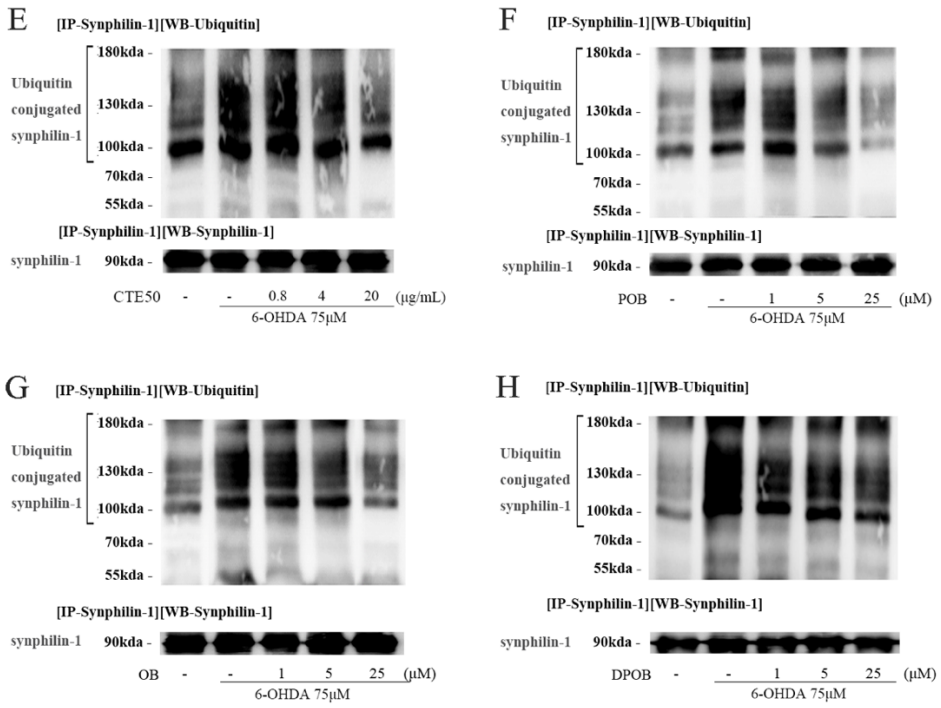

Figure 28. Inhibitory effects of CTE50 and three orobol derivatives against 6-OHDA-induced polyubiquitination of synphilin-1.

Cells were simultaneously treated with 6-OHDA (75 μM) and (E) CTE50 or (F – H) three orobol derivatives for 48 h. The polyubiquitination of synphilin-1 was determined by immunoprecipitation and western blot analysis. Representative data from three independent experiments are shown.

3.8. A proteasome inhibitor (MG-132) diminished the protective effects of CTE50 and the three orobol derivatives against 6-OHDA-induced neuronal cell death and proteasome dysfunction

It has been reported that proteasome inhibition induces dopaminergic neuronal cell degeneration and apoptosis (Park et al., 2011). In contrast, proteasome activation enhances survival in a neuronal model of neurodegenerative disease (Seo et al., 2007). To investigate whether the neuroprotective effects of CTE50 and the three orobol derivatives are due to the amelioration of proteasomal dysfunction, MG132, a proteasome inhibitor, was co-applied with the samples. As shown in Fig. 29, CTE50 (20 μg/mL) and three orobol derivatives (25 μM) protected against 6-OHDA-induced neuronal cell death; however, co-treatment with MG132 (1 μM, non-cytotoxic concentration) significantly blocked the protective effects of CTE50 and the three orobol derivatives against 6-OHDA-induced cell death. Additionally, MG132 (1 μM) blocked the recovery effects of CTE50 and the three orobol derivatives against 6-OHDA-induced proteasome dysfunction (Fig. 30).

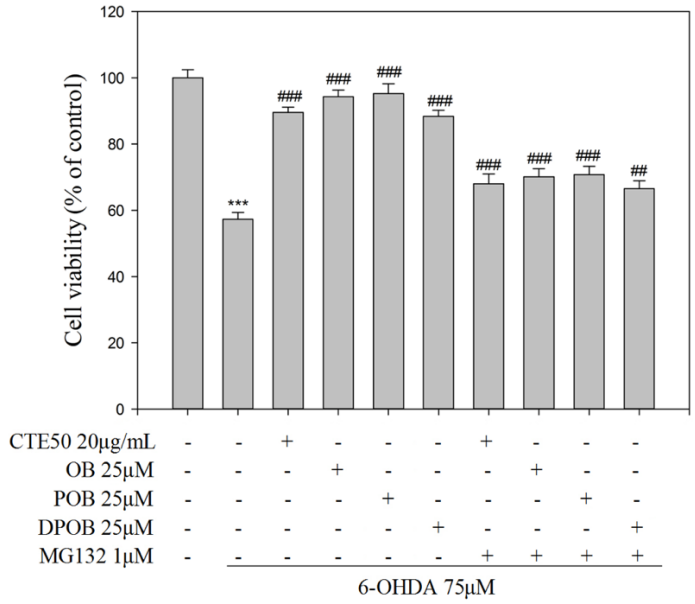

Figure 29. Inhibitory effects of MG132 on the protective effects of CTE50 and three orobol derivatives against 6-OHDA-induced neuronal cell death.

The protective effects of CTE50 and three orobol derivatives 6-OHDA-induced neuronal cell death were blocked by MG132. Cell viability was measured by the MTT reduction assay. (Data represent the mean ± SD of three independent experiments. (***$p<0.001$ versus control group, $^{\#}p<0.05$, $^{\#\#}p<0.01$, and $^{\#\#\#}p<0.001$ versus 6-OHDA-induced group)

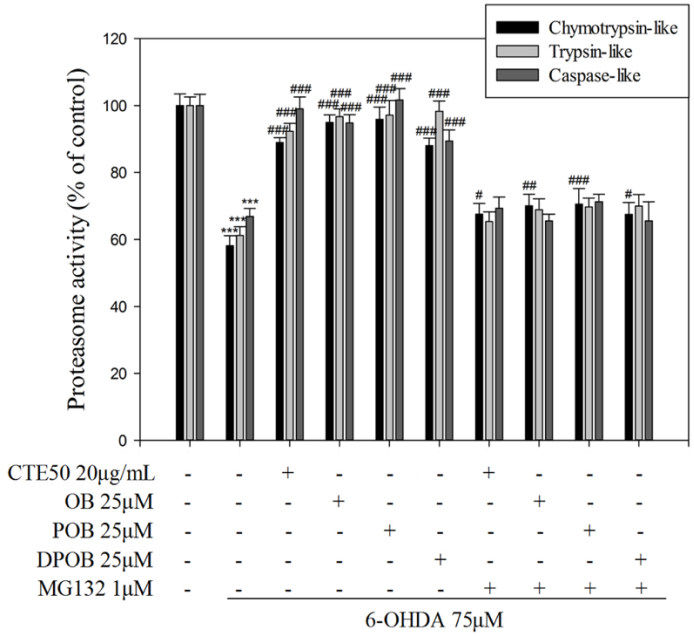

Figure 30. Inhibitory effects of MG132 on the protective effects of CTE50 and three orobol derivatives against 6-OHDA-induced proteasome dysfunction.

The protective effects of CTE50 and three orobol derivatives against 6-OHDA-induced proteasome dysfunction were blocked by MG132. Three types of proteasome activity were measured using a multi-plate reader with fluorophore-linked peptide substrates. Data represent the mean ± SD of three independent experiments. (***$p<0.001$ versus control group, $^{\#}p<0.05$, $^{\#\#}p<0.01$, and $^{\#\#\#}p<0.001$ versus 6-OHDA-induced group)

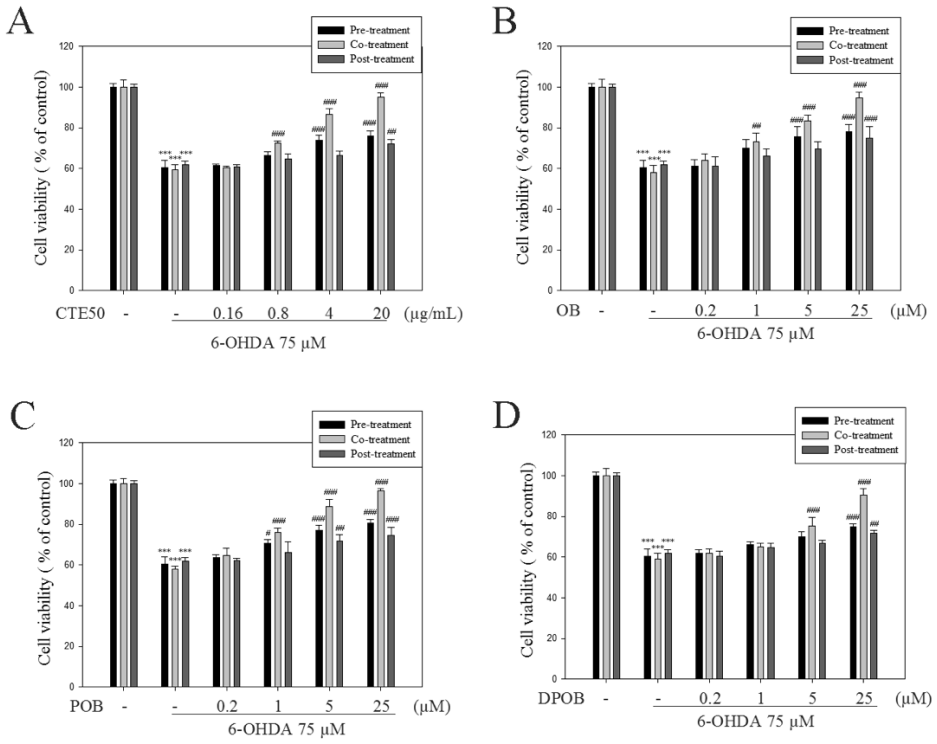

Figure 31. Comparison of neuroprotective effect of CTE50 and three orobol derivatives (OB, POB, and DPOB) against 6-OHDA-induced neurotoxicity by pre-, co-, and post treatment.

In pre-treatment group, cells were cultured in 96-well plate for 24 h, and CTE50 or orobol derivatives pre-treated for 48h. After 48h, medium was changed and cells were treated with 6-OHDA (75 μM) for 48 h. In co-treatment group, cells were cultured, and CTE50 or orobol derivatives were simultaneously treated with 6-OHDA for 48 h. In post-treatment group, cells were cultured, and treated with 6-OHDA for 48 h. After 48h, medium was

changed and cells were treated CTE50 or orobol derivatives for 48 h. Cell viability were measured by MTT reduction assay. Data represent the mean ± SD of three independent experiments. (***$p<0.001$ versus control group, $^{\#}p<0.05$, $^{\#\#}p<0.01$, and $^{\#\#\#}p<0.001$ versus 6-OHDA-induced group)

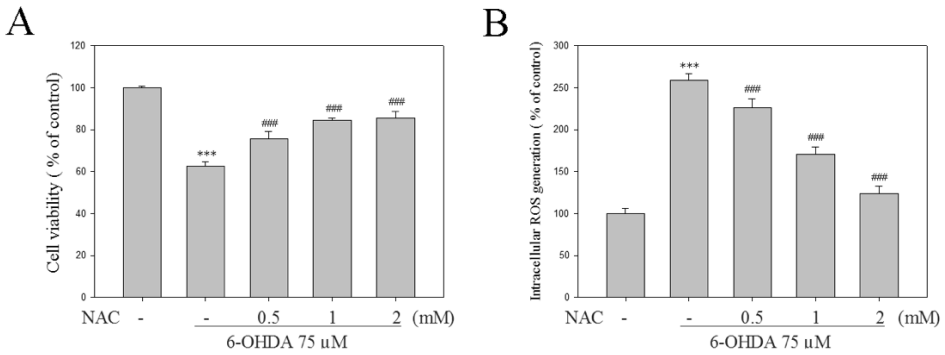

Figure 32. The effects of N-acetylcystein (NAC) against 6-OHDA-induced neurotoxicity and ROS generation.

Cells were cultured in 96-well plate for 24 h, and NAC was simultaneously treated with 6-OHDA (75 μM) for 48 h. Cell viability were measured by MTT reduction assay (A). Cells were cultured in 12-well plate for 24h, and NAC were simultaneously treated with 6-OHDA (75 μM) for 48 h. The relative fluorescence intensities of total 10,000 events by FACs analysis with DCFH-DA dye were quantified (B). Data represent the mean ± SD of three independent experiments. (***$p<0.001$ versus control group, $^{###}p<0.001$ versus 6-OHDA-induced group)

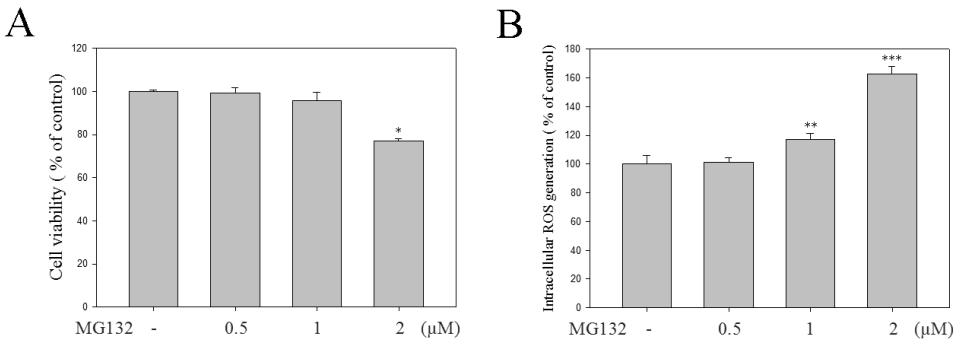

Figure 33. The effect of MG132 on neurotoxicity and ROS generation.

Cells were cultured in 96-well plate for 24 h, and MG132 was for 48 h. Cell viability were measured by MTT reduction assay (A). Cells were cultured in 12-well plate for 24h, and MG132 were for 48 h. The relative fluorescence intensities of total 10,000 events by FACS analysis with DCFH-DA dye were quantified (B). Data represent the mean ± SD of three independent experiments. (*$p<0.05$, **$p<0.01$, ***$p<0.001$ versus control group)

4. Discussion

As the world's population is rapidly ageing, the number of patients suffering from PD is increasing significantly. Although the cause of PD has not been definitively verified, recent research findings have suggested that oxidative stress and the impairment of the proteasome are major events in its pathogenesis (Ciechanover and Kwon, 2015). Oxidative stress has been implicated in ageing and neurodegenerative diseases such as PD. Oxidative stress induces the oxidation and aggregation of proteins in the brain (Butterfield and Kanski, 2001). In addition, excessive oxidative stress advances cellular apoptosis through the accumulation of oxidized proteins (Klovekorn and Munch, 1998). Many studies have reported that protein homeostasis is essential for cellular physiology and that the proteasome is responsible for selectively degrading targets including short-lived, damaged or misfolded protein, which comprise approximately 80% of all intracellular proteins. Hence, considerable interest has been paid to the importance of the role of the proteasome. The ubiquitination process is activated by ubiquitin-activating enzymes (E1), ubiquitin-conjugating enzymes (E2), and ubiquitin-transferring enzymes (E3). Through a sequential enzymatic reaction, proteins

are polyubiquitinated by E3 ligase. The polyubiquitin chain is recognized by the regulatory domain of the proteasome, in which the target protein is degraded by the catalytic core domain (Amm et al., 2014). Under normal conditions, polyubiquitinated proteins are rapidly degraded and do not accumulate. The accumulation of polyubiquitinated proteins is observed when excessive intracellular ROS, cellular stress, and diverse stress impair proteasome function (Elkon et al., 2004), and the accumulation of polyubiquitinated proteins induces neurotoxicity and neurodegeneration. Thus, the restoration of proteasome activity through the down-regulation of intracellular ROS is one of the primary mechanisms regulating ubiquitin-conjugated proteins, Lewy body-associated α-synuclein, and synphilin-1 proteins and the protection against neuronal cell death.

In the present study, 6-OHDA-induced ROS generation decreased in a concentration-dependent manner when cells were treated with different concentrations of CTE50 or the three orobol derivatives, and these compounds significantly elicited their neuroprotective effects against 6-OHDA-induced cell death and inhibited 6-OHDA-induced changes in cell morphology including shrinkage and rounding. In addition, we evaluated the inhibitory effects of CTE50 and the three orobol derivatives on the levels of cleaved caspase-9, caspase-3 and PARP, which are apoptosis signal factors; 6-OHDA

treatment increased the levels of cleaved caspase-9, caspase-3 and PARP protein; however, these increases were inhibited by co-treatment with CTE50 and the three orobol derivatives. A previous study demonstrated that the inhibitory effect of (-)-epigallocatechin-3-gallate (EGCG) on ROS generation led to a suppression of apoptosis (Ning et al., 2016). In our results, the inhibitory effects of CTE50 and three orobol derivatives on ROS generation are also concomitant with the protection against neuronal cell death and the activation of apoptosis signalling markers. Based on the neuroprotective effects of three orobol derivatives, we evaluated structure-bioactivity relationship (SAR). The compounds with two hydroxy groups at C-3′ and C-4′ in B-ring of flavonoid (**1** – **5**) exhibited neuroprotective effects, whereas the others with one hydroxy group at C-4' (**6** – **9**) did not. This suggested that the hydroxy group in the B-ring of flavonoid influences neuroprotective effects. The neuroprotective effect of prenyl-groups is not clear from 9 isolates to evaluate SAR. Therefore, further study will be necessary to evaluate SAR with prenylated flavonoids on neuroprotective activity.

A recent study emphasized the role of the proteasome in neurodegenerative disease and showed that proteasome inhibition induced neurotoxicity via the accumulation of polyubiquitinated proteins and protein aggregation (Canu et al., 2000). As neuronal cells are vulnerable to the accumulation of

polyubiquitinated proteins, several neurodegenerative diseases are related to the neurotoxicity resulting from protein accumulation. It has been shown that proteasome activity can gradually decrease with ageing and environmental stress, among other reasons, which results in a reduced ability to degrade misfolded proteins, contributing to the development of pathological protein aggregates (Ciechanover and Kwon, 2015). In cellular models, proteasome inhibition induced apoptosis and neuronal cell degeneration (Park et al., 2011; Sun et al., 2006), whereas proteasome activation enhanced neuronal cell survival (Seo et al., 2007). Thus, the protection against proteasome dysfunction could be a possible therapeutic strategy for neuroprotection. To investigate the mechanism underlying the protective effects of CTE50 and the three orobol derivatives against 6-OHDA-induced neuronal cell death, chymotrypsin-, trypsin-, and caspase-like proteasome activities were measured in SH-SY5Y cells. Our results showed that 6-OHDA significantly inhibited all three types of proteasome activities due to excessive ROS generation, and these results correlate with previously reported studies (Elkon et al., 2004). CTE50 and the three orobol derivatives at concentration of 20 μg/mL and 25 μM, respectively, attenuated 6-OHDA-induced dysfunction of the proteasome and nearly restored proteasome activities to normal levels. Additionally, we measured the levels of ubiquitin-conjugated proteins and

found an increase following 6-OHDA treatment. However, CTE50 (20 μg/mL) and the three orobol derivatives (25 μM) attenuated the 6-OHDA-induced increase in ubiquitin-conjugated protein levels to almost normal. These results suggested that 6-OHDA-induced proteasome dysfunction triggers the accumulation of ubiquitin-conjugated proteins, leading to neuronal cell death; however, CTE50 and the three orobol derivatives prevented the dysfunction of ubiquitin proteasome system (UPS) and protected against neuronal cell death. The impairment of UPS is involved in the formation of Lewy bodies, which is a characteristic hallmark of PD. Lewy bodies are composed of abnormal filamentous aggregates containing α-synuclein, and synphilin-1 has been found to colocalize with α-synuclein in Lewy bodies. It has been demonstrated that the overexpression of α-synuclein in *Drosophila* and *C. elegans* induced neuronal cell loss (Kontopoulos et al., 2006; Pesah et al., 2005). It has also been reported that α-synuclein filaments and oligomers themselves inhibited proteasome activities (Lindersson et al., 2004). Synphilin-1 has been reported to enhance the aggregation and neurotoxicity of α-synuclein (Buttner et al., 2010) and to promote inclusion formation under conditions of proteasome inhibition. Additionally, it has been reported that synphilin-1 inhibits the degradation of α-synuclein by the proteasome and thus increases the half-life of α-synuclein (Alvarez-Castelao and Castano, 2011).

Therefore, it has been suggested that the regulation of α-synuclein and synphilin-1 through UPS is important for neuroprotection (Sidhu et al., 2004). It was also previously reported that a relationship exists between proteasome dysfunction and neuronal cell death. Proteasome inhibition triggers a dramatic activation of the pro-apoptotic caspase-3,-9, PARP and DNA fragment (Sun et al., 2006; Yuan et al., 2008). The proteasome inhibitor MG132 induces dopaminergic neuronal cell degeneration and apoptosis (Park et al., 2011), and bortezomib, a proteasome inhibitor, induces caspase-dependent apoptosis. In contrast, a proteasome activator enhances the survival of neuronal cells (Seo et al., 2007), and betulinic acid and demethylsuberosin, reported to be proteasome activators, showed neuroprotective effects (Eksioglu-Demiralp et al., 2010; Kim, B-H et al., 2015). In our results, 6-OHDA-induced proteasome dysfunction resulted in the polyubiquitination of α-synuclein and synphilin-1 protein. However, CTE50 and the three orobol derivatives reduced the levels of 6-OHDA-induced polyubiquitination of α-synuclein and synphilin-1 protein in addition to ameliorating the dysfunction of proteasome activities. Furthermore, treatment with MG132, a proteasome inhibitor, significantly reduced the protective effects of CTE50 and the three orobol derivatives against 6-OHDA-induced neuronal cell death and proteasome dysfunction, suggesting that their neuronal cell protective effects are partly due to the

protection against proteasome dysfunction. In spite of the evidence for neuroprotection by orobol derivatives, there has been little research reported on the blood-brain barrier (BBB) permeability of orobol derivatives. However, some studies have demonstrated that isoflavones and several metabolites have been proven to transverse the BBB (Chandrasekharan and Aglin, 2013; Youdim et al., 2003). Therefore, BBB permeability of orobol and its derivatives should be studied to elucidate its potential for permeation across BBB in the further study.

5. Conclusion

In conclusion, this study demonstrated that CTE50 and three orobol derivatives protected against neuronal cell death and ROS generation, and attenuated proteasome dysfunction, the accumulation of ubiquitin-conjugated proteins, and the levels of polyubiquitinated α-synuclein and synphilin-1, the constituents of Lewy bodies. However, the neuroprotective effects of CTE50 and three orobol derivatives and the attenuation of proteasome dysfunction were significantly inhibited by MG132, suggesting their neuroprotective effects are partly due to the protection of the ubiquitin/proteasome-dependent degradation of α-synuclein and synphilin-1. Based on the results, it was suggested that CTE50 and the three orobol derivatives might be promising candidates for the therapy of neurodegenerative diseases such as PD.

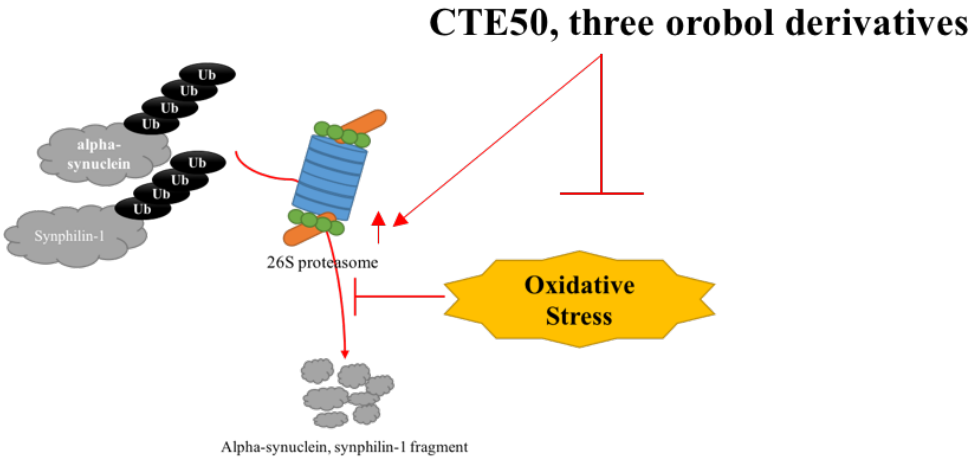

Figure 34. A scheme of protective effects of CTE50 and three orobol derivatives on 6-OHDA-induced neuronal cell death via enhancing proteasome activity and the ubiquitin/proteasome-dependent degradation of α-synuclein and synphilin-1.

CTE50 and three orobol derivatives protected against neuronal cell death, ROS generation, and accumulation of ubiquitin-conjugated proteins, polyubiquitinated α-synuclein and synphilin-1 via protecting proteasome dysfunction.

Chapter 3

Protective effects of TH3-125-4 (TH20) from the root barks of *Cudrania tricuspidata* on CCCP-induced neuronal cell death via the inhibition of USP30 deubiquitinating enzyme in Parkin knock down SH-SY5Y cells

1. Introduction

Mitophagy, a specialized autophagy pathway that mediates the clearance of damaged mitochondria by lysosomes, is important for mitochondrial quality control. Defective mitochondria, if left uncleared, can be a source of oxidative stress and compromise the health of the entire mitochondrial network. Parkinson's disease is characterized prominently, but not solely, by loss of dopaminergic neurons in the substantia nigra. Although the pathogenic mechanisms of Parkinson's disease are unclear, several lines of evidence propose that mitochondrial dysfunction is central to the disease. Most compellingly, familial Parkinson's disease can be caused by mutations in the ubiquitin ligase parkin and protein kinase PINK1 (Valente et al., 2004), both of which maintain healthy mitochondria via regulating mitochondrial dynamics and quality control (Narendra and Youle, 2011). Genetic studies established that PINK1 acts upstream of parkin (Park, J et al., 2006a). PINK1 recruits parkin from the cytoplasm to the surface of damaged mitochondria, leading to parkin-mediated ubiquitination of mitochondrial outer membrane proteins and deletion of damaged mitochondria by mitophagy (Narendra et al., 2010; Chan et al., 2011). Parkinson's disease-associated mutations in PINK1

or parkin impair parkin recruitment, mitochondrial ubiquitination, and/or mitophagy (Matsuda et al., 2010; Vives-Bauza et al., 2010). In the context of the inherently high mitochondrial oxidative stress in substantia nigra dopamine neurons, loss of parkin-mediated mitophagy could explain the greater susceptibility of substantia nigra neurons to neurodegeneration. Thus, promoting mitophagy and enhancing mitochondrial quality control could benefit dopaminergic neurons. Recent studies reported that deubiquitinating enzyme antagonizes the role of parkin e3 ligase. In culture of dopaminergic cells overexpressing parkin, Ubiquitin-specific protease (USP) 15, 30 blocks ubiquitination of mitochondrial proteins by parkin and inhibits lysosomal delivery of mitochondria and mitophagy (Nakamura and Hirose, 2008) . USP 30 can counteract parkin-mediated ubiquitination and degradation of mitochondrial Rho GTPase 1 (MIRO1) and translocase of outer mitochondrial membrane 20 (TOM20), two mitochondrial proteins, after mitochondrial damage. Also, USP30 can inhibit parkin-mediated ubiquitination of mitofusin 1, 2 (Mfn1,2), mitochondria fusion proteins. In cells transfected with green-fluorescent-protein-parkin (GFP-parkin) and expressing pathogenic parkin mutations, the mitophagy process is deficient. In this model, a knockdown of USP30 protein restores mitophagy, allowing cells to overcome parkin deficiency. Finally, using PINK1 or parkin mutant Drosophilia, the authors

demonstrated that USP30 suppression maintained mitochondrial health, improved climbing capability, and prevented dopamine depletion (Park, J et al., 2006b). Finally, in flies treated by paraquat, a mitochondrial toxin inducing parkinsonism, knockdown of USP30 rescued climbing ability, improved flies' survival, and prevented dopamine depletion (Tanner et al., 2011). All of these experiments show that USP30 plays a major role in dopaminergic cell dysfunction by altering mitophagy and that inhibiting this protein could represent a promising strategy for PD treatment. In this study, we evaluated the inhibitory effects of the isolated compounds from *C. tricuspidata* on USP15, 30. Also, the study investigated the potential effects on neuroprotection, parkin mediated mitophagy, mitochondrial membrane potential against CCCP-induced SH-SY5Y cells and parkin knock down SH-SY5Y cells.

2. Material and methods

2.1. Chemicals and reagents

Carbonyl cyanide 3-chlorophenylhydrazone (CCCP), JC-1, MG132, CCK-8, mitotracker, and PR-619 were purchased from Sigma-Aldrich (St. Louis, MO, USA). Dulbecco's modified Eagle's medium (DMEM) and fetal bovine serum (FBS) were purchased from Gibco BRL (Rockville, MD, USA). Hybond-polyvinylidene difluoride (PVDF) membranes were purchased from Amersham Pharmacia Biotechnology Inc. (Piscataway, NJ, USA). PRO-PREP protein extraction solution and WEST-Queen® ECL solution were purchased from iNtRON Biotech Inc. (Kyunggi, Korea). USP15, USP30, tetra ubiquitin peptides were purchased from Bio-Vision, Inc. (Milpitas, CA, USA) Parkin siRNA, scrambled siRNA, Mfn1, Mfn2, ubiquitin, USP15, USP30, OPA1, VDAC, alpha-tubulin, parkin, LC3-II first antibody, secondary antibody and FITC-conjugated secondary antibody were purchased from Santa Cruz Biotechnology, Inc. (Santa Cruz, CA, USA)

2.2. Preparation of TH3-125-4 (TH20)

Cudrania tricuspidata was stored at the Korea Forest Research Institute at Southern Forest Research Center (Jinju, Korea) in September 2008. A voucher specimen (accession number KH1-4-090814) was kept at the Department of Biosystems and Biotechnology at Korea University (Seoul, Korea). TH3-125-4 (TH20) was isolated from the roots of *Cudrania tricuspidata* and the structure of TH3-125-4 (TH20) was determined by spectroscopic methods, and the purity was more than 98% (Wei and Yu, 2008). TH3-125-4 (TH20) was dissolved in DMSO and diluted with PBS to obtain the proper concentration. Final concentration of DMSO was less than 0.1% and it didn't influence the performed assays.

2.3. Cell cultures

The human neuroblastoma cell line SH-SY5Y (ATCC No. CRL-2266) was purchased from the American Type Culture Collection (Manassas, VA, USA) and cultured in DMEM supplemented with 10 % heat-inactivated FBS and 1 % penicillin/streptomycin at 37 ºC in a humidified 5 % CO_2 atmosphere.

2.4. Measurement of cell viability

SH-SY5Y cells were seeded at a density of 1×10^5 cells/200 μL/well in 96-well plates for 24 h, and the cells were pre-treated with isolated compounds from *C. tricuspidata* for 24 h followed by subsequent treatment with CCCP (10 μM) for an additional 24 h. To evaluate the effect of parkin, cells were transfected with scrambled siRNA or parkin siRNA for 48 h and its final concentration was 100 nM. After transfected cells were treated with isolated compounds and CCCP (10 μM), cell viability was determined using a CCK-8 and measured by ELISA (Koo et al., 2011).

2.5. Measurement of mitochondrial membrane potential by JC-1 staining

SH-SY5Y cells were seeded at a density of 2×10^5 cells/2 mL/well in 6-well plates for 24 h, and the cells were pre-treated with isolated compounds for 24 h followed by subsequent treatment with CCCP (10 μM) for an additional 8 h. Mitochondrial membrane potential was determined using a JC-1 dyes. Briefly, the cells were washed with PBS, and then incubated with 10 μg/mL of JC-1 for 30 min at 37 ºC in the dark. The cells were then washed with PBS. The fluorescence intensities were measured by flow cytometry (BD FACSCalibur ™).

2.6. Measurement of intracellular ROS by Flow cytometry

ROS levels in cells were measured with the 2',7'-dichlorofluorescein diacetate (DCFH-DA) method (Munch et al., 1998a). Briefly, the cells were washed with PBS, and then incubated with 4 μM of DCFH-DA for 30 min at 37 ºC in the dark. The cells were then washed with PBS. The fluorescence intensities were measured by flow cytometry (BD FACSCalibur ^{TM}).

2.7. Mitochondrial and cytosolic fraction preparations

The mitochondrial and cytosolic proteins were extracted with a commercial kit (Mitochondria/Cytosol Fractionation Kit) according to the manufacturer's procedure (Bio-Vision, Milpitas, CA,). Briefly, the cells were incubated in cytosolic fraction buffer on ice for 15 min and homogenize cells in an ice-cold dounce tissue grinder. After homogenize, centrifuged for 10 min at 700 x g in a microcentrifuge at 4 ºC. Transfer the supernatant to a fresh 1.5-ml tube, and centrifuge at 10,000 x g in a microcentrifuge for 30 min at 4 ºC. Collect supernatant as a cytosolic fraction and mitochondrial pellet were washed with cold PBS, extracted completely with mitochondrial fraction buffer.

2.8. Parkin knock down via the transfection of small interfering RNA (siRNA)

The transfection with scrambled siRNA or parkin siRNA were progressed at final concentrations of 100 nM for 48 h by Lipofectamine 2000 (Invitrogen, Carlsbad, CA) prior to treatment with isolated compounds and CCCP (10 μM) as recommended by the manufacturer's guidelines.

2.9. Measurement of protein expression

The cells were collected, washed with PBS and lysed with a PRO-PREP protein extraction solution at -20 ºC for 20 min. After centrifugation at 13,000 x g for 30 min, the supernatant was used as the total protein extracts. Western blot analysis was accomplished as previously described method (Ham et al., 2013).

2.10. Immunoprecipitation assay

Immunoprecipitation was performed as previously described with slight modifications (Chen et al., 2014). After treatment, cells were washed three times with PBS and homogenized and lysed in cold-lysis buffer (50 mM Tris, 1 mM PMSF, 150 mM NaCl, 50 mM NaF, 1% Nonidet P-40, 0.25% sodium deoxycholate, 10 mM sodium pyrophosphate) and centrifuged at 14,000 × g (10 min, 4 °C), and the supernatant was transferred to a new ep-tube and incubated with 2 μg of Mfn1 or Mfn2 antibody overnight at 4 °C. The next

day, A/G plus agarose beads were added and incubated overnight at 4 °C followed by 3 washes in cold-lysis buffer. The loading samples were adjusted to total volume of 30 μL with lysis buffer, and the immune-complexes were eluted at 95 °C on a heating block for 5 min, vortexed, and spun down by centrifugation at 15,000 × g for 10 min.

2.11. Measurement of mitophagy by fluorescence microscope

The culture dish was coated with 0.2 % gelatin at 37 °C for 30 min and dried at RT on a clean bench. The SH-SY5Y cells were plated at a density of 5×10^4 cells/200 μL/well in coated dishes for 24 h and CCCP for 8 h. After treatment, the cells were washed with 1x PBS/Tween-20 buffer (pH 7.4) (PBST) once. The cells were fixed with 4 % paraformaldehyde for 30 min at room temperature (RT). After washing with PBST, the blocking steps were performed with 1 % BSA in PBST. Next, the cells were incubated with the primary antibody at 4 °C overnight. The next day, the cells were washed with PBST 3 times and incubated with FITC-conjugated secondary antibody for 1 h at RT. After 1 h, the cells were washed with PBST 3 times, and DAPI staining was performed for 5 min at RT. Lastly, the PBST washing and mounting steps were conducted.

2.12. Measurement of deubiquitinating enzyme activity

DUB assay buffer is composed of 20 mM HEPES at pH7.2, 100 mM NaCl, 0.05 % Tween 20, 0.1 mg/mL BSA, 1 mM DTT. Purified DUBs at optimal concentrations (USP 15, 50 nmol/L; USP30, 50 nmol/L) were incubated in DUB buffer containing isolated compounds (indicated concentration), vehicle alone (DMSO), or PR-619, (positive control for DUB inhibition) in a 100 μL reaction volume for 30 to 60 minutes at 37 °C. The reaction was initiated by the addition of 500 nmol/L Ub-AMC, and the release of AMC fluorescence was recorded at excitation/emission of 380/480 using a fluorometer.

2.13. Measurement of ubiquitin chain disassembly

In vitro disassembly of purified polyubiquitin chains (K48/K63 linked) was performed as described earlier (Dayal et al., 2009). USP30 (50 ng) prepared in DUB buffer was incubated with K48- or K63-linked chains (1 μg) and isolated compound for 15 min at 37 °C. The extent of chain disassembly was assessed by Western blotting.

2.14. Statistical analysis

All experimental data are expressed as mean value ± standard deviation. Statistical significance between multiple groups was determined by one-way

ANOVA (PRISM Graph Pad, San Diego, CA, USA). When ANOVA had a significant difference, *post hoc* Bonferroni's multiple comparison tests was conducted. *P* value less than 0.05 was regarded to be statistically significant.

3. Results

3.1. Inhibitory effect of TH3-125-4 (TH20) on deubiquitinating enzymes, USP15, USP30.

The isolated compounds from *C. tricuspidata* were evaluated to determine its inhibitory effects on deubiquitinating enzyme (DUB) activity. As shown in Table. 4, twelve isolated compounds inhibited USP15, USP30 activity. Among twelve isolated compounds, TH3-125-4 (TH20) showed potent inhibitory effects on USP30 with an IC_{50} values of 38.1 μM. TH20 inhibited USP30 enzyme activity concentration-dependently manner (Fig. 36). However, TH20 did not show inhibitory effect on USP15, total DUB enzyme activity. PR-619, a non-selective DUB inhibitor, significantly inhibited USP15, USP30, and total DUB enzyme activities, respectively (Fig. 37). The result of PR-619 was correlated with previous reports.

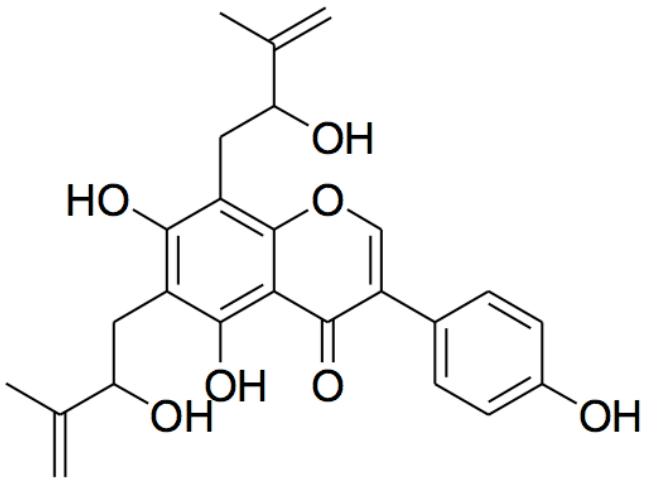

Figure 35. Chemical structures of TH3-125-4 (TH20)

Table 4. Inhibitory effect of isolated compounds from *C.tricuspidata* on deubiquitinating enzymes (USP15, USP30, Total DUB enzymes)

No.	Sample	USP15 inhibitory effect IC_{50} (μM)	USP30 inhibitory effect IC_{50} (μM)	Total DUB inhibitory effect IC_{50} (μM)
1	**TH3-125-4 (TH20)**	**>160**	**38.1**	**>160**
2	TH4-165-3K(TH49)	69.9	>160	>160
3	TH4-165-7 (TH50)	>160	60.5	>160
4	TH4-199-1K1 (TH59)	>160	82.3	>160
5	TH4-199-1K2 (TH60)	57.6	>160	>160
6	TH4-199-2K1 (TH61)	50.8	>160	>160
7	TH4-199-2K2 (TH62)	>160	83.7	>160

Table 4. Continued

No.	Sample	USP15 inhibitory effect IC_{50} (μM)	USP30 inhibitory effect IC_{50} (μM)	Total DUB inhibitory effect IC_{50} (μM)
8	TH5-17-5 (TH72)	>160	78.8	>160
9	JY1-154-2 (JY23)	150.7	>160	>160
10	JY1-164-4 (JY26)	132.2	>160	>160
11	JY1-190-1 (JY51)	130.8	>160	>160
12	JY1-191-3 (JY53)	155.2	>160	>160
…	…	…	…	…
129	JY1-134-5	>160	>160	>160
130	**PR619**	**4**	**6.7**	**8.5**

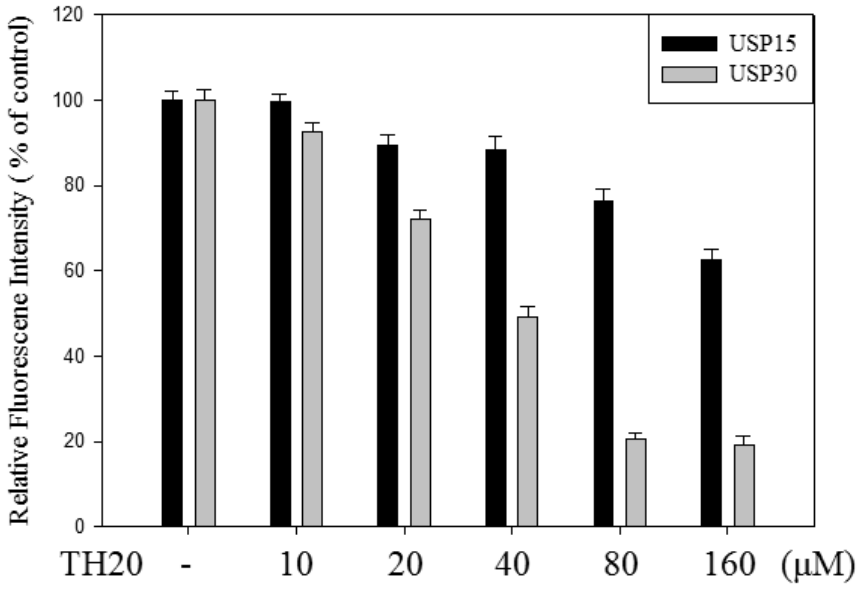

Figure 36. Inhibitory effects of TH3-125-4 (TH20) on USP15 and USP30 enzyme activities.

TH20 was incubated with 1 x DUB assay buffer for 30 min. DUB enzyme activities were measured by multiplate reader with fluorophore-linked Ub-AMC peptide substrates. The relative fluorescence intensity was indicated. Data represent the mean ± SD of three independent experiments.

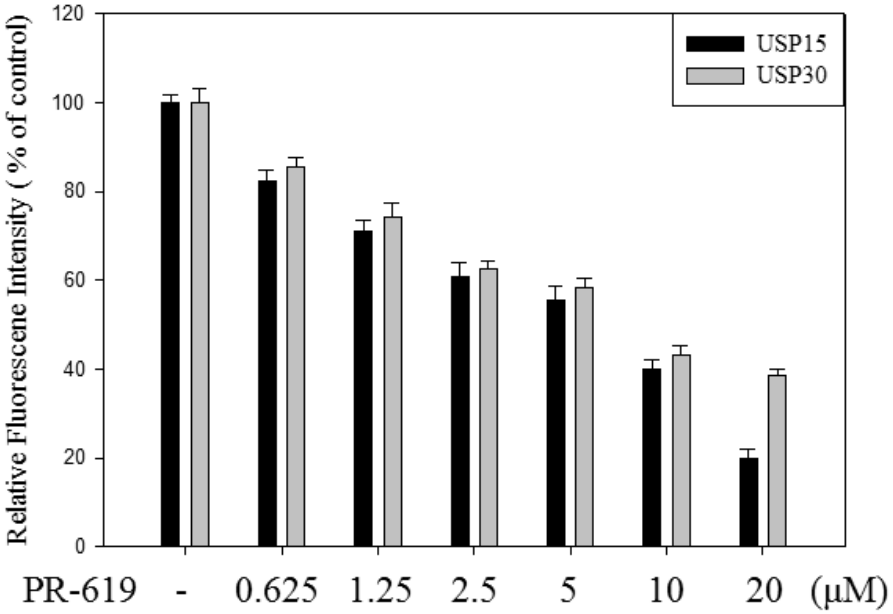

Figure 37. Inhibitory effects of PR-619 on USP15 and USP30 enzyme activities.

PR-619 was incubated with 1 x DUB assay buffer for 30 min. DUB enzyme activities were measured by multiplate reader with fluorophore-linked Ub-AMC peptide substrates. The relative fluorescence intensity was indicated. Data represent the mean ± SD of three independent experiments.

3.2. Effect of TH3-125-4 (TH20) on ubiquitin chain disassembly

The polyubiquitin chains (K48/K63 linked) are formed by e3 ligase like a parkin. The polyubiquitin chains are resolved by DUB. The incubation polyubiquitin chain with USP30 significantly induced disassembly of tetra ubiquitin. However, incubation with TH3-125-4 (TH20) inhibited disassembly of tetra ubiquitin at a concentration-dependent manner. The 80 μM of TH20 completely blocked the degradation of tetra ubiquitin. The results were correlated with inhibitory effects on USP30 activity in Fig. 38.

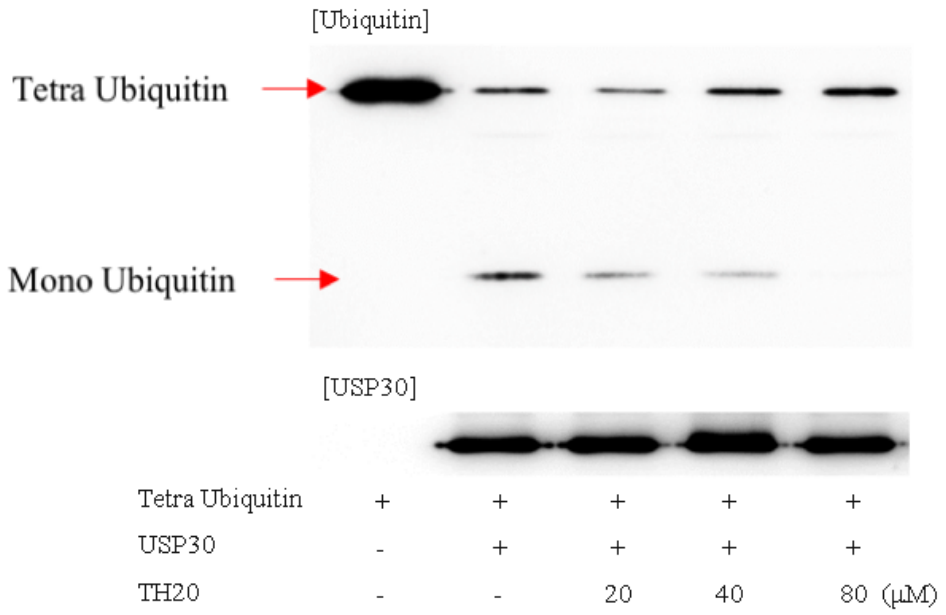

Figure 38. Inhibitory effects of TH3-125-4 (TH20) on USP30 enzyme mediated tetra ubiquitin disassembly.

TH20 was incubated with 1 x DUB assay buffer for 30 min. USP30 enzyme activities were measured by western blot assay with tetra ubiquitin peptide substrates. Representative data from three independent experiments are shown.

3.3. The protective effects of TH3-125-4 (TH20) against CCCP-induced neuronal cell death in parkin knock down SH-SY5Y cells.

The previous study revealed that parkin knock down cells were increased the vulnerability against CCCP neurotoxin. In the results, parkin siRNA transfected SH-SY5Y cells were more vulnerable to CCCP induce than scramble siRNA transfected SH-SY5Y cells. Also, USP15 or USP30 siRNA-transfected SH-SY5Y cells significantly protected the CCCP-induced cell death (Fig.39 and 40). Pre-treatment of TH20 protected CCCP-induced parkin knock down cell death at a concentration dependent manner. However, TH20 did not protect CCCP-induced scramble knock down cell death (Fig. 41).

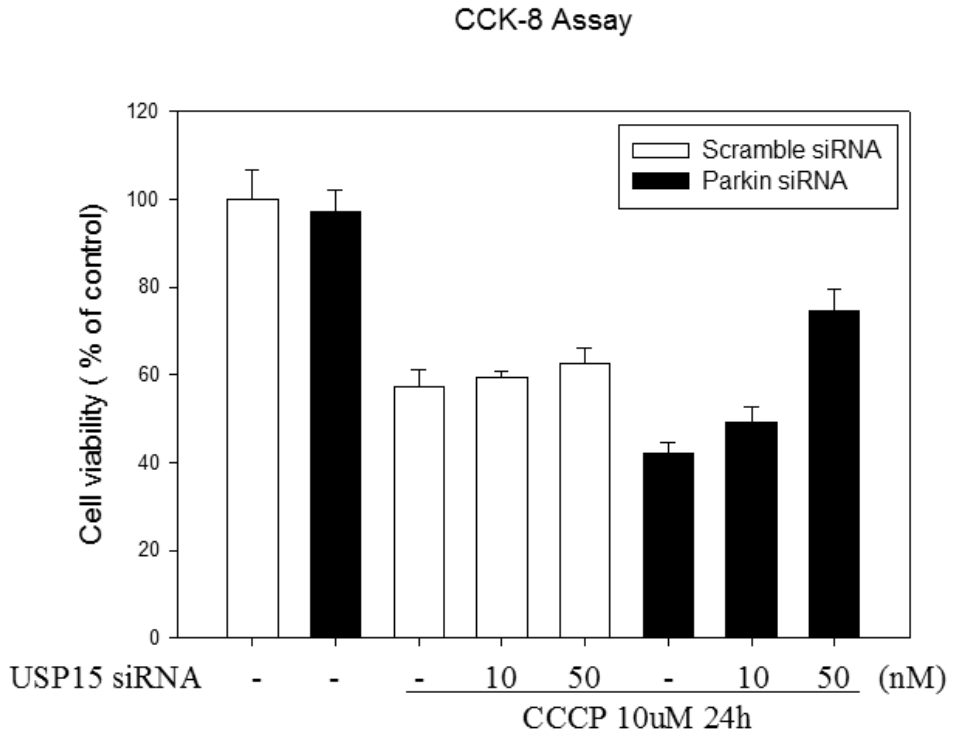

Figure 39. The protective effects of USP15 siRNA against CCCP-induced neuronal cell death in parkin knock down SH-SY5Y cells.

The cells were double-transfected with different concentrations of USP15 siRNA (10 - 50 nM) and Parkin siRNA or scramble siRNA (100 nM) for 48 h. After 24h, cells were subsequently treated with CCCP (10 μM) for another 24 h. The cell viability was determined by CCK-8 assay.

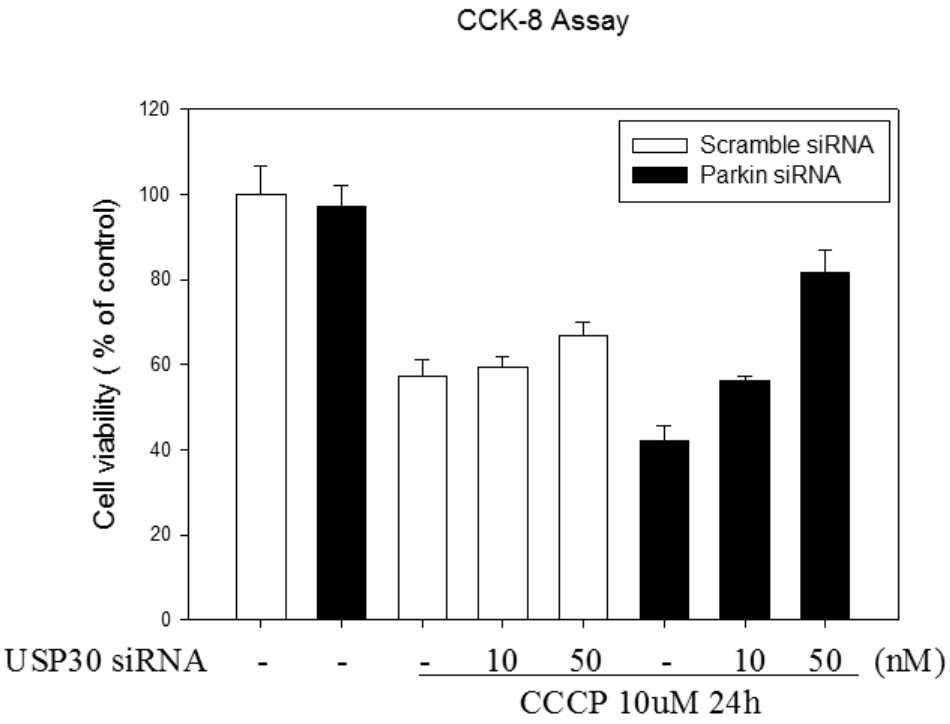

Figure 40. The protective effects of TH3-125-4 (TH20) against CCCP-induced neuronal cell death in parkin knock down SH-SY5Y cells.

The cells were double-transfected with different concentrations of USP30 siRNA (10 - 50 nM) and Parkin siRNA or scramble siRNA (100 nM) for 48 h. After 24h, cells were subsequently treated with CCCP (10 μM) for another 24 h. The cell viability was determined by CCK-8 assay.

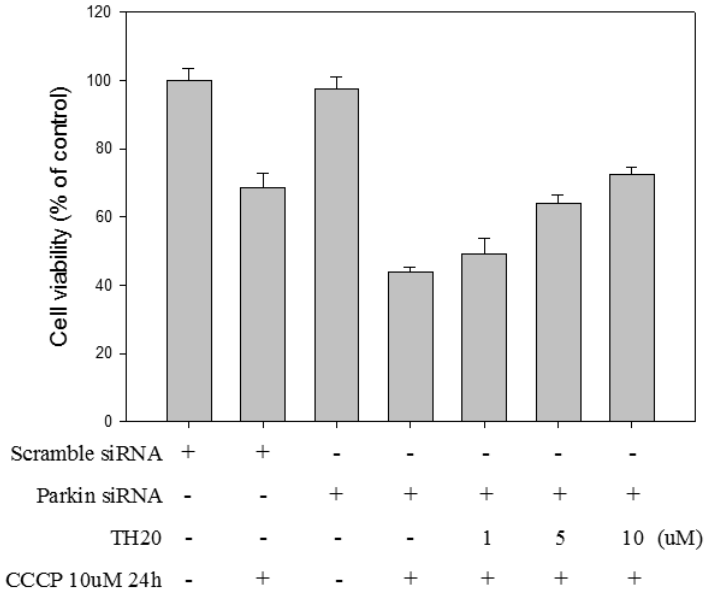

Figure 41. The protective effects of TH3-125-4 (TH20) against CCCP-induced neuronal cell death in parkin knock down SH-SY5Y cells.

The cells were pre-treated with different concentrations of TH20 (1 - 10 μM) for 24 h and subsequently treated with CCCP (10 μM) for another 24 h. The cells were transfected with Parkin siRNA or scramble siRNA (100 nM) for 48 h before the treatment with TH20. The cell viability was determined by CCK-8 assay.

3.4. Inhibitory effect of TH3-125-4 (TH20) on USP30 protein expression in SH-SY5Y cells.

We evaluated USP15, USP30 protein expression in SH-SY5Y cells. Among twelve isolated compounds, TH20 inhibited USP30 protein expression (Fig. 42). However, TH20 did not affect the protein expression of USP15. The protein expression of USP30 were gradually decreased by TH20 treatment at a concentration dependent manner. PR-619, a non-selective DUB inhibitor, did not affect the protein expression of USP15, USP30 (Fig. 43). The concentration of TH20 and PR-619 used in this experiment did not show cytotoxicity.

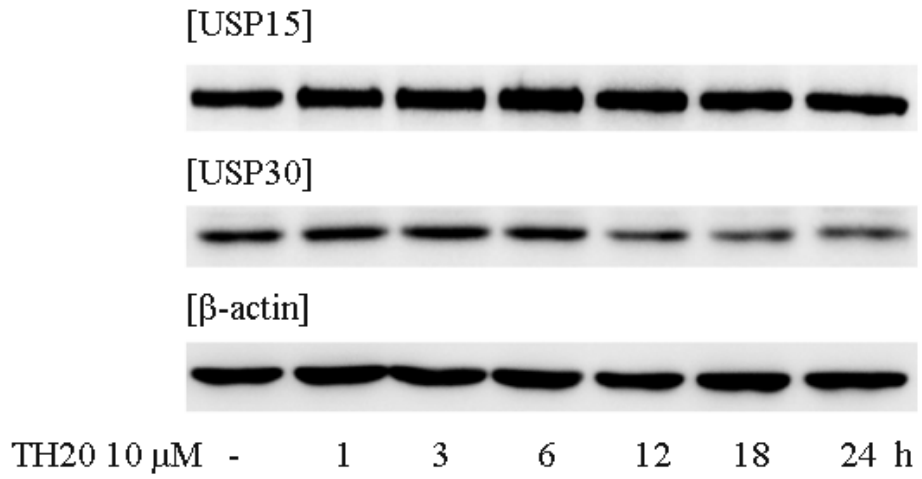

Figure 42. Inhibitory effect of TH3-125-4 (TH20) on USP30 protein expression in SH-SY5Y cells.

The cells were treated with TH20 (10 μM) for different durations (0 - 24 h). After treatment, the total protein was extracted and determined protein expression level by western blot assay. Representative data from three independent experiments are shown.

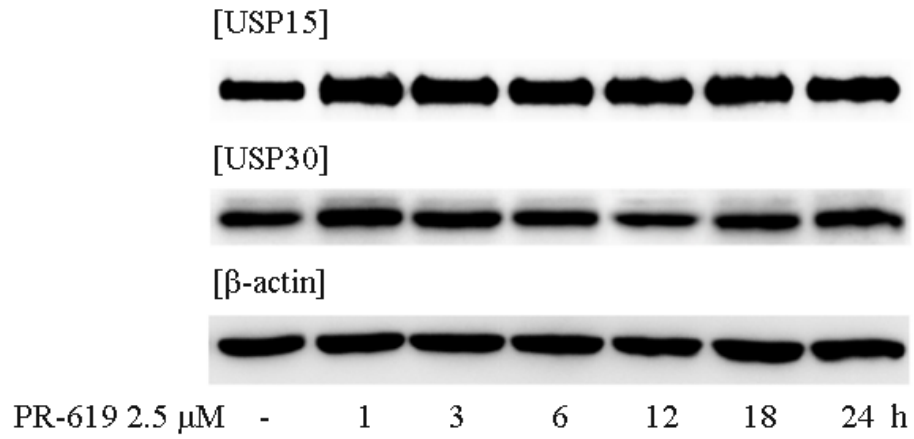

Figure 43. The protective effects of TH3-125-4 (TH20) against CCCP-induced neuronal cell death in parkin knock down SH-SY5Y cells.

The cells were treated with PR-619 (2.5 μM) for different durations (0 - 24 h). After treatment, the total protein was extracted and determined protein expression level by western blot assay. Representative data from three independent experiments are shown.

3.5. Effect of TH3-125-4 (TH20) on CCCP-induced disruption of mitochondrial membrane potential.

CCCP induces the rapid collapse of mitochondrial membrane potential (MMP) in SH-SY5Y cells. In our results, CCCP-induced collapse of MMP was peaked at 8 h. To evaluate the effect of TH20 on MMP, SH-SY5Y cell were pre-treated by TH20 for 24h. After then, MMP was disrupted by CCCP for 8h. TH20 did not protected CCCP-induced disruption of MMP (Fig. 44). The 10 μM of TH20 treatment slightly protected CCCP-induced collapse of MMP. However, the protective effect of TH20 was not significant result.

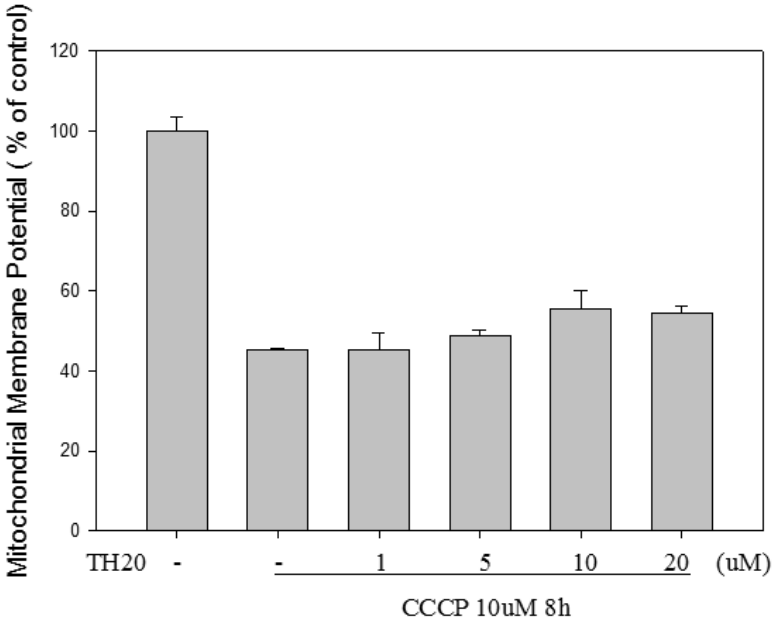

Figure 44. Effect of TH3-125-4 (TH20) on CCCP-induced disruption of mitochondrial membrane potential.

The cells were pre-treated with different concentrations of TH20 (1 - 10 μM) for 24 h and subsequently treated with CCCP (10 μM) for another 8 h. The cells were stained with JC-1 dyes for 30 min and determined by FACS analysis using FL-1 and FL-2 channel. The values of fluorescence intensity were obtained from histogram statistic of CellQuest software.

4. Discussion

Parkinson's disease is the most common neurodegenerative movement disorder. Although most cases are sporadic, several genes have been recently linked to familial PD, and loss-of-function mutations in Park2, the gene coding for the ubiquitin ligase Parkin, represent the most common recessive cause (Kitada et al., 1998). Parkin-null Drosophila melanogaster exhibit a severe phenotype, with the loss of dopaminergic neurons, disrupted spermatogenesis, and swollen and disordered mitochondria appearing before degeneration of their indirect flight muscles (Greene et al., 2003). The role of parkin in mitochondria phenotype was demonstrated. Parkin is selectively recruited to dysfunctional mitochondria in mammalian cells, and that after recruitment, Parkin mediates the engulfment of mitochondria by autophagosomes and their subsequent degradation. The results suggest that loss of Parkin activity may allow the accumulation of dysfunctional mitochondria, leading to neuron loss in PD, and that Parkin normally functions to survey mitochondrial activity and maintain mitochondrial fidelity by activating the autophagy of damaged organelles (Narendra et al., 2008). A recent proteomic study in human cells showed that Parkin ubiquitinates over

100 sites in more than 30 different MOM proteins, including Mfn1,2, in response to mitochondrial depolarization (Sarraf et al., 2013). In a recent research, deubiquitinating enzymes were reported that it can be an antagonist of parkin e3 ligase and inhibit parkin-mediated mitophagy. Among diverse DUBs, USP15 and USP30 were emerged as a major factor in opposing parkin e3 ligase activity. USP15, -30 deubiquitinates parkin-mediated mitochondrial fusion, fission proteins (Bingol et al., 2014; Cornelissen et al., 2014). Hence, the inhibition of USP15,-30 could be a therapeutic implication for familial PD.

In the current study, we identified a small natural compound, TH3-125-4 (TH20) derived from *C. tricuspidata*, which potently inhibits USP30 enzyme activity. However, TH20 did not significantly affect USP15 and total DUB enzyme activity. The inhibition of USP30 enzyme activity has a major role in PINK1-Parkin mediated mitophagy. It was reported that UPS30 physically interacts with Mfn1, 2 and decreases ubiquitination of Mfn1and Mfn2, whereas mutation of the active cysteine (C77) in the catalytic domain to serine abolishes its deubiquitinase activity, and thus the USP30-C77S mutant is unable to affect the ubiquitination of Mfns. Furthermore, it was demonstrated that inhibition of USP30 could lead to enhanced ubiquitination of Mfn1 or Mfn2, which promotes mitochondrial fusion (Yue et al., 2014). Hence, inhibitory effect of TH20 on USP30 enzyme activity could enhance PINK1-

Parkin mediated mitophagy. When the cells were transfected with Parkin siRNA, CCCP-induced neuronal cell death was increased comparing scramble siRNA treated SH-SY5Y. While TH20 treatment protected CCCP-induced neuronal cell death in Parkin K.D. SH-SY5Y cells, TH20 did not show protective effect against CCCP-induced neuronal cell death in scramble K.D. SH-SY5Y cells. Also, TH20 did not protect CCCP-induced disruption of MMP. The neuroprotective effect of TH20 in Parkin K.D. SH-SY5Y cells was predicted to be due to the DUB inhibitory effect, and the experiment for the DUB inhibitory effect was carried out. TH20 inhibited the enzymatic activity of USP30, while the inhibitory effect on USP15 and total DUB activity was weak. In addition, TH20 decreased the protein expression of USP30 in SH-SY5Y cells. Based on our results, we suggest that the protective effect of TH20 on CCCP-induced neuronal cell death in Parkin K.D. SH-SY5Y cells is mainly inhibition of USP30 enzyme activity. Further studies are needed to validate the hypothesis of the study, such as the effects of TH20 on Mfn1,2, OPA1, VDAC, LC3-beta, and p62 which are one of Parkin-mediated mitophagy factors. We are under investigating the effect of TH20 on Parkin-mediated mitophagy factors.

5. Conclusion

In conclusion, this study demonstrated that TH20 protected against CCCP-induced neuronal cell death in Parkin K.D. SH-SY5Y cells. Also, TH20 significantly inhibited USP30 enzyme activity and disassembly of polyubiquitin chain in *in vitro* assay. Our results showed that the protein expression of USP30 was decreased by treatment with TH20. Based on our results, we suggest that TH20 might be promising candidates for the therapy of familiar PD via restoring Parkin-mediated mitophagy.

References

Alfieri, A, Srivastava, S, Siow, RC, Modo, M, Fraser, PA, Mann, GE. 2011. Targeting the Nrf2-Keap1 antioxidant defence pathway for neurovascular protection in stroke. *The Journal of physiology* **589**(Pt 17): 4125-4136.

Alvarez-Castelao, B, Castano, JG. 2011. Synphilin-1 inhibits alpha-synuclein degradation by the proteasome. *Cell Mol Life Sci* **68**(15): 2643-2654.

Amm, I, Sommer, T, Wolf, DH. 2014. Protein quality control and elimination of protein waste: the role of the ubiquitin-proteasome system. *Biochim Biophys Acta* **1843**(1): 182-196.

Betarbet, R, Sherer, TB, Greenamyre, JT. 2005. Ubiquitin-proteasome system and Parkinson's diseases. *Exp Neurol* **191 Suppl 1**: S17-27.

Bingol, B, Tea, JS, Phu, L, Reichelt, M, Bakalarski, CE, Song, QH, et al. 2014. The mitochondrial deubiquitinase USP30 opposes parkin-mediated mitophagy. *Nature* **510**(7505): 370-+.

Bochkov, VN, Oskolkova, OV, Birukov, KG, Levonen, AL, Binder, CJ, Stockl, J. 2010. Generation and biological activities of oxidized phospholipids. *Antioxid Redox Signal* **12**(8): 1009-1059.

Bradford, MM. 1976. A rapid and sensitive method for the quantitation of microgram quantities of protein utilizing the principle of protein-dye binding. *Anal Biochem* **72**: 248-254.

Butterfield, DA, Kanski, J. 2001. Brain protein oxidation in age-related neurodegenerative disorders that are associated with aggregated proteins. *Mech Ageing Dev* **122**(9): 945-962.

Buttner, S, Delay, C, Franssens, V, Bammens, T, Ruli, D, Zaunschirm, S, et al. 2010. Synphilin-1 enhances alpha-synuclein aggregation in yeast and contributes to cellular stress and cell death in a Sir2-dependent manner. *PLoS One* **5**(10): e13700.

Canu, N, Barbato, C, Ciotti, MT, Serafino, A, Dus, L, Calissano, P. 2000. Proteasome involvement and accumulation of ubiquitinated proteins in cerebellar granule neurons undergoing apoptosis. *J Neurosci* **20**(2): 589-599.

Chan, NC, Salazar, AM, Pham, AH, Sweredoski, MJ, Kolawa, NJ, Graham, RLJ, et al. 2011. Broad activation of the ubiquitin-proteasome system by Parkin is critical for mitophagy. *Hum Mol Genet* **20**(9): 1726-1737.

Chandrasekharan, S, Aglin, A. 2013. Pharmacokinetics of dietary isoflavones. *Journal of Steroids & Hormonal Science* **2014**.

Chen, S, Zhu, P, Guo, HM, Solis, RS, Wang, YQ, Ma, YN, et al. 2014. Alpha1 catalytic subunit of AMPK modulates contractile function of cardiomyocytes through phosphorylation of troponin I. *Life Sciences* **98**(2): 75-82.

Chen, X, Guo, C, Kong, J. 2012. Oxidative stress in neurodegenerative diseases. *Neural Regen Res* **7**(5): 376-385.

Ciechanover, A, Kwon, YT. 2015. Degradation of misfolded proteins in neurodegenerative diseases: therapeutic targets and strategies. *Exp Mol Med* **47**: e147.

Cookson, MR. 2005. The biochemistry of Parkinson's disease*. *Annu. Rev. Biochem.* **74**: 29-52.

Cornelissen, T, Haddad, D, Wauters, F, Van Humbeeck, C, Mandemakers, W, Koentjoro, B, et al. 2014. The deubiquitinase USP15 antagonizes Parkin-mediated mitochondrial ubiquitination and mitophagy. *Hum Mol Genet* **23**(19): 5227-5242.

Dahlmann, B. 2007. Role of proteasomes in disease. *BMC Biochem* **8 Suppl 1**: S3.

Dayal, S, Sparks, A, Jacob, J, Allende-Vega, N, Lane, DP, Saville, MK. 2009. Suppression of the Deubiquitinating Enzyme USP5 Causes the

Accumulation of Unanchored Polyubiquitin and the Activation of p53. *Journal of Biological Chemistry* **284**(8): 5030-5041.

Dinkova-Kostova, AT, Talalay, P. 2010. NAD(P)H:quinone acceptor oxidoreductase 1 (NQO1), a multifunctional antioxidant enzyme and exceptionally versatile cytoprotector. *Arch Biochem Biophys* **501**(1): 116-123.

Dodel, RC, Du, Y, Bales, KR, Ling, Z, Carvey, PM, Paul, SM. 1999. Caspase-3-like proteases and 6-hydroxydopamine induced neuronal cell death. *Brain research. Molecular brain research* **64**(1): 141-148.

Doskeland, AP, Flatmark, T. 2002. Ubiquitination of soluble and membrane-bound tyrosine hydroxylase and degradation of the soluble form. *Eur J Biochem* **269**(5): 1561-1569.

Eksioglu-Demiralp, E, Kardas, ER, Ozgul, S, Yagci, T, Bilgin, H, Sehirli, O, et al. 2010. Betulinic acid protects against ischemia/reperfusion-induced renal damage and inhibits leukocyte apoptosis. *Phytother Res* **24**(3): 325-332.

Elkon, H, Melamed, E, Offen, D. 2004. Oxidative stress, induced by 6-hydroxydopamine, reduces proteasome activities in PC12 cells - Implications for the pathogenesis of Parkinson's disease. *Journal of Molecular Neuroscience* **24**(3): 387-400.

Espinosa-Diez, C, Miguel, V, Mennerich, D, Kietzmann, T, Sanchez-Perez, P, Cadenas, S, et al. 2015. Antioxidant responses and cellular adjustments to oxidative stress. *Redox Biol* **6**: 183-197.

Farooqui, T, Farooqui, AA. 2011. Lipid-mediated oxidative stress and inflammation in the pathogenesis of Parkinson's disease. *Parkinson's disease* **2011**: 247467.

Fraser, JA, Saunders, RD, McLellan, LI. 2002. Drosophila melanogaster glutamate-cysteine ligase activity is regulated by a modifier subunit with a mechanism of action similar to that of the mammalian form. *The Journal of biological chemistry* **277**(2): 1158-1165.

Fujimoto, T, Hano, Y, Nomura, T. 1984. Components of Root Bark of Cudrania tricuspidata l.1,2 Structures of Four New Isoprenylated Xanthones, Cudraxanthones A, B, C and D. *Planta Med* **50**(3): 218-221.

Ganora, L. 2009. Herbal constituents: Foundations of phytochemistry. *Lisa Ganora, Louisville, CO*.

Greene, JC, Whitworth, AJ, Kuo, I, Andrews, LA, Feany, MB, Pallanck, LJ. 2003. Mitochondrial pathology and apoptotic muscle degeneration in Drosophila parkin mutants. *P Natl Acad Sci USA* **100**(7): 4078-4083.

Ham, A, Kim, DW, Kim, KH, Lee, SJ, Oh, KB, Shin, J, et al. 2013. Reynosin protects against neuronal toxicity in dopamine-induced SH-SY5Y cells and 6-hydroxydopamine-lesioned rats as models of Parkinson's disease: Reciprocal up-regulation of E6-AP and down-regulation of alpha-synuclein. *Brain Res* **1524**: 54-61.

Hano, Y, Matsumoto, Y, Shinohara, K, Sun, JY, Nomura, T. 1991. Structures of Four New Isoprenylated Xanthones, Cudraxanthones L,

M, N, and O from Cudrania tricuspidata1,2. *Planta Med* **57**(2): 172-175.

Hiep, NT, Kwon, J, Kim, DW, Hwang, BY, Lee, HJ, Mar, W, et al. 2015. Isoflavones with neuroprotective activities from fruits of Cudrania tricuspidata. *Phytochemistry* **111**: 141-148.

Huang, Q, Figueiredo-Pereira, ME. 2010. Ubiquitin/proteasome pathway impairment in neurodegeneration: therapeutic implications. *Apoptosis* **15**(11): 1292-1311.

Jeong, CH, Choi, GN, Kim, JH, Kwak, JH, Jeong, HR, Kim, DO, et al. 2010. Protective Effects of Aqueous Extract from Cudrania tricuspidata on Oxidative Stress-induced Neurotoxicity. *Food Science and Biotechnology* **19**(4): 1113-1117.

Jeong, JY, Jo, YH, Lee, KY, Do, SG, Hwang, BY, Lee, MK. 2014. Optimization of pancreatic lipase inhibition by Cudrania tricuspidata fruits using response surface methodology. *Bioorg Med Chem Lett* **24**(10): 2329-2333.

Jung, T, Grune, T. 2013. The proteasome and the degradation of oxidized proteins: Part I-structure of proteasomes. *Redox Biol* **1**: 178-182.

Kang, DG, Hur, TY, Lee, GM, Oh, H, Kwon, TO, Sohn, EJ, et al. 2002. Effects of Cudrania tricuspidata water extract on blood pressure and renal functions in NO-dependent hypertension. *Life sciences* **70**(22): 2599-2609.

Kang, KW, Lee, SJ, Kim, SG. 2005. Molecular mechanism of nrf2 activation by oxidative stress. *Antioxidants & redox signaling* **7**(11-12): 1664-1673.

Kanthasamy, A, Jin, H, Mehrotra, S, Mishra, R, Kanthasamy, A, Rana, A. 2010. Novel cell death signaling pathways in neurotoxicity models of dopaminergic degeneration: relevance to oxidative stress and neuroinflammation in Parkinson's disease. *Neurotoxicology* **31**(5): 555-561.

Kaufmann, SH, Desnoyers, S, Ottaviano, Y, Davidson, NE, Poirier, GG. 1993. Specific proteolytic cleavage of poly(ADP-ribose) polymerase: an early marker of chemotherapy-induced apoptosis. *Cancer research* **53**(17): 3976-3985.

Kim, B-H, Kwon, J, Lee, D, Mar, W. 2015. Neuroprotective Effect of Demethylsuberosin, a Proteasome Activator, against MPP+-induced Cell Death in Human Neuroblastoma SH-SY5Y Cells. *Planta Medica Letters* **2**(01): e15-e18.

Kim, D-W, Lee, K-t, Kwon, J, Lee, HJ, Lee, D, Mar, W. 2015. Neuroprotection against 6-OHDA-induced oxidative stress and apoptosis in SH-SY5Y cells by 5, 7-Dihydroxychromone: Activation of the Nrf2/ARE pathway. *Life sciences* **130**: 25-30.

Kitada, T, Asakawa, S, Hattori, N, Matsumine, H, Yamamura, Y, Minoshima, S, et al. 1998. Mutations in the parkin gene cause autosomal recessive juvenile parkinsonism. *Nature* **392**(6676): 605-608.

Klovekorn, P, Munch, J. 1998. Variable optical delay line with diffraction-limited autoalignment. *Appl Opt* **37**(10): 1903-1904.

Kontopoulos, E, Parvin, JD, Feany, MB. 2006. Alpha-synuclein acts in the nucleus to inhibit histone acetylation and promote neurotoxicity. *Hum Mol Genet* **15**(20): 3012-3023.

Koo, U, Nam, KW, Ham, A, Lyu, D, Kim, B, Lee, SJ, et al. 2011. Neuroprotective effects of 3alpha-acetoxyeudesma-1,4(15),11(13)-trien-12,6alpha-olide against dopamine-induced apoptosis in the human neuroblastoma SH-SY5Y cell line. *Neurochem Res* **36**(11): 1991-2001.

Kuida, K, Haydar, TF, Kuan, CY, Gu, Y, Taya, C, Karasuyama, H, et al. 1998. Reduced apoptosis and cytochrome c-mediated caspase activation in mice lacking caspase 9. *Cell* **94**(3): 325-337.

Lee, Ha, H, Lee, JK, Seo, CS, Lee, NH, Jung, DY, et al. 2012. The fruits of Cudrania tricuspidata suppress development of atopic dermatitis in NC/Nga mice. *Phytother Res* **26**(4): 594-599.

Lee, IK, Kim, CJ, Song, KS, Kim, HM, Koshino, H, Uramoto, M, et al. 1996. Cytotoxic benzyl dihydroflavonols from Cudrania tricuspidata. *Phytochemistry* **41**(1): 213-216.

Lee, T, Kwon, J, Lee, D, Mar, W. 2015. Effects of Cudrania tricuspidata Fruit Extract and Its Active Compound, 5,7,3 ',4 '-Tetrahydroxy-6,8-diprenylisoflavone, on the High-Affinity IgE Receptor-Mediated Activation of Syk in Mast Cells. *Journal of Agricultural and Food Chemistry* **63**(22): 5459-5467.

Leutner, S, Czech, C, Schindowski, K, Touchet, N, Eckert, A, Muller, WE. 2000. Reduced antioxidant enzyme activity in brains of mice transgenic for human presenilin-1 with single or multiple mutations. *Neuroscience letters* **292**(2): 87-90.

Lim, JH, Kim, KM, Kim, SW, Hwang, O, Choi, HJ. 2008. Bromocriptine activates NQO1 via Nrf2-PI3K/Akt signaling: Novel cytoprotective mechanism against oxidative damage. *Pharmacol Res* **57**(5): 325-331.

Lindersson, E, Beedholm, R, Hojrup, P, Moos, T, Gai, W, Hendil, KB, et al. 2004. Proteasomal inhibition by alpha-synuclein filaments and oligomers. *J Biol Chem* **279**(13): 12924-12934.

Matsuda, N, Sato, S, Shiba, K, Okatsu, K, Saisho, K, Gautier, CA, et al. 2010. PINK1 stabilized by mitochondrial depolarization recruits Parkin to damaged mitochondria and activates latent Parkin for mitophagy. *J Cell Biol* **189**(2): 211-221.

McNaught, KS, Jenner, P. 2001. Proteasomal function is impaired in substantia nigra in Parkinson's disease. *Neurosci Lett* **297**(3): 191-194.

Meyer, T, Munch, C, Volkel, H, Booms, P, Ludolph, AC. 1998. The EAAT2 (GLT-1) gene in motor neuron disease: absence of mutations in amyotrophic lateral sclerosis and a point mutation in patients with hereditary spastic paraplegia. *Journal of neurology, neurosurgery, and psychiatry* **65**(4): 594-596.

Munch, G, Cunningham, AM, Riederer, P, Braak, E. 1998a. Advanced glycation endproducts are associated with Hirano bodies in Alzheimer's disease. *Brain research* **796**(1-2): 307-310.

Munch, G, Gerlach, M, Sian, J, Wong, A, Riederer, P. 1998b. Advanced glycation end products in neurodegeneration: more than early markers of oxidative stress? *Annals of neurology* **44**(3 Suppl 1): S85-88.

Nakamura, N, Hirose, S. 2008. Regulation of mitochondrial morphology by USP30, a deubiquitinating enzyme present in the mitochondrial outer membrane. *Mol Biol Cell* **19**(5): 1903-1911.

Narendra, D, Tanaka, A, Suen, DF, Youle, RJ. 2008. Parkin is recruited selectively to impaired mitochondria and promotes their autophagy. *J Cell Biol* **183**(5): 795-803.

Narendra, DP, Jin, SM, Tanaka, A, Suen, DF, Gautier, CA, Shen, J, et al. 2010. PINK1 Is Selectively Stabilized on Impaired Mitochondria to Activate Parkin. *Plos Biol* **8**(1).

Narendra, DP, Youle, RJ. 2011. Targeting Mitochondrial Dysfunction: Role for PINK1 and Parkin in Mitochondrial Quality Control. *Antioxid Redox Sign* **14**(10): 1929-1938.

Nguyen, T, Nioi, P, Pickett, CB. 2009. The Nrf2-antioxidant response element signaling pathway and its activation by oxidative stress. *J Biol Chem* **284**(20): 13291-13295.

Ning, W, Wang, S, Liu, D, Fu, L, Jin, R, Xu, A. 2016. Potent effects of peracetylated (-)-epigallocatechin-3-gallate against hydrogen peroxide-induced damage in human epidermal melanocytes via attenuation of oxidative stress and apoptosis. *Clin Exp Dermatol* **41**(6): 616-624.

Okamoto, Y, Suzuki, A, Ueda, K, Ito, C, Itoigawa, M, Furukawa, H, et al. 2006. Anti-estrogenic activity of prenylated isoflavones from Millettia pachycarpa: implications for pharmacophores and unique mechanisms. *Journal of health science* **52**(2): 186-191.

Park, HS, Jun do, Y, Han, CR, Woo, HJ, Kim, YH. 2011. Proteasome inhibitor MG132-induced apoptosis via ER stress-mediated apoptotic pathway and its potentiation by protein tyrosine kinase p56lck in human Jurkat T cells. *Biochem Pharmacol* **82**(9): 1110-1125.

Park, J, Lee, SB, Lee, S, Kim, Y, Song, S, Kim, S, et al. 2006a. Mitochondrial dysfunction in Drosophila PINK1 mutants is complemented by parkin. *Nature* **441**(7097): 1157-1161.

Park, J, Lee, SB, Lee, S, Kim, Y, Song, S, Kim, S, et al. 2006b. Mitochondrial dysfunction in Drosophila PINK1 mutants is complemented by parkin. *Nature* **441**(7097): 1157-1161.

Park, KH, Park, YD, Han, JM, Im, KR, Lee, BW, Jeong, IY, et al. 2006. Anti-atherosclerotic and anti-inflammatory activities of catecholic xanthones and flavonoids isolated from Cudrania tricuspidata. *Bioorg Med Chem Lett* **16**(21): 5580-5583.

Park, SH, Jang, JH, Chen, CY, Na, HK, Surh, YJ. 2010. A formulated red ginseng extract rescues PC12 cells from PCB-induced oxidative cell

death through Nrf2-mediated upregulation of heme oxygenase-1 and glutamate cysteine ligase. *Toxicology* **278**(1): 131-139.

Pesah, Y, Burgess, H, Middlebrooks, B, Ronningen, K, Prosser, J, Tirunagaru, V, et al. 2005. Whole-mount analysis reveals normal numbers of dopaminergic neurons following misexpression of alpha-Synuclein in Drosophila. *Genesis* **41**(4): 154-159.

Pompella, A, Visvikis, A, Paolicchi, A, De Tata, V, Casini, AF. 2003. The changing faces of glutathione, a cellular protagonist. *Biochem Pharmacol* **66**(8): 1499-1503.

Qiu, J, Chen, L, Zhu, Q, Wang, D, Wang, W, Sun, X, et al. 2012. Screening natural antioxidants in peanut shell using DPPH-HPLC-DAD-TOF/MS methods. *Food chemistry* **135**(4): 2366-2371.

Rahman, K. 2007. Studies on free radicals, antioxidants, and co-factors. *Clinical interventions in aging* **2**(2): 219-236.

Ramos-Gomez, M, Kwak, MK, Dolan, PM, Itoh, K, Yamamoto, M, Talalay, P, et al. 2001. Sensitivity to carcinogenesis is increased and chemoprotective efficacy of enzyme inducers is lost in nrf2 transcription factor-deficient mice. *Proceedings of the National Academy of Sciences of the United States of America* **98**(6): 3410-3415.

Rizzardini, M, Terao, M, Falciani, F, Cantoni, L. 1993. Cytokine induction of haem oxygenase mRNA in mouse liver. Interleukin 1 transcriptionally activates the haem oxygenase gene. *The Biochemical journal* **290 (Pt 2)**: 343-347.

Sarraf, SA, Raman, M, Guarani-Pereira, V, Sowa, ME, Huttlin, EL, Gygi, SP, et al. 2013. Landscape of the PARKIN-dependent ubiquitylome in response to mitochondrial depolarization. *Nature* **496**(7445): 372-+.

Seo, H, Sonntag, KC, Kim, W, Cattaneo, E, Isacson, O. 2007. Proteasome activator enhances survival of Huntington's disease neuronal model cells. *PLoS One* **2**(2): e238.

Seo, WG, Pae, HO, Oh, GS, Chai, KY, Yun, YG, Chung, HT, et al. 2001. Ethyl acetate extract of the stem bark of Cudrania tricuspidata induces apoptosis in human leukemia HL-60 cells. *Am J Chin Med* **29**(2): 313-320.

Shiotsuka, S, Isonishi, S. 2001. Differential sensitization by orobol in proliferating and quiescent human ovarian carcinoma cells. *Int J Oncol* **18**(2): 337-342.

Sidhu, A, Wersinger, C, MOUSSA, CEH, Vernier, P. 2004. The role of α-synuclein in both neuroprotection and neurodegeneration. *Annals of the New York Academy of Sciences* **1035**(1): 250-270.

Su, ZY, Shu, L, Khor, TO, Lee, JH, Fuentes, F, Kong, AN. 2013. A perspective on dietary phytochemicals and cancer chemoprevention: oxidative stress, nrf2, and epigenomics. *Topics in current chemistry* **329**: 133-162.

Sun, F, Anantharam, V, Zhang, D, Latchoumycandane, C, Kanthasamy, A, Kanthasamy, AG. 2006. Proteasome inhibitor MG-132 induces dopaminergic degeneration in cell culture and animal models. *Neurotoxicology* **27**(5): 807-815.

Sun, X, Huang, L, Zhang, M, Sun, S, Wu, Y. 2010. Insulin like growth factor-1 prevents 1-mentyl-4-phenylphyridinium-induced apoptosis in PC12 cells through activation of glycogen synthase kinase-3beta. *Toxicology* **271**(1-2): 5-12.

Tai, HC, Schuman, EM. 2008. Ubiquitin, the proteasome and protein degradation in neuronal function and dysfunction. *Nat Rev Neurosci* **9**(11): 826-838.

Tanner, CM, Kamel, F, Ross, GW, Hoppin, JA, Goldman, SM, Korell, M, et al. 2011. Rotenone, Paraquat, and Parkinson's Disease. *Environ Health Persp* **119**(6): 866-872.

Tucker, JL, 3rd, Munchus, GM, 3rd. 1998. The predictors of quality care. *Military medicine* **163**(11): 754-757.

Turkseven, S, Kruger, A, Mingone, CJ, Kaminski, P, Inaba, M, Rodella, LF, et al. 2005. Antioxidant mechanism of heme oxygenase-1 involves an increase in superoxide dismutase and catalase in experimental diabetes. *Am J Physiol Heart Circ Physiol* **289**(2): H701-707.

Uddin, GM, Jeon, JS, Kim, CY. 2011. Isolation of Prenylated Isoflavonoids from Cudrania tricuspidata Fruits that Inhibit A2E Photooxidation. *Natural Product Sciences* **17**(3): 206-211.

Uttara, B, Singh, AV, Zamboni, P, Mahajan, RT. 2009. Oxidative stress and neurodegenerative diseases: a review of upstream and downstream antioxidant therapeutic options. *Current neuropharmacology* **7**(1): 65-74.

Valente, EM, Abou-Sleiman, PM, Caputo, V, Muqit, MM, Harvey, K, Gispert, S, et al. 2004. Hereditary early-onset Parkinson's disease caused by mutations in PINK1. *Science* **304**(5674): 1158-1160.

Vives-Bauza, C, Zhou, C, Huang, Y, Cui, M, de Vries, RLA, Kim, J, et al. 2010. PINK1-dependent recruitment of Parkin to mitochondria in mitophagy. *P Natl Acad Sci USA* **107**(1): 378-383.

Wei, G, Yu, B. 2008. Isoflavone glycosides: Synthesis and evaluation as alpha-glucosidase inhibitors. *Eur J Org Chem*(18): 3156-3163.

Wojcik, C, DeMartino, GN. 2003. Intracellular localization of proteasomes. *Int J Biochem Cell Biol* **35**(5): 579-589.

Youdim, KA, Dobbie, MS, Kuhnle, G, Proteggente, AR, Abbott, NJ, Rice-Evans, C. 2003. Interaction between flavonoids and the blood–brain barrier: in vitro studies. *Journal of neurochemistry* **85**(1): 180-192.

Yuan, BZ, Chapman, JA, Reynolds, SH. 2008. Proteasome Inhibitor MG132 Induces Apoptosis and Inhibits Invasion of Human Malignant Pleural Mesothelioma Cells. *Transl Oncol* **1**(3): 129-140.

Yue, W, Chen, ZH, Liu, HY, Yan, C, Chen, M, Feng, D, et al. 2014. A small natural molecule promotes mitochondrial fusion through inhibition of the deubiquitinase USP30. *Cell Res* **24**(4): 482-496.

Zhang, M, An, C, Gao, Y, Leak, RK, Chen, J, Zhang, F. 2013. Emerging roles of Nrf2 and phase II antioxidant enzymes in neuroprotection. *Progress in neurobiology* **100**: 30-47.

Zuo, Y, Xiang, B, Yang, J, Sun, X, Wang, Y, Cang, H, et al. 2009. Oxidative modification of caspase-9 facilitates its activation via disulfide-mediated interaction with Apaf-1. *Cell research* **19**(4): 449-457.

국문초록

꾸지뽕나무로부터 분리한 유효성분물질의 파킨슨병 세포모델에서의 신경보호효과: Ubiquitin-proteasome system 및 Nrf2-ARE 관련 기전에 관한 효과연구

김 동 우

약학과 천연물과학 전공

서울대학교 약학대학 대학원

파킨슨 병은 운동 장애, 기억 상실, 운동 부조 및 도파민 신경의 손실등의 특징을 보이는 퇴행성 뇌질환이다. 파킨슨 병의 원인은 명확하게 특정되지 않았지만 산화적 스트레스, 유비퀴틴 – 프로테아좀 기능저하, mitophagy 기능이상은 세포 기능 장애 및 과도한 독성단백질의 축적 및 미토콘드리아 장애를 초래하며 주요 병인으로 간주되고있다. 신경독성으로 알려진 6-OHDA, CCCP 는 라디칼과 같은 과도한 활성산소종을 유도하거나 미토콘드리아의 기능이상을 유도함으로써 도파민 뉴런을 파괴하고 단백질 산화 및

신경 세포 사멸을 일으킨다. 산화적스트레스는 다양한 분자병리학적 기전을 통해 세포사멸을 유발하며, 유비퀴틴 – 프로테아좀 기능저하는 독성 단백질의 과다축적을 유도하고 이로인해 신경 세포사를 초래한다. Mitophagy 의 기능이상은 제거해야할 미토콘드리아의 과축적을 유발하여 신경 세포사를 초래한다. 현재 개발중인 새로운 치료법은 도파민 뉴런을 보호하는 것을 목적으로 하고 있다. 본 연구에서 파킨슨 병의 치료제제로써 가능성 있는 선도 화합물을 발견하기 위해 SH-SY5Y 신경아종 세포에서 6-OHDA, CCCP 로 유도한 뇌세포 사멸 보호효과 및 관련 기전에 대하여 연구하였다.

첫번째로, 꾸지뽕나무 뿌리로부터 분리한 5,7-Dihydroxychromone (DHC)의 Nrf2/ARE 기전 활성화를 통한 6-OHDA 로 유도한 뇌세포사멸 보호효과를 연구하고자 하였다. 6-OHDA 로 유도한 SH-SY5Y 뇌세포 사멸은 DHC 처리에 의해 농도의존적으로 감소하는 결과를 보였으며, 세포내 활성산소종 역시 DHC 처리에 의해 감소하는 결과를 확인하였다. 이에 DHC 의 뇌세포사멸 보호효과의 기전을 확인하고자, DHC 의 Nrf2 nuclear translocation 에 대해

연구하였고, DHC 처리에 의해 Nrf2 의 핵안으로 이동이 증가함을 확인하였다. 이어진 연구에 의해 핵안으로 이동한 Nrf2 가 ARE 와 binding 하는 것을 확인할 수 있었으며, 이로인해 phase 2 antioxidant enzyme 의 발현량이 증가하는 결과를 확인하였다. 이어진 실험에서 Nrf2 knock down 시킨 세포주에서 DHC 의 뇌세포사멸 보호효과는 현저히 감소되는 결과를 확인하였다. 즉, DHC 의 6-OHDA 로 유도한 뇌세포사멸의 보호효과가 Nrf2/ARE 기전을 통한 phase 2 antioxidant enzyme 의 활성화를 통한것임을 증명할 수 있었다. 최종적으로 Nrf2/ARE 기전의 활성화를 통한 퇴행성뇌질환 예방 및 치료제 선도물질로써 가능성을 제시할 수 있다.

두번째로, 꾸지뽕나무 열매로부터 분리한 Orobol 유도체 및 에탄올 추출물을 이용하여 6-OHDA 로 유도한 뇌세포 사멸 및 ubiquitin-proteasome system 에 대한 효과를 연구 하였다. 꾸지뽕나무 열매 50% 에탄올 추출물 및 orobol, 6-prenylorobol, 6,8-diprenylorobol 이 6-OHDA 로 유도한 SH-SY5Y 뇌세포사멸 보호효과가 가장 우수하였다. 또한, 50% 에탄올 추출물 및 orobol 유도체는 6-OHDA 로 유도한 proteasome dysfunction 을 효과적으로

보호하는 결과를 보였다. Proteasome 보호효과를 통해 파킨슨 질환의 주요 독성 단백질 중 하나인 a-synuclein, synphilin-1 의 제거를 효과적으로 유도하였다. 하지만 proteasome inhibitor 인 MG132 를 처리함에 따라 50% 에탄올 추출물 및 orobol 유도체의 세포사멸 보호효과 및 proteasome 보호효과가 현저히 저하되는 결과를 보였다. 즉, 꾸지뽕나무 열매 50% 에탄올 추출물 및 orobol 유도체는 ubiquituin-proteasome system 의 정상화를 통해 a-synuclein, synphilin-1 의 제거를 유도하고, apoptosis, 활성산소종 생성을 억제하며 뇌세포를 효과적으로 보호함을 증명할 수 있었다. 최종적으로 proteasome 보호효과를 통한 퇴행성 뇌질환 예방 및 치료제의 선도물질로써의 가능성을 제시할 수 있다.

마지막으로, 꾸지뽕나무로부터 분리한 유효물질이 deubiquitinating 효소에 미치는 영향을 연구 하였다. 꾸지뽕나무 뿌리로부터 분리된 TH3-125-4 (TH20)는 Parkin K.D. SH-SY5Y 세포주에서 CCCP 로 유도한 신경 세포 사멸을 보호하였다. TH20 은 deubiquitinating 효소로 알려진 USP30 의 활성을 효과적으로 억제하였으며, USP30 의 polyubiquitin 분해활성 역시 억제하는 효과를 보였다. 또한, TH20 은

USP30 의 단백질 발현을 감소시켰다. 연구 결과에 따르면 TH20 은 Parkin 매개 mitophagy 를 정상적으로 회복하여 유전형 파킨슨 병의 치료제 선도물질로써의 가능성을 보였다.

주요어: 꾸지뽕나무, 산화적 스트레스, 6-OHDA, 뇌세포사멸 보호, 5,7-Dihydroxychromone, Nrf2/ARE pathway, orobol 유도체, 프로테아좀 활성, ubiquitination, deubiquitinating 효소, PINK1, Parkin, mitophagy

학번: 2012-21566

First-Author publications

Journal of Functional Foods 29 (2017) 104–114

Contents lists available at ScienceDirect

Journal of Functional Foods

journal homepage: www.elsevier.com/locate/jff

Orobol derivatives and extracts from *Cudrania tricuspidata* fruits protect against 6-hydroxydomamine-induced neuronal cell death by enhancing proteasome activity and the ubiquitin/proteasome-dependent degradation of α-synuclein and synphilin-1

Dong-Woo Kim [a], Jaeyoung Kwon [b], Su Jin Sim [c], Dongho Lee [d,**], Woongchon Mar [a,*]

[a] Natural Products Research Institute, College of Pharmacy, Seoul National University, Seoul 08826, Republic of Korea
[b] Natural Constituents Research Center, Korea Institute of Science and Technology (KIST) Gangneung Institute, Gangneung 25451, Republic of Korea
[c] Forest Medicinal Resources Research Center, National Institute of Forest Science, Yeongju 36040, Republic of Korea
[d] Department of Biosystems and Biotechnology, Korea University, Seoul 02841, Republic of Korea

ARTICLE INFO

Article history:
Received 8 September 2016
Received in revised form 21 November 2016
Accepted 9 December 2016

Keywords:
Cudrania tricuspidata
Orobol derivatives
Proteasome activity
Polyubiquitination
Neuroprotection
6-OHDA

ABSTRACT

We investigated the neuroprotective effects of orobol derivatives and ethanol extracts from *Cudrania tricuspidata* fruits. Among the nine isolates from a 50% ethanol extract from *Cudrania tricuspidata* fruits (CTE50), orobol (OB), 6-prenylorobol (POB), and 6,8-diprenylorobol (DPOB) showed neuroprotective effects in 6-OHDA-induced SH-SY5Y cell death. In addition, CTE50 and the three orobol derivatives (OB, POB, and DPOB) attenuated the cleavage of caspase-3, caspase-9, and PARP and inhibited the excessive generation of ROS. Furthermore, it enhanced the 6-OHDA-induced dysfunction of proteasome activity and reduced the accumulation of ubiquitin conjugated-proteins and the polyubiquitination of α-synuclein and synphilin-1. The proteasome inhibitor MG132 blocked the neuroprotective effects and the enhanced proteasome activity produced by CTE50 and the three orobol derivatives. These results demonstrate that CTE50 and three orobol derivatives protect against 6-OHDA-induced neurotoxicity by enhancing the ubiquitin/proteasome-dependent degradation of α-synuclein and synphilin-1, suggesting that they might be possible candidates for the treatment of neurodegenerative diseases.

1. Introduction

Cudrania tricuspidata (Moraceae) is a subtropical tree that is widely distributed in Korea, China, and Japan. The fruits of *C. tricuspidata* are used in jams, juices, and a fermented alcoholic beverage with sugar, and they are commercially produced as food in Korea. In addition, the root, stem, leaf, and fruits of this plant have been reported to have anti-atherosclerotic, anti-inflammatory and antioxidant activities (Jeong et al., 2010; Lee et al., 2012; Park et al., 2006). Recent studies have demonstrated that the fruit of *C. tricuspidata* inhibited pancreatic lipase (Jeong et al., 2014), protected neuronal cells against oxidative stress-induced toxicity (Jeong et al., 2010), and inhibited IgE-mediated allergic and inflammatory responses (Lee, Kwon, Lee, & Mar, 2015). The compounds isolated from *C. tricuspidata* are primarily xanthones and flavones in addition to some alkaloids, lignins, coumarins, polysaccharides, and chromones (Fujimoto, Hano, & Nomura, 1984; Hano, Matsumoto, Shinohara, Sun, & Nomura, 1991; Hiep et al., 2015; Lee et al., 1996; Seo et al., 2001). The isoflavones from the fruits of *C. tricuspidata* have been reported to exert protective effects against 6-hydroxydopamine (6-OHDA)-induced neurotoxicity (Hiep et al., 2015) and to have inhibitory effects against IgE-mediated allergic and inflammatory responses (Lee et al., 2015). Orobol (OB), 6-prenylorobol (POB) and 6,8-diprenylorobol (DPOB) are prenylated isoflavones. It was reported that OB increases cisplatin sensitivity in human ovarian carcinoma (Shiotsuka & Isonishi, 2001) and that DPOB shows anti-estrogenic activity (Okamoto et al., 2006) and inhibits lipofuscin fluorophore-mediated photo oxidation (Uddin, Jeon, & Kim, 2011).

Abbreviations: 6-OHDA, 6-hydroxydomamine; PD, Parkinson's disease; PARP, poly (ADP-ribose) polymerase; ROS, reactive oxygen species; UPP, ubiquitin-proteasome pathway; UPS, ubiquitin-proteasome system; CTE50, 50% ethanol extract from *Cudrania tricuspidata* fruits; OB, orobol; POB, 6-prenylorobol; DPOB, 6,8-diprenylorobol.

* Corresponding author.
** Corresponding author.
E-mail addresses: dongholee@korea.ac.kr (D. Lee), mars@snu.ac.kr (W. Mar).

http://dx.doi.org/10.1016/j.jff.2016.12.017
1756-4646/

Parkinson's disease (PD) is characterized by severe motor deficits, cogwheel rigidity, bradykinesia, and the loss of dopaminergic neurons. The aetiology of PD has not been clearly identified; however, oxidative stress is thought to be a common factor that leads to cellular dysfunction and neurodegeneration. Reactive oxygen species (ROS) are mainly produced as a by-product of cellular metabolism and oxidative phosphorylation. Non-neutralized ROS produce oxidative stress in cellular organisms and lead to abnormal molecular activities (Bochkov et al., 2010). In particular, the pathological events that occur in PD have been suggested to be linked to protein oxidation caused by oxidative stress (Butterfield & Kanski, 2001), and excessive intracellular ROS induce apoptosis that is characterized by the cleavage of caspase-3, caspase-9 and poly ADP-ribose polymerase (PARP) (Klovekorn & Munch, 1998). The neurotoxin 6-OHDA destroys dopaminergic and noradrenergic neurons in the brain by inducing excessive ROS such as superoxide radicals, which leads to protein oxidation and neuronal cell death (Kanthasamy et al., 2010).

The proteasome plays a key role in the selective degradation of oxidized proteins via ubiquitin-mediated processes, and its role is essential for cellular protein maintenance (Jung & Grune, 2013; Tai & Schuman, 2008). The diversity in E3 ubiquitin ligases confers specificity in selecting substrate proteins, and ubiquitin-tagged proteins are targeted by the proteasome for selective ubiquitin-dependent protein degradation. The catalytic domain of the proteasome contains chymotrypsin, trypsin, and caspases type, and each type has a different role in protein degradation (Huang & Figueiredo-Pereira, 2010). In general, high levels of ubiquitinated proteins do not accumulate in normal cells because they are rapidly degraded by the ubiquitin-proteasome pathway (UPP). However, dysfunctions in the ubiquitination machinery or in the proteolytic activities of the proteasome are associated with multiple pathological conditions, such as excessive intracellular ROS, cellular stress, and diverse stress. These factors impair the normal states of the ubiquitin-proteasome system (UPS) and induce the accumulation of polyubiquitinated misfolded proteins and oxidized proteins, thus leading to dysfunction in the ubiquitin-proteasome system. Subsequently, this induces protein aggregation, further inhibits proteasome activity, generates additional cellular stress, and ultimately leads to cell death (Dahlmann, 2007). Recent research has suggested that oxidative stress-induced proteasome dysfunction might play a key role in neurodegenerative diseases and that rescuing the decrease in proteasome activity could be a new therapeutic strategy (Seo, Sonntag, Kim, Cattaneo, & Isacson, 2007). Additionally, dysfunction in proteasome activity was observed in the substantia nigra of PD patients, suggesting that the impairment of the UPS is involved in the formation of Lewy bodies and in dopaminergic neuronal cell death in PD (McNaught & Jenner, 2001). Lewy bodies are characteristic hallmarks of PD and are composed of primarily α-synuclein and synphilin-1 along with ubiquitin and other fibrils. α-synuclein, a small acidic protein composed of 140 amino acids, is abundant in the human brain; is also found in the heart, muscles, and other tissues; and is a naturally unfolded protein with the ability to self-aggregate. The aggregation process of α-synuclein results in potential cell damage, leading to dopaminergic neuronal loss in Parkinson's disease (Cookson, 2005). α-synuclein also associates with other protein partners in the cell, including a significant interaction with synphilin-1. It has been reported that synphilin-1 is a presynaptic protein that could be a modulator of UPS, and the overexpression of synphilin-1 promotes the formation of inclusions under conditions of proteasome inhibition. Additionally, synphilin-1 inhibits the degradation of α-synuclein by the proteasome, thus increasing its half-life (Alvarez-Castelao & Castano, 2011). Therefore, it is possible that the inhibition Lewy body-associated protein accumulation through the protection against proteasome dysfunction could be a key aspect of PD treatment.

In our previous reports, we investigated the neuroprotective effect of different extracts (0–100% ethanol ratio) containing isoflavones from *C. tricuspidata* fruits (Hiep et al., 2015). Here, nine isolates obtained from 50% ethanol extract from *C. tricuspidata* fruits (CTE50) were evaluated for their neuroprotective potential against 6-OHDA-induced cell death in SH-SY5Y human neuroblastoma cells. We focused on the potential effects on apoptosis, intracellular ROS generation, proteasome activities, polyubiquitination of Lewy body-associated α-synuclein and synthilin-1 against 6-OHDA-induced SH-SY5Y cells.

2. Materials and methods

2.1. Reagents

6-Hydroxydopamine (6-OHDA), and 2′,7′-dichlorfluorescein-diacetate (DCFH-DA) were purchased from Sigma-Aldrich (St. Louis, MO, USA). MG132 was purchased from Enzo Life Sciences (Farmingdale, NY, USA). Dulbecco's modified Eagle's medium (DMEM) and foetal bovine serum (FBS) were purchased from Hyclone™ Thermo Scientific (Wyman Street Waltham, MA, USA). Hybond®-Polyvinylidene difluoride (PVDF) membranes were purchased from Amersham Pharmacia Biotechnology Inc. (Piscataway, NJ, USA). PRO-PREP protein extraction solution and WEST-ZOL® ECL solution were purchased from iNtRON Biotech Inc. (Kyunggi, Korea). Antibodies against ubiquitin, α-synuclein, synphilin-1, β-actin, caspase-3, cleaved caspase-3, caspase-9, cleaved caspase-9, PARP, and A/G Plus-Agarose and secondary antibodies were purchased from Santa Cruz Biotechnology, Inc. (CA, USA)

2.2. Preparation of ethanol extracts from C. tricuspidata fruits

The fruits of *C. tricuspidata* were collected from the Korea Forest Research Institute, Southern Forest Research Center (Jinju, Korea). A voucher specimen (accession no. KH1-5-090904) was deposited at the Department of Biosystems and Biotechnology, Korea University (Seoul, Korea). The dry fruit of *C. tricuspidata* (3.4 kg) was ground into powder form and sifted through a 120-mesh sieve. The dry powder (7 g) was refluxed three times for 1 h each by means of a heating mantle with 250 mL of 0%, 30%, 50%, 70%, or 100% ethanol in round 500-mL flasks. The combined extracts were filtered and concentrated in vacuo to yield 2.85 g, 2.71 g, 2.57 g, 2.67 g, and 2.1 g, respectively.

2.3. Isolation and identification of compounds from CTE50

Nine isoflavones, namely, orobol (**1**, 0.0021%), 6-prenylorobol (**2**, 0.0100%), 6,8-diprenylorobol (**3**, 0.0015%), millewanins H and G (**4** and **5**, 0.0029 and 0.0045%), alpinumisoflavone (**6**, 0.0762%), 4′-*O*-methylalpinumisoflavone (**7**, 0.0046%), erysenegalensein E (**8**, 0.0181%), and 6,8-diprenylgenistein (**9**, 0.0055%), were isolated from the fruits of *C. tricuspidata*. The chemical structures were determined by interpretation of spectroscopic data, including MS and NMR spectra, as compared to the previously reported literature (supplementary data 1). The detailed isolation procedures are included in the supplementary materials and methods. The purity of each compound was more than 95%.

2.4. Ultra-Performance Liquid Chromatography (UPLC) analysis

The CTE50 was analysed using an Acquity UPLC system (Waters, Millford, MA, USA) with an Acquity UPLC BEH C18 column (1.7 μm, 2.1 × 150 mm i.d.). The mobile phase consisted of solvent A (0.05% formic acid in water) and solvent B (acetonitrile), which flowed at rate of 0.3 mL/min. The starting eluent was 40% B at 0 min, and the

proportion of B was increased linearly to 100% from 0 to 10 min, held constant at 100% for 11.5 min, and then returned to the initial condition over the course of 1.5 min to re-equilibrate the column. The sample injection volume was 4 μL for extract and 2 μL for compounds (CTE50: 3 mg/mL, OB, POB, and DPOB: 0.2 mg/mL). The column and sample managers were maintained at 35 and 15 °C, respectively, and the UV detection wavelength was monitored at 265 nm.

2.5. SH-SY5Y cell culture

The human neuroblastoma cell line SH-SY5Y (ATCC No. CRL-2266) was purchased from the American Type Culture Collection (Manassas, VA, USA) and cultured in DMEM supplemented with 10% heat-inactivated FBS and 1% penicillin/streptomycin at 37 °C in a humidified 5% CO_2 atmosphere. Test samples were dissolved in 10% DMSO, and the cells were treated within non-cytotoxic concentration ranges of test samples at a final concentration of 0.1% DMSO.

2.6. Measurement of cell viability

SH-SY5Y cells were plated at a density of 1×10^5 cells/200 μL/well in 96-well plates for 24 h, and the cells were simultaneously treated with 6-OHDA and test samples (0.16–20 μg/mL of 0–100% CTE; 0.2–25 μM of nine isolates) for 48 h. After treatment, cell viability was evaluated using the MTT assay as previously described (Koo et al., 2011). Briefly, the medium was removed, and the cells were incubated with fresh medium containing 0.5 mg/mL MTT for 4 h at 37 °C, after which the medium was gently removed. Formazan crystals were dissolved in 100 μL DMSO, and absorbance was measured at 540 nm using a microplate reader (SpectraMax M5, Molecular Devices, USA).

2.7. Measurement of intracellular ROS by flow cytometry

Intracellular ROS levels were measured by the 2′,7′-dichloro fluorescein diacetate (DCFH-DA) method as described previously (Kim et al., 2015). Briefly, SH-SY5Y cells were plated at a density of 1×10^6 cells/1 mL/well in 12-well plates for 24 h, simultaneously treated with 6-OHDA (75 μM) and test samples (0.16–20 μg/mL of 0–100% CTE, 0.2–25 μM of isolates) for 48 h, and washed three times with PBS. DCFH-DA (4 μM/mL in PBS) was then added, and afterwards, the cells were incubated for 30 min at 37 °C in the dark. The cells were then washed 3 times with PBS, and the fluorescence intensities of a total of 10,000 events were measured by the FL-1 channel of a flow cytometer (BD FACS Calibur™).

2.8. Measurement of proteasome activity in 6-OHDA-induced SH-SY5Y cells

Proteasome activity was determined using SH-SY5Y cells as previously described (Kim, Kwon, Lee, & Mar, 2015). Briefly, cells (1.0×10^5 cells/300 μL/well) were plated in 48-well plates for 24 h and then simultaneously treated with 6-OHDA (75 μM) and samples (0.16–20 μg/mL of CTE50, 0.2–25 μM of nine isolates) for 48 h. After washing twice with PBS, cells were lysed by freeze-thawing 3 times (between −70 °C and 37 °C, 5 min each) and scraped into PBS buffer. Supernatants were collected by centrifugation at 15,000 rpm (15 min, 4 °C), and the total protein concentration was determined by the Bradford method (Bradford, 1976). The proteolytic activity of the proteasomes was evaluated with a 20S proteasome activity kit (APT 280; Millipore, USA). In brief, supernatants (40 μg) were incubated for 2 h at 37 °C in the provided buffer with fluorophore-linked peptide substrates. Suc-LLVY-AMC (40 μM), Boc-LRR-AMC (40 μM), and Z-LLE-MCA (80 μM) were used as the substrates for chymotrypsin-, trypsin- and caspase-like protease activities, respectively. Reaction mixtures without cell lysates were used as negative controls, and aminomethylcoumarin (AMC) or methylcoumarylamide (MCA) fluorescence was measured at excitation/emission wavelengths of 380/460 and 380/440 nm, respectively, using a microplate reader (SpectraMax M5, Molecular Devices, USA).

2.9. Immunoprecipitation assay

Immunoprecipitation was performed as previously described with slight modifications (Chen et al., 2014). Briefly, SH-SY5Y cells were plated at a density of 2×10^6 cells/4 mL in 100-mm dishes for 24 h. The cells were then simultaneously treated with 6-OHDA (75 μM) and samples (0.8–20 μg/mL of CTE50, 1–25 μM of three orobol derivatives) for 48 h and washed three times with PBS. SH-SY5Y cells were homogenized and lysed in cold-lysis buffer (50 mM Tris, 1 mM PMSF, 150 mM NaCl, 50 mM NaF, 1% Nonidet P-40, 0.25% sodium deoxycholate, 10 mM sodium pyrophosphate) and centrifuged at 14,000g (10 min, 4 °C), and the supernatant was transferred to a new ep-tube and incubated with 2 μg of α-synuclein or synphilin-1 antibody overnight at 4 °C. The next day, A/G plus agarose beads were added and incubated overnight at 4 °C followed by 3 washes in cold-lysis buffer. The loading samples were adjusted to total volume of 30 μL with lysis buffer, and the immune-complexes were eluted at 95 °C on a heating block for 5 min, vortexed, and spun down by centrifugation at 15,000g for 10 min.

2.10. Western blot analysis

SH-SY5Y cells were plated at a density of 2×10^6 cells/4 mL in 60-mm dishes for 24 h. The cells were then simultaneously treated with 6-OHDA (75 μM) and samples (0.16–20 μg/mL of CTE50, 0.2–25 μM of three orobol derivatives) for 48 h, washed three times with PBS, and lysed with a PRO-PREP protein extraction solution at −20 °C for 20 min. After centrifugation at 13,000 rpm for 30 min, the supernatant was used as the total protein extract. Western blot analysis was accomplished as previously described (Ham et al., 2013). Briefly, protein extracts were separated by electrophoresis on a SDS-PAGE gel and then transferred to PVDF membranes. Then, the PVDF membranes were incubated overnight at 4 °C with primary antibodies followed by a 1-h incubation at RT with the secondary antibody. The blots were developed using WEST-Queen® ECL solution and analysed using LAS4000 (GE Healthcare, UK)

2.11. Statistical analysis

All experimental data are expressed as the mean ± standard deviation. Statistical significance between multiple groups was determined by one-way ANOVA (PRISM Graph Pad, San Diego, CA, USA). When the ANOVA showed a significant difference, Bonferroni's multiple comparison *post hoc* tests were conducted. A P value less than 0.05 was considered statistically significant.

3. Results

3.1. Protective effects against 6-OHDA-induced neuronal cell death in SH-SY5Y cells

Ethanol is often used to extract bioactive compounds from plant materials, and the bioactivity of plant extracts depends on the ratio of water to ethanol used in the extraction process (Ganora, 2009). We evaluated the neuroprotective effects within non-cytotoxic

Table 1
Inhibitory effects of ethanol extracts and isolates from the fruits of *C. tricuspidata* against 6-OHDA-induced cell death and ROS generation in SH-SY5Y cells.

Extract/Compound	Neuroprotective effect against 6-OHDA-induced cell death (EC_{50} value)	Inhibitory effect against 6-OHDA-induced ROS generation (IC_{50} value)
0% ethanol extract of *C. tricuspidata* fruit	>20 μg/mL	>20 μg/mL
30% ethanol extract of *C. tricuspidata* fruit	5.4 ± 0.8 μg/mL	10.2 ± 1.2 μg/mL
50% ethanol extract of *C. tricuspidata* fruit	3.3 ± 0.3 μg/mL	6.7 ± 0.7 μg/mL
70% ethanol extract of *C. tricuspidata* fruit	7.8 ± 0.9 μg/mL	14.2 ± 1.1 μg/mL
100% ethanol extract of *C. tricuspidata* fruit	>20 μg/mL	>20 μg/mL
(**1**) orobol	6.4 ± 0.5 μM	7.2 ± 0.6 μM
(**2**) 6-prenylorobol	4.5 ± 0.3 μM	5.9 ± 0.4 μM
(**3**) 6,8-diprenylorobol	10.1 ± 0.8 μM	17.3 ± 1.0 μM
(**4**) millewanin H	15.2 ± 1.3 μM	19.2 ± 1.5 μM
(**5**) millewanin G	18.5 ± 2.1 μM	22.4 ± 2.4 μM
(**6**) alpinumisoflavone	>25 μM	>25 μM
(**7**) 4′-O-methylalpinumisoflavone	>25 μM	>25 μM
(**8**) erysenegalensein E	>25 μM	>25 μM
(**9**) 6,8-diprenylgenistein	>25 μM	>25 μM

The EC_{50} & IC_{50} values were determined in a semi-logarithmic graph with 4 different concentrations. The values are presented as the mean ± standard deviation of three independent experiments.

concentration ranges from different CTE extracts (0%, 30%, 50%, 70%, and 100% ethanol) and nine isolates. As shown in Table 1, CTE50 showed the most potent protective effects with an EC_{50} value of 3.3 μg/mL. The constituents of CTE50 were identified using UPLC, and nine isolates were obtained (Fig. 1). Among the nine isolates, three orobol derivatives (OB, POB, and DPOB) significantly attenuated 6-OHDA-induced neurotoxicity with EC_{50} values of 6.4 μM, 4.5 μM, and 10.1 μM, respectively (Table. 1). As shown in Fig. S1, 6-OHDA-induced neuronal cell death was observed by the morphology of cells: 6-OHDA resulted in cellular morphological changes including cell shrinkage and rounding. However, treatment with CTE50 (20 μg/mL) or the three orobol derivatives (25 μM) ameliorated the 6-OHDA-induced morphological changes to almost normal levels. As shown in Fig. 2, the 6-OHDA-induced group showed a significant decrease in cell viability compared to the vehicle-treated group. However, CTE50 (0.16–20 μg/mL) or the three orobol derivatives (0.2–25 μM) protected 6-OHDA-induced neuronal cell death in a concentration-dependent manner. Additionally, we examined the comparison of neuroprotective effect of CTE50 and three orobol derivatives against 6-OHDA-induced neurotoxicity by pre-, co-, and post treatment. Among three groups, co-treatment group exerted potent neuroprotective effects (Fig. S5).

3.2. Inhibition of 6-OHDA-induced intracellular ROS generation

Excessive intracellular ROS induce cellular stress and neuronal cell death, and it has been reported that ROS play important roles in the pathogenesis of neurodegenerative diseases. As shown in Table 1, CTE50 showed the most potent inhibition of 6-OHDA-induced ROS generation with an IC_{50} value of 6.7 μg/mL. Among the nine compounds derived from CTE50, the three orobol derivatives showed a significant inhibitory effect against 6-OHDA-induced intracellular ROS generation with IC_{50} values of 7.2 μM (OB), 5.9 μM (POB), and 17.3 μM (DPOB). As shown in Figs. 2, 6-OHDA-treated cells showed strong DCF fluorescence intensities compared to vehicle-treated cells. The amount of intracellular ROS was decreased in a concentration-dependent manner when cells were treated with CTE50 (0.8–20 μg/mL) or the three orobol derivatives (1–25 μM).

3.3. Neuroprotective effects against 6-OHDA-induced apoptosis

It has been reported that 6-OHDA induces ROS-dependent apoptosis, which is characterized by the cleavage of caspase-9, caspase-3 and PARP. Excessive ROS accumulation results in the activation of the caspases (caspase-9 and caspase-3), and activated caspase-3 cleaves the DNA repair protein PARP; cleaved, activated PARP is final apoptotic marker. To investigate the inhibitory effects of CTE50 and three orobol derivatives on the levels of cleaved caspase-9, caspase-3, and PARP protein, we performed a western blot assay. As shown in Fig. 3, the cleavage levels of caspase-9, caspase-3, and PARP were increased when the SH-SY5Y cells were exposed to 6-OHDA. However, CTE50 (0.16–20 μg/mL) or the three orobol derivatives (0.2–25 μM) inhibited the cleavage of caspase-9, caspase-3, and PARP protein in a concentration-dependent manner in 6-OHDA-induced SH-SY5Y cells.

3.4. Protective effects against 6-OHDA-induced dysfunction of proteasome activity

Proteasome function is essential for cellular physiology and protein degradation. To evaluate the effects of CTE50 and the nine isolates against the dysfunction of proteasome activity induced by 6-OHDA in SH-SY5Y cells, we measured the activities of chymotrypsin-, trypsin- and caspase-like proteases. As shown in Table 2 and Fig. S3A, 6-OHDA significantly inhibited all three different types of proteasome activities; however, CTE50 most potently attenuated the 6-OHDA-induced dysfunction of proteasome activities from extracts (0–100%) with an EC_{50} value of 1.2 μg/mL (chymotrypsin-like), 1.5 μg/mL (trypsin-like), and 6.7 μg/mL (caspase-like). The three orobol derivatives at the concentration of 25 μM prominently protected against 6-OHDA-induced dysfunction of the proteasome and almost restored the activities to normal levels. (Fig. S3B–D).

3.5. Inhibition of 6-OHDA-induced ubiquitin-conjugated proteins

Proteasome dysfunction causes a reduction in the degradation of misfolded proteins, consequently resulting in the accumulation of polyubiquitinated proteins. To investigate the inhibitory effects of CTE50 and the three orobol derivatives against 6-OHDA-induced ubiquitin conjugated-protein formation, we performed western blot analysis. As shown in Figs. 3, 6-OHDA increased the levels of high molecular ubiquitin-conjugated proteins. When cells were treated with different concentrations of CTE50 (0.16–20 μg/mL) (Fig. 4A) or the three orobol derivatives (0.2–25 μM) (Fig. 4B–D), the levels of ubiquitin-conjugated proteins were decreased to normal in a concentration-dependent manner. CTE50 (20 μg/mL) and

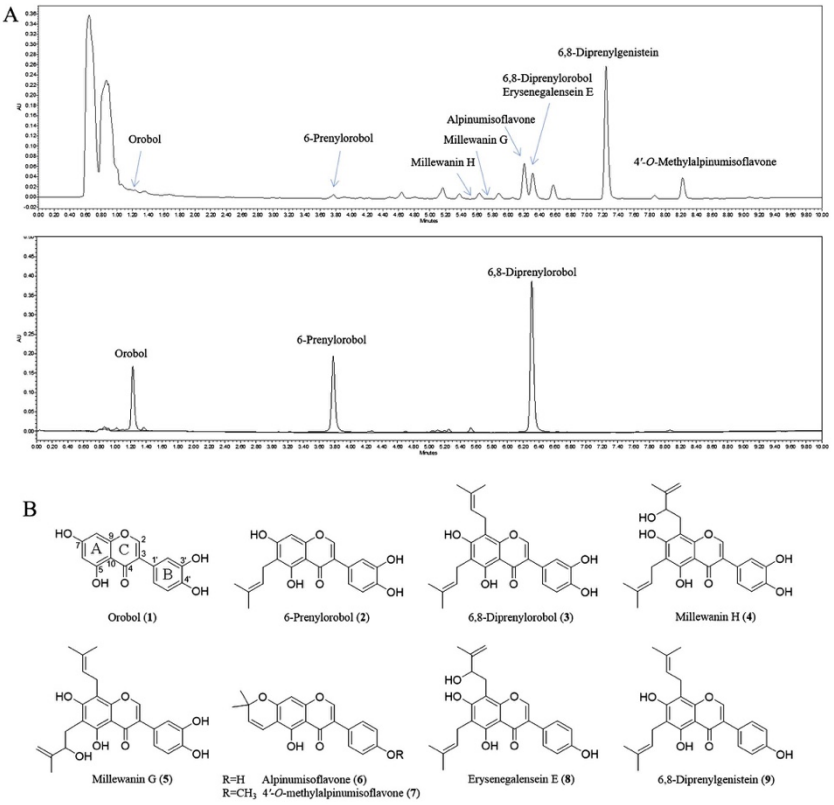

Fig. 1. UPLC chromatograms and structures of isolates from CTE50. (A) UPLC chromatogram of CTE50 and isolates from CTE50. Nine compounds were isolated from CTE50. Among nine isolates, orobol, 6-prenylorobol, and 6,8-diprenylorobol were selected for further study. The selected three orobol derivatives were confirmed the elution time for identification (B) Chemical structures of the isolates. The isolated compounds are orobol (**1**), 6-prenylorobol (**2**), 6,8-diprenylorobol (**3**), millewanin H (**4**), millewanin G (**5**), alpinumisoflavone (**6**), 4′-O-methylalpinumisoflavone (**7**), erysenegalensein E (**8**), and 6,8-diprenylgenistein (**9**).

the three orobol derivatives (25 μM) restored the ubiquitin-conjugated proteins to almost normal levels.

3.6. Inhibition of 6-OHDA-induced poly-ubiquitination of α-synuclein, and synphilin-1

Physiologically, polyubiquitinated proteins are normally rapidly degraded by the proteasome. However, dysfunction in proteasome activity increases the polyubiquitination of α-synuclein and synphilin-1, inducing neurotoxicity. As shown in Figs. 5, 6-OHDA increased the polyubiquitination of α-synuclein. When the cells were treated with different concentrations of CTE50 (0.8–20 μg/mL) or the three orobol derivatives (1–25 μM), the polyubiquitination of α-synuclein was restored to almost normal levels in a concentration-dependent manner (Fig. 5A–D). Additionally, as shown in Figs. 5, 6-OHDA increased the polyubiquitination of synphilin-1; however, CTE50 (0.8–20 μg/mL) and the three orobol derivatives (1–25 μM) reduced the polyubiquitinated synphilin-1 to almost normal levels in a concentration-dependent manner (Fig. 5E–H).

3.7. A proteasome inhibitor (MG-132) diminished the protective effects of CTE50 and the three orobol derivatives against 6-OHDA-induced neuronal cell death and proteasome dysfunction

It has been reported that proteasome inhibition induces dopaminergic neuronal cell degeneration and apoptosis (Park, Jun do, Han, Woo, & Kim, 2011). In contrast, proteasome activation

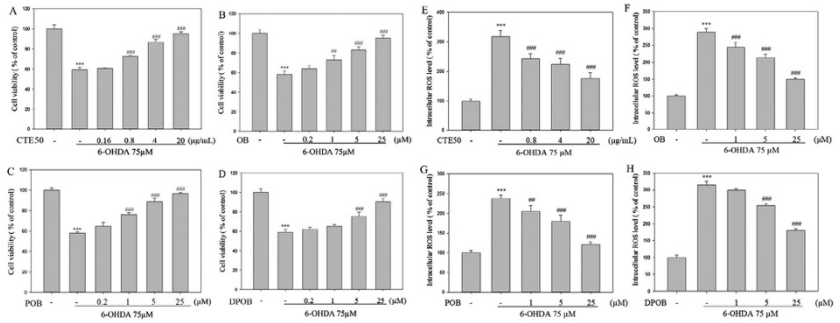

Fig. 2. Inhibitory effects of CTE50 and three orobol derivatives (OB, POB, and DPOB) against 6-OHDA-induced neurotoxicity and ROS generation. (A–D) Cells were cultured in 96-well plate for 24 h, and CTE50 or orobol derivatives were simultaneously treated with 6-OHDA (75 μM) for 48 h. Cell viability were measured by MTT reduction assay. (E–H) Cells were cultured in 12-well plate for 24 h, and CTE50 or three orobol derivatives were simultaneously treated with 6-OHDA (75 μM) for 48 h. The relative fluorescence intensities of total 10,000 events by FACs analysis were quantified. Data represent the mean ± SD of three independent experiments. (*** $p < 0.001$ versus control group, ## $p < 0.01$ and ### $p < 0.001$ versus 6-OHDA-induced group.)

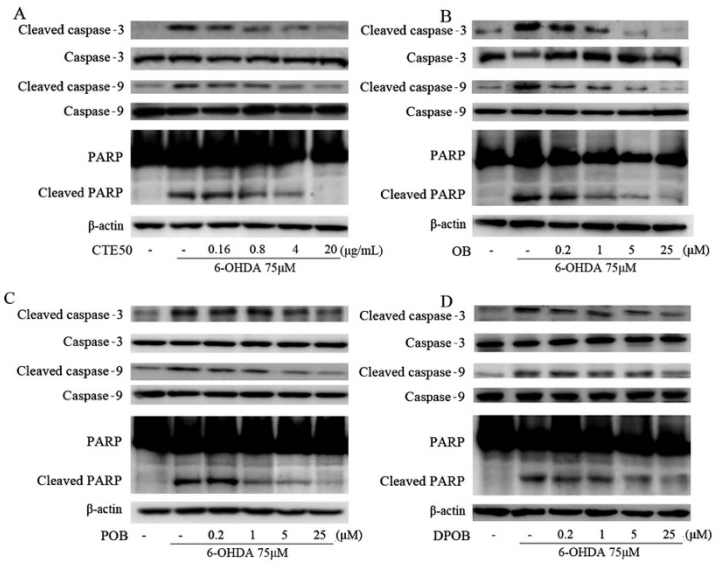

Fig. 3. Inhibitory effects of CTE50 and three orobol derivatives against 6-OHDA-induced apoptotic markers. Cells were simultaneously treated with 6-OHDA (75 μM) and (A) CTE50 or (B – D) three orobol derivatives for 48 h. The levels of cleaved caspase-9, caspase-3 and PARP were assessed by western blot; β-actin was used as a housekeeping protein. Representative data from three independent experiments are shown.

enhances survival in a neuronal model of neurodegenerative disease (Seo et al., 2007). To investigate whether the neuroprotective effects of CTE50 and the three orobol derivatives are due to the amelioration of proteasomal dysfunction, MG132, a proteasome inhibitor, was co-applied with the samples. As shown in Fig. 6A, CTE50 (20 μg/mL) and three orobol derivatives (25 μM) protected against 6-OHDA-induced neuronal cell death; however, co-treatment with MG132 (1 μM, non-cytotoxic concentration)

Table 2
The protective effects of ethanol extracts and isolates from the fruits of *C. tricuspidata* against 6-OHDA-induced proteasome dysfunction in SH-SY5Y cells.

Extract/Compound	Protective effect against 6-OHDA-induced dysfunction of proteasome activities		
	Chymotrypsin-like (EC_{50} value)	Trypsin-like (EC_{50} value)	Caspase-like (EC_{50} value)
0% ethanol extract of *C. tricuspidata* fruit	>20 μg/mL	>20 μg/mL	>20 μg/mL
30% ethanol extract of *C. tricuspidata* fruit	5.4 ± 0.4 μg/mL	9.5 ± 0.6 μg/mL	18.5 ± 1.5 μg/mL
50% ethanol extract of *C. tricuspidata* fruit	1.2 ± 0.3 μg/mL	1.5 ± 0.4 μg/mL	6.7 ± 0.8 μg/mL
70% ethanol extract of *C. tricuspidata* fruit	7.8 ± 0.7 μg/mL	13.2 ± 1.2 μg/mL	>20 μg/mL
100% ethanol extract of *C. tricuspidata* fruit	>20 μg/mL	>20 μg/mL	>20 μg/mL
(**1**) orobol	7.4 ± 0.3 μM	3.7 ± 0.3 μM	2.9 ± 0.2 μM
(**2**) 6-prenylorobol	6.8 ± 0.7 μM	3.9 ± 0.4 μM	1.3 ± 0.2 μM
(**3**) 6,8-diprenylorobol	7.9 ± 0.4 μM	4.2 ± 0.4 μM	1.8 ± 0.1 μM
(**4**) millewanin H	22.1 ± 2.0 μM	24.4 ± 2.1 μM	6.8 ± 0.4 μM
(**5**) millewanin G	24.4 ± 1.5 μM	5.9 ± 0.3 μM	1.2 ± 0.3 μM
(**6**) alpinumisoflavone	>25 μM	>25 μM	>25 μM
(**7**) 4′-O-methylalpinumisoflavone	>25 μM	>25 μM	>25 μM
(**8**) erysenegalensein E	>25 μM	>25 μM	>25 μM
(**9**) 6,8-diprenylgenistein	>25 μM	>25 μM	>25 μM

The EC_{50} values were determined in a semi-logarithmic graph with 4 different concentrations. The values are presented as the mean ± standard deviation of three independent experiments.

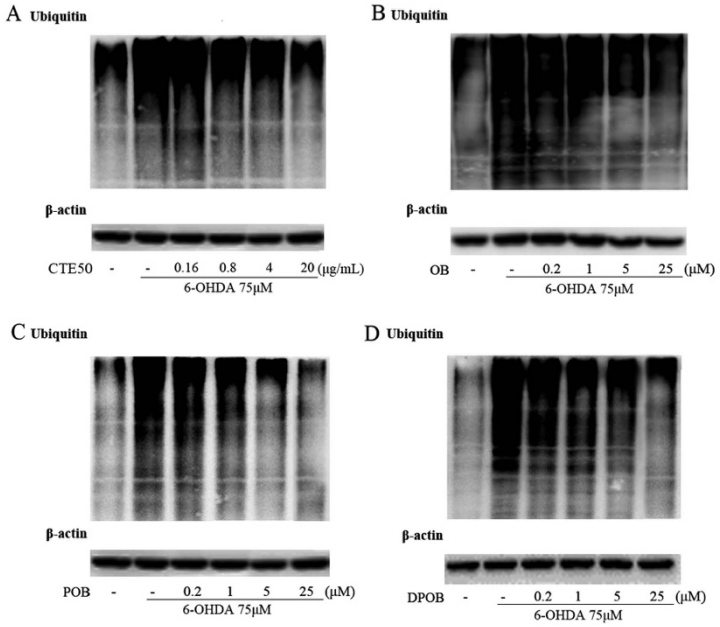

Fig. 4. Inhibitory effects of CTE50 and three orobol derivatives against 6-OHDA-induced ubiquitin-conjugated proteins. Cells were simultaneously treated with 6-OHDA (75 μM) and (A) CTE50 or (B–D) three orobol derivatives for 48 h. The levels of ubiquitin-conjugated proteins were determined by western blot; β-actin was used as a housekeeping protein. Representative data from three independent experiments are shown.

significantly blocked the protective effects of CTE50 and the three orobol derivatives against 6-OHDA-induced cell death. Additionally, MG132 (1 μM) blocked the recovery effects of CTE50 and the three orobol derivatives against 6-OHDA-induced proteasome dysfunction (Fig. 6B).

4. Discussion

As the world's population is rapidly ageing, the number of patients suffering from PD is increasing significantly. Although the cause of PD has not been definitively verified, recent research

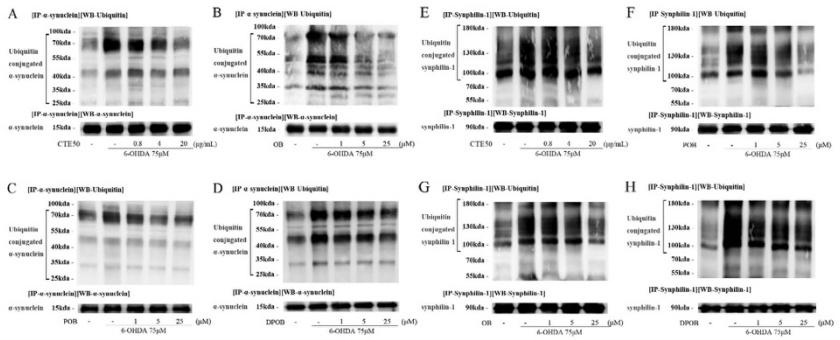

Fig. 5. Inhibitory effects of CTE50 and three orobol derivatives against 6-OHDA-induced polyubiquitination of α-synuclein and synphilin-1. Cells were simultaneously treated with 6-OHDA (75 μM) and (A, E) CTE50 or (B–D, F–H) three orobol derivatives for 48 h. The polyubiquitination of α-synuclein and synphilin-1 was determined by immunoprecipitation and western blot analysis. Representative data from three independent experiments are shown.

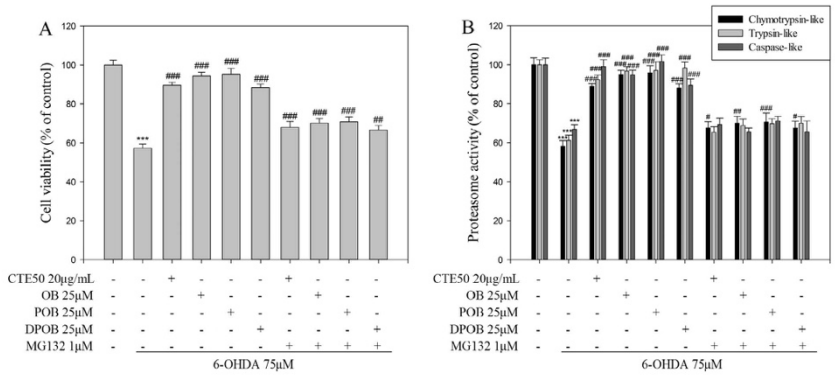

Fig. 6. Inhibitory effects of MG132 on the protective effects of CTE50 and three orobol derivatives against 6-OHDA-induced neuronal cell death and proteasome dysfunction. (A) The protective effects of CTE50 and three orobol derivatives 6-OHDA-induced neuronal cell death were blocked by MG132. Cell viability was measured by the MTT reduction assay. (B) The protective effects of CTE50 and three orobol derivatives against 6-OHDA-induced proteasome dysfunction were blocked by MG132. Three types of proteasome activity were measured using a multi-plate reader with fluorophore-linked peptide substrates. Data represent the mean ± SD of three independent experiments. (*** $p < 0.001$ versus control group, # $p < 0.05$, ## $p < 0.01$, and ### $p < 0.001$ versus 6-OHDA-induced group.)

findings have suggested that oxidative stress and the impairment of the proteasome are major events in its pathogenesis (Ciechanover & Kwon, 2015). Oxidative stress has been implicated in ageing and neurodegenerative diseases such as PD. Oxidative stress induces the oxidation and aggregation of proteins in the brain (Butterfield & Kanski, 2001). In addition, excessive oxidative stress advances cellular apoptosis through the accumulation of oxidized proteins (Klovekorn & Munch, 1998). Many studies have reported that protein homeostasis is essential for cellular physiology and that the proteasome is responsible for selectively degrading targets including short-lived, damaged or misfolded protein, which comprise approximately 80% of all intracellular proteins. Hence, considerable interest has been paid to the importance of the role of the proteasome. The ubiquitination process is activated by ubiquitin-activating enzymes (E1), ubiquitin-conjugating enzymes (E2), and ubiquitin-transferring enzymes (E3). Through a sequential enzymatic reaction, proteins are polyubiquitinated by E3 ligase. The polyubiquitin chain is recognized by the regulatory domain of the proteasome, in which the target protein is degraded by the catalytic core domain (Amm, Sommer, & Wolf, 2014). Under normal conditions, polyubiquitinated proteins are rapidly degraded and do not accumulate. The accumulation of polyubiquitinated proteins is observed when excessive intracellular ROS, cellular stress, and diverse stress impair proteasome function (Elkon, Melamed, & Offen, 2004), and the accumulation of polyubiquitinated proteins induces neurotoxicity and neurodegeneration. Thus, the restoration of proteasome activity through the down-regulation of intracellular ROS is one of the primary

mechanisms regulating ubiquitin-conjugated proteins, Lewy body-associated α-synuclein, and synphilin-1 proteins and the protection against neuronal cell death.

In the present study, 6-OHDA-induced ROS generation decreased in a concentration-dependent manner when cells were treated with different concentrations of CTE50 or the three orobol derivatives, and these compounds significantly elicited their neuroprotective effects against 6-OHDA-induced cell death and inhibited 6-OHDA-induced changes in cell morphology including shrinkage and rounding. In addition, we evaluated the inhibitory effects of CTE50 and the three orobol derivatives on the levels of cleaved caspase-9, caspase-3 and PARP, which are apoptosis signal factors; 6-OHDA treatment increased the levels of cleaved caspase-9, caspase-3 and PARP protein; however, these increases were inhibited by co-treatment with CTE50 and the three orobol derivatives. A previous study demonstrated that the inhibitory effect of (−)-epigallocatechin-3-gallate (EGCG) on ROS generation led to a suppression of apoptosis (Ning et al., 2016). In our results, the inhibitory effects of CTE50 and three orobol derivatives on ROS generation are also concomitant with the protection against neuronal cell death and the activation of apoptosis signalling markers. Based on the neuroprotective effects of three orobol derivatives, we evaluated structure-bioactivity relationship (SAR). The compounds with two hydroxy groups at C-3′ and C-4′ in B-ring of flavonoid (**1–5**) exhibited neuroprotective effects, whereas the others with one hydroxy group at C-4′ (**6–9**) did not. This suggested that the hydroxy group in the B-ring of flavonoid influences neuroprotective effects. The neuroprotective effect of preny groups is not clear from 9 isolates to evaluate SAR. Therefore, further study will be necessary to evaluate SAR with prenylated flavonoids on neuroprotective activity.

A recent study emphasized the role of the proteasome in neurodegenerative disease and showed that proteasome inhibition induced neurotoxicity via the accumulation of polyubiquitinated proteins and protein aggregation (Canu et al., 2000). As neuronal cells are vulnerable to the accumulation of polyubiquitinated proteins, several neurodegenerative diseases are related to the neurotoxicity resulting from protein accumulation. It has been shown that proteasome activity can gradually decrease with ageing and environmental stress, among other reasons, which results in a reduced ability to degrade misfolded proteins, contributing to the development of pathological protein aggregates (Ciechanover & Kwon, 2015). In cellular models, proteasome inhibition induced apoptosis and neuronal cell degeneration (Park et al., 2011; Sun et al., 2006), whereas proteasome activation enhanced neuronal cell survival (Seo et al., 2007). Thus, the protection against proteasome dysfunction could be a possible therapeutic strategy for neuroprotection. To investigate the mechanism underlying the protective effects of CTE50 and the three orobol derivatives against 6-OHDA-induced neuronal cell death, chymotrypsin-, trypsin-, and caspase-like proteasome activities were measured in SH-SY5Y cells. Our results showed that 6-OHDA significantly inhibited all three types of proteasome activities due to excessive ROS generation, and these results correlate with previously reported studies (Elkon et al., 2004). CTE50 and the three orobol derivatives at concentration of 20 μg/mL and 25 μM, respectively, attenuated 6-OHDA-induced dysfunction of the proteasome and nearly restored proteasome activities to normal levels. Additionally, we measured the levels of ubiquitin-conjugated proteins and found an increase following 6-OHDA treatment. However, CTE50 (20 μg/mL) and the three orobol derivatives (25 μM) attenuated the 6-OHDA-induced increase in ubiquitin-conjugated protein levels to almost normal. These results suggested that 6-OHDA-induced proteasome dysfunction triggers the accumulation of ubiquitin-conjugated proteins, leading to neuronal cell death; however, CTE50 and the three orobol derivatives prevented the dysfunction of ubiquitin proteasome system (UPS) and protected against neuronal cell death. The impairment of UPS is involved in the formation of Lewy bodies, which is a characteristic hallmark of PD. Lewy bodies are composed of abnormal filamentous aggregates containing α-synuclein, and synphilin-1 has been found to colocalize with α-synuclein in Lewy bodies. It has been demonstrated that the overexpression of α-synuclein in *Drosophila* and *C. elegans* induced neuronal cell loss (Kontopoulos, Parvin, & Feany, 2006; Pesah et al., 2005). It has also been reported that α-synuclein filaments and oligomers themselves inhibited proteasome activities (Lindersson et al., 2004). Synphilin-1 has been reported to enhance the aggregation and neurotoxicity of α-synuclein (Buttner et al., 2010) and to promote inclusion formation under conditions of proteasome inhibition. Additionally, it has been reported that synphilin-1 inhibits the degradation of α-synuclein by the proteasome and thus increases the half-life of α-synuclein (Alvarez-Castelao & Castano, 2011). Therefore, it has been suggested that the regulation of α-synuclein and synphilin-1 through UPS is important for neuroprotection (Sidhu, Wersinger, Moussa, & Vernier, 2004). It was also previously reported that a relationship exists between proteasome dysfunction and neuronal cell death. Proteasome inhibition triggers a dramatic activation of the pro-apoptotic caspase-3,-9, PARP and DNA fragment (Sun et al., 2006; Yuan, Chapman, & Reynolds, 2008). The proteasome inhibitor MG132 induces dopaminergic neuronal cell degeneration and apoptosis (Park et al., 2011), and bortezomib, a proteasome inhibitor, induces caspase-dependent apoptosis. In contrast, a proteasome activator enhances the survival of neuronal cells (Seo et al., 2007), and betulinic acid and demethylsuberosin, reported to be proteasome activators, showed neuroprotective effects (Eksioglu-Demiralp et al., 2010; Kim, Kwon et al., 2015). In our results, 6-OHDA-induced proteasome dysfunction resulted in the polyubiquitination of α-synuclein and synphilin-1 protein. However, CTE50 and the three orobol derivatives reduced the levels of 6-OHDA-induced polyubiquitination of α-synuclein and synphilin-1 protein in addition to ameliorating the dysfunction of proteasome activities. Furthermore, treatment with MG132, a proteasome inhibitor, significantly reduced the protective effects of CTE50 and the three orobol derivatives against 6-OHDA-induced neuronal cell death and proteasome dysfunction, suggesting that their neuronal cell protective effects are partly due to the protection against proteasome dysfunction. In spite of the evidence for neuroprotection by orobol derivatives, there has been little research reported on the blood-brain barrier (BBB) permeability of orobol derivatives. However, some studies have demonstrated that isoflavones and several metabolites have been proven to transverse the BBB (Chandrasekharan & Aglin, 2013; Youdim et al., 2003). Therfore, BBB permeability of orobol and its derivatives should be studied to elucidate its potential for permeation across BBB in the further study.

In conclusion, this study demonstrated that CTE50 and three orobol derivatives protected against neuronal cell death and ROS generation, and attenuated proteasome dysfunction, the accumulation of ubiquitin-conjugated proteins, and the levels of polyubiquitinated α-synuclein and synphilin-1, the constituents of Lewy bodies. However, the neuroprotective effects of CTE50 and three orobol derivatives and the attenuation of proteasome dysfunction were significantly inhibited by MG132, suggesting their neuroprotective effects are partly due to the protection of the ubiquitin/proteasome-dependent degradation of α-synuclein and synphilin-1. Based on our results, we suggest that CTE50 and the three orobol derivatives might be promising candidates for the therapy of neurodegenerative diseases such as PD.

Conflict of interest

The authors have declared that there are no conflicts of interest.

Acknowledgements

This work was supported by the Basic Science Research Program through the National Research Foundation of Korea (NRF) (Grant No. NRF-2013R1A1A2008111) and the BK21 Plus Program through the National Research Foundation (NRF) funded by the Ministry of Education of Korea.

Appendix A. Supplementary material

Supplementary data associated with this article can be found, in the online version, at http://dx.doi.org/10.1016/j.jff.2016.12.017.

References

Alvarez-Castelao, B., & Castano, J. G. (2011). Synphilin-1 inhibits alpha-synuclein degradation by the proteasome. *Cellular and Molecular Life Sciences, 68*(15), 2643–2654. http://dx.doi.org/10.1007/s00018-010-0592-3.

Amm, I., Sommer, T., & Wolf, D. H. (2014). Protein quality control and elimination of protein waste: the role of the ubiquitin-proteasome system. *Biochimica et Biophysica Acta, 1843*(1), 182–196. http://dx.doi.org/10.1016/j.bbamcr.2013.06.031.

Bochkov, V. N., Oskolkova, O. V., Birukov, K. G., Levonen, A. L., Binder, C. J., & Stockl, J. (2010). Generation and biological activities of oxidized phospholipids. *Antioxidants & Redox Signaling, 12*(8), 1009–1059. http://dx.doi.org/10.1089/ars.2009.2597.

Bradford, M. M. (1976). A rapid and sensitive method for the quantitation of microgram quantities of protein utilizing the principle of protein-dye binding. *Analytical Biochemistry, 72*, 248–254.

Butterfield, D. A., & Kanski, J. (2001). Brain protein oxidation in age-related neurodegenerative disorders that are associated with aggregated proteins. *Mechanisms of Ageing and Development, 122*(9), 945–962.

Buttner, S., Delay, C., Franssens, V., Bammens, T., Ruli, D., Zaunschirm, S., ... Winderickx, J. (2010). Synphilin-1 enhances alpha-synuclein aggregation in yeast and contributes to cellular stress and cell death in a Sir2-dependent manner. *PLoS One, 5*(10), e13700. http://dx.doi.org/10.1371/journal.pone.0013700.

Canu, N., Barbato, C., Ciotti, M. T., Serafino, A., Dus, L., & Calissano, P. (2000). Proteasome involvement and accumulation of ubiquitinated proteins in cerebellar granule neurons undergoing apoptosis. *Journal of Neuroscience, 20*(2), 589–599.

Chandrasekharan, S., & Aglin, A. (2013). Pharmacokinetics of dietary isoflavones. *Journal of Steroids & Hormonal Science, 2014*.

Chen, S., Zhu, P., Guo, H. M., Solis, R. S., Wang, Y. Q., Ma, Y. N., ... Li, J. (2014). Alpha1 catalytic subunit of AMPK modulates contractile function of cardiomyocytes through phosphorylation of troponin I. *Life Sciences, 98*(2), 75–82. http://dx.doi.org/10.1016/j.lfs.2014.01.006.

Ciechanover, A., & Kwon, Y. T. (2015). Degradation of misfolded proteins in neurodegenerative diseases: therapeutic targets and strategies. *Experimental & Molecular Medicine, 47*, e147. http://dx.doi.org/10.1038/emm.2014.117.

Cookson, M. R. (2005). The biochemistry of Parkinson's disease». *Annual Review of Biochemistry, 74*, 29–52.

Dahlmann, B. (2007). Role of proteasomes in disease. *BMC Biochemistry, 8*(Suppl 1), S3. http://dx.doi.org/10.1186/1471-2091-8-S1-S3.

Eksioglu-Demiralp, E., Kardas, E. R., Ozgul, S., Yagci, T., Bilgin, H., Sehirli, O., ... Sener, G. (2010). Betulinic acid protects against ischemia/reperfusion-induced renal damage and inhibits leukocyte apoptosis. *Phytotherapy Research, 24*(3), 325–332. http://dx.doi.org/10.1002/ptr.2929.

Elkon, H., Melamed, E., & Offen, D. (2004). Oxidative stress, induced by 6-hydroxydopamine, reduces proteasome activities in PC12 cells - Implications for the pathogenesis of Parkinson's disease. *Journal of Molecular Neuroscience, 24*(3), 387–400. http://dx.doi.org/10.1385/jmn:24:3:387.

Fujimoto, T., Hano, Y., & Nomura, T. (1984). Components of root bark of cudrania tricuspidata 11,2 structures of four new isoprenylated xanthones, cudraxanthones A, B, C and D. *Planta Medica, 50*(3), 218–221. http://dx.doi.org/10.1055/s-2007-969682.

Ganora, L. (2009). *Herbal constituents: Foundations of phytochemistry*. Louisville CO: Lisa Ganora.

Ham, A., Kim, D. W., Kim, K. H., Lee, S. J., Oh, K. B., Shin, J., & Mar, W. (2013). Reynosin protects against neuronal toxicity in dopamine-induced SH-SY5Y cells and 6-hydroxydopamine-lesioned rats as models of Parkinson's disease: Reciprocal up-regulation of E6-AP and down-regulation of alpha-synuclein. *Brain Research, 1524*, 54–61. http://dx.doi.org/10.1016/j.brainres.2013.05.036.

Hano, Y., Matsumoto, Y., Shinohara, K., Sun, J. Y., & Nomura, T. (1991). Structures of four new isoprenylated xanthones, cudraxanthones L, M, N, and O from cudrania tricuspidata1,2. *Planta Medica, 57*(2), 172–175. http://dx.doi.org/10.1055/s-2006-960059.

Hiep, N. T., Kwon, J., Kim, D. W., Hwang, B. Y., Lee, H. J., Mar, W., & Lee, D. (2015). Isoflavones with neuroprotective activities from fruits of *Cudrania tricuspidata*. *Phytochemistry, 111*, 141–148. http://dx.doi.org/10.1016/j.phytochem.2014.10.021.

Huang, Q., & Figueiredo-Pereira, M. E. (2010). Ubiquitin/proteasome pathway impairment in neurodegeneration: therapeutic implications. *Apoptosis, 15*(11), 1292–1311. http://dx.doi.org/10.1007/s10495-010-0466-z.

Jeong, C. H., Choi, G. N., Kim, J. H., Kwak, J. H., Jeong, H. R., Kim, D. O., & Heo, H. J. (2010). Protective effects of aqueous extract from cudrania tricuspidata on oxidative stress-induced neurotoxicity. *Food Science and Biotechnology, 19*(4), 1113–1117. http://dx.doi.org/10.1007/s10068-010-0158-z.

Jeong, J. Y., Jo, Y. H., Lee, K. Y., Do, S. G., Hwang, B. Y., & Lee, M. K. (2014). Optimization of pancreatic lipase inhibition by *Cudrania tricuspidata* fruits using response surface methodology. *Bioorganic & Medicinal Chemistry Letters, 24*(10), 2329–2333. http://dx.doi.org/10.1016/j.bmcl.2014.03.067.

Jung, T., & Grune, T. (2013). The proteasome and the degradation of oxidized proteins: Part I-structure of proteasomes. *Redox Biology, 1*, 178–182. http://dx.doi.org/10.1016/j.redox.2013.01.004.

Kanthasamy, A., Jin, H., Mehrotra, S., Mishra, R., Kanthasamy, A., & Rana, A. (2010). Novel cell death signaling pathways in neurotoxicity models of dopaminergic degeneration: Relevance to oxidative stress and neuroinflammation in Parkinson's disease. *Neurotoxicology, 31*(5), 555–561. http://dx.doi.org/10.1016/j.neuro.2009.12.003.

Kim, B.-H., Kwon, J., Lee, D., & Mar, W. (2015). Neuroprotective effect of demethylsuberosin, a proteasome activator, against MPP+-induced Cell death in human neuroblastoma SH-SY5Y cells. *Planta Medica Letters, 2*(01), e15–e18.

Kim, D.-W., Lee, K.-T., Kwon, J., Lee, H. J., Lee, D., & Mar, W. (2015). Neuroprotection against 6-OHDA-induced oxidative stress and apoptosis in SH-SY5Y cells by 5, 7-dihydroxychromone: Activation of the Nrf2/ARE pathway. *Life Sciences, 130*, 25–30.

Klovekorn, P., & Munch, J. (1998). Variable optical delay line with diffraction-limited autoalignment. *Applied Optics, 37*(10), 1903–1904.

Kontopoulos, E., Parvin, J. D., & Feany, M. B. (2006). Alpha-synuclein acts in the nucleus to inhibit histone acetylation and promote neurotoxicity. *Human Molecular Genetics, 15*(20), 3012–3023. http://dx.doi.org/10.1093/hmg/ddl243.

Koo, U., Nam, K. W., Ham, A., Lyu, D., Kim, B., Lee, S. J., ... Shin, J. (2011). Neuroprotective effects of 3alpha-acetoxyeudesma-1,4(15),11(13)-trien-12,6alpha-olide against dopamine-induced apoptosis in the human neuroblastoma SH-SY5Y cell line. *Neurochemical Research, 36*(11), 1991–2001. http://dx.doi.org/10.1007/s11064-011-0523-1.

Lee Ha, H., Lee, J. K., Seo, C. S., Lee, N. H., Jung, D. Y., ... Shin, H. K. (2012). The fruits of *Cudrania tricuspidata* suppress development of atopic dermatitis in NC/Nga mice. *Phytotherapy Research, 26*(4), 594–599. http://dx.doi.org/10.1002/ptr.3577.

Lee, I. K., Kim, C. J., Song, K. S., Kim, H. M., Koshino, H., Uramoto, M., & Yoo, I. D. (1996). Cytotoxic benzyl dihydroflavonols from *Cudrania tricuspidata*. *Phytochemistry, 41*(1), 213–216.

Lee, T., Kwon, J., Lee, D., & Mar, W. (2015). Effects of *Cudrania tricuspidata* fruit extract and its active compound, 5,7,3',4'-Tetrahydroxy-6,8-diprenylisoflavone, on the high-affinity IgE receptor-mediated activation of syk in mast cells. *Journal of Agricultural and Food Chemistry, 63*(22), 5459–5467. http://dx.doi.org/10.1021/acs.jafc.5b00903.

Lindersson, E., Beedholm, R., Hojrup, P., Moos, T., Gai, W., Hendil, K. B., & Jensen, P. H. (2004). Proteasomal inhibition by alpha-synuclein filaments and oligomers. *Journal of Biological Chemistry, 279*(13), 12924–12934. http://dx.doi.org/10.1074/jbc.M306390200.

McNaught, K. S., & Jenner, P. (2001). Proteasomal function is impaired in substantia nigra in Parkinson's disease. *Neuroscience Letters, 297*(3), 191–194.

Ning, W., Wang, S., Liu, D., Fu, L., Jin, R., & Xu, A. (2016). Potent effects of peracetylated (−)-epigallocatechin-3-gallate against hydrogen peroxide-induced damage in human epidermal melanocytes via attenuation of oxidative stress and apoptosis. *Clinical and Experimental Dermatology, 41*(6), 616–624. http://dx.doi.org/10.1111/ced.12855.

Okamoto, Y., Suzuki, A., Ueda, K., Ito, C., Itoigawa, M., Furukawa, H., ... Kojima, N. (2006). Anti-estrogenic activity of prenylated isoflavones from Millettia pachycarpa: Implications for pharmacophores and unique mechanisms. *Journal of Health Science, 52*(2), 186–191.

Park, H. S., Jun do, Y., Han, C. R., Woo, H. J., & Kim, Y. H. (2011). Proteasome inhibitor MG132-induced apoptosis via ER stress-mediated apoptotic pathway and its potentiation by protein tyrosine kinase p56lck in human Jurkat T cells. *Biochemical Pharmacology, 82*(9), 1110–1125. http://dx.doi.org/10.1016/j.bcp.2011.07.085.

Park, K. H., Park, Y. D., Han, J. M., Im, K. R., Lee, B. W., Jeong, I. Y., ... Lee, W. S. (2006). Anti-atherosclerotic and anti-inflammatory activities of catecholic xanthones and flavonoids isolated from *Cudrania tricuspidata*. *Bioorganic & Medicinal Chemistry Letters, 16*(21), 5580–5583. http://dx.doi.org/10.1016/j.bmcl.2006.08.032.

Pesah, Y., Burgess, H., Middlebrooks, B., Ronningen, K., Prosser, J., Tirunagaru, V., ... Mardon, G. (2005). Whole-mount analysis reveals normal numbers of dopaminergic neurons following misexpression of alpha-Synuclein in Drosophila. *Genesis, 41*(4), 154–159. http://dx.doi.org/10.1002/gene.20106.

Seo, W. G., Pae, H. O., Oh, G. S., Chai, K. Y., Yun, Y. G., Chung, H. T., ... Kwon, T. O. (2001). Ethyl acetate extract of the stem bark of Cudrania tricuspidata induces apoptosis in human leukemia HL-60 cells. *American Journal of Chinese Medicine, 29*(2), 313–320. http://dx.doi.org/10.1142/S0192415X01000332.

Seo, H., Sonntag, K. C., Kim, W., Cattaneo, E., & Isacson, O. (2007). Proteasome activator enhances survival of Huntington's disease neuronal model cells. *PLoS One, 2*(2), e238. http://dx.doi.org/10.1371/journal.pone.0000238.

Shiotsuka, S., & Isonishi, S. (2001). Differential sensitization by orobol in proliferating and quiescent human ovarian carcinoma cells. *International Journal of Oncology, 18*(2), 337–342.

Sidhu, A., Wersinger, C., Moussa, C. E. H., & Vernier, P. (2004). The role of α-synuclein in both neuroprotection and neurodegeneration. *Annals of the New York Academy of Sciences, 1035*(1), 250–270.

Sun, F., Anantharam, V., Zhang, D., Latchoumycandane, C., Kanthasamy, A., & Kanthasamy, A. G. (2006). Proteasome inhibitor MG-132 induces dopaminergic degeneration in cell culture and animal models. *Neurotoxicology, 27*(5), 807–815. http://dx.doi.org/10.1016/j.neuro.2006.06.006.

Tai, H. C., & Schuman, E. M. (2008). Ubiquitin, the proteasome and protein degradation in neuronal function and dysfunction. *Nature Reviews Neuroscience, 9*(11), 826–838. http://dx.doi.org/10.1038/nrn2499.

Uddin, G. M., Jeon, J. S., & Kim, C. Y. (2011). Isolation of prenylated isoflavonoids from *Cudrania tricuspidata* fruits that inhibit A2E photooxidation. *Natural Product Sciences, 17*(3), 206–211.

Youdim, K. A., Dobbie, M. S., Kuhnle, G., Proteggente, A. R., Abbott, N. J., & Rice-Evans, C. (2003). Interaction between flavonoids and the blood–brain barrier: in vitro studies. *Journal of Neurochemistry, 85*(1), 180–192.

Yuan, B. Z., Chapman, J. A., & Reynolds, S. H. (2008). Proteasome inhibitor MG132 induces apoptosis and inhibits invasion of human malignant pleural mesothelioma cells. *Transl Oncol, 1*(3), 129–140.

Life Sciences 130 (2015) 25–30

Contents lists available at ScienceDirect

Life Sciences

journal homepage: www.elsevier.com/locate/lifescie

Neuroprotection against 6-OHDA-induced oxidative stress and apoptosis in SH-SY5Y cells by 5,7-Dihydroxychromone: Activation of the Nrf2/ARE pathway ☆

Dong-Woo Kim [a], Kyoung-tae Lee [b], Jaeyoung Kwon [c], Hak Ju Lee [b], Dongho Lee [c,*], Woongchon Mar [a,**]

[a] Natural Products Research Institute, College of Pharmacy, Seoul National University, Seoul 151-742, Republic of Korea
[b] Division of Wood Chemistry & Microbiology, Department of Forest Products, Korea Forest Research Institute, Seoul 130-712, Republic of Korea
[c] Department of Biosystems and Biotechnology, Korea University, Seoul 136-713, Republic of Korea

ARTICLE INFO

Article history:
Received 31 October 2014
Received in revised form 3 February 2015
Accepted 28 February 2015
Available online 26 March 2015

Keywords:
5,7-Dihydroxychromone
Oxidative stress
6-OHDA
Nrf2/ARE pathway
Neuroprotection
Cudrania tricuspidata

ABSTRACT

Aims: The aim of this study was to prove the neuroprotective effect of 5,7-Dihydroxychromone (DHC) through the Nrf2/ARE signaling pathway. To elucidate the mechanism, we investigated whether 6-hydroxydopamine (6-OHDA)-induced neurotoxicity in SH-SY5Y cells could be attenuated by DHC via activating the Nrf2/ARE signal and whether DHC could down-regulate 6-OHDA-induced excessive ROS generation

Main methods: To evaluate the neuroprotective effect of DHC against 6-OHDA-induced apoptosis, FACS analysis was performed using PI staining. The inhibitory effect of DHC against 6-OHDA-induced ROS generation was evaluated by DCFH-DA staining assay. Additionally, translocation of Nrf2 to the nucleus and increased Nrf2/ARE binding activity, which subsequently resulted in the up-regulation of the Nrf2-dependent antioxidant gene expressions including HO-1, NQO1, and GCLc, were evaluated by Western blotting and EMSA.

Key findings: Pre-treatment of DHC, one of the constituents of *Cudrania tricuspidata*, significantly protects 6-OHDA-induced neuronal cell death and ROS generation. Also, DHC inhibited the expression of activated caspase-3 and caspase-9 and cleaved PARP in 6-OHDA-induced SH-SY5Y cells. DHC induced the translocation of Nrf2 to the nucleus and increased Nrf2/ARE binding activity which results in the up-regulation of the expression of Nrf2-dependent antioxidant genes, including HO-1, NQO1, and GCLc. The addition of Nrf2 siRNA abolished the neuroprotective effect of DHC against 6-OHDA-induced neurotoxicity and the expression of Nrf2-mediated antioxidant genes.

Significance: Activation of Nrf2/ARE signal by DHC exerted neuroprotective effects against 6-OHDA-induced oxidative stress and apoptosis. This finding will give an insight that activating Nrf2/ARE signal could be a new potential therapeutic strategy for neurodegenerative disease.

1. Introduction

The incidence of neurodegenerative diseases is increasing with the continuous growth of the elderly population. Although the causes of neurodegenerative diseases have not been clearly elucidated, recent studies have demonstrated that reactive oxygen species (ROS) might be one of the important factors in neurotoxicity that occurs in neurodegenerative diseases [3]. Increased ROS production causes impairment to cell organelles. Many studies have confirmed the benefits of antioxidants in reducing oxidative stress in neurons and protecting against neurodegenerative diseases [1].

In response to excessive ROS, the cellular expressions and bioactivity of numerous antioxidant enzymes are changed via initiating the upstream factor NF-E2-related factor 2 (Nrf2)/antioxidant response element (ARE) complex [12]. The Nrf2/ARE signal has an important effect on the induction of antioxidant gene expression, and it has been reported that the activation of Nrf2 is an important signal which can neutralize oxidative stress [24]. Under normal state, Nrf2 is localized in the cytoplasm and is subject to ubiquitination and proteasomal degradation. However, antioxidant agents block the elimination of Nrf2 from the cytosolic Nrf2 complex, which induces nuclear translocation of Nrf2 and subsequently makes the Nrf2/ARE complex mediate the induction of many antioxidant enzyme genes, such as heme oxygenase 1 (HO-1), NAD(P)H:quinone oxidoreductase (NQO1), and glutamate–cysteine ligase catalytic (GCLc) subunit [27]. Numerous research results reported that Nrf2 and Nrf2 dependent antioxidant genes are potent factors for developing the therapy of neurodegenerative diseases due to its ability to regulate the excessive oxidative stress and inflammation.

☆ English language in this manuscript was edited and revised by a professional editorial service, Elsevier Language Editing (Kidlington, UK. http://webshop.elsevier.com).

* Corresponding author. Tel.: +82 2 3290 3017; fax: +82 2 953 0737.
** Corresponding author. Tel.: +82 2 880 2473; fax: +82 2 888 9122.
E-mail address: dongholee@korea.ac.kr (D. Lee), mars@snu.ac.kr (W. Mar).

http://dx.doi.org/10.1016/j.lfs.2015.02.026
0024-3205/

A recent study demonstrated that the extracts of *Cudrania tricuspidata* protect neurons against oxidative stress-induced cytotoxicity [6] and have inhibitory effects on nitric oxide synthase (NOS) [7]. It was also reported that 5,7-Dihydroxychromone (DHC), from *C. tricuspidata*, has an antioxidant activity [19]. However, the neuroprotective effects of DHC and the related mechanisms of neuroprotection were poorly elucidated.

In this study, we demonstrated that the neuroprotective effects of DHC against 6-OHDA-induced neurotoxicity via the induction of the Nrf2/ARE-mediated signal.

2. Materials and methods

2.1. Materials

Propidium iodide (PI), 6-hydroxydopamine (6-OHDA), and 2′,7′-dichlorofluorescein-diacetate (DCFH-DA) were purchased from Sigma-Aldrich (St. Louis, MO, USA). Dulbecco's modified Eagle's medium (DMEM) and fetal bovine serum (FBS) were purchased from Gibco BRL (Rockville, MD, USA). Hybond-polyvinylidene difluoride (PVDF) membranes were purchased from Amersham Pharmacia Biotechnology Inc. (Piscataway, NJ, USA). Easy-Blue® total RNA extraction solution, PRO-PREP protein extraction solution and WEST-ZOL® ECL solution were purchased from iNtRON Biotech Inc. (Kyunggi, Korea). SuPrimeScript RT premix®, and SYBR HS Prime qPCR premix® were purchased from Genet Bio (Daejeon, Korea). Nrf2 siRNA, scrambled siRNA, Nrf2, HO-1, NQO1, GCLc, LaminB1, α-tubulin, β-actin, caspase-3, caspase-9, PARP, secondary antibody and FITC-conjugated secondary antibody were purchased from Santa Cruz Biotechnology, Inc. (Santa Cruz, CA, USA).

2.2. Preparation of DHC

C. tricuspidata was stored at the Korea Forest Research Institute at the Southern Forest Research Center (Jinju, Korea) in September 2008. A voucher specimen (accession number KH1-4-090814) was kept at the Department of Biosystems and Biotechnology at Korea University (Seoul, Korea). 5,7-Dihydroxychromone (DHC) was isolated from the roots of *C. tricuspidata* and the structure of DHC was determined by spectroscopic methods, and the purity was more than 98.5% [26]. DHC was dissolved in DMSO and diluted with PBS to obtain the proper concentration of DHC. The final concentration of DMSO was less than 0.1% and it didn't influence the performed assays.

2.3. SH-SY5Y cell culture

The human neuroblastoma cell line SH-SY5Y (ATCC No. CRL-2266) was purchased from the American Type Culture Collection (Manassas, VA, USA) and cultured in DMEM supplemented with 10% heat-inactivated FBS and 1% penicillin/streptomycin at 37 °C in a humidified 5% CO_2 atmosphere.

2.4. Measurement of cell viability

SH-SY5Y cells were seeded at a density of 2×10^5 cells/2 mL/well in 6-well plates for 24 h, and the cells were pre-treated with DHC (0.4, 2, or 10 μM) for 24 h followed by subsequent treatment with 6-OHDA (100 μM) for an additional 24 h. To evaluate the effect of Nrf2, cells were transfected with scrambled siRNA or Nrf2 siRNA for 48 h and its final concentration was 50 nM. After transfected cells were treated with DHC (10 μM) and 6-OHDA (100 μM), cell viability was determined using a propidium iodide (PI) staining and measured by flow cytometry (BD FACSCalibur™). Also, cell viability was evaluated using MTT assay as previously described [10].

2.5. Measurement of intracellular ROS by flow cytometry

ROS levels in cells were measured with the 2′,7′-dichlorofluorescein diacetate (DCFH-DA) method [15]. Briefly, the cells were washed with PBS, and then incubated with 4 μM of DCFH-DA for 30 min at 37 °C in the dark. The cells were then washed with PBS. The fluorescence intensities were measured by flow cytometry (BD FACSCalibur™).

2.6. Nuclear and cytosolic lysate preparations

The nuclear and cytosolic proteins were extracted with a commercial kit (Nuclear Extract Kit) according to the manufacturer's procedure (Active Motif, Carlsbad, CA). Briefly, the cells were incubated in hypotonic buffer on ice for 15 min, homogenized with detergent, and centrifuged for 30 s at 14,000 ×*g* in a microcentrifuge at 4 °C. The supernatant was used as the cytosolic proteins. The nuclear pellets were washed with cold PBS, extracted completely with lysis buffer for 30 min on ice and centrifuged for 10 min at 14,000 ×*g* in a microcentrifuge at 4 °C. The supernatant was used as the nuclear proteins.

2.7. Electrophoretic mobility shift assay (EMSA)

To determine the Nrf2–ARE binding activity, an electrophoretic mobility shift assay (EMSA) was accomplished as previously described [14]. Briefly, the nuclear proteins from the SH-SY5Y cells were reacted with ^{32}P-end-labeled 22-mer double-stranded oligonucleotide containing the Nrf2 sequence for 30 min at 37 °C. The DNA–protein complexes were electrophoresed and gels were dried. The binding signals were visualized by BAS-1500 (Fuji, Tokyo, Japan).

2.8. Nrf2 knockout via the transfection of small interfering RNA (siRNA)

The transfection with scrambled siRNA or Nrf2 siRNA were progressed at the final concentrations of 50 nM for 48 h by Lipofectamine 2000 (Invitrogen, Carlsbad, CA) prior to treatment with DHC (10 μM) and 6-OHDA (100 μM) as recommended by the manufacturer's guidelines.

2.9. Western blot analysis

The SH-SY5Y cells were collected, washed with PBS and lysed with a PRO-PREP protein extraction solution at − 20 °C for 20 min. After centrifugation at 13,000 ×*g* for 30 min, the supernatant was used as the total protein extracts. Western blot analysis was accomplished as in previously described method [5].

2.10. Immunocytochemical staining

The culture dish was coated with 0.2% gelatin at 37 °C for 30 min and dried at RT on a clean bench. The SH-SY5Y cells were plated at a density of 5×10^4 cells/200 μL/well in coated dishes for 24 h and incubated with DHC (0.4, 2, or 10 μM) for 6 h. After treatment with DHC, the cells were washed with 1× PBS/Tween-20 buffer (pH 7.4) (PBST) once. The cells were fixed with 4% paraformaldehyde for 30 min at room temperature (RT). After washing with PBST, the blocking steps were performed with 1% BSA in PBST. Next, the cells were incubated with the primary antibody at 4 °C overnight. The next day, the cells were washed with PBST 3 times and incubated with FITC-conjugated secondary antibody for 1 h at RT. After 1 h, the cells were washed with PBST 3 times, and DAPI staining was performed for 5 min at RT. Lastly, the PBST washing and mounting steps were conducted.

2.11. Statistical analysis

All experimental data are expressed as mean value ± standard deviation. Statistical significance between multiple groups was determined

by one-way ANOVA (PRISM Graph Pad, San Diego, CA, USA). When ANOVA had a significant difference, post-hoc Bonferroni multiple comparison tests was conducted. A p value less than 0.05 was regarded to be statistically significant.

3. Results

3.1. Protective effect of DHC against 6-OHDA-induced neuronal cell death

The protective effects of DHC (Fig. 1A) on SH-SY5Y cells were evaluated to determine the non-cytotoxic dose range (data not shown). The percentage of cell necrosis was evaluated with PI staining. As shown in Fig. 1C, the percentage of PI-stained dead cells induced by 6-OHDA increased to 44.5% compared to the vehicle-treated group (8.7%). In contrast, 6-OHDA-induced cell death was dose-dependently prevented by DHC treatments at concentrations of 0.4, 2 and 10 μM within the non-toxic dose range. DHC (10 μM) treatment elicited its neuroprotective effects against 6-OHDA by decreasing the percentage of PI-positive cells to 13.8%, whereas treatment with Nrf2 siRNA and DHC (10 μM) reduced the neuroprotective effect by increasing the percentage of PI-positive cells to 50.1%. Also, the neuroprotective effect of DHC was evaluated by MTT assay (Fig. 1B). The result of the MTT assay was correlated with the PI staining assay.

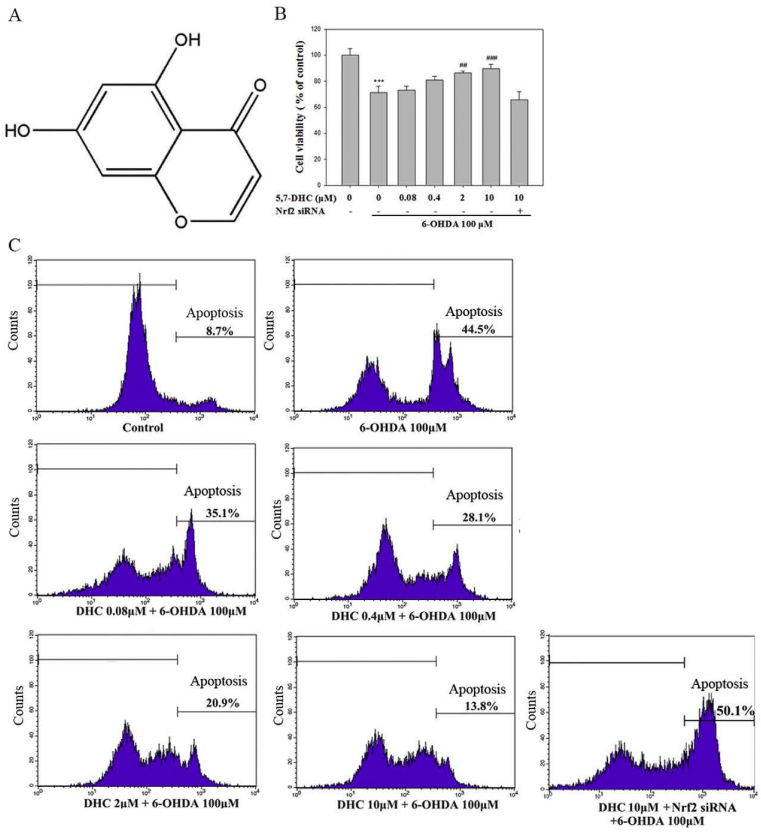

Fig. 1. (A) Chemical structure of 5,7-Dihydroxychromone (DHC). (B) Effects of DHC against 6-OHDA-induced cell death in SH-SY5Y cells were measured by MTT reduction assay and (C) illustrated by PI staining and FACS analysis using the FL-2 channel. The cells were pre-treated with different concentrations of DHC (0.4–10 μM) for 24 h and subsequently treated with 6-OHDA (100 μM) for another 24 h. The cells were transfected with Nrf2 siRNA (50 nM) for 48 h before the treatment with DHC (10 μM). (***$p < 0.001$ versus control group, ##$p < 0.01$ and ###$p < 0.001$ versus 6-OHDA-induced group).

3.2. Inhibitory effect of DHC against 6-OHDA-induced intracellular ROS generation

Intracellular ROS were detected by a DCFH-DA dye, which can be diffused to the cell membrane and deacetylated by esterase to the 2′,7′-dichlorodihydrofluorescein (DCFH), which is swiftly converted into the dichlorofluorescein (DCF) emitting fluorescence by ROS. As shown in Fig. 2, the 6-OHDA-induced cells exhibited higher DCF fluorescence intensities than the vehicle-treated cells. The amount of ROS generation was decreased in a dose-dependent manner when the 6-OHDA-induced cells were treated with different concentrations of DHC (0.4–10 μM). The 6-OHDA-induced group generated an approximately 5-fold greater amount of ROS than that of the vehicle-treated group. When the DHC (10 μM)-treated cells were treated with 6-OHDA, the ROS level was approximately 2-fold greater than that of the vehicle-treated group. However, the inhibitory effect of DHC (10 μM) on intracellular ROS generation disappeared upon treatment with Nrf2 siRNA, and the combined treatment with Nrf2 siRNA and DHC (10 μM) produced a similar ROS generation compared to the 6-OHDA-treated group.

3.3. Effects of DHC on induction of the nuclear Nrf2 and binding affinity of Nrf2/ARE in SH-SY5Y cells

Nrf2 in nucleus has a binding affinity to the ARE region and the Nrf2/ARE complex induces the transcription of ARE-mediated antioxidant genes. DHC increased the induction of nuclear Nrf2 with a peak effect that occurred at 6 h. As shown in Fig. 3A, the nuclear Nrf2 was dose-dependently increased by DHC treatment (0.08–10 μM) at 6 h (Fig. 3B). The increase of nuclear Nrf2 by DHC was visualized by immunocytochemistry in Fig. 3C. To elucidate the binding activity between Nrf2 and ARE, an electrophoretic mobility gel-shift assay (EMSA) was performed. As shown in Fig. 4, DHC (2 μM) drastically increased the Nrf2–ARE binding activity and the maximum binding activity was observed at 12 h.

3.4. Effects of DHC on HO-1, NQO1 and GCLc protein expression in SH-SY5Y cells

The protein levels of HO-1, NQO1, and GCLc, which are reported as major phase II antioxidant enzymes that are transcribed upon Nrf2/ARE binding, were measured in the SH-SY5Y cells. As shown in Fig. 5A and B, HO-1, NQO1, and GCLc protein expression levels were increased in a time- and dose-dependent manner by DHC treatment. As shown in Fig. 5B, HO-1, NQO1, and GCLc protein expression levels at 24 h were gradually increased by DHC treatment (0.08–10 μM). Upon Nrf2 siRNA treatment, the increased protein expression levels of HO-1, NQO1, and GCLc induced by DHC treatment (10 μM) were drastically reduced to a near-baseline level (Fig. 5C). These results revealed that Nrf2/ARE binding is a key step in the transcriptions of HO-1, NQO1, and GCLc proteins.

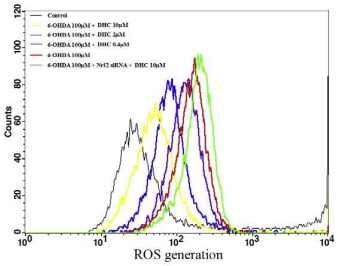

Fig. 2. Effects of DHC against 6-OHDA-induced intracellular ROS generation in SH-SY5Y cells illustrated by DCFH-DA staining and FACS analysis using the FL-1 channel. The cells were pre-treated with different concentrations of DHC (0.4–10 μM) for 24 h and subsequently treated with 6-OHDA (100 μM) for another 24 h. The cells were transfected with Nrf2 siRNA (50 nM) for 48 h before treatment with DHC (10 μM).

3.5. The inhibitory effects of DHC on the 6-OHDA-induced apoptotic signal

The inhibitory effects of DHC on the expressions of cleaved caspase-9, caspase-3, and PARP during the process of apoptosis were evaluated. ROS accumulation is known to activate caspase-9 and caspase-3, and activated caspase-3 cleaves PARP. As shown in Fig. 6, the cleaved caspase-9, caspase-3, and PARP were over-expressed when the SH-SY5Y cells were induced by 6-OHDA. However, the over-expression of these cleaved proteins was dose-dependently inhibited by DHC treatment (0.08–10 μM).

4. Discussion

Neurodegenerative diseases may occur without obvious causes or be the result of numerous circumstances that cause the impairment of cellular performance in neuron and ultimately cell death. Due to the rapid aging of the populations of societies across the world, the number of patients suffering from the neurodegenerative disease is also increasing. Although the causes of these diseases have not been clearly elucidated, recent studies have revealed that ROS is composed of their pathogenesis [3]. Because of their abundant iron contents and relatively deficient antioxidant defense system, neuronal cells are vulnerable to excessive ROS and electrophile related stress. It has been suggested that ROS is highly involved in the neurotoxicity of neurodegenerative disease [16]. Over the past decade, many studies of antioxidant enzymes have resulted in progress in the treatment and prevention of diseases [20]. In this context, it has been suggested that the coordinated expression of phase II antioxidant enzymes via the induction of nuclear Nrf2 could be a promising strategy for protection against oxidative stress-related neurodegenerative diseases.

The effects of DHC (Fig. 1A) have not been thoroughly examined, particularly in relation to protection against neuronal cell death. In this report, DHC was found to protect against neuronal cell death and the ROS generation in 6-OHDA-induced SH-SY5Y cells. It was reported that caspase-9 could be cleaved by ROS generation [28]. Cleaved caspase-9 induces activation of caspase-3 by making a cleaved form of caspase-3, which is the important caspase involved in the apoptotic process and neuronal cell death caused by 6-OHDA [2,11]. PARP is cleaved by an active form of caspase-3, and this cleaved PARP loses the ability to participate in DNA repair, which results in apoptosis. PARP cleavage by the active form of caspase-3 is a reliable indicator of apoptosis [9]. In our results, DHC prevented the 6-OHDA-induced cleavages of caspase-3, caspase-9, and PARP, which inhibited the activation of the apoptotic cascade in the SH-SY5Y cells. Moreover, DHC down-regulated the ROS level, which was increased by treatment with 6-OHDA. Based on its results, we suggest that this anti-apoptotic effect of DHC is associated with the down-regulation of ROS.

The effects of the Nrf2/ARE signaling pathway on ROS generation were also evaluated. Our results revealed that treatment with DHC inhibited the generation of 6-OHDA-induced ROS, which affect the early and late stages of apoptosis. The ability of DHC to inhibit ROS generation seems to be an important factor in neuronal cell protection. DHC also increased the induction of nuclear Nrf2, which has a binding affinity to ARE and activates ARE-driven phase II antioxidant enzymes; NQO1, HO-1, and GCLc. Nrf2 is regarded as a key regulator of antioxidant defensive responses and a sensor of cellular redox status [8]. Many lines of research have proven the importance of Nrf2-related antioxidant enzymes in neuroprotection [17]. It has been also reported that the levels of antioxidant genes are considerably decreased in Nrf2-K.O. mice and the expression levels of antioxidant enzymes were eliminated

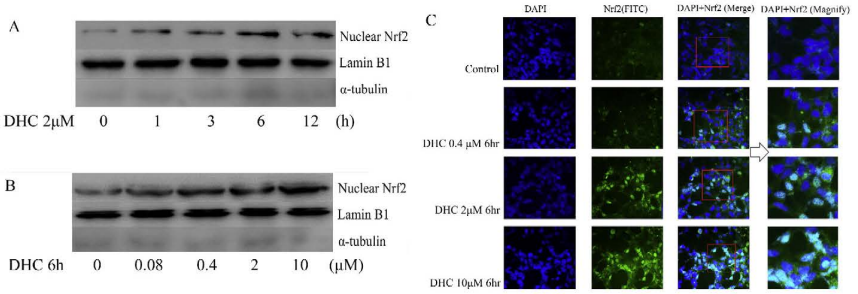

Fig. 3. Effects of DHC on the nuclear translocation of Nrf2 in SH-SY5Y cells illustrated by Western blot analysis and immunocytochemistry. (A) The cells were treated with DHC (2 μM) for different durations (0–12 h). (B) The cells were treated with different concentrations of DHC (0.4–10 μM) for 6 h. Representative data from three independent experiments are shown. (C) The cells were treated with DHC (0.4–10 μM) for 6 h, and the nuclei were visualized with DAPI staining. Nrf2 was detected with FITC-conjugated antibodies. Cellular morphologies were visualized with a fluorescence microscope (400×). Representative images from three independent experiments are shown.

by Nrf2-siRNA in in vitro models [21]. NQO1, HO-1, and GCLc are representative antioxidant enzymes whose expressions are increased by diverse environmental stimulus including ROS and thiol-reactive substances [4,22,23]. NQO1 has been reported to be a potentially attractive therapeutic target for protecting cells from oxidative damage because it makes a stable form of hydroquinone by catalyzing quinone [13]. Moreover, it has been reported that HO-1 catalyzes heme to carbon monoxide, biliverdin and iron, which exerts potent antioxidant effects [3]. GCLc participates in glutathione synthesis and prevents the impairment of cellular function from excessive ROS [18]. Many studies have shown that these antioxidant enzymes have powerful antioxidant effects, and it has been suggested that the regulation of antioxidant enzymes might be a key factor in the prevention of age-related diseases [25]. Our results revealed that DHC treatment induced the nuclear translocation of Nrf2, which resulted in the increases in NQO1, HO-1, and GCLc at the level of protein expression, suggesting that the neuroprotective effects of DHC against 6-OHDA-induced cell death are involved in the inhibition of ROS generation. Based on our research, we expect that one of the neuroprotective effects exerted by DHC is the increased induction of the Nrf2/ARE signal. When the cells were transfected with Nrf2 siRNA, the protective effects of DHC against 6-OHDA-induced neurotoxicity and ROS generation were inhibited. Moreover, the increased protein expression levels of NQO1, HO-1, and GCLc by DHC treatment (10 μM) were also drastically reduced to basal levels by treatment with Nrf2 siRNA. Our results showed that the neuroprotective effects of DHC are due to the activation of the Nrf2/ARE signaling pathways and the subsequent inhibition of ROS generation.

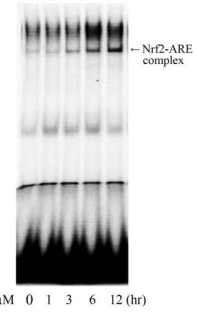

Fig. 4. Effects of DHC on the binding activity of Nrf2–ARE. The cells were treated with DHC (2 μM) for different durations (0–12 h), and the nuclear extracts were incubated with [γ-^{32}P]-labeled oligonucleotides harboring an ARE consensus sequence. Nrf2–ARE binding activity was measured via an electrophoretic mobility gel-shift assay (EMSA).

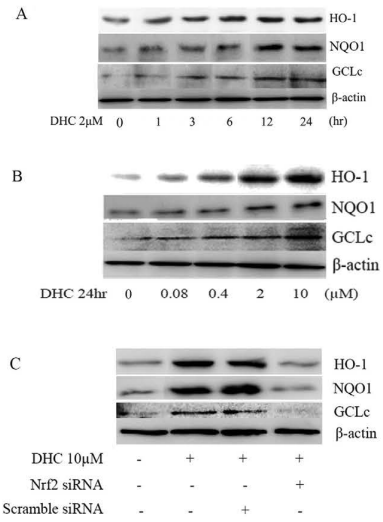

Fig. 5. Effects of DHC on the expressions of the HO-1, NQO1, and GCLc proteins in the SH-SY5Y cells illustrated by Western blot analysis. (A) The cells were treated with DHC (2 μM) for different durations (0–24 h). (B) The cells were treated with different concentrations of DHC (0.08–10 μM) for 24 h. (C) The cells were transfected with Nrf2 siRNA (50 nM) or scrambled siRNA (50 nM) prior to treatment with DHC (10 μM) for 48 h. Representative data from three independent experiments are shown.

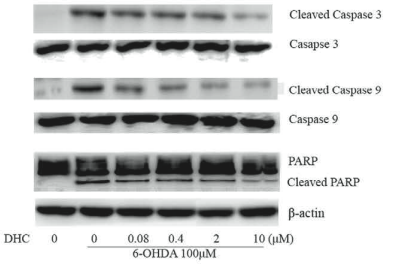

Fig. 6. Inhibitory effects of DHC on the expressions of cleaved caspase-9, caspase-3 and PARP illustrated by Western blot analysis. The cells were pre-treated with different concentrations of DHC (0.4–10 μM) for 24 h and subsequently treated with 6-OHDA (100 μM) for another 24 h. Representative data from three independent experiments are shown.

5. Conclusion

The present study demonstrated that DHC prevented 6-OHDA-induced neurotoxicity via the induction of the Nrf2/ARE signal, which subsequently led to the overexpression of antioxidant enzymes, including NQO1, HO-1, and GCLc. As a result of these effects, DHC inhibited the generation of ROS and neuronal cell death in 6-OHDA-induced SH-SY5Y cells. Our study suggests that DHC can be a promising neuroprotective candidate in the therapy of neurodegenerative diseases such as Parkinson's disease.

Conflict of interest statement

The authors declare that there are no conflicts of interest.

Acknowledgments

This work was supported by the Basic Science Research Program through the National Research Foundation (NRF) of Korea (Grant no. NRF-2013R1A1A2008111) and the BK21 plus program in 2015 through the National Research Foundation (NRF) funded by the Ministry of Education of Korea. The author appreciates Korea University and the Korea Forest Research Institute for supporting the plant materials.

References

[1] A. Alfieri, S. Srivastava, R.C. Siow, M. Modo, P.A. Fraser, G.E. Mann, Targeting the Nrf2–Keap1 antioxidant defence pathway for neurovascular protection in stroke, J. Physiol. 589 (2011) 4125–4136.
[2] R.C. Dodel, Y. Du, K.R. Bales, Z. Ling, P.M. Carvey, S.M. Paul, Caspase-3-like proteases and 6-hydroxydopamine induced neuronal cell death, Brain Res. Mol. Brain Res. 64 (1999) 141–148.
[3] T. Farooqui, A.A. Farooqui, Lipid-mediated oxidative stress and inflammation in the pathogenesis of Parkinson's disease, Park. Dis. 2011 (2011) 247467.
[4] J.A. Fraser, R.D. Saunders, I.I. McLellan, *Drosophila melanogaster* glutamate–cysteine ligase activity is regulated by a modifier subunit with a mechanism of action similar to that of the mammalian form, J. Biol. Chem. 277 (2002) 1158–1165.
[5] A. Ham, D.W. Kim, K.H. Kim, S.J. Lee, K.B. Oh, J. Shin, W. Mar, Reynosin protects against neuronal toxicity in dopamine-induced SH-SY5Y cells and 6-hydroxydopamine-lesioned rats as models of Parkinson's disease: reciprocal up-regulation of E6-AP and down-regulation of alpha-synuclein, Brain Res. 1524 (2013) 54–61.
[6] C.H. Jeong, G.N. Choi, J.H. Kim, J.H. Kwak, H.R. Jeong, D.O. Kim, H.J. Heo, Protective effects of aqueous extract from *Cudrania tricuspidata* on oxidative stress-induced neurotoxicity, Food Sci. Biotechnol. 19 (2010) 1113–1117.
[7] D.G. Kang, T.Y. Hur, G.M. Lee, H. Oh, T.O. Kwon, E.J. Sohn, H.S. Lee, Effects of *Cudrania tricuspidata* water extract on blood pressure and renal functions in NO-dependent hypertension, Life Sci. 70 (2002) 2599–2609.
[8] K.W. Kang, S.J. Lee, S.G. Kim, Molecular mechanism of nrf2 activation by oxidative stress, Antioxid. Redox Signal. 7 (2005) 1664–1673.
[9] S.H. Kaufmann, S. Desnoyers, Y. Ottaviano, N.E. Davidson, G.G. Poirier, Specific proteolytic cleavage of poly(ADP-ribose) polymerase: an early marker of chemotherapy-induced apoptosis, Cancer Res. 53 (1993) 3976–3985.
[10] U. Koo, K.W. Nam, A. Ham, D. Lyu, B. Kim, S.J. Lee, K.H. Kim, K.B. Oh, W. Mar, J. Shin, Neuroprotective effects of 3alpha-acetoxyeudesma-1,4(15),11(13)-trien-12,6alpha-olide against dopamine-induced apoptosis in the human neuroblastoma SH-SY5Y cell line, Neurochem. Res. 36 (2011) 1991–2001.
[11] K. Kuida, T.F. Haydar, C.Y. Kuan, Y. Gu, C. Taya, H. Karasuyama, M.S. Su, P. Rakic, R.A. Flavell, Reduced apoptosis and cytochrome c-mediated caspase activation in mice lacking caspase 9, Cell 94 (1998) 325–337.
[12] S. Leutner, C. Czech, K. Schindowski, N. Touchet, A. Eckert, W.E. Muller, Reduced antioxidant enzyme activity in brains of mice transgenic for human presenilin-1 with single or multiple mutations, Neurosci. Lett. 292 (2000) 87–90.
[13] J.H. Lim, K.M. Kim, S.W. Kim, O. Hwang, H.J. Choi, Bromocriptine activates NQO1 via Nrf2-PI3K/Akt signaling: novel cytoprotective mechanism against oxidative damage, Pharmacol. Res. 57 (2008) 325–331.
[14] T. Meyer, C. Munch, H. Volkel, P. Booms, A.C. Ludolph, The EAAT2 (GLT^{-1}) gene in motor neuron disease: absence of mutations in amyotrophic lateral sclerosis and a point mutation in patients with hereditary spastic paraplegia, J. Neurol. Neurosurg. Psychiatry 65 (1998) 594–596.
[15] G. Munch, A.M. Cunningham, P. Riederer, E. Braak, Advanced glycation endproducts are associated with Hirano bodies in Alzheimer's disease, Brain Res. 796 (1998) 307–310.
[16] G. Munch, M. Gerlach, J. Sian, A. Wong, P. Riederer, Advanced glycation end products in neurodegeneration: more than early markers of oxidative stress? Ann. Neurol. 44 (1998) S85–S88.
[17] S.H. Park, J.H. Jang, C.Y. Chen, H.K. Na, Y.J. Surh, A formulated red ginseng extract rescues PC12 cells from PCB-induced oxidative cell death through Nrf2-mediated upregulation of heme oxygenase-1 and glutamate cysteine ligase, Toxicology 278 (2010) 131–139.
[18] A. Pompella, A. Visvikis, A. Paolicchi, V. De Tata, A.F. Casini, The changing faces of glutathione, a cellular protagonist, Biochem. Pharmacol. 66 (2003) 1499–1503.
[19] J. Qiu, L. Chen, Q. Zhu, D. Wang, W. Wang, X. Sun, X. Liu, F. Du, Screening natural antioxidants in peanut shell using DPPH–HPLC–DAD–TOF/MS methods, Food Chem. 135 (2012) 2366–2371.
[20] K. Rahman, Studies on free radicals, antioxidants, and co-factors, Clin. Interv. Aging 2 (2007) 219–236.
[21] M. Ramos-Gomez, M.K. Kwak, P.M. Dolan, K. Itoh, M. Yamamoto, P. Talalay, T.W. Kensler, Sensitivity to carcinogenesis is increased and chemoprotective efficacy of enzyme inducers is lost in nrf2 transcription factor-deficient mice, Proc. Natl. Acad. Sci. U. S. A. 98 (2001) 3410–3415.
[22] M. Rizzardini, M. Terao, F. Falciani, L. Cantoni, Cytokine induction of haem oxygenase mRNA in mouse liver. Interleukin 1 transcriptionally activates the haem oxygenase gene, Biochem. J. 290 (Pt 2) (1993) 343–347.
[23] Z.Y. Su, L. Shu, T.O. Khor, J.H. Lee, F. Fuentes, A.N. Kong, A perspective on dietary phytochemicals and cancer chemoprevention: oxidative stress, nrf2, and epigenomics, Top. Curr. Chem. 329 (2013) 133–162.
[24] X. Sun, L. Huang, M. Zhang, S. Sun, Y. Wu, Insulin like growth factor-1 prevents 1-mentyl-4-phenylphyridinium-induced apoptosis in PC12 cells through activation of glycogen synthase kinase-3beta, Toxicology 271 (2010) 5–12.
[25] B. Uttara, A.V. Singh, P. Zamboni, R.T. Mahajan, Oxidative stress and neurodegenerative diseases: a review of upstream and downstream antioxidant therapeutic options, Curr. Neuropharmacol. 7 (2009) 65–74.
[26] G. Wei, B. Yu, Isoflavone glycosides: synthesis and evaluation as alpha-glucosidase inhibitors, Eur. J. Org. Chem. 3156-3163 (2008).
[27] M. Zhang, C. An, Y. Gao, R.K. Leak, J. Chen, F. Zhang, Emerging roles of Nrf2 and phase II antioxidant enzymes in neuroprotection, Prog. Neurobiol. 100 (2013) 30–47.
[28] Y. Zuo, B. Xiang, J. Yang, X. Sun, Y. Wang, H. Cang, J. Yi, Oxidative modification of caspase-9 facilitates its activation via disulfide-mediated interaction with Apaf-1, Cell Res. 19 (2009) 449–457.

BRAIN RESEARCH ▮ (▮▮▮▮) ▮▮▮–▮▮▮

Available online at www.sciencedirect.com

SciVerse ScienceDirect

www.elsevier.com/locate/brainres

Research Report

Reynosin protects against neuronal toxicity in dopamine-induced SH-SY5Y cells and 6-hydroxydopamine-lesioned rats as models of Parkinson's disease: Reciprocal up-regulation of E6-AP and down-regulation of α-synuclein

Ahrom Ham[a,1], Dong-Woo Kim[a,1], Kyeong Ho Kim[b], Sung-Jin Lee[c], Ki-Bong Oh[d], Jongheon Shin[a,*], Woongchon Mar[a,**]

[a]Natural Products Research Institute, College of Pharmacy, Seoul National University, 599 Gwanak-ro, Gwanak-gu, Seoul 151-742, Republic of Korea
[b]College of Pharmacy, Kangwon National University, Chuncheon 200-701, Republic of Korea
[c]Department of Animal Biotechnology, Kangwon National University, Chuncheon 200-701, Republic of Korea
[d]School of Agricultural Biotechnology, Seoul National University, 599 Gwanak-ro, Gwanak-gu, Seoul 151-742, Republic of Korea

ARTICLE INFO

Article history:
Accepted 22 May 2013

Keywords:
Reynosin
α-Synuclein
E6-associated protein
Neuroprotection
6-OHDA lesion
Parkinson's disease

ABSTRACT

Aggregation of α-synuclein (ASYN) is considered a major determinant of neuronal loss in Parkinson's disease (PD). E6-associated protein (E6-AP), an E3 ubiquitin protein ligase, has been known to promote the degradation of α-synuclein. The aim of this study was to assess the effects of the sesquiterpene lactone reynosin on dopamine (DA)-induced neuronal toxicity and regulation of E6-associated protein and α-synuclein proteins in both in vitro and in vivo models of Parkinson's disease. Usi"ng flow cytometry and western blot analysis, we determined that reynosin significantly protected both against cell death from dopamine-induced toxicity in human neuroblastoma SH-SY5Y cells and against the loss of tyrosine hydroxylase (TH)-positive cells in 6-hydroxydopamine (6-OHDA)-lesioned rats (a rodent Parkinson's disease model system). In addition, reynosin made up-regulation of E6-associated protein expression and down-regulation of the over-expression of α-synuclein protein in both dopamine-treated SH-SY5Y cells and 6-hydroxydopamine-lesioned rats. These results suggest that the protective effect of reynosin against dopamine-induced neuronal cell death may be due to the reciprocal up-regulation of E6-associated protein and down-regulation of α-synuclein protein expression.

*Corresponding author. Fax: +82 2 762 8322.
**Corresponding author. Fax: +82 2 880 2474.
E-mail addresses: shinj@snu.ac.kr (J. Shin), mars@snu.ac.kr (W. Mar).
[1]These authors contributed equally to this work.

0006-8993/$ - see front matter © 2013 Elsevier B.V. All rights reserved.
http://dx.doi.org/10.1016/j.brainres.2013.05.036

Please cite this article as: Ham, A., et al., Reynosin protects against neuronal toxicity in dopamine-induced SH-SY5Y cells and 6-hydroxydopamine-lesioned rats as models of Parkinson's disease: Reciprocal up-regulation of E6-AP and down-regulation of α-synuclein. Brain Research (2013), http://dx.doi.org/10.1016/j.brainres.2013.05.036

1. Introduction

Parkinson's disease (PD) is the second most common neurodegenerative disorder after Alzheimer's disease and is neuropathologically characterized by severe motor deficits caused by neuronal cell death (Golde, 2009). PD is neuropathologically characterized by a selective loss of nigrostriatal dopaminergic neurons (Nicotra and Parvez, 2002) and the presence of brainstem-type Lewy bodies, a hallmark of idiopathic PD composed of an abnormal aggregation of α-synuclein (ASYN), inside neurons (Dedov et al., 2001).

The presence of ASYN as a main component of Lewy bodies suggests that the aggregation of this protein is a key pathogenic event in PD; moreover, patients with PD exhibit the accumulation of ASYN in the substantia nigra. Phosphorylation of ASYN has been suggested to an important factor both for the cytoplasmic inclusion formation (Chu and Kordower, 2007; Smith et al., 2005) and the conformational changes. It induced the abnormal aggregation of ASYN that are considered to lead to neuronal cell loss (Chu et al., 2006). Over-expression of ASYN also caused its aggregation in the brain and induced neurodegeneration in an animal model (Feany and Bender, 2000; Kirik et al., 2002). Recently, it was reported that E6-associated protein (E6-AP), an E3 ubiquitin-protein ligase with a limited role in protein folding, promotes the degradation of polyglutamine proteins mediated by the ubiquitin–proteasome pathway; in addition, E6-AP possibly functions as a cellular quality control ubiquitin ligase (Mishra et al., 2009). Moreover, E6-AP is recruited to juxtanuclear aggregates of ASYN, which may play a critical regulatory role in the degradation of ASYN (Mulherkar et al., 2009).

It has been suggested that an imbalance between cytoplasmic and vesicular dopamine (DA) may cause neuronal degeneration (Barzilai et al., 2001), and this degeneration may be a factor in the dopaminergic damage observed in PD. In this study, neurotoxicity elicited by DA in SH-SY5Y cells was used as an in vitro model of PD (Asanuma et al., 2003; Gomez-Santos et al., 2003; Miyazaki and Asanuma, 2008), and 6-hydroxydopamine (6-OHDA)-lesioned rats were used as an in vivo model of PD (Foyet et al., 2011) to evaluate the neuroprotective effects of reynosin.

Reynosin, a sesquiterpene lactone isolated from the leaves of *Laurus nobilis* L. (Lauraceae), has been reported to have pharmacological actions such as the reduction of ethanol concentration in rat blood and nitric oxide production (Yoshikawa et al., 2000). In a previous study, we reported that spirafolide, another sesquiterpene lactone from *Laurus nobilis* L. (Lauraceae), has neuroprotective effects in human SH-SY5Y cells (Ham et al., 2010).

The aim of this study was to determine whether reynosin protects neuronal cells against DA toxicity through the regulation of E6-AP and ASYN protein expression in human dopaminergic cells and 6-OHDA-induced lesioned rat, as in vitro and in vivo models of PD, respectively. To our knowledge, this is the first report demonstrating the neuroprotective effects of reynosin in the context of the regulation of E6-AP and ASYN protein expression. These results suggest the therapeutic potential of reynosin in neurodegenerative diseases such as PD.

2. Results

2.1. Protection from DA-induced cell death by reynosin

SH-SY5Y cells were treated with reynosin to evaluate possible toxic effects at concentrations ranging from 0.08 μM to 50 μM (final 0.5% DMSO, v/v) for 48 h (data not shown). The neuroprotective effect of reynosin against DA-induced cell death was evaluated within the non-toxic dose range. As shown in Fig. 1B, treatment of SH-SY5Y cells with DA (600 μM) for 24 h resulted in important changes in cellular morphology; specifically, a reduction in the amount of cytoplasm and decrease in cell adherence were observed. However, cells reverted to normal shape, when pre-treated with reynosin (2 μM) for 24 h before DA treatment (24 h). In addition, treatment of cells with DA for 24 h (600 μM) reduced the viability to 29.2% ($p<0.001$) compared to vehicle-treated cells (control group), whereas DA-induced cell death was significantly prevented by reynosin pre-treatment for 24 h at concentrations of 0.08, 0.4, and 2 μM in a dose-dependent manner. The viability was 31.8%, 41.5% ($p<0.01$), and 76.8% ($p<0.001$), respectively (EC_{50}, 3.6 μM) as compared to the control group (Fig. 1C and D). Apomorphine (APO) was used as a positive control compound. APO is a non-selective dopamine agonist which activates both D_1-like and D_2-like receptors and used in the treatment of PD (Millan et al., 2002). The protective effect of reynosin against DA-induced cell death was approximately 5 times more potent than that of APO (a positive control compound) (EC_{50}, 18.2 μM).

2.2. Effects of reynosin on E6-AP and ASYN protein expression in SH-SY5Y cells

The protein expression levels of E6-AP and ASYN were detected by western blot analysis in SH-SY5Y cells. In DA-treated cells, E6-AP protein expression decreased but ASYN protein expression increased in a time-dependent manner. In particular, a dramatic increase in ASYN protein expression was observed after 15 h of DA treatment, whereas the E6-AP levels were reduced gradually. On the basis of these results, DA treatment for 15 h was used in subsequent experiments.

The level of E6-AP protein expression in the DA treatment group was reduced to 0.5-fold ($p<0.01$) compared with the control group, whereas, after pre-treatment with reynosin (0.08, 0.4, and 2 μM) for 24 h, E6-AP protein expression was dose-dependently increased to 0.6-, 0.7-, and 0.9-fold ($p<0.01$) compared with the control group, respectively. Interestingly, treatment with APO (2 μM) resulted in E6-AP protein expression that was only 0.6-fold that of the control group, indicating that reynosin is 1.5-fold more potent than APO at a concentration of 2 μM (Fig. 2C).

In addition, DA-treatment increased ASYN expression to 2.6-fold ($p<0.001$) compare with the control group, whereas pre-treatment with reynosin (0.08, 0.4, and 2 μM) for 24 h reduced ASYN expression in a dose-dependent manner to 1.8-, 1.3- ($p<0.01$), and 1.1-fold ($p<0.001$) compare with the control group, respectively (Fig. 2D). Interestingly, APO did not affect DA-induced over-expression of the ASYN protein at the concentration tested (2 μM) (Fig. 2D). In conclusion,

Please cite this article as: Ham, A., et al., Reynosin protects against neuronal toxicity in dopamine-induced SH-SY5Y cells and 6-hydroxydopamine-lesioned rats as models of Parkinson's disease: Reciprocal up-regulation of E6-AP and down-regulation of α-synuclein. Brain Research (2013), http://dx.doi.org/10.1016/j.brainres.2013.05.036

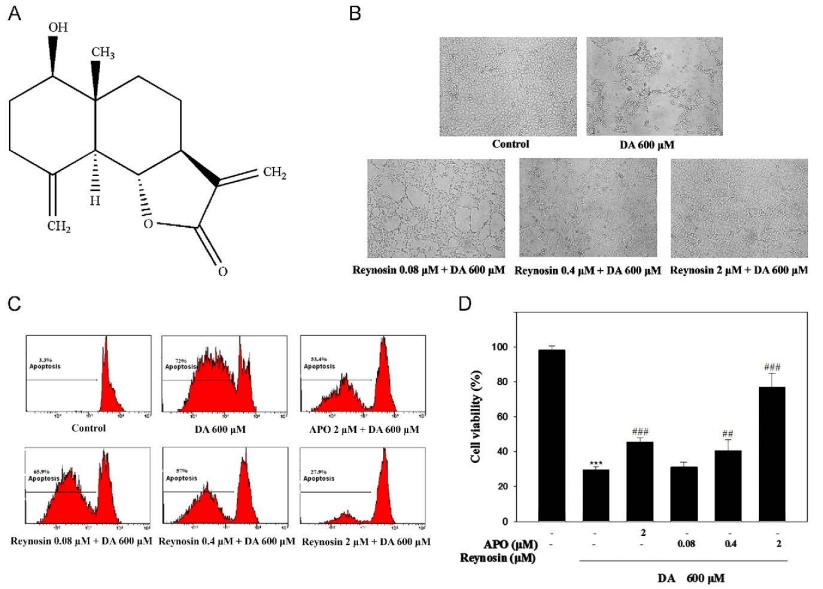

Fig. 1 – Reynosin protects against DA induced neuronal cell death in SH-SY5Y cells. (A) Chemical structure of reynosin. (B) Cellular morphological changes. Cells were pre-treated with reynosin (0.08, 0.4, and 2 μM) for 24 h, followed by DA treatment (600 μM) for an additional 24 h. (C) Effects on DA-induced cell death as observed by PI staining and FACS analysis. (D) Histograms show the proportion of dead cells relative to total cells. APO was used as a positive control compound. Plots were calculated from the flow cytometry histogram distributions (mean ± SD, $n \geq 5$) (‾$p < 0.001$ versus control group, $^{\#\#}p < 0.01$ and $^{\#\#\#}p < 0.001$ versus DA-treated group).

reynosin treatment reversed the concomitant down-regulation of E6-AP and up-regulation of ASYN proteins by DA.

2.3. *Effects of reynosin on TH-positive dopaminergic neurons in the substantia nigra in 6-OHDA-lesioned rats*

TH, the rate limiting enzyme in DA synthesis, was used as a marker for dopaminergic neurons in the substantia nigra (Masliah et al., 2000). TH-positive neurons in the substantia nigra were detected by immunohistochemistry (Fig. 3A). The effect of the various treatments on dopaminergic neurons was quantified by calculating the ratio of TH-positive neurons in the substantia nigra from the ipsilateral hemisphere to those from the contralateral hemisphere (I/C ratio). In the 6-OHDA-lesioned group, a significant loss of TH-positive neurons was observed. The I/C ratio of the sham group was 0.9 and that of the 6-OHDA lesion group was 0.3 ($p < 0.001$). The I/C ratio of reynosin treatment in 6-OHDA-lesioned rats was 0.4, 0.5 ($p < 0.001$), and 0.8 ($p < 0.001$) at doses of 0.2, 1, and 5 mg/kg, respectively, whereas treatment with APO, at 5 mg/kg, resulted in an I/C ratio of 0.7 ($p < 0.001$) (Fig. 3B).

2.4. *Effects of reynosin on E6-AP and ASYN protein expression in 6-OHDA-lesioned rats*

The effects of reynosin on the expression of E6-AP and ASYN proteins were determined in the rat model of PD. In the substantia nigra of 6-OHDA-lesioned rats, E6-AP protein expression was reduced to 0.39-fold ($p < 0.001$) compared with sham group, and the ASYN protein expression was increased to 2.3-fold ($p < 0.001$). However, treatment with reynosin (0.2, 1, and 5 mg/kg) in a lesioned rat increased the E6-AP protein expression to 0.44-, 0.52-, and 0.69-fold ($p < 0.05$) compare with the sham group and concomitantly decreased the ASYN protein expression to 2.1-, 1.5- ($p < 0.01$), and 1.3-fold ($p < 0.001$), respectively (Fig. 4). Interestingly, APO (5 mg/kg) reduced the E6-AP protein expression to 0.66-fold to that of sham group, which is similar to the effect caused by reynosin

Please cite this article as: Ham, A., et al., Reynosin protects against neuronal toxicity in dopamine-induced SH-SY5Y cells and 6-hydroxydopamine-lesioned rats as models of Parkinson's disease: Reciprocal up-regulation of E6-AP and down-regulation of α-synuclein. Brain Research (2013), http://dx.doi.org/10.1016/j.brainres.2013.05.036

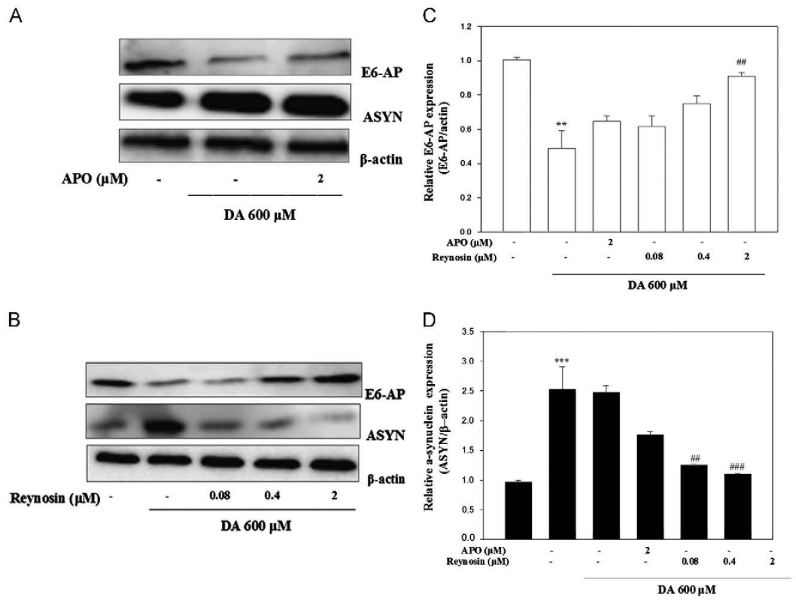

Fig. 2 – The effects of reynosin on the levels of ASYN and E6-AP protein expression were demonstrated by western blot analysis in SH-SY5Y cells treated with DA. (A and B) SH-SY5Y cells were pre-treated for 24 h with different concentrations of reynosin (0.08, 0.4, and 2 μM) or APO (2 μM) followed by treatment with DA (600 μM) for 15 h. Representative western blots using ASYN and E6-AP antibodies are presented. (C and D) Relative protein expression levels were normalized to β-actin expression. Data obtained from at least 5 independent experiments are shown and presented as the mean ± SD ($^{**}p<0.01$ and $^{***}p<0.001$ versus control group, $^{\#\#}p<0.01$ and $^{\#\#\#}p<0.001$ versus DA-treated group).

(5 mg/kg). However, APO did not affect the over-expression of the ASYN protein in lesioned rats. These results are consistent with the in vitro results obtained from SH-SY5Y cells.

3. Discussion

In this study, reynosin isolated from *Laurus nobilis* L. (Lauraceae) extract was evaluated for its neuroprotective effects in SH-SY5Y cells (Fig. 1) and in 6-OHDA-lesioned rats (Fig. 3) as in vitro and in vivo PD models, respectively. It has been reported that infusion of 6-OHDA causes a rapid and consistent loss of TH immunoreactivity in the substantia nigra (Masliah et al., 2000). In the present study, a significant loss of TH-positive neurons was observed in the substantia nigra of rats at 7 days after 6-OHDA lesion, and the number of TH-positive neurons in each group was illustrated in the representative photomicrographs, and quantified by image analysis (Fig. 3). Treatment with reynosin (i.p., once, 1 h after 6-OHDA lesion) significantly protected against the loss of TH-positive neurons from 6-OHDA-induced toxicity in the substantia nigra in a dose-dependent manner. This protective effect of reynosin was 1.2 times more potent than that of the APO, positive control compound, (Watanabe et al., 2004) at doses of 5 mg/kg.

It has been reported that many patients with PD have mutations in specific genes such as ASYN, and over-expression and mutation of ASYN are two of the most important pathogenic events in PD (Hughes et al., 1993). It has been reported that cells expressing mutant ASYN were more vulnerable to oxidative stress (Kanda et al., 2000). It also has been reported that Lewy bodies, abnormal protein inclusions, are the most common pathological hallmark of PD, and the main component of Lewy bodies is ASYN; thus, aggregation of this protein is believed to be a key pathogenic event in PD. In addition, aggregation of insoluble ASYN may remove soluble ASYN protofibrils, and this action is thought to induce greater toxicity of ASYN (Conway et al., 2001) and further aggregation of ASYN. Aggregation of ASYN is potentiated by exposure to a variety of stimuli such as mitochondrial inhibition and oxidative stress that are observed in PD pathology (Bennett, 2005). Extracellular DA is a stressor agent

Please cite this article as: Ham, A., et al., Reynosin protects against neuronal toxicity in dopamine-induced SH-SY5Y cells and 6-hydroxydopamine-lesioned rats as models of Parkinson's disease: Reciprocal up-regulation of E6-AP and down-regulation of α-synuclein. Brain Research (2013), http://dx.doi.org/10.1016/j.brainres.2013.05.036

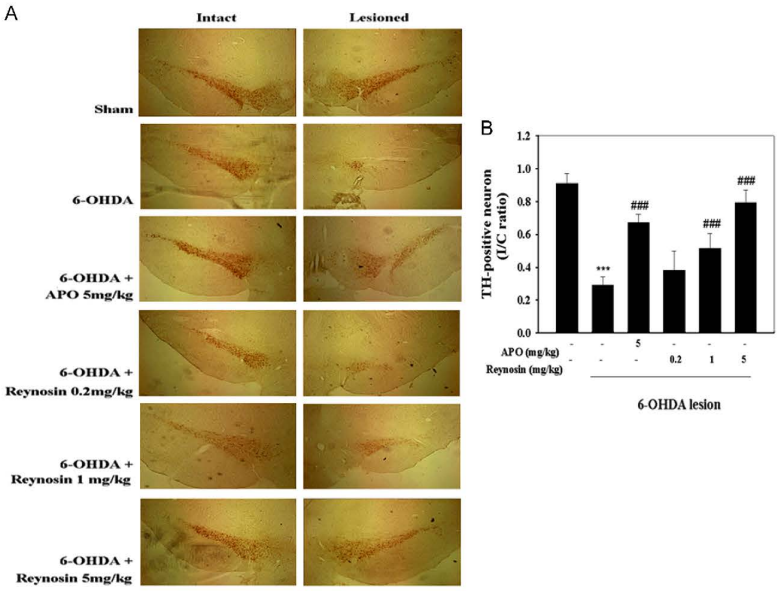

Fig. 3 – Neuroprotective effects of reynosin on TH-positive neurons in the substantia nigra in 6-OHDA-lesioned rats. (A) Photomicrograph of TH-positive neurons in both ipsilateral and contralateral hemispheres. Rats were divided into 4 groups; sham, 6-OHDA-lesioned, APO treatment (5 mg/kg), and reynosin treatment (0.2, 1, and 5 mg/kg) groups. (B) The effect of treatment on dopaminergic neurons was quantified by calculating the ratio of TH-positive neurons in the substantia nigra from the ipsilateral hemisphere to those from the contralateral hemisphere (*i*/C ratio). Each group represents the data from more than 9 rats, and mean values obtained from 5 sections from each rat were used ($^{***}p<0.001$ versus sham group, $^{###}p<0.001$ versus 6-OHDA-lesioned group).

that promotes ASYN over-expression (Gomez-Santos et al., 2003), and it has been reported that ASYN expression was significantly increased between 6 and 24 h after treatment with DA (Gomez-Santos et al., 2005). Our results demonstrated that DA-induced ASYN over-expression was significantly down-regulated by pre-treatment with reynosin in a dose-dependent manner in SH-SY5Y cells. However, pre-treatment with APO did not affect ASYN protein expression levels at the concentration tested (Fig. 2).

There are some disorders have been identified due to the malfunction of E3 ligases, including autosomal recessive juvenile PD (Jiang and Beaudet, 2004). Cell survival ultimately depends on the shift in equilibrium between the formation and clearance of improperly folded proteins. E6-AP, which plays a critical role in preventing the misfolding and the aggregation of proteins, is likely to control ubiquitin ligase activity, and it was presumed that E6-AP plays an important role in protein misfolding-related neurodegenerative disorders such as PD (Mishra et al., 2008). E6-AP has been shown to interact with Hsp70/Hsc70 chaperones and promotes the degradation of aggregate proteins (Mishra et al., 2009). The role of E6-AP is not limited polyglutamine or ASYN but misfolded proteins in general and E6-AP might act as a cellular quality control ligase. E6-AP has been shown to be located in Lewy bodies of the PD brain, and the endogenous E6-AP co-localizes with ASYN in intracellular inclusions in neuroblastoma cells. Over-expression of E6-AP enhances degradation of wild-type as well as mutant forms of ASYN by ubiquitination, indicating that E6-AP plays critical regulatory role in the degradation of AYN (Mulherkar et al., 2009). In addition, E6-AP regulates cell proliferation by proteasomal degradation of p53, tumor suppressor protein (Scheffner, 1998). It also promotes cell growth and proliferation by regulating the PI3K–AKT pathway (Srinivasan and Nawaz, 2011). E6-AP promotes SOD1 aggresomes degradation and suppresses cell toxicity along with heat shock protein 70 (Mishra et al., 2013). In the present study, decreased E6-AP protein expression level by DA was rescued by treatment with reynosin in both SH-SY5Y cells and 6-OHDA-lesioned rats (Fig. 2). Furthermore, treatment with reynosin

Please cite this article as: Ham, A., et al., Reynosin protects against neuronal toxicity in dopamine-induced SH-SY5Y cells and 6-hydroxydopamine-lesioned rats as models of Parkinson's disease: Reciprocal up-regulation of E6-AP and down-regulation of α-synuclein. Brain Research (2013), http://dx.doi.org/10.1016/j.brainres.2013.05.036

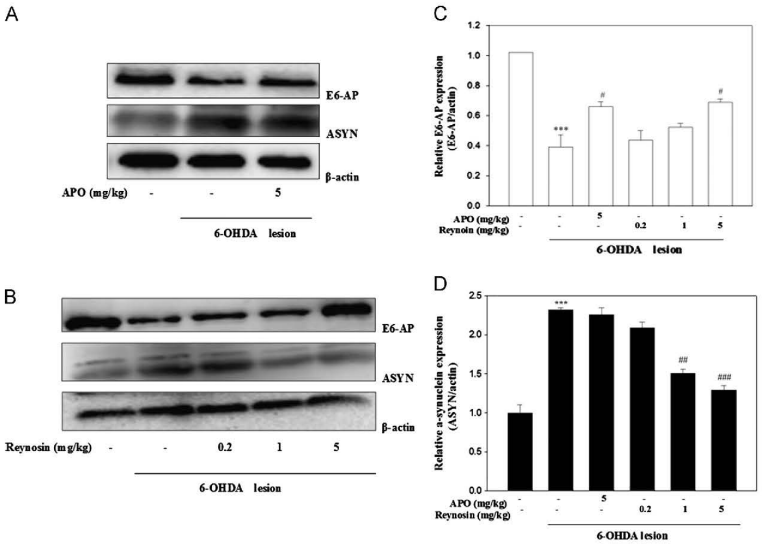

Fig. 4 – Effects of reynosin on the levels of ASYN and E6-AP protein expression in 6-OHDA-lesioned rats. (A and B) Rats were i. p. injected once with 0.2, 1, and 5 mg/kg of reynosin or 5 mg/kg of APO at 1 h after 6-OHDA lesion. The representative expression levels of ASYN and E6-AP protein are presented. (C and D) The mean values of ASYN and E6-AP were normalized to β-actin expression ($^{\sim}p<0.001$ versus sham group, $^{\#}p<0.05$, $^{\#\#}p<0.01$, and $^{\#\#\#}p<0.001$ versus 6-OHDA-lesioned group).

in 6-OHDA-lesioned rats down-regulated the over-expression of ASYN and simultaneously led to recovery of the down-regulated E6-AP protein expression (Fig. 4), consistent with the in vitro results.

In conclusion, our findings suggest that reynosin protects against DA-induced cell death and the resultant decrease in TH-positive neuronal loss in 6-OHDA-lesioned rats through the down-regulation of ASYN concomitant with the up-regulation of E6-AP protein expression. Our result, the reciprocal up-regulation of E6-AP and down-regulation of ASYN by reynosin, is the first reports about the neuroprotective effects of reynosin on in vitro and in vivo PD models, suggesting that reynosin might be a potential candidate for treatment of neurodegenerative diseases such as PD.

4. Experimental procedures

4.1. Reagents

Reynosin (98.2% purity) was provided by Prof. Jongheon Shin (Seoul National University, Korea). Dopamine (DA), apomorphine (APO), 6-OHDA, and propidium iodide (PI) were purchased from Sigma-Aldrich (St Louis, MO, USA). Dulbecco's modified Eagle's medium (DMEM) and fetal bovine serum (FBS) were purchased from Gibco BRL (Rockville, MD, USA). Hybond-polyvinylidene difluoride (PVDF) membrane was purchased from Amersham Pharmacia Biotechnology Inc. (Piscataway, NJ, USA). Protein extraction solution was purchased from iNtRON Biotech Inc. (Seoul, Korea).

4.2. Cell culture and neuronal cell protection test

Human neuroblastoma SH-SY5Y cells (ATCC no. CRL-2266) were cultured in DMEM supplemented with 10% heat-inactivated FBS and 1% penicillin/streptomycin (Meiji Seika, Tokyo, Japan), at 37 °C in a humidified 5% CO2 atmosphere. SH-SY5Y cells were cultured for 24 h and then treated with reynosin (0.08, 0.4, and 2 μM) or 2 μM of APO (a positive control compound) (Hara et al., 2006) for 24 h, followed by subsequent treatment with DA (600 μM) for an additional 24 h. Cell viability was analyzed by flow cytometry (FACS) (Calibur, Becton Dickinson, USA) using PI staining (Yang et al., 2009).

4.3. Animal

Male Sprague-Dawley rats were purchased from Samtako Bio Korea (Osan, Korea) and housed in groups (2–3 rats/cage) at room temperature for 1 week prior to the experiments in a humidity-controlled environment with a 12/12-light-dark cycle and unlimited access to food and water. All animal experiments were performed with the approval of the Institutional

Please cite this article as: Ham, A., et al., Reynosin protects against neuronal toxicity in dopamine-induced SH-SY5Y cells and 6-hydroxydopamine-lesioned rats as models of Parkinson's disease: Reciprocal up-regulation of E6-AP and down-regulation of α-synuclein. Brain Research (2013), http://dx.doi.org/10.1016/j.brainres.2013.05.036

Animal Care and Use Committee of Seoul National University, and in accordance with the requirements of European Directive 2010/63/EU. All efforts were made to minimize the number of animals used and their suffering. After experiments, all of the animals were sacrificed by overdose of anesthetics.

4.4. 6-OHDA lesion and APO/reynosin treatment

Injection of 6-OHDA into the rat substantia nigra was used as an animal model of PD (Ungerstedt, 1968). Rats weighing approximately 250 g were randomly divided into 4 groups: the sham group (vehicle solution, $n \geq 9$), the 6-OHDA-lesioned group (6-OHDA, $n \geq 9$), the APO treatment group (6-OHDA +APO, $n \geq 9$), and the reynosin treatment group (6-OHDA +reynosin, $n \geq 9$). The sham and 6-OHDA groups were intraperitoneally (i.p.) injected with the vehicle solution (1% EtOH/saline). The treatment groups were intraperitoneally injected with reynosin (0.2, 1, and 5 mg/kg, dissolved in 1% EtOH/saline) or APO (5 mg/kg, dissolved in 1% EtOH/saline) 1 h after 6-OHDA injection into the left substantia nigra. APO has been reported to have neuroprotective effects against 6-OHDA-lesioned nigrostriatal damage in the rat (Yuan et al., 2006) and was used as a positive control compound. At the beginning of the experiment, rats were anesthetized with ketamine (80 mg/kg, i.p.; Ketaset®; Fort Dodge, IA, USA) followed by xylazine (10 mg/kg, i.p.; Rompun®, Bayer, UK), and placed in a stereotaxic frame (Dae-Jong Instrument Industry Co., Seoul, Korea). 6-OHDA dissolved at a concentration of 5 μg/μl in saline containing 0.1% ascorbic acid was injected at a final dose of 20 μg into the substania nigra 4.8 mm posterior, 1.8 mm lateral and 7.8 mm ventral to the bregma and dura at a rate of 1 μl/min, using a Hamilton 10-μl syringe, according to the previously described procedure (Paxinos and Watson, 1998). After the 4 min of 6-OHDA injection at a rate of 1 μl/ml, the needle was kept in place for another 5 min to allow complete diffusion of 6-OHDA and then slowly removed at a rate of 1 mm/min. In the sham group, vehicle solution was injected instead of 6-OHDA. Next, the bone hole was sealed with restorative cement (GC Co., Tokyo, Japan) and then clipped. After 6-OHDA lesions, the animals were returned to their cages for 1 week.

4.5. Immunohistochemistry

TH-positive neurons were detected using the anti-TH antibody (Chemicon International, Temecula, CA, USA) and the Vectastain Elite ABC kit (Vector Laboratories, Burlingame, CA, USA) (Iancu et al., 2005). In brief, sections were incubated in PBS mixed with 3% goat serum and 0.2% Triton X-100 for 12 h, followed by an anti-mouse TH antibody at a dilution of 1:333 at 4 °C for another 24 h. The sections were then washed in 0.01 M PBS 3 times, incubated with secondary anti-mouse HRP-conjugated IgG antibody (1:1000; Santa Cruz Biotechnology, Inc., CA, USA) at room temperature for 1 h, and an avidin/biotin/peroxidase complex solution for another 1 h. The sections were subsequently stained with a diaminobenzidine immunohistochemistry kit (Vector Laboratories, CA, USA) and then mounted using cover slips and mounting fluid.

4.6. Image capture and analysis

Image analysis was performed using an optical microscope connected to a computerized image analysis system equipped with dedicated software (Viewfinder Lite software, Olympus, Japan). The average signal intensity of TH-positive neurons was determined. The effects on dopaminergic neurons were quantified by calculating the ratio of TH-positive neurons in the substantia nigra from the ipsilateral hemisphere to those from the contralateral hemisphere (I/C ratio) (Armentero et al., 2006; Blandini et al., 2004). For each animal, 4 or 5 sections were evaluated and pooled to provide the mean intensity value used to calculate the ratio ($n \geq 9$).

4.7. Western blot analysis

SH-SY5Y cells were cultured for 24 h and pre-treated within non-cytotoxic dose ranges of reynosin (0.08, 0.4, and 2 μM) or 2 μM of APO for 24 h, with a subsequent DA treatment for an additional 15 h. Proteins were extracted with a PRO-PREP protein extraction solution.

For animal-based (in vivo) western blotting, the rats were sacrificed and their brain tissues were rapidly obtained. The striatum from individual rats were dissected out and homogenized in 1% sodium dodecyl sulfate (SDS) TBST buffer, followed by boiling and centrifugation. Proteins from the brain tissue were prepared with a PRO-PREP protein extraction solution.

For western blotting analyses, equal amounts of protein were loaded onto each lane, separated by SDS-PAGE on a 10% gel, and transferred to a PVDF membrane. The membranes were incubated overnight at 4 °C with the anti-rabbit primary antibody for ASYN (1: 1000; Immuno-Biological Laboratories Co. Ltd., Gunma, Japan) and E6-AP (1:1000; Santa Cruz, CA, USA), followed by incubation for 1 h at room temperature with the secondary antibody (1:5000; anti-rabbit HRP-conjugated IgG, Santa Cruz, USA). Bands were analyzed using the LAS1000 (Fuji, Japan) image analyzer. After the blot was stripped and reprobed with anti-β-actin mouse antibody (1:5000; Santa Cruz, CA, USA), it was used as an internal control.

4.8. Statistical analysis

All experimental data are presented as the mean value ± standard deviation. Statistical significance between multiple groups was analyzed by one-way ANOVA (PRISM GraphPad, San Diego, CA, USA). When ANOVA showed a significant difference, post hoc Bonferroni's multiple comparison tests were performed. P values less than 0.05 were considered to be statistically significant.

Acknowledgments

This work was supported by the Basic Science Research Program through the National Research Foundation of Korea (NRF) funded by the Ministry of Education, Science and Technology (Grant no. 2010-0028078).

Please cite this article as: Ham, A., et al., Reynosin protects against neuronal toxicity in dopamine-induced SH-SY5Y cells and 6-hydroxydopamine-lesioned rats as models of Parkinson's disease: Reciprocal up-regulation of E6-AP and down-regulation of α-synuclein. Brain Research (2013), http://dx.doi.org/10.1016/j.brainres.2013.05.036

Appendix A. Supporting information

Supplementary data associated with this article can be found in the online version at http://dx.doi.org/10.1016/j.brainres.2013.05.036.

REFERENCES

Armentero, M.T., et al., 2006. Prolonged blockade of NMDA or mGluR5 glutamate receptors reduces nigrostriatal degeneration while inducing selective metabolic changes in the basal ganglia circuitry in a rodent model of Parkinson's disease. Neurobiol. Dis. 22, 1–9.

Asanuma, M., Miyazaki, I., Ogawa, N., 2003. Dopamine- or L-DOPA-induced neurotoxicity: the role of dopamine quinone formation and tyrosinase in a model of Parkinson's disease. Neurotoxic. Res. 5, 165–176.

Barzilai, A., Melamed, E., Shirvan, A., 2001. Is there a rationale for neuroprotection against dopamine toxicity in Parkinson's disease?. Cell Mol. Neurobiol. 21, 215–235.

Bennett, M.C., 2005. The role of alpha-synuclein in neurodegenerative diseases. Pharmacol. Ther. 105, 311–331.

Blandini, F., et al., 2004. Neuroprotective effect of rasagiline in a rodent model of Parkinson's disease. Exp. Neurol. 187, 455–459.

Chu, Y., et al., 2006. Nurr1 in Parkinson's disease and related disorders. J. Comp. Neurol. 494, 495–514.

Chu, Y., Kordower, J.H., 2007. Age-associated increases of alpha-synuclein in monkeys and humans are associated with nigrostriatal dopamine depletion: is this the target for Parkinson's disease?. Neurobiol. Dis. 25, 134–149.

Conway, K.A., et al., 2001. Kinetic stabilization of the alpha-synuclein protofibril by a dopamine-alpha-synuclein adduct. Science 294, 1346–1349.

Dedov, V.N., Cox, G.C., Roufogalis, B.D., 2001. Visualisation of mitochondria in living neurons with single- and two-photon fluorescence laser microscopy. Micron 32, 653–660.

Feany, M.B., Bender, W.W., 2000. A drosophila model of Parkinson's disease. Nature 404, 394–398.

Foyet, H.S., et al., 2011. Methanolic extract of Hibiscus asper leaves improves spatial memory deficits in the 6-hydroxydopamine-lesion rodent model of Parkinson's disease. J. Ethnopharmacol. 133, 773–779.

Golde, T.E., 2009. The therapeutic importance of understanding mechanisms of neuronal cell death in neurodegenerative disease. Mol. Neurodegener. 4, 8.

Gomez-Santos, C., et al., 2003. Dopamine induces autophagic cell death and alpha-synuclein increase in human neuroblastoma SH-SY5Y cells. J. Neurosci. Res. 73, 341–350.

Gomez-Santos, C., et al., 2005. Induction of C/EBP beta and GADD153 expression by dopamine in human neuroblastoma cells. Relationship with alpha-synuclein increase and cell damage. Brain Res. Bull. 65, 87–95.

Ham, A., et al., 2010. Spirafolide from bay leaf (*Laurus nobilis*) prevents dopamine-induced apoptosis by decreasing reactive oxygen species production in human neuroblastoma SH-SY5Y cells. Arch. Pharm. Res. 33, 1953–1958.

Hara, H., Ohta, M., Adachi, T., 2006. Apomorphine protects against 6-hydroxydopamine-induced neuronal cell death through activation of the Nrf2-ARE pathway. J. Neurosci. Res. 84, 860–866.

Hughes, A.J., et al., 1993. Subcutaneous apomorphine in Parkinson's disease: response to chronic administration for up to five years. Mov. Disord. 8, 165–170.

Iancu, R., et al., 2005. Behavioral characterization of a unilateral 6-OHDA-lesion model of Parkinson's disease in mice. Behav. Brain Res. 162, 1–10.

Jiang, Y.H., Beaudet, A.L., 2004. Human disorders of ubiquitination and proteasomal degradation. Curr. Opin. Pediatr. 16, 419–426.

Kanda, S., et al., 2000. Enhanced vulnerability to oxidative stress by alpha-synuclein mutations and C-terminal truncation. Neuroscience 97, 279–284.

Kirik, D., et al., 2002. Parkinson-like neurodegeneration induced by targeted overexpression of alpha-synuclein in the nigrostriatal system. J. Neurosci. 22, 2780–2791.

Masliah, E., et al., 2000. Dopaminergic loss and inclusion body formation in alpha-synuclein mice: implications for neurodegenerative disorders. Science 287, 1265–1269.

Millan, M.J., et al., 2002. Differential actions of antiparkinson agents at multiple classes of monoaminergic receptor. I. A multivariate analysis of the binding profiles of 14 drugs at 21 native and cloned human receptor subtypes. J. Pharmacol. Exp. Ther. 303, 791–804.

Mishra, A., et al., 2008. E6-AP promotes misfolded polyglutamine proteins for proteasomal degradation and suppresses polyglutamine protein aggregation and toxicity. J. Biol. Chem. 283, 7648–7656.

Mishra, A., et al., 2009. The ubiquitin ligase E6-AP is induced and recruited to aggresomes in response to proteasome inhibition and may be involved in the ubiquitination of Hsp70-bound misfolded proteins. J. Biol. Chem. 284, 10537–10545.

Mishra, A., et al., 2013. E6-AP association promotes SOD1 aggresomes degradation and suppresses toxicity. Neurobiol. Aging 34(4) (1310), e11–e23.

Miyazaki, I., Asanuma, M., 2008. Dopaminergic neuron-specific oxidative stress caused by dopamine itself. Acta Med. Okayama 62, 141–150.

Mulherkar, S.A., Sharma, J., Jana, N.R., 2009. The ubiquitin ligase E6-AP promotes degradation of alpha-synuclein. J. Neurochem. 110, 1955–1964.

Nicotra, A., Parvez, S., 2002. Apoptotic molecules and MPTP-induced cell death. Neurotoxicol. Teratol. 24, 599–605.

Paxinos, G., Watson, C., 1998. The Rat Brain in Stereotaxic Coordinates. Academic Press, San Diego.

Scheffner, M., 1998. Ubiquitin, E6-AP, and their role in p53 inactivation. Pharmacol. Ther. 78, 129–139.

Smith, W.W., et al., 2005. Alpha-synuclein phosphorylation enhances eosinophilic cytoplasmic inclusion formation in SH-SY5Y cells. J. Neurosci. 25, 5544–5552.

Srinivasan, S., Nawaz, Z., 2011. E3 ubiquitin protein ligase, E6-associated protein (E6-AP) regulates PI3K–Akt signaling and prostate cell growth. Biochim. Biophys. Acta 1809, 119–127.

Ungerstedt, U., 1968. 6-Hydroxy-dopamine induced degeneration of central monoamine neurons. Eur. J. Pharmacol. 5, 107–110.

Watanabe, H., et al., 2004. Protective effects of neuronal nitric oxide synthase inhibitor in mouse brain against MPTP neurotoxicity: an immunohistological study. Eur. Neuropsychopharmacol. 14, 93–104.

Yang, F., et al., 2009. Role of autophagy and proteasome degradation pathways in apoptosis of PC12 cells overexpressing human alpha-synuclein. Neurosci. Lett. 454, 203–208.

Yoshikawa, M., et al., 2000. Alcohol absorption inhibitors from bay leaf (Laurus nobilis): structure-requirements of sesquiterpenes for the activity. Bioorg. Med. Chem. 8, 2071–2077.

Yuan, H., et al., 2006. R-apomorphine protects against 6-hydroxydopamine-induced nigrostriatal damage in rat. Neurosci. Bull. 22, 331–338.

Please cite this article as: Ham, A., et al., Reynosin protects against neuronal toxicity in dopamine-induced SH-SY5Y cells and 6-hydroxydopamine-lesioned rats as models of Parkinson's disease: Reciprocal up-regulation of E6-AP and down-regulation of α-synuclein. Brain Research (2013), http://dx.doi.org/10.1016/j.brainres.2013.05.036

A Thesis for the Degree of Doctor of Philosophy in Pharmacology

Neuroprotection of active principles from the *Cudrania tricuspidata* in *in vitro* models of Parkinson's disease: Effect on the ubiquitin-proteasome system and Nrf2-ARE pathway

꾸지뽕나무로부터 분리한 유효성분물질의 파킨슨병 세포모델에서의 신경보호효과: Ubiquitin-proteasome system 및 Nrf2-ARE 관련 기전에 관한 효과연구

August, 2017

By

Dong-Woo Kim

Natural Products Science Major, College of Pharmacy

Doctor Course in the Graduate School

Seoul National University

Abstract

Neuroprotection of active principles from the *Cudrania tricuspidata* in *in vitro* models of Parkinson's disease: Effect on the ubiquitin-proteasome system and Nrf2- ARE pathway

Dong-Woo Kim

Natural Products Science Major

College of Pharmacy

Doctor Course in the Graduate School

Seoul National University

Parkinson's disease (PD) is characterized by severe motor deficits, cogwheel rigidity, bradykinesia, and the loss of dopaminergic neurons. The aetiology of PD has not been clearly identified; however, oxidative stress is thought to be a common factor that leads to cellular dysfunction and neurodegeneration. In particular, the pathological events that occur in PD have been suggested to be linked to protein oxidation caused by oxidative stress, and excessive intracellular ROS induce apoptosis that is characterized by the cleavage of caspase-3, caspase-9 and poly

ADP-ribose polymerase (PARP). The neurotoxin 6-hydroxydopamine (6-OHDA), Carbonyl cyanide 3-chlorophenylhydrazone (CCCP) destroys dopaminergic and noradrenergic neurons in the brain by inducing excessive ROS such as superoxide radicals, which leads to protein oxidation and neuronal cell death. Also, ubiquitin-proteasome system play a key role in the etiology of PD. The proteasome selective degrades oxidized proteins via ubiquitin-mediated processes, and its role is essential for cellular protein maintenance. However, dysfunctions in the ubiquitination machinery or in the proteolytic activities of the proteasome induce the accumulation of polyubiquitinated misfolded proteins and oxidized proteins. Subsequently, this induces protein aggregation, further inhibits proteasome activity, generates additional cellular stress, and ultimately leads to neuronal cell death. Additionally, mitophagy play a major role in the etiology of PD. Mitophagy, a specialized autophagy pathway that mediates the clearance of damaged mitochondria by lysosomes, is important for mitochondrial quality control. Defective mitochondria, if left uncleared, can be a source of oxidative stress and compromise the health of the entire mitochondrial network. The several lines of evidence propose that mitochondrial dysfunction is central to the disease. PD-associated mutations in PINK1 or parkin impair parkin recruitment, mitochondrial ubiquitination, and/or mitophagy. In the context of the inherently high mitochondrial oxidative stress in substantia nigra dopamine neurons, loss of parkin-mediated mitophagy could explain the greater susceptibility of substantia nigra

neurons to neurodegeneration. Thus, promoting mitophagy and enhancing mitochondrial quality control could benefit dopaminergic neurons. The current therapeutic drugs are based on prohibiting the progress of PD through treatment of dopamine agonist or dopamine precursor. New therapies in development are aimed at protecting dopaminergic neurons. In this study, the effects of natural products on 6-OHDA, CCCP-mediated signaling in SH-SY5Y neuroblastoma cell were investigated to discover new lead compounds for the treatment of PD.

Cudrania tricuspidata (Moraceae) is a subtropical tree that is widely distributed in Korea, China, and Japan. The fruits of *C. tricuspidata* are used in jams, juices, and a fermented alcoholic beverage with sugar, and they are commercially produced as food in Korea. Also, the cortex and root bark of *C. tricuspidata* have been used as a traditional medicine for inflammation and tumors. A recent study demonstrated that the extracts of *C. tricuspidata* protect neurons against oxidative stress-induced cytotoxicity and inhibitory effects on nitric oxide synthase (NOS). The compounds isolated from *C. tricuspidata* are primarily xanthones and flavones in addition to some alkaloids, lignins, coumarins, polysaccharides, and chromones. The isoflavones and chromones from *C. tricuspidata* have been reported to exert protective effects against 6-OHDA-induced neurotoxicity and to have inhibitory effects against IgE-mediated allergic and inflammatory responses.

In first chapter, it was investigated that 5,7-dihydroxychromone (DHC) isolated from the roots of *C. tricuspidata* for its neuronal cell protection and inhibition of

the generation of ROS in 6-OHDA-induced SH-SY5Y cells. Flow cytometric analysis revealed that DHC protected against the 6-OHDA-induced generation of ROS and protected against neuronal cell death. Additionally, DHC increased the nuclear translocation of Nrf2 and the binding of Nrf2 to ARE, which subsequently resulted in the up-regulation of the expression of Nrf2-dependent antioxidant genes, including heme oxygenase 1 (HO-1), NAD(P)H quinone oxidoreductase 1 (NQO1) and glutamate-cysteine ligase, catalytic subunit (GCLc). DHC inhibited the expression of cleaved caspase-3 and caspase-9 and PARP in 6-OHDA-induced SH-SY5Y cells. The addition of Nrf2 siRNA abolished the neuroprotective effect of DHC against 6-OHDA-induced cell death and the expression of Nrf2-mediated antioxidant genes. These findings suggest that the neuroprotective effect of DHC against 6-OHDA-induced toxicity is partly due to the induction of Nrf2-mediated antioxidant gene expression via the activation of the Nrf2-ARE signaling pathway in SH-SY5Y cells.

In the second chapter, the effects of ethanol extract from the fruits of *C. tricuspidata* (CTE) and it active compounds were studied. Among the nine isolates from a 50% ethanol extract from *C. tricuspidata* fruits (CTE50), orobol (OB), 6-prenylorobol (POB), and 6,8-diprenylorobol (DPOB) showed neuroprotective effects in 6-OHDA-induced SH-SY5Y cell death. In addition, CTE50 and the three orobol derivatives (OB, POB, and DPOB) attenuated the cleavage of caspase-3, caspase-9, and PARP and inhibited the excessive generation of ROS. Furthermore,

it enhanced the 6-OHDA-induced dysfunction of proteasome activity and reduced the accumulation of ubiquitin conjugated-proteins and the polyubiquitination of α-synuclein and synphilin-1. The proteasome inhibitor MG132 blocked the neuroprotective effects and the enhanced proteasome activity produced by CTE50 and the three orobol derivatives. These results demonstrate that CTE50 and three orobol derivatives protect against 6-OHDA-induced neurotoxicity by enhancing the ubiquitin/proteasome-dependent degradation of α-synuclein and synphilin-1, suggesting that they might be possible candidates for the treatment of neurodegenerative diseases.

In the third chapter, the effects of active compounds from the *C. tricuspidata* extracts on deubiquitinating enzymes were studied. TH3-125-4 (TH20) isolated from the root barks of the *C. tricuspidata* protected against CCCP-induced neuronal cell death in Parkin K.D. SH-SY5Y cells. Also, TH20 significantly inhibited USP30 enzyme activity and disassembly of polyubiquitin chain in *in vitro* assay. Additionally, TH20 decreased protein expression of USP30. Based on the results, it was suggested that TH20 might be promising candidates for the therapy of familiar PD via restoring Parkin-mediated mitophagy.

Keywords : *Cudrania tricuspidata*, oxidative stress, 6-OHDA, neuroprotection, 5,7-Dihydroxychromone, Nrf2/ARE pathway, orobol derivatives, proteasome activity, ubiquitination, deubiquitinating enzyme, PINK1, Parkin, mitophagy

Student number **:** 2012-21566

Table of Contents

Abstract · · ·

2.6 Measurement of intracellular ROS by Flow cytometry · · · · · · · · · · · ·13

2.7 Nuclear and cytosolic lysate preparations ·13

2.8 Electrophoretic mobility shift assay (EMSA)· · · · · · · · · · · · · · · · · · · 14

2.9 Nrf2 knockout via the transfection of small interfering RNA (siRNA)·

· · · · · · · · · · · · · · · · · · · ·

SH-SY5Y cells · · ·

3.5 Effects of CTE50 and three orobol derivatives on proteasome subunit mRNA expression · · ·

3.2 Effect of TH3-125-4 (TH20) on ubiquitin chain disassembly · · · · · · 123

3.3 The protective effects of TH3-125-4 (TH20) against CCCP-induced neuronal cell death in parkin knock down SH-SY5Y cells · · · · · · · · · · · 125

3.4 Inhibitory effect of TH3-125-4 (TH20) on USP30 protein expression in SH-SY5Y cells· · · · · · · · · · · ·

List of Figures

Figure 13. Effects of DHC on the mRNA expressions of NQO1 in SH-SY5Y cells· · · ·

Figure 23. Inhibitory effects of CTE50 and three orobol derivatives against 6-OHDA-induced apoptotic markers · 77

Figure 24. Protective effects of CTE50 and three orobol derivatives (OB, POB, and DPOB) against 6-OHDA-induced dysfunction of proteasome activities in SH-SY5Y cells ·80

Figure 25. Effects of CTE50 and three orobol derivatives (OB, POB, and DPOB) on mRNA expression of proteasome subunits in SH-SY5Y cells · · · · · · ·83

Figure 26. Inhibitory effects of CTE50 and three orobol derivatives against 6-OHDA-induced ubiquitin-conjugated proteins · · · · · · · · · · · · · · · · · · ·85

Figure 27. Inhibitory effects of CTE50 and three orobol derivatives against 6-OHDA-induced polyubiquitination of α-synuclein · 87

Figure 28. Inhibitory effects of CTE50 and three orobol derivatives against 6-OHDA-induced polyubiquitination of synphilin-1· · · · · · · · · · · · · · · · · · · ·88

Figure 29. Inhibitory effects of MG132 on the protective effects of CTE50 and three orobol derivatives against 6-OHDA-induced neuronal cell death · · · · 90

Figure 30. Inhibitory effects of MG132 on the protective effects of CTE50 and three orobol derivatives against 6-OHDA-induced proteasome dysfunction · · · · · · · · · · · · · · · · · · ·

neuronal cell death in parkin knock down SH-SY5Y cells · · · · · · · ·128

Figure 42. Inhibitory effect of TH3-125-4 (TH20) on USP30 protein expression in SH-SY5Y cells · · · · · · ·

List of Tables

Chapter 1

Neuroprotection against 6-OHDA-induced oxidative stress and apoptosis in SH-SY5Y cells by 5,7-Dihydroxychromone

: Activation of the Nrf2/ARE pathway

1. Introduction

The incidence of neurodegenerative diseases is increasing with the continuous growth of the elderly population. Although the causes of neurodegenerative diseases have not been clearly elucidated, recent studies have demonstrated that reactive oxygen species (ROS) might be one of the important factors in the neurotoxicity that occurs in neurodegenerative diseases (Farooqui and Farooqui, 2011). Cells exposed to environment fortified with oxygen constantly generate oxygen free radicals. ROS includes oxygen-related free radicals and reactive species, and they are produced as a result of aerobic metabolism. Formation of ROS can occur in two ways: enzymatic and non-enzymatic responses. Enzymatic responses generating free radicals include those involved in the mitochondrial respiratory chain, phagocytosis, prostaglandin synthesis and the cytochrome P450 system. The non-enzymatic process can also occur through oxidative phosphorylation (*i.e.* aerobic respiration) in the mitochondria. ROS is generated from either endogenous or exogenous sources. Endogenous free radicals are generated from immune cell activation, inflammation, mental stress, excessive exercise, ischemia, infection, cancer and aging. Exogenous ROS result from air and water

pollution, cigarette smoke, alcohol, heavy or transition metals (Cd, Hg, Pb, Fe, As), certain drugs (cyclosporine, tacrolimus, gentamycin, bleomycin), industrial solvents, cooking (smoked meat, used oil, fat) and radiation. After penetrated into the body by different ways, these exogenous agents are decomposed or metabolized into free radicals (Chen et al., 2012). Increased ROS production causes impairment to cell organelles. Many studies have confirmed the benefits of antioxidants in reducing oxidative stress in neurons and protecting against neurodegenerative diseases (Alfieri et al., 2011). In response to excessive ROS, the cellular expressions and bioactivity of numerous antioxidant enzymes are changed via initiating the upstream factor NF-E2-related factor 2 (Nrf2)/antioxidant response elements (AREs) complex (Leutner et al., 2000).

The Nrf2/ARE signal has an important effect on the induction of antioxidant gene expression, and it has been reported that the activation of Nrf2 is an important signal which can neutralize oxidative stress (Sun et al., 2010). Nrf2 activity is regulated partly by Keap1 protein, which was initially proposed to act by binding and tethering the transcription factor in the cytoplasm. Activation of Nrf2 in response to stress signals was thought to result from a interruption of this association, releasing Nrf2 for translocation into the nucleus to affect its transcriptional activity. Independently, Nrf2 has been

found to be a highly unstable protein, subject to proteolytic degradation catalyzed by the proteasome via the ubiquitin-dependent pathway. In this case, activation of Nrf2 was suggested to be dependent on mechanisms that increase its stability, leading to its accumulation in the cell. The unstable nature of the Nrf2 protein and its regulation through this dynamic mechanism suggest that Nrf2 is unlikely to be joined in a passive complex in the cytoplasm. This was supported by a number of studies demonstrating a more active role of Keap1 in its repression of Nrf2 activity. Keap1 appears to promote Nrf2 ubiquitylation in a constitutive manner through the cullin-3-dependent pathway. That Nrf2 is constantly degraded in non-stressed cells implies that Keap1 is a constitutively active protein and that it promotes Nrf2 ubiquitylation in an unregulated manner. This is supported by the observation that overexpression of Keap1 leads to increased levels of ubiquitin-conjugated forms of Nrf2 in cells, indicating that Keap1 is expressed as a functionally active protein. Thus, interaction between the two proteins is more likely a transient encounter rather than a sustained association. Given that the steady-state level of Nrf2 in the cell is maintained in part through its constitutive expression, requiring *de novo* gene transcription and protein synthesis, the pathway through which Nrf2 activity is regulated, from synthesis to degradation, requires examination in further detail (Nguyen et al., 2009). In

summary, under normal state, Nrf2 is localized in the cytoplasm and is subject to ubiquitination and proteasomal degradation. However, antioxidant agents block the elimination of Nrf2 from the cytosolic Nrf2 complex, which induces nuclear translocation of Nrf2 and subsequently makes the Nrf2/ARE complex to mediate the induction of many antioxidant enzyme genes, such as heme oxygenase 1 (HO-1), NAD(P)H: quinone oxidoreductase (NQO1), and glutamate-cysteine ligase catalytic subunit (GCLc) (Zhang et al., 2013).

The heme-heme oxygenase (HO) system is a controller of endothelial cell integrity and oxidative stress. HO-1 and HO-2, two isoforms of HO, are viewed as having a major role in the construction of carbon monoxide (CO) and bilirubin and in heme breakdown. The fact that HO-1 is strongly induced by oxidant stress and its substrate heme, in conjunction with the ability of HO-1, to protect against oxidative insult suggests a countervailing system to oxidative stress damage. The antioxidant effects of HO-1 arise from its capacity to increase reduced glutathione levels and to degrade heme, as well as from the elaboration of biliverdin and bilirubin, which have potent antioxidant properties. CO, a product of HO, is not an antioxidant, but it does have an antiapoptotic effect. Furthermore, CO is a vasodilator that has been shown to enhance endothelial function and plays an important role in regulating basal and constrictor-induced vascular tone (Turkseven et al., 2005).

NQO1 has multiple protective roles that include and extend beyond its catalytic function. It is a widely-distributed FAD-dependent flavoprotein that catalyzes the reduction of quinones, quinoneimines, nitroaromatics, and azo dyes. NQO1 was discovered and named DT-diaphorase in the late 1950s, and shown to be identical to the dicoumarol-inhibited vitamin K reductase described. The classical direct antioxidant role of NQO1 is characteristic in its catalytic mechanism: the obligatory two-electron reduction of a wide array of quinones to their corresponding hydroquinones by using either NADPH or NADH as the hydride donor. In doing so, NQO1 diverts quinone electrophiles from participating in reactions that could lead to either sulfhydryl depletion, or to one-electron reductions that can produce semiquinones and various reactive oxygen intermediates as a result of redox cycling. In addition, the hydroquinone products of the NQO1 reaction can be further metabolized to glucuronide and sulfate conjugates, thereby facilitating their excretion. Remarkably, quinone reductases have been found in a wide range of eukaryotic organisms ranging from yeast to mammals. Although in many systems much remains to be learned about the complicated details of the function and regulation of these enzymes, it is clear that in all cases quinone reductases are at the forefront of the cellular defense by providing multiple layers of protection (Dinkova-Kostova and Talalay, 2010).

Glutathione (GSH) is considered the most abundant molecule among endogenous antioxidants. GSH is a reduced peptide consisting of three-residues (γ-l-glutamyl-l-cysteinyl glycine) which can donate an electron with the consequence that two electrons donating GSH molecules form oxidized GSSG. In humans, GSH is almost uniquely present in a quite high concentration (1–10 mM) which allows to scavenge ROS either directly or indirectly. It can directly react with O^{2-} and some other ROS, but its indirect ROS-scavenging functions, such as revitalizing other antioxidants, are likely more important; e.g. it can reduce dehydroascorbic acid which is formed in the reconversion of α-tocopheroxyl radical to α-tocopherol, a lipophilic chain breaking antioxidant, which interacts with the polyunsaturated acyl groups of lipids, stabilizes membranes and scavenges various reactive oxygen species and lipid oxy-radicals. As an antioxidant it reacts with ROS, RNS and radicals produced in association with electron transport, xenobiotic metabolism and inflammatory responses. GSH is synthesized from its constituent amino acids forming a tripeptide thiol and this synthesis requires two ATP-dependent steps. The first and limiting synthesis is catalyzed by γ-glutamyl-cysteine ligase (GCL) and the second step mediated by GSH synthetase (GS). GCL is a heterodimeric enzyme composed by a heavy subunit, GCLc with catalytic activity and a smaller one, GCLm that has a regulatory role on the other

subunit. GSH homeostasis in the cell is not only regulated by its de novo synthesis, but also by other factors such as utilization, recycling and cellular export. This redox cycle is known as the GSH cycle and incorporates other important antioxidant, redox-related enzymes. Nearly every eukaryotic cell, from plants to yeast to humans, expresses a form of the GCL protein for the purpose of synthesizing GSH. To further highlight the critical nature of this enzyme, genetic knockdown of GCL results in embryonic lethality. Furthermore, dysregulation of GCL enzymatic function and activity is known to be involved in the vast majority of human diseases, such as diabetes, Parkinson's disease, Alzheimer's disease, COPD, HIV/AIDS, and cancer. This typically involves impaired function leading to decreased GSH biosynthesis, reduced cellular antioxidant capacity, and the induction of oxidative stress (Espinosa-Diez et al., 2015). Numerous research results reported that Nrf2 and Nrf2 dependent antioxidant genes are potent factors for developing the therapy of neurodegenerative diseases due to its abilities to regulate the excessive oxidative stress and inflammation. A recent study demonstrated that the extracts of *Cudrania tricuspidata* protect neurons against oxidative stress-induced cytotoxicity (Jeong et al., 2010) and have inhibitory effects on nitric oxide synthase (NOS) (Kang et al., 2002). It was also reported that 5,7-Dihydroxychromone (DHC), from *Cudrania*

tricuspidata, has an antioxidant activity (Qiu et al., 2012). However, neuroprotective effects of DHC and the related mechanisms of neuroprotection were poorly elucidated.

In this study, it was demonstrated that neuroprotective effects of DHC against 6-OHDA-induced neurotoxicity via the induction of the Nrf2/ARE-mediated signal.

2. Materials and methods

2.1. Chemicals and reagents

Propidium iodide (PI), 6-hydroxydopamine (6-OHDA), and 2',7'-dichlorfluorescein-diacetate (DCFH-DA) were purchased from Sigma-Aldrich (St. Louis, MO, USA). Dulbecco's modified Eagle's medium (DMEM) and fetal bovine serum (FBS) were purchased from Gibco BRL (Rockville, MD, USA). Hybond-polyvinylidene difluoride (PVDF) membranes were purchased from Amersham Pharmacia Biotechnology. (Piscataway, NJ, USA). Easy-Blue® total RNA extraction solution, PRO-PREP protein extraction solution and WEST-ZOL® ECL solution were purchased from iNtRON Biotech. (Kyunggi, Korea). SuPrimeScript RT premix®, and SYBRs HS Prime qPCR premix® were purchased from Genet Bio (Daejeon, Korea). Nrf2 siRNA, scrambled siRNA, Nrf2, HO-1, NQO1, GCLc, LaminB1, α-tubulin, β-actin, caspase-3, caspase-9, PARP, secondary antibody and FITC-conjugated secondary antibody were purchased from Santa Cruz Biotechnology. (Santa Cruz, CA, USA)

2.2. Preparation of 5,7-dihydroxychromone (DHC)

Cudrania tricuspidata was stored at the Korea Forest Research Institute at Southern Forest Research Center (Jinju, Korea) in September 2008. A voucher specimen (accession number KH1-4-090814) was kept at the Department of Biosystems and Biotechnology at Korea University (Seoul, Korea). 5,7-Dihydroxychromone (DHC) was isolated from the roots of *Cudrania tricuspidata* and the structure of DHC was determined by spectroscopic methods, and the purity was more than 98.5% (Wei and Yu, 2008). DHC was dissolved in DMSO and diluted with PBS to obtain the proper concentration of DHC. Final concentration of DMSO was less than 0.1% and it didn't influence the performed assays.

2.3. Cell cultures

The human neuroblastoma cell line SH-SY5Y (ATCC No. CRL-2266) was purchased from the American Type Culture Collection (Manassas, VA, USA) and cultured in DMEM supplemented with 10 % heat-inactivated FBS and 1 % penicillin/streptomycin at 37 ºC in a humidified 5 % CO_2 atmosphere.

2.4. Measurement of cell viability

SH-SY5Y cells were seeded at a density of 1×10^5 cells/200 μL/well in 96-well plates for 24 h, and the cells were pre-treated with DHC (0.4, 2, or 10 μM) for 24 h followed by subsequent treatment with 6-OHDA (100 μM) for an additional 24 h. To evaluate the effect of Nrf2, cells were transfected with scrambled siRNA or Nrf2 siRNA for 48 h and its final concentration was 50 nM. After transfected cells were treated with DHC (10 μM) and 6-OHDA (100 μM),-cell viability was determined using a MTT (3-(4,5-Dimethylthiazol-2-yl)-2,5-Diphenyltetrazolium Bromide) and measured by ELISA (Koo et al., 2011).

2.5. Measurement of cell necrosis by propidium iodide staining

SH-SY5Y cells were seeded at a density of 2×10^5 cells/2 mL/well in 6-well plates for 24 h, and the cells were pre-treated with DHC (0.4, 2, or 10 μM) for 24 h followed by subsequent treatment with 6-OHDA (100 μM) for an additional 24 h. To evaluate the effect of Nrf2, cells were transfected with scrambled siRNA or Nrf2 siRNA for 48 h and its final concentration was 50 nM. After transfected cells were treated with DHC (10 μM) and 6-OHDA (100

μM),-cell viability was determined using a propidium iodide (PI) staining and measured by flow cytometry (BD FACSCalibur ^{TM}) (Koo et al., 2011).

2.6. Measurement of intracellular ROS by Flow cytometry

ROS levels in cells were measured with the 2',7'-dichlorofluorescein diacetate (DCFH-DA) method (Munch et al., 1998a). Briefly, the cells were washed with PBS, and then incubated with 4 μM of DCFH-DA for 30 min at 37 ºC in the dark. The cells were then washed with PBS. The fluorescence intensities were measured by flow cytometry (BD FACSCalibur ^{TM} San Jose, CA, USA).

2.7. Nuclear and cytosolic lysate preparations

The nuclear and cytosolic proteins were extracted with a commercial kit (Nuclear Extract Kit) according to the manufacturer's procedure (Active Motif, Carlsbad, CA). Briefly, the cells were incubated in hypotonic buffer on ice for 15 min, homogenized with detergent, and centrifuged for 30 sec at 14,000 x g in a microcentrifuge at 4 ºC. The supernatant was used as the cytosolic proteins. The nuclear pellets were washed with cold PBS, extracted completely with lysis buffer for 30 min on ice and centrifuged for 10 min at 14,000 x g in a microcentrifuge at 4 ºC. The supernatant was used as the nuclear proteins.

2.8. Electrophoretic mobility shift assay (EMSA)

To determine the Nrf2-ARE binding activity, an electrophoretic mobility shift assay (EMSA) was accomplished as previously described (Meyer et al., 1998). Briefly, the nuclear proteins from the SH-SY5Y cells were reacted with ^{32}P-end-labeled 22-mer double-stranded oligonucleotide containing the Nrf2 sequence for 30 min at 37 ºC. The DNA-protein complexes were electrophoresed and gels were dried. The binding signals were visualized by BAS-1500 (Fuji, Tokyo, Japan).

2.9. Nrf2 knockout via the transfection of small interfering RNA (siRNA)

The transfection with scrambled siRNA or Nrf2 siRNA were progressed at final concentrations of 50 nM for 48 h by Lipofectamine 2000 (Invitrogen, Carlsbad, CA) prior to treatment with DHC (10 μM) and 6-OHDA (100 μM) as recommended by the manufacturer's guidelines.

2.10. Measurement of mRNA expression

After treatments, total RNA was isolated from SH-SY5Y cells by easy-BLUE® and cDNA was synthesized by using SuPrimeScript RT premix® according to the manufacturer's procedure. The synthesized cDNA was used for PCR and the primer pair sequence were listed as follows:

HO-1 5-TGCTCGCATGAACACTCTG-3 (Sense) and

5- TCCTCTGTCAGCAGTGCC-3 (antisense);

NQO1 5-AGCCCAGATATTGTGGCTGA-3 (Sense) and

5-AAGCCACAGAAATGCAGAATG-3 (antisense);

GCLc 5-AGGCCAACATGCGAAAC-3 (Sense) and

5-CGGATATTTCTTGTTAAGGTACTGG-3 (antisense);

GAPDH 5-CTCTGCTCCTCCTGTTCGAC-3 (Sense) and

5-ACGACCAAATCCGTTGACTC-3 (antisense). The cycle condition was as follow; 94℃ for 20s, 56℃ for 20s, 72℃ for 30s and 40 cycles. PCR were performed by using SYBRs HS Prime qPCR premix® in an ABI 7300 real-time PCR (Applied Bio systems, CA, USA). Ct (threshold cycle) values were obtained using the Sequence Detection Software version1.2.3 (Applied Bio systems, CA, USA). To evaluate quantification of the changes in target gene expression, we used the $2^{-\triangle\triangle Ct}$ method (Tucker and Munchus, 1998). Fold change=$2^{-\triangle\triangle Ct}$, $\triangle\triangle Ct = (Ct_{\text{target gene}} - Ct_{GAPDH}) - (Ct_{\text{control}} - Ct_{GAPDH})$

2.11. Measurement of protein expression

The SH-SY5Y cells were collected, washed with PBS and lysed with a PRO-PREP protein extraction solution at -20 ºC for 20 min. After centrifugation at 13,000 x g for 30 min, the supernatant was used as the total protein extracts. Western blot analysis was accomplished as previously described method (Ham et al., 2013).

2.12. Nuclear translocation of Nrf2 using fluorescence microscope

The culture dish was coated with 0.2 % gelatin at 37 °C for 30 min and dried at RT on a clean bench. The SH-SY5Y cells were plated at a density of 5×10^4 cells/200 μL/well in coated dishes for 24 h and incubated with DHC (0.4, 2, or 10 μM) for 6 h. After treatment with DHC, the cells were washed with 1x PBS/Tween-20 buffer (pH 7.4) (PBST) once. The cells were fixed with 4 % paraformaldehyde for 30 min at room temperature (RT). After washing with PBST, the blocking steps were performed with 1 % BSA in PBST. Next, the cells were incubated with the primary antibody at 4 °C overnight. The next day, the cells were washed with PBST 3 times and incubated with FITC-conjugated secondary antibody for 1 h at RT. After 1 h, the cells were washed with PBST 3 times, and DAPI staining was performed for 5 min at RT. Lastly, the PBST washing and mounting steps were conducted.

2.13. Statistical analysis

All experimental data are expressed as mean value ± standard deviation. Statistical significance between multiple groups was determined by one-way ANOVA (PRISM Graph Pad, San Diego, CA, USA). When ANOVA had a significant difference, *post hoc* Bonferroni's multiple comparison tests was conducted. *P* value less than 0.05 was regarded to be statistically significant.

3. Results

3.1. Protective effect of DHC against 6-OHDA-induced neuronal cell death.

The protective effects of DHC (Fig. 2) on SH-SY5Y cells were evaluated to determine the non-cytotoxic dose range (data not shown). The percentage of cell necrosis was evaluated with PI staining. As shown in Fig. 3, the percentage of PI-stained dead cells induced by 6-OHDA increased to 44.5 % compared to the vehicle-treated group (8.7 %). In contrast, 6-OHDA-induced cell death was dose-dependently prevented by DHC treatments at concentrations of 0.4, 2 and 10 μM within the non-toxic dose range. DHC (10 μM) treatment elicited its neuroprotective effects against 6-OHDA by decreasing the percentage of PI-positive cells to 13.8 %, whereas treatment with Nrf2 siRNA and DHC (10 μM) reduced the neuroprotective effect by increasing the percentage of PI-positive cells to 50.1 %. Also, the neuroprotective effect of DHC was evaluated by MTT assay (Fig. 4). The result of MTT assay was correlated with PI staining assay.

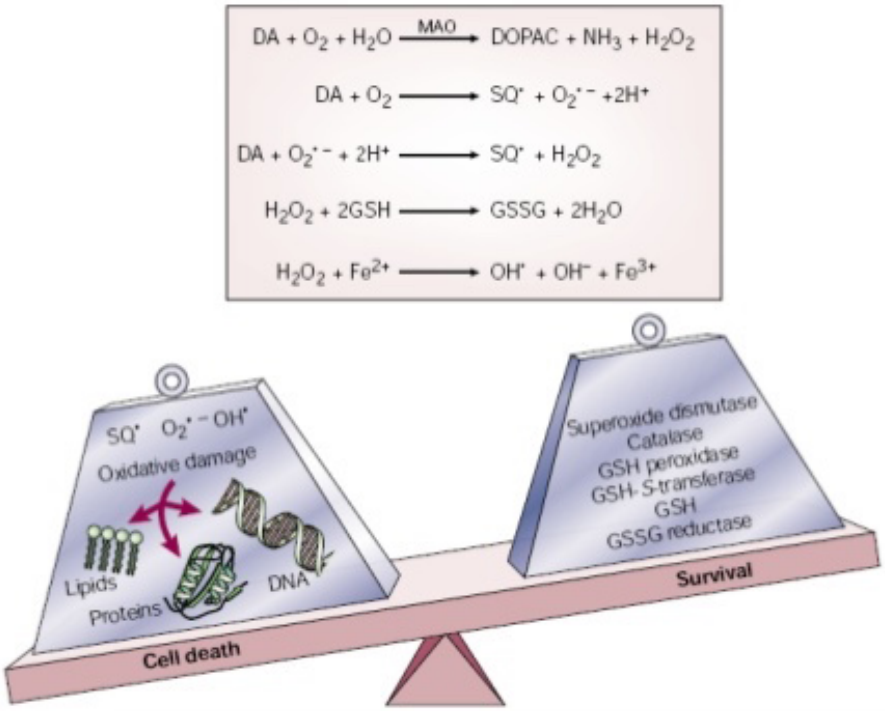

Figure 1. Scheme of oxidative stress and antioxidant enzymes in neuronal cell.

Table 1. The protective effect of isolated compounds from *Cudrania tricuspidata* root barks against 6-OHDA-induced neuronal cell death.

No.	Sample	6-OHDA-induced neuronal cell death MTT EC_{50} (μM)
1	**JY1-13-2**	**12.9**
2	**JY1-14-1**	**7.2**
3	JY1-15-1	>40
4	JY1-19-1	>40
5	JY1-19-2	>40
6	JY1-29-2	>40
7	JY1-30-1	>40
8	**JY1-36-1**	**9.5**
9	**JY1-37-2**	**9.2**
10	**JY1-53-2**	**15.5**
11	JY1-54-1	>40
12	JY1-54-3	>40
13	**JY1-56-2**	**9.1**
14	JY1-59-2	>40
15	JY1-64-2	>40
16	JY1-69-3	>40
17	**JY1-88-2**	**30.2**
18	JY1-88-3	>40
19	**JY1-89-7**	**8**
20	JY1-89-9	>40
21	JY1-89-11	>40

22	JY1-89-12	>40

Table 1. Continued

No.	Sample	6-OHDA-induced neuronal cell death MTT EC_{50} (μM)
23	JY1-91-7	>40
24	JY1-97-1	>40
25	JY1-62-1	>40
26	JY1-64-4	>40
27	JY1-64-5	>40
28	JY1-64-7	>40
29	JY1-88-13	>40
30	JY1-89-8	>40
31	JY1-99-1	>40
32	JY1-99-2	>40
33	JY1-101-1	>40
34	JY1-101-4	>40
35	JY1-102-4	>40
36	JY1-104-3	>40
37	JY1-120-3	>40
38	JY1-146-1	>40
39	JY1-153-2	>40
40	JY1-154-2	>40
41	JY1-158-2	>40
42	JY1-162-1	>40
43	JY1-164-4	>40

44	JY1-164-5	>40
45	JY1-165-8	>40

Table 1. Continued

No.	Sample	6-OHDA-induced neuronal cell death MTT EC_{50} (μM)
46	JY1-166-3	>40
47	JY1-167-6	>40
48	JY1-168-6	>40
49	JY1-170-5	>40
50	JY1-170-6	>40
51	JY1-172-2	>40
52	JY1-173-1	>40
53	JY1-179-6	>40
54	JY1-179-8	>40
55	JY1-179-9	>40
56	**JY1-180-4 (5,7-Dihydroxychromone ;DHC)**	**1.9**

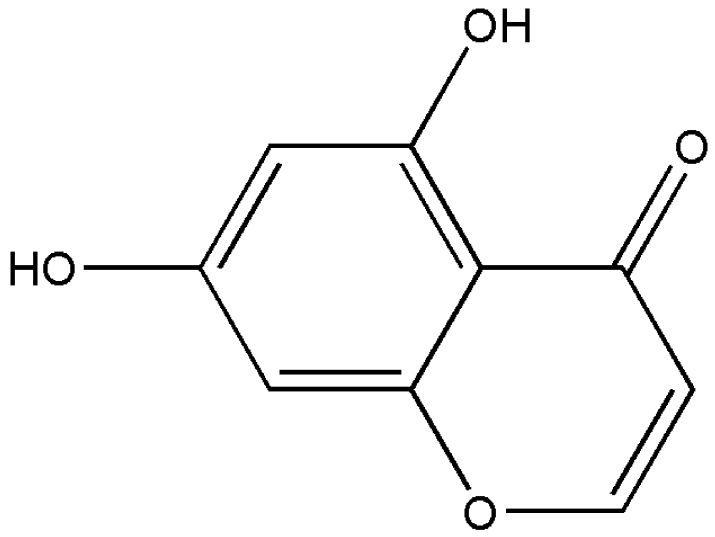

Figure 2. Chemical structure of 5,7-Dihydroxychromone (DHC).

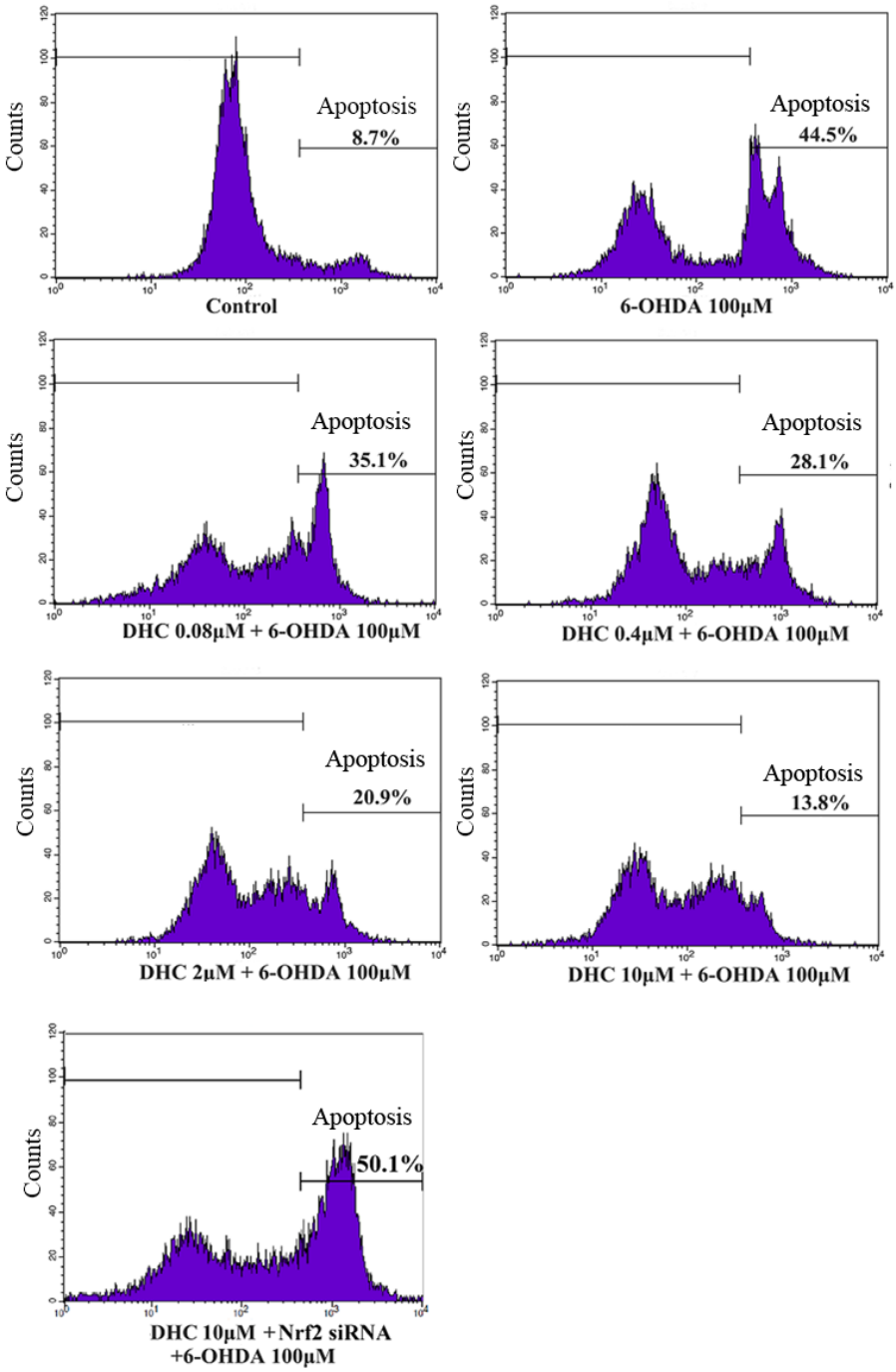
Counts
Apoptosis
8.7%
Control
Apoptosis
44.5%
6-OHDA 100μM
Apoptosis
35.1%
DHC 0.08μM + 6-OHDA 100μM
Apoptosis
28.1%
DHC 0.4μM + 6-OHDA 100μM
Apoptosis
20.9%
DHC 2μM + 6-OHDA 100μM
Apoptosis
13.8%
DHC 10μM + 6-OHDA 100μM
Apoptosis
50.1%
DHC 10μM +Nrf2 siRNA
+6-OHDA 100μM

Figure 3. Effects of DHC against 6-OHDA-induced cell necrosis in SH-SY5Y cells.

The cells were pre-treated with different concentrations of DHC (0.08 - 10 μM) for 24 h and subsequently treated with 6-OHDA (100 μM) for another 24 h. The cells were transfected with Nrf2 siRNA (50 nM) for 48 h before the treatment with DHC (10 μM). The cells were stained with PI dyes for 30 min and determined by FACS analysis using FL-2 channel. The values of fluorescence intensity were obtained from histogram statistic of CellQuest software.

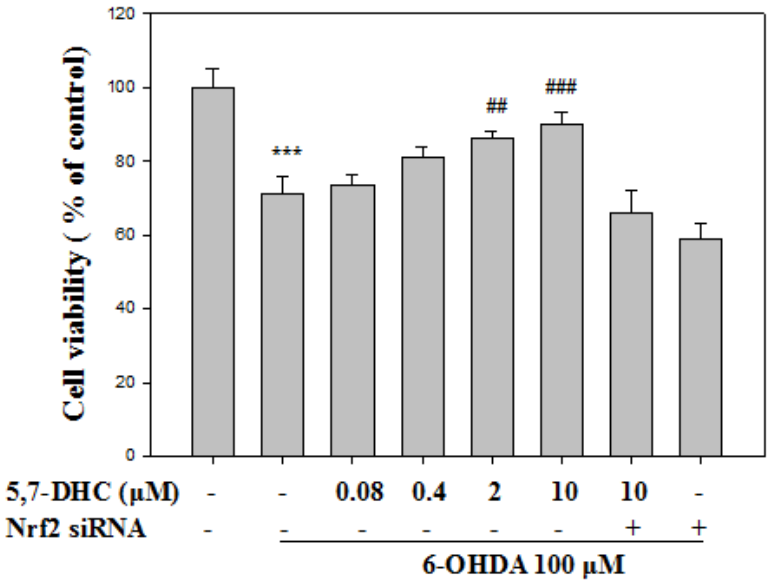

Figure 4. Effects of DHC against 6-OHDA-induced cell death in SH-SY5Y cells.

The cells were pre-treated with different concentrations of DHC (0.08 - 10 μM) for 24 h and subsequently treated with 6-OHDA (100 μM) for another 24 h. The cells were transfected with Nrf2 siRNA (50 nM) for 48 h before the treatment with DHC (10 μM). The cell viability was determined by MTT assay. ($^{***}p<0.001$ versus control group, $^{\#\#}p<0.01$ and $^{\#\#\#}p<0.001$ versus 6-OHDA-induced group)

3.2. Inhibitory effect of DHC against 6-OHDA-induced intracellular ROS generation.

Intracellular ROS were detected by DCFH-DA dye, which can be diffused to the cell membrane and deacetylated by esterase to the 2',7'-dichlorodihydrofluorescin (DCFH), which is swiftly converted into the dichlorofluorescein (DCF) emitting fluorescence by ROS. As shown in Fig. 5, the 6-OHDA-induced cells exhibited higher DCF fluorescence intensities than the vehicle-treated cells. The amount of ROS generation was decreased in a dose-dependent manner when the 6-OHDA-induced cells were treated with different concentrations of DHC (0.4 - 10 μM). The 6-OHDA-induced group generated approximately 5-fold greater amount of ROS than that of the vehicle-treated group. When the DHC (10 μM)-treated cells were treated with 6-OHDA, the ROS level was approximately 2-fold greater than that of the vehicle-treated group. However, the inhibitory effect of DHC (10 μM) on intracellular ROS generation disappeared upon treatment with Nrf2 siRNA, and the combined treatment with Nrf2 siRNA and DHC (10 μM) produced the similar ROS generation compared to the 6-OHDA-treated group.

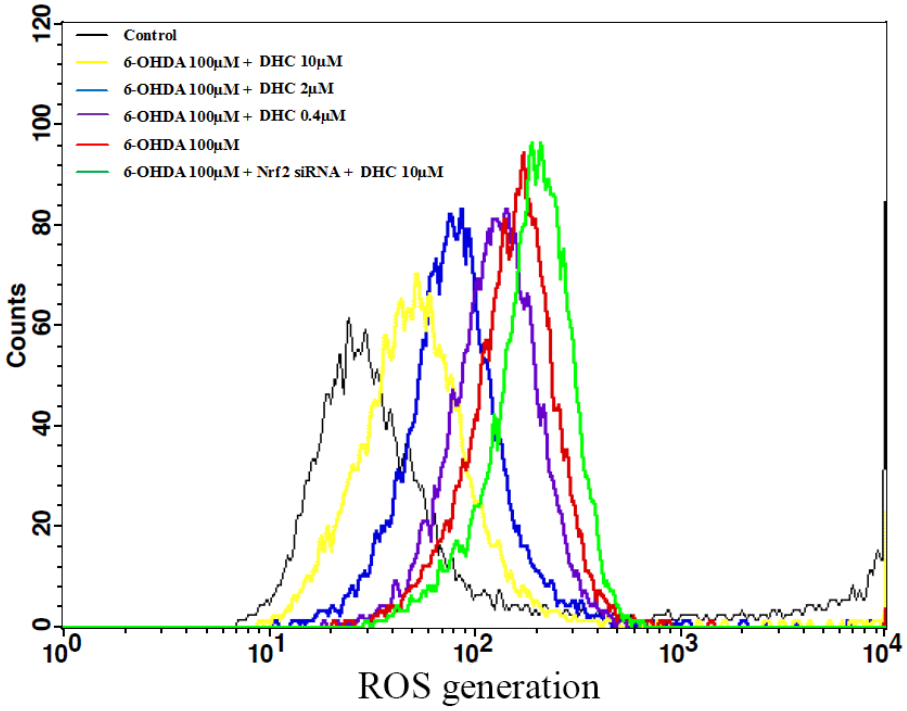

Figure 5. Effects of DHC against 6-OHDA-induced intracellular ROS generation in SH-SY5Y cells.

The cells were pre-treated with different concentrations of DHC (0.4 - 10 μM) for 24 h and subsequently treated with 6-OHDA (100 μM) for another 24 h. The cells were transfected with Nrf2 siRNA (50 nM) for 48 h before the treatment with DHC (10 μM). The cells were stained with DCFH-DA dyes for 30 min and determined by FACS analysis using FL-1 channel. The values of fluorescence intensity were obtained from histogram statistic of CellQuest software.

3.3. Effects of DHC on induction of the nuclear Nrf2 and binding affinity of Nrf2/ARE in SH-SY5Y cells

Nrf2 in nucleus has a binding affinity to the ARE region and Nrf2/ARE complex induces the transcription of ARE-mediated antioxidant genes. DHC increased the induction of nuclear Nrf2 with a peak effect that occurred at 6 h. As shown in Fig. 6, the nuclear Nrf2 was dose-dependently increased by DHC treatment (0.08 - 10 μM) at 6 h (Fig. 7). The increase of nuclear Nrf2 by DHC was visualized by immunocytochemistry in Fig. 8. To elucidate the binding activity between Nrf2 and ARE, an electrophoretic mobility gel-shift assay (EMSA) was performed. As shown in Fig. 9, DHC (2 μM) drastically increased Nrf2-ARE binding activity and the maximum binding activity was observed at 12 h.

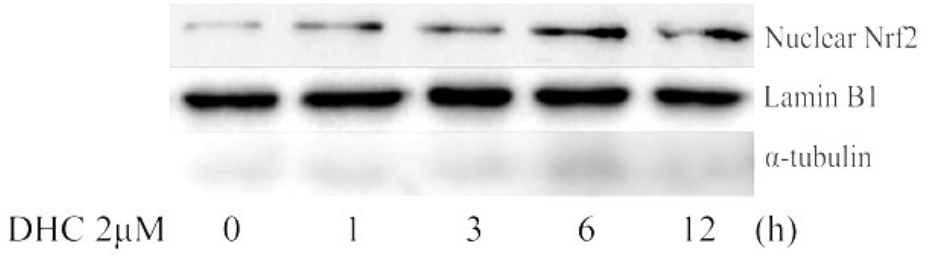

Figure 6. Effects of DHC on the nuclear translocation of Nrf2 in SH-SY5Y cells.

The cells were treated with DHC (2 μM) for different durations (0 - 12 h). The nuclear protein was extracted. Lamin B1 was used for nuclear marker and α-tubulin was used for cytosol marker. The protein expression levels of Nrf2, Lamin B1, and α-tubulin were determined by western blot analysis. Representative data from three independent experiments are shown.

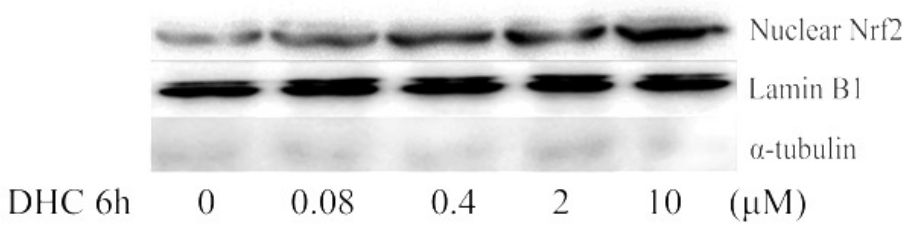

Figure 7. Effects of DHC on the nuclear translocation of Nrf2 in SH-SY5Y cells.

The cells were treated with different concentrations of DHC (0.4 - 10 μM) for 6 h. The nuclear protein was extracted. Lamin B1 was used for nuclear marker and α-tubulin was used for cytosol marker. The protein expression levels of Nrf2, Lamin B1, and α-tubulin were determined by western blot analysis. Representative data from three independent experiments are shown.

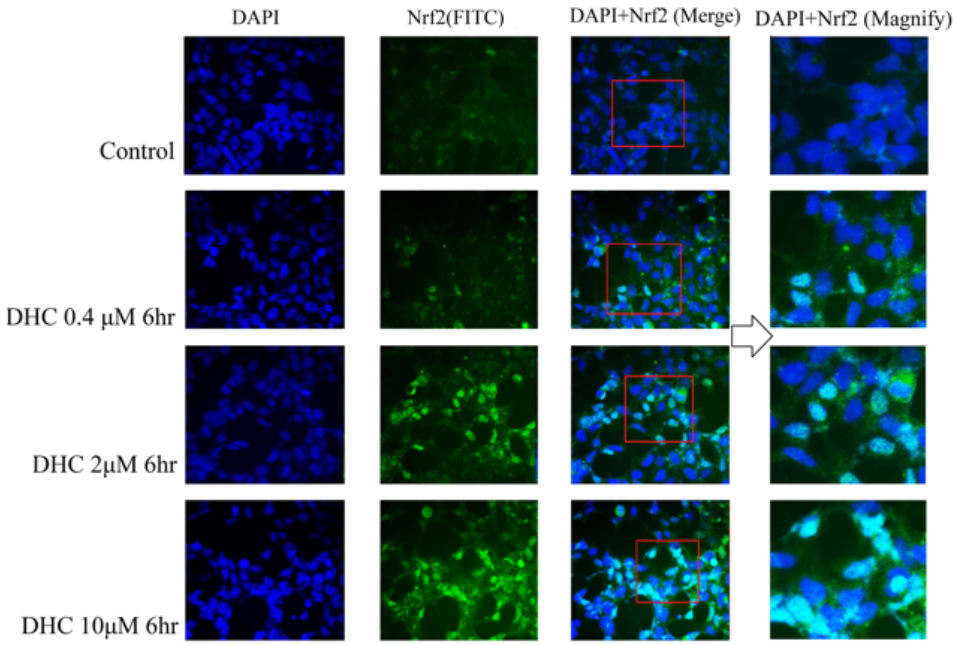

Figure 8. Effects of DHC on the nuclear translocation of Nrf2 in SH-SY5Y cells.

The cells were treated with DHC (0.4 - 10 μM) for 6 h. Cells were fixed and the nuclei were visualized with DAPI staining. Nrf2 was detected with FITC-conjugated antibodies. Cellular morphologies were visualized with a fluorescence microscope (×400). Representative images from three independent experiments are shown.

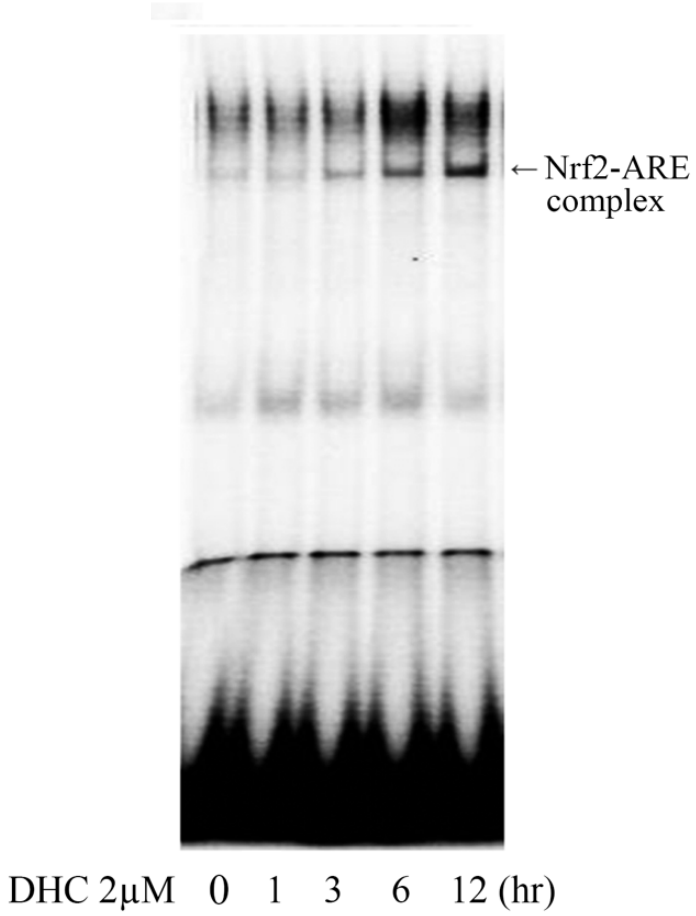

Figure 9. Effects of DHC on the binding activity of Nrf2-ARE.

The cells were treated with DHC (2 μM) for different durations (0 - 12 h), and the nuclear extracts were incubated with [γ-^{32}P]-labeled oligonucleotides harboring an ARE consensus sequence. Nrf2-ARE binding activity was measured via an electrophoretic mobility gel-shift assay (EMSA).

3.4. Effects of DHC on HO-1, NQO1 and GCLc protein expression in SH-SY5Y cells.

The protein levels of HO-1, NQO1, and GCLc, which are reported as a major phase II antioxidant enzymes that are transcribed upon Nrf2/ARE binding, were measured in the SH-SY5Y cells. As shown in Fig. 10, HO-1, NQO1, and GCLc protein expression levels were increased in a time- and dose-dependent manner by DHC treatment. As shown in Fig. 10 (B), HO-1, NQO1, and GCLc protein expression levels at 24 h were gradually increased by DHC treatment (0.08 - 10 μM). Upon Nrf2 siRNA treatment, the increased protein expression levels of HO-1, NQO1, and GCLc induced by DHC treatment (10 μM) were drastically reduced to a near-baseline level (Fig. 11). These results revealed that Nrf2/ARE binding is a key step in the transcriptions of HO-1, NQO1, and GCLc proteins.

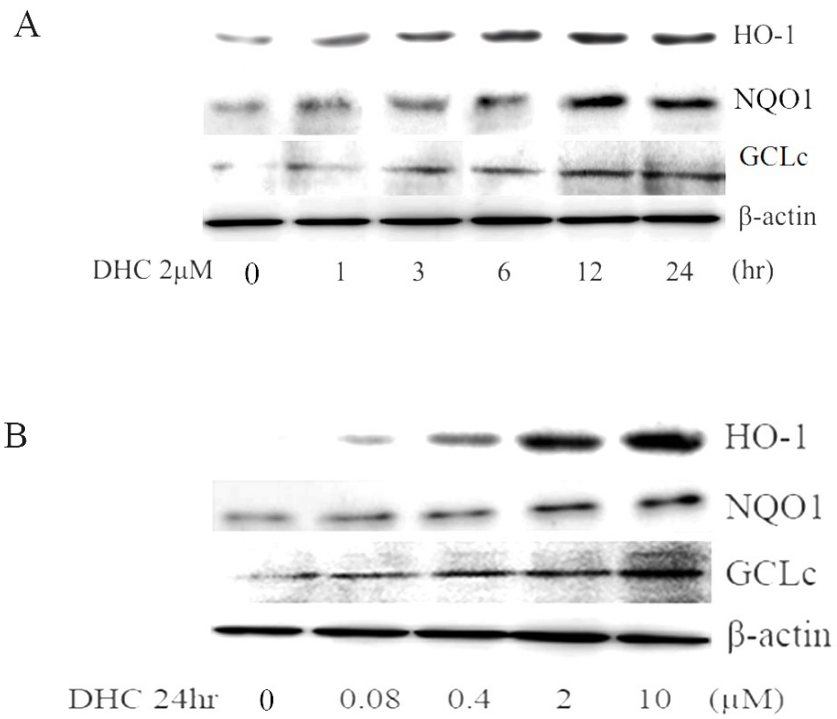

Figure 10. Effects of DHC on the expressions of the HO-1, NQO1, and GCLc proteins in the SH-SY5Y cells.

The cells were treated with DHC (2 μM) for different durations (0 - 24 h) **(A)**. The cells were treated with different concentrations of DHC (0.08 - 10 μM) for 24 h **(B)**. After treatment, the total protein was extracted and determined protein expression level by western blot assay. Representative data from three independent experiments are shown.

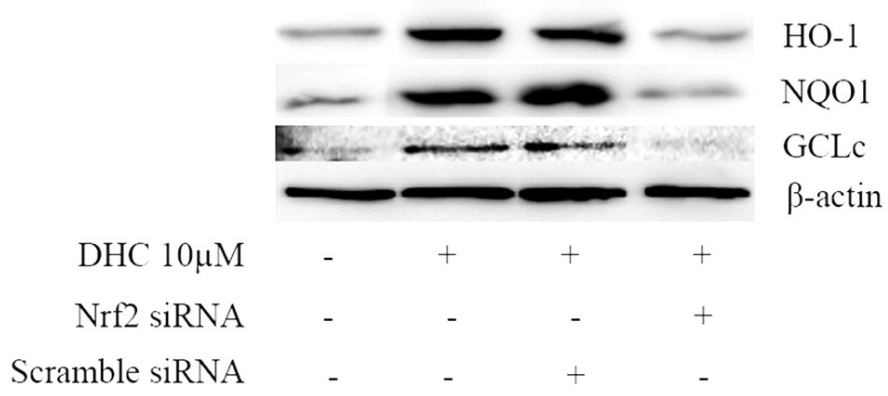

Figure 11. Effects of DHC on the expressions of the HO-1, NQO1, and GCLc proteins in Nrf2 siRNA treated SH-SY5Y cells.

The cells were transfected with Nrf2 siRNA (50 nM) or scrambled siRNA (50 nM) prior to treatment with DHC (10 μM) for 48 h. After DHC treatment, the total protein was extracted and evaluated HO-1, NQO1, and GCLc protein expression level by western blot assay. Representative data from three independent experiments are shown.

3.5. Effects of DHC on HO-1, NQO1 and GCLc mRNA expression in SH-SY5Y cells

The mRNA levels of HO-1, NQO1, and GCLc, which are reported as a major phase II antioxidant enzymes that are transcribed upon Nrf2/ARE binding, were measured in the SH-SY5Y cells. As shown in Fig. 12 - 14, HO-1, NQO1, and GCLc mRNA expression levels were increased in concentration-dependent manner by DHC treatment. HO-1, NQO1, and GCLc mRNA expression levels at 24 h were gradually increased by DHC treatment (0.08 - 10 μM). These results revealed that Nrf2/ARE binding is a key step in the transcriptions of HO-1, NQO1, and GCLc mRNA.

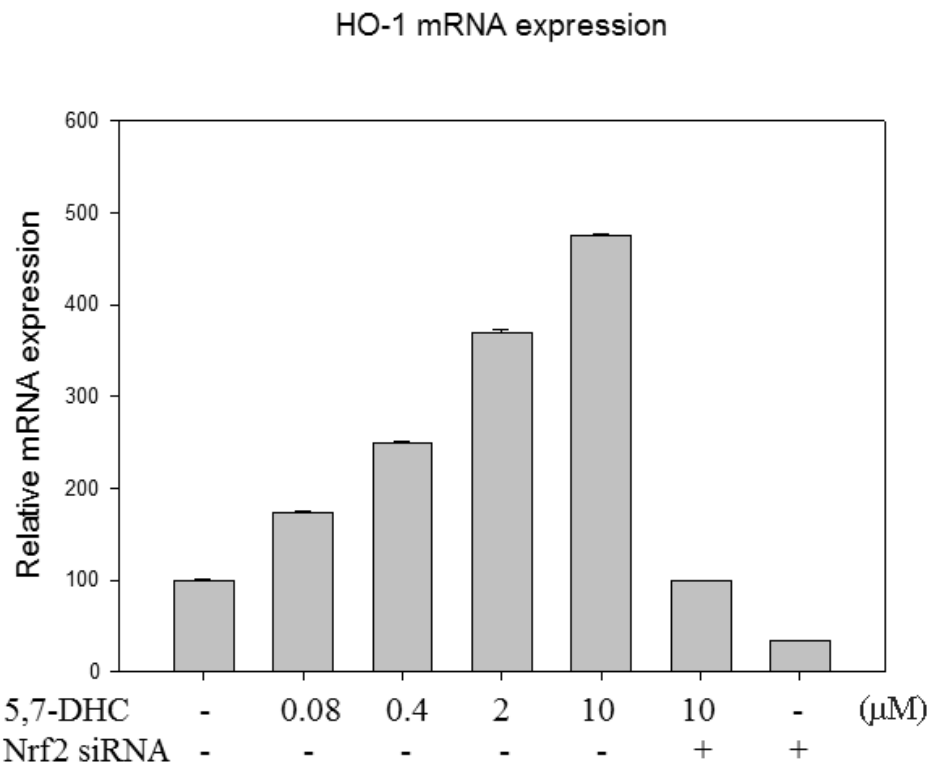

Figure 12. Effects of DHC on the mRNA expressions of HO-1 in SH-SY5Y cells.

The cells were transfected with Nrf2 siRNA (50 nM) or scrambled siRNA (50 nM) for 48 h prior to treatment with DHC (0.08 - 10 μM). After DHC treatment for 24h, the total RNA was extracted. The mRNA expression levels of HO-1 was determined by qRT-PCR analysis. Data represent the mean ± SD of three independent experiments.

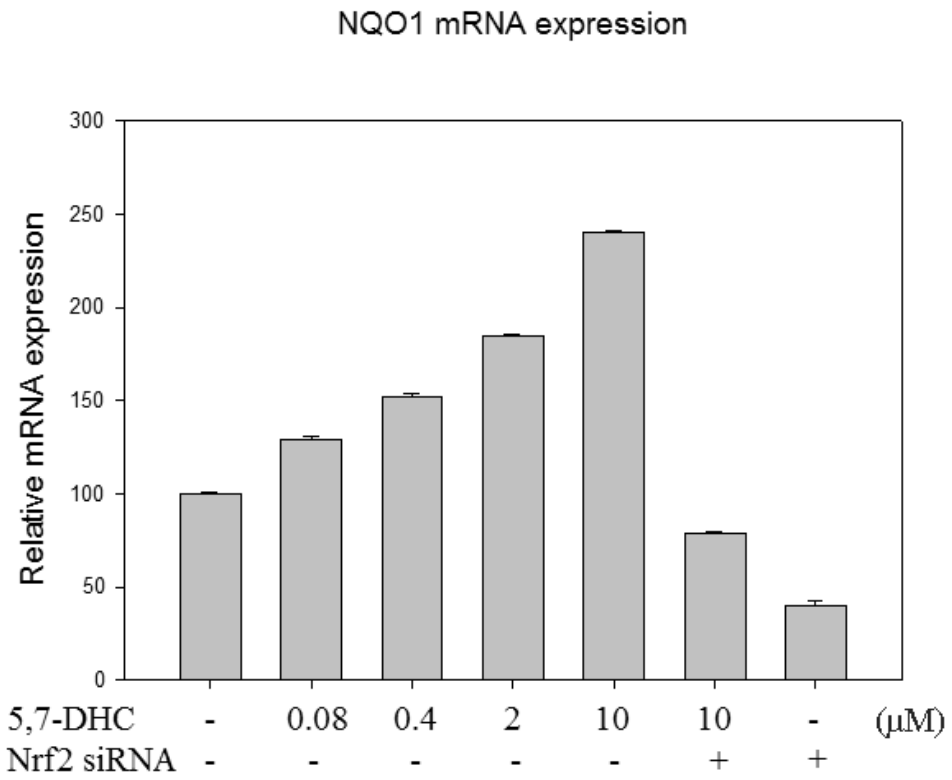

Figure 13. Effects of DHC on the mRNA expressions of NQO1 in SH-SY5Y cells.

The cells were transfected with Nrf2 siRNA (50 nM) or scrambled siRNA (50 nM) for 48 h prior to treatment with DHC (0.08 - 10 μM). After DHC treatment for 24h, the total RNA was extracted. The mRNA expression levels of NQO1 was determined by qRT-PCR analysis. Data represent the mean ± SD of three independent experiments.

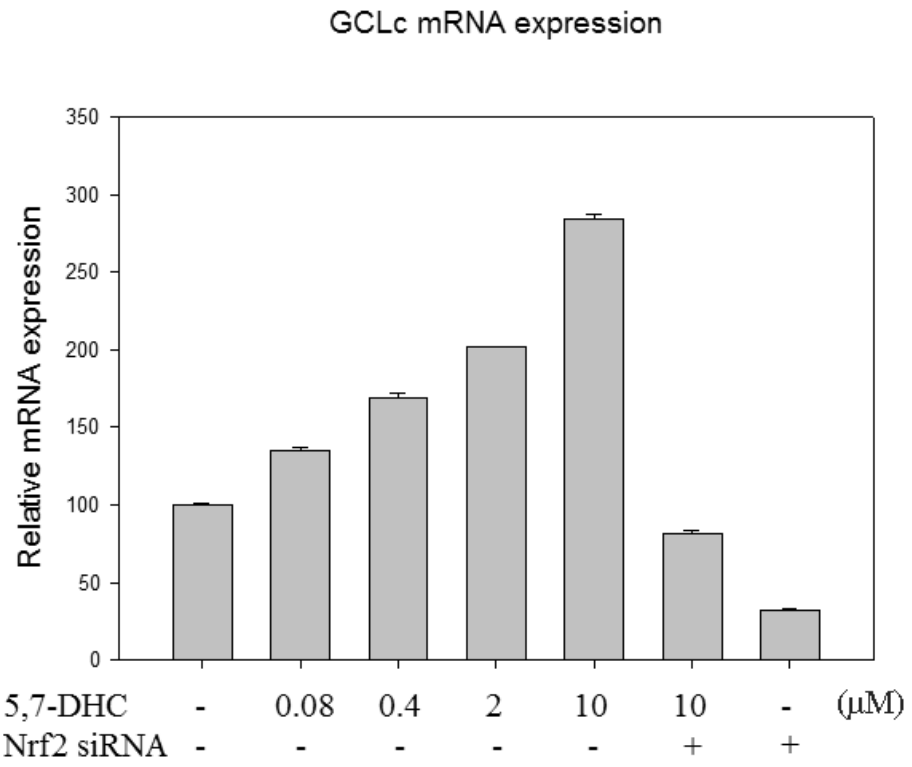

Figure 14. Effects of DHC on the mRNA expressions of GCLc in SH-SY5Y cells.

The cells were transfected with Nrf2 siRNA (50 nM) or scrambled siRNA (50 nM) for 48 h prior to treatment with DHC (0.08 - 10 μM). After DHC treatment for 24h, the total RNA was extracted. The mRNA expression levels of GCLc was determined by qRT-PCR analysis. Data represent the mean ± SD of three independent experiments.

3.6. The inhibitory effects of DHC on the 6-OHDA-induced apoptotic signal.

The inhibitory effects of DHC on the expressions of cleaved caspase-9, caspase-3, and PARP during the process of apoptosis were evaluated. ROS accumulation is known to activate caspase-9 and caspase-3, and activated caspase-3 cleaves PARP. As shown in Fig. 15, the cleaved caspase-9, caspase-3, and PARP were over-expressed when the SH-SY5Y cells were induced by 6-OHDA. However, the over-expression of these cleaved proteins was concentration-dependently inhibited by DHC treatment (0.08 - 10 μM).

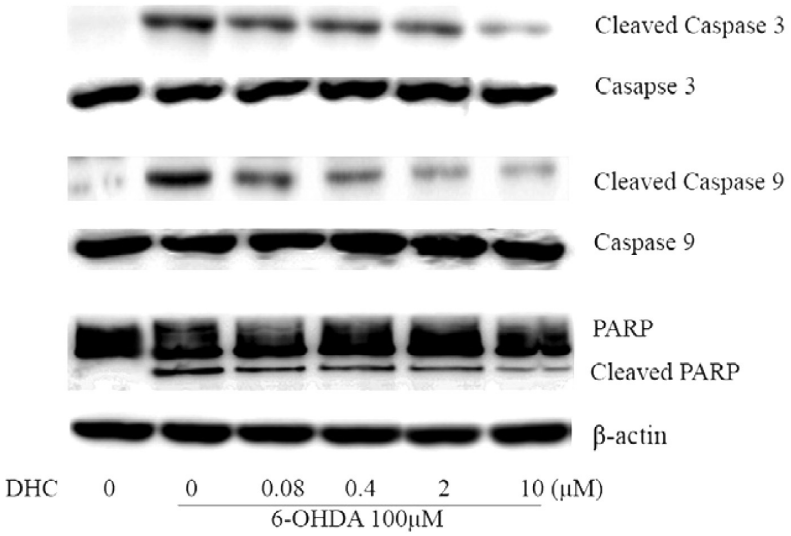

Figure 15. Inhibitory effects of DHC on the expressions of cleaved caspase-9, caspase-3 and PARP protein.

The cells were pre-treated with different concentrations of DHC (0.08 - 10 μM) for 24 h and subsequently treated with 6-OHDA (100 μM) for another 24 h. Then, each cell lysate was subjected to western blot analysis. Representative data from three independent experiments are shown.

4. Discussion

Neurodegenerative diseases may occur without obvious causes or be the result of numerous circumstances that cause the impairment of cellular performance in neuron and ultimately cell death. Due to the rapid aging of the populations of societies across the world, the number of patients suffering from the neurodegenerative disease is also increasing. Although the causes of these diseases have not been clearly elucidated, recent studies have revealed that ROS is composed of their pathogenesis (Farooqui and Farooqui, 2011). Because of their abundant iron contents and relatively deficient antioxidant defense system, neuronal cells are vulnerable to excessive ROS and electrophile related stress. It has been suggested that ROS is highly involved in the neurotoxicity of neurodegenerative disease (Munch et al., 1998b). Over the past decade, many studies of antioxidant enzymes have resulted in progress in the treatment and prevention of diseases (Rahman, 2007). In this context, it has been suggested that the coordinated expression of phase II antioxidant enzymes via the induction of nuclear Nrf2 could be a promising strategy for protection against oxidative stress-related neurodegenerative diseases.

The effects of DHC (Fig. 2) have not been thoroughly examined, particularly in relation to protection against neuronal cell death. In this report, DHC was found to protect against neuronal cell death and the ROS generation in 6-OHDA-induced SH-SY5Y cells. It was reported that caspase-9 could be cleaved by the ROS generation (Zuo et al., 2009). Cleaved caspase-9 induces activation of caspase-3 by making cleaved form of caspase-3, which is the important caspase involved in the apoptotic process and neuronal cell death caused by 6-OHDA (Dodel et al., 1999; Kuida et al., 1998). PARP is cleaved by active form of caspase-3, and this cleaved PARP loses the ability to participate in DNA repair, which results in apoptosis. PARP cleavage by active form of caspase-3 is a reliable indicator of apoptosis (Kaufmann et al., 1993). In our results, DHC prevented the 6-OHDA-induced cleavages of caspase-3, caspase-9, and PARP, which inhibited the activation of the apoptotic cascade in the SH-SY5Y cells. Moreover, DHC down-regulated the ROS level, which was increased by treatment with 6-OHDA. Based on its results, we suggest that this anti-apoptotic effect of DHC is associated with the down-regulation of ROS.

The effects of the Nrf2/ARE signaling pathway on the ROS generation were also evaluated. Our results revealed that treatment with DHC inhibited the generation of 6-OHDA-induced ROS, which affect the early and late stages

of apoptosis. The ability of DHC to inhibit ROS generation seems to be an important factor in neuronal cell protection. DHC also increased the induction of nuclear Nrf2, which has a binding affinity to ARE and activates ARE-driven phase II antioxidant enzymes; NQO1, HO-1, and GCLc. Nrf2 is regarded as a key regulator of antioxidant defensive responses and a sensor of cellular redox status (Kang et al., 2005). Many lines of research have proven the importance of Nrf2-related antioxidant enzymes in neuroprotection (Park et al., 2010). It has been also reported that the levels of antioxidant genes are considerably decreased in Nrf2-K.O. mice and the expression levels of antioxidant enzymes were eliminated by Nrf2-siRNA in *in vitro* models (Ramos-Gomez et al., 2001). NQO1, HO-1, and GCLc are representative antioxidant enzymes whose expressions are increased by diverse environmental stimulus including ROS and thiol-reactive substances (Rizzardini et al., 1993; Su et al., 2013; Fraser et al., 2002). NQO1 has been reported to be a potentially attractive therapeutic target for protecting cells from oxidative damage because it makes stable form of hydroquinone by catalyzing quinone (Lim et al., 2008). Moreover, it has been reported that HO-1 catalyzes heme to carbon monoxide, biliverdin and iron, which exerts potent antioxidant effects (Farooqui and Farooqui, 2011). CGLc participates in glutathione synthesis and prevents the impairment of cellular function from

the excessive ROS (Pompella et al., 2003). Many studies have shown that these antioxidant enzymes have powerful antioxidant effects, and it has been suggested that the regulation of antioxidant enzymes might be a key factor in the prevention of age-related disease (Uttara et al., 2009). Our results revealed that DHC treatment induced the nuclear translocation of Nrf2, which resulted in the increases in NQO1, HO-1, and CGLc at the level of protein expression, suggesting that the neuroprotective effects of DHC against 6-OHDA-induced cell death are involved in the inhibition of ROS generation. Based on our research, we expect that one of the neuroprotective effects exerted by DHC is the increased induction of the Nrf2/ARE signal. When the cells were transfected with Nrf2 siRNA, the protective effects of DHC against 6-OHDA-induced neurotoxicity and ROS generation were inhibited. Moreover, the increased protein expression levels of NQO1, HO-1, and GCLc by DHC treatment (10 μM) were also drastically reduced to basal levels by treatment with Nrf2 siRNA. The results revealed that the neuroprotective effects of DHC are due to the activation of Nrf2/ARE signal pathways and the subsequent inhibition of ROS generation.

5. Conclusion

The present study demonstrated that DHC prevented 6-OHDA-induced neurotoxicity via the induction of Nrf2/ARE signal, which subsequently led to the overexpression of antioxidant enzymes, including NQO1, HO-1, and CGLc. As a result of these effects, DHC inhibited the generation of ROS and neuronal cell death in 6-OHDA-induced SH-SY5Y cells. Our study suggests that DHC can be a promising neuroprotective candidate in the therapy of neurodegenerative diseases such as Parkinson's disease.

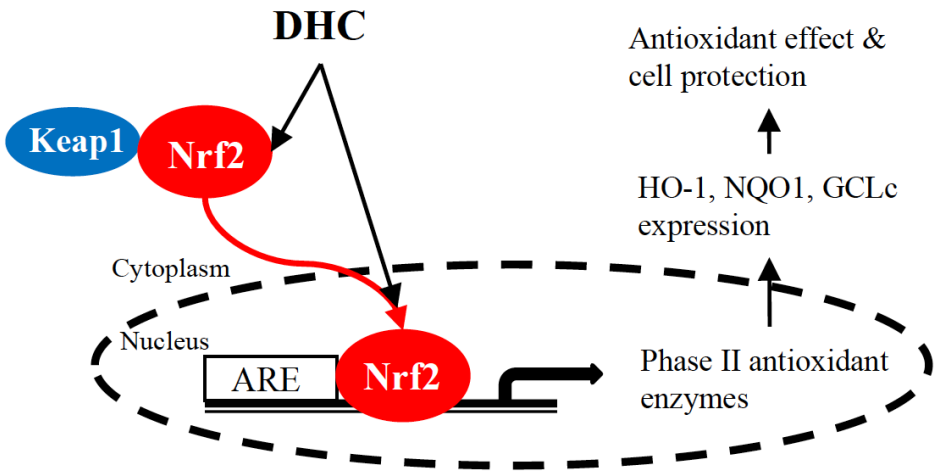

Figure 16. A scheme of protective effects of DHC on 6-OHDA-induced neuronal cell death via activation of Nrf2/ARE signal.

DHC protected 6-OHDA-induced neurotoxicity via the induction of Nrf2/ARE signal, which subsequently led to the overexpression of antioxidant enzymes, including NQO1, HO-1, and CGLc. As a result of these effects, DHC inhibited the generation of ROS and neuronal cell death in 6-OHDA-induced SH-SY5Y cells.

Chapter 2

Orobol derivatives and extracts from *Cudrania tricuspidata* fruits protect against 6-hydroxydopamine-induced neuronal cell death by enhancing proteasome activity and the ubiquitin/proteasome-dependent degradation of α-synuclein and synphilin-1

1. Introduction

Cudrania tricuspidata (Moraceae) is a subtropical tree that is widely distributed in Korea, China, and Japan. The fruits of *C. tricuspidata* are used in jams, juices, and a fermented alcoholic beverage with sugar, and they are commercially produced as food in Korea. In addition, the root, stem, leaf, and fruits of this plant have been reported to have anti-atherosclerotic, anti-inflammatory and antioxidant activities (Lee et al., 2012; Park, KH et al., 2006; Jeong et al., 2010). Recent studies have demonstrated that the fruit of *C. tricuspidata* inhibited pancreatic lipase (Jeong et al., 2014), protected neuronal cells against oxidative stress-induced toxicity (Jeong et al., 2010), and inhibited IgE-mediated allergic and inflammatory responses (Lee et al., 2015). The compounds isolated from *C. tricuspidata* are primarily xanthones and flavones in addition to some alkaloids, lignins, coumarins, polysaccharides, and chromones (Hano et al., 1991; Lee et al., 1996; Seo et al., 2001; Fujimoto et al., 1984; Hiep et al., 2015). The isoflavones from the fruits of *C. tricuspidata* have been reported to exert protective effects against 6-hydroxydopamine (6-OHDA)-induced neurotoxicity (Hiep et al., 2015) and to have inhibitory effects against IgE-mediated allergic and inflammatory

responses (Lee et al., 2015). Orobol (OB), 6-prenylorobol (POB) and 6,8-diprenylorobol (DPOB) are prenylated isoflavones. It was reported that OB increases cisplatin sensitivity in human ovarian carcinoma (Shiotsuka and Isonishi, 2001) and that DPOB shows anti-estrogenic activity (Okamoto et al., 2006) and inhibits lipofuscin fluorophore-mediated photo oxidation (Uddin et al., 2011).

Parkinson's disease (PD) is characterized by severe motor deficits, cogwheel rigidity, bradykinesia, and the loss of dopaminergic neurons. The aetiology of PD has not been clearly identified; however, oxidative stress is thought to be a common factor that leads to cellular dysfunction and neurodegeneration. Reactive oxygen species (ROS) are mainly produced as a by-product of cellular metabolism and oxidative phosphorylation. Non-neutralized ROS produce oxidative stress in cellular organisms and lead to abnormal molecular activities (Bochkov et al., 2010). In particular, the pathological events that occur in PD have been suggested to be linked to protein oxidation caused by oxidative stress (Butterfield and Kanski, 2001), and excessive intracellular ROS induce apoptosis that is characterized by the cleavage of caspase-3, caspase-9 and poly ADP-ribose polymerase (PARP) (Klovekorn and Munch, 1998). The neurotoxin 6-OHDA destroys dopaminergic and noradrenergic neurons in the brain by inducing excessive ROS such as superoxide radicals,

which leads to protein oxidation and neuronal cell death (Kanthasamy et al., 2010).

The proteasome plays a key role in the selective degradation of oxidized proteins via ubiquitin-mediated processes, and its role is essential for cellular protein maintenance (Tai and Schuman, 2008; Jung and Grune, 2013). The ubiquitin-proteasome system (UPS) is responsible for the degradation of many cellular proteins, except membrane and extracellular proteins, which after endocytosis are degraded within the lysosomes. In addition, misfolded, mutant, and oxidatively damaged proteins are also degraded by the UPS. Proteins to be degraded are first marked by covalent attachment of a polyubiqutin chain to a lysine residue on the substrate. The polyubiquitinated protein is then degraded by a large proteolytic complex, the 26S proteasome. Monoubiquitinylation, on the other hand, regulates transcription, translation, protein trafficking, DNA repair, and numerous other cellular functions. Polyubiquitination of a target protein is accomplished through a series of enzyme-mediated reactions that are required to ensure specificity and activate the ubiquitinmoiety. First, activated ubiquitin is generated by ubiquitin-activating enzyme (E1), which forms a thiol ester linkage between a cysteine residue and carboxy-terminalglycine in ubiquitin in an ATP-dependent manner. The activated ubiquitin is transferred to one of the several

ubiquitin carrier proteins or ubiquitin conjugating enzymes (E2s) via the formation of another thiol linkage. Finally, ubiquitin is ligated to the lysine residue of the protein substrate that is specifically bound to an E3 ligase. Parkin, involved in familial PD, is an example of such an E3 ligase. Additional activated ubiquitin moieties can be attached to internal lysine residues within the ubiquitin to form polyubiquitin linkages, which then act as the degradation sign that is recognized by the 26S proteasome complex (Dahlmann, 2007). A minimum of four ubiquitin moieties is required for efficient targeting to the proteasome. Selectivity of ubiquitination and recognition of substrates are largely mediated by E3s. There are more E2s than E1s, and more E3s than E2s so at each step the number of proteins that can possibly be involved increases, as does the specificity of binding to the next component. It is the E3, either alone or in combination with its bound E2, that determines the specificity of substrate recognition (Betarbet et al., 2005).

Proteasomes are existing in the cytoplasm, perinuclear regions, and nuclei of all eukaryotic cells. Their relative abundance within these compartments is extremely variable. In the cytoplasm, proteasomes are associated with centrosomes, cytoskeletal networks, and the outer surface of the endoplasmic reticulum. In the nucleus, proteasomes are present throughout the nucleoplasm but not in the nucleoli. Impairment of

the proteolytic pathway results in accumulation of proteasomes in these locations, forming organized aggregates. Aggregates located in the pericentrosomal areas have been termed “aggresomes”. Aggresomes are known to damage proteasomal function and promote apoptosis (Wojcik and DeMartino, 2003).

The 26S proteasome consists of a catalytic core—the 20S proteasome. The 20S proteasome is made up of 28 subunits assembled as two outer and two inner heptameric rings stacked axially to form a hollow cylindrical structure wherein proteolysis occurs (Doskeland and Flatmark, 2002). The two inner rings of the 20S proteasome are composed of seven different β-subunits each. The three different catalytic sites (chymotrypsin-like, trypsin-like, and caspase-like-peptide hydrolytic sites) of the proteasome reside on the inner surface of the inner rings, thereby preventing indiscriminate degradation of proteins (Huang and Figueiredo-Pereira, 2010). The noncatalytic outer rings, comprising of seven different α-subunits, serve as an anchor for the 19S (PA700) multisubunit ATPase containing proteasome activator or regulator. The 19S complex determines substrate specificity and consists of at least six ATPases and more than 15 additional subunits that lack the capacity to bind to ATP. The 19S regulatory complex serves at least three ATP-dependent functions: it selectively opens the channel through the 20S proteasome,

unfolds ubiquitinated proteins to allow entry into the catalytic core, and cleaves off the polyubiquitinated chain from the substrate. The degradation products of proteasomal catalysis are small peptides and amino acids that can be recycled to produce new proteins. At the same time, polyubiquitin chains, released from targeted proteins, are then disassembled by ubiquitin carboxy-terminal hydrolases to produce monomeric ubiquitin molecules that can be reused. Recent research has suggested that oxidative stress-induced proteasome dysfunction might play a key role in neurodegenerative diseases and that rescuing the decrease in proteasome activity could be a new therapeutic strategy (Seo et al., 2007). Additionally, dysfunction in proteasome activity was observed in the substantia nigra of PD patients, suggesting that the impairment of the UPS is involved in the formation of Lewy bodies and in dopaminergic neuronal cell death in PD (McNaught and Jenner, 2001). Lewy bodies are characteristic hallmarks of PD and are composed of primarily α-synuclein and synphilin-1 along with ubiquitin and other fibrils. α-synuclein, a small acidic protein composed of 140 amino acids, is abundant in the human brain; is also found in the heart, muscles, and other tissues; and is a naturally unfolded protein with the ability to self-aggregate. The aggregation process of α-synuclein results in potential cell damage, leading to dopaminergic neuronal loss in Parkinson's disease (Cookson, 2005).

α-synuclein also associates with other protein partners in the cell, including a significant interaction with synphilin-1. It has been reported that synphilin-1 is a presynaptic protein that could be a modulator of UPS, and the overexpression of synphilin-1 promotes the formation of inclusions under conditions of proteasome inhibition. Additionally, synphilin-1 inhibits the degradation of α-synuclein by the proteasome, thus increasing its half-life (Alvarez-Castelao and Castano, 2011). Therefore, it is possible that the inhibition Lewy body-associated protein accumulation through the protection against proteasome dysfunction could be a key aspect of PD treatment.

In our previous reports, we investigated the neuroprotective effect of different extracts (0 – 100% ethanol ratio) containing isoflavones from *C. tricuspidata* fruits (Hiep et al., 2015). Here, nine isolates obtained from 50% ethanol extract from *C. tricuspidata* fruits (CTE50) were evaluated for their neuroprotective potential against 6-OHDA-induced cell death in SH-SY5Y human neuroblastoma cells. The study focused on the potential effects on apoptosis, intracellular ROS generation, proteasome activities, polyubiquitination of Lewy body-associated α-synuclein and synphilin-1 against 6-OHDA-induced SH-SY5Y cells.

2. Materials and methods

2.1. Chemicals and reagents

6-Hydroxydopamine (6-OHDA), and 2',7'-dichlorfluorescein-diacetate (DCFH-DA) were purchased from Sigma-Aldrich (St. Louis, MO, USA). MG132 was purchased from Enzo Life Sciences (Farmingdale, NY, USA). Dulbecco's modified Eagle's medium (DMEM) and foetal bovine serum (FBS) were purchased from Hyclone™ Thermo Scientific (Wyman Street Waltham, MA, USA). Hybond®-Polyvinylidene difluoride (PVDF) membranes were purchased from Amersham Pharmacia Biotechnology Inc. (Piscataway, NJ, USA). PRO-PREP protein extraction solution and WEST-ZOL® ECL solution were purchased from iNtRON Biotech Inc. (Kyunggi, Korea). Antibodies against ubiquitin, α-synuclein, synphilin-1, β-actin, caspase-3, cleaved caspase-3, caspase-9, cleaved caspase-9, PARP, and A/G Plus-Agarose and secondary antibodies were purchased from Santa Cruz Biotechnology, Inc. (CA, U.S.A.)

2.2. Preparation of ethanol extracts from the fruits of *C. tricuspidata* (CTE)

The fruits of *C. tricuspidata* were collected from the Korea Forest Research Institute, Southern Forest Research Center (Jinju, Korea). A voucher specimen (accession no. KH1-5-090904) was deposited at the Department of Biosystems and Biotechnology, Korea University (Seoul, Korea). The dry fruit of *C. tricuspidata* (3.4 kg) was ground into powder form and sifted through a 120-mesh sieve. The dry powder (7 g) was refluxed three times for 1 h each by means of a heating mantle with 250 mL of 0, 30, 50 70, or 100% ethanol in round 500-mL flasks. The combined extracts were filtered and concentrated in vacuo to yield 2.85 g, 2.71 g, 2.57 g, 2.67 g, and 2.1 g, respectively.

2.3. Ultra performance liquid chromatography (UPLC) analysis of CTE50

The CTE50 was analysed using an Acquity UPLC system (Waters, Millford, MA, USA) with an Acquity UPLC BEH C18 column (1.7 μm, 2.1 × 150 mm i.d.). The mobile phase consisted of solvent A (0.05% formic acid in water) and solvent B (acetonitrile), which flowed at rate of 0.3 mL/min. The starting eluent was 40% B at 0 min, and the proportion of B was increased linearly to 100% from 0 to 10 min, held constant at 100% for 11.5 min, and then returned to the initial condition over the course of 1.5 min to re-equilibrate the column.

The sample injection volume was 4 μL for extract and 2 μL for compounds (CTE50: 3 mg/mL, OB, POB, and DPOB: 0.2 mg/mL). The column and sample managers were maintained at 35 and 15 °C, respectively, and the UV detection wavelength was monitored at 265 nm.

2.4. Isolation and identification of compounds from CTE50

Nine isoflavones, namely, orobol (**1**, 0.0021%), 6-prenylorobol (**2**, 0.0100%), 6,8-diprenylorobol (**3**, 0.0015%), millewanins H and G (**4** and **5**, 0.0029 and 0.0045%), alpinumisoflavone (**6**, 0.0762%), 4′-*O*-methylalpinumisoflavone (**7**, 0.0046%), erysenegalensein E (**8**, 0.0181%), and 6,8-diprenylgenistein (**9**, 0.0055%), were isolated from the fruits of *C. tricuspidata*. The chemical structures were determined by interpretation of spectroscopic data, including MS and NMR spectra, as compared to the previously reported literature (supplementary data 1). The detailed isolation procedures are included in the supplementary materials and methods. The purity of each compound was more than 95%.

2.5. Cell cultures

The human neuroblastoma cell line SH-SY5Y (ATCC No. CRL-2266) was purchased from the American Type Culture Collection (Manassas, VA, USA)

and cultured in DMEM supplemented with 10% heat-inactivated FBS and 1% penicillin/streptomycin at 37 ºC in a humidified 5% CO_2 atmosphere. Test samples were dissolved in 10% DMSO, and the cells were treated within non-cytotoxic concentration ranges of test samples at a final concentration of 0.1% DMSO.

2.6. Measurement of cell viability

SH-SY5Y cells were plated at a density of 1×10^5 cells/200 μL/well in 96-well plates for 24 h, and the cells were simultaneously treated with 6-OHDA and test samples (0.16 – 20 μg/mL of 0 – 100% CTE; 0.2 – 25 μM of nine isolates) for 48 h. After treatment, cell viability was evaluated using the MTT assay as previously described (Koo et al., 2011). Briefly, the medium was removed, and the cells were incubated with fresh medium containing 0.5 mg/mL MTT for 4 h at 37 ºC, after which the medium was gently removed. Formazan crystals were dissolved in 100 μL DMSO, and absorbance was measured at 540 nm using a microplate reader (SpectraMax M5, Molecular Devices, USA).

2.7. Measurement of intracellular ROS by flow cytometry

Intracellular ROS levels were measured by the 2',7'-dichlorofluorescein diacetate (DCFH-DA) method as described previously (Kim, D-W et al.,

2015). Briefly, SH-SY5Y cells were plated at a density of 1×10^6 cells/1 mL/well in 12-well plates for 24 h, simultaneously treated with 6-OHDA (75 μM) and test samples (0.16 – 20 μg/mL of 0 – 100% CTE, 0.2 – 25 μM of isolates) for 48 h, and washed three times with PBS. DCFH-DA (4 μM/mL in PBS) was then added, and afterwards, the cells were incubated for 30 min at 37 ºC in the dark. The cells were then washed 3 times with PBS, and the fluorescence intensities of a total of 10,000 events were measured by the FL-1 channel of a flow cytometer (BD FACS Calibur™).

2.8. Measurement of proteasome activity

Proteasome activity was determined using SH-SY5Y cells as previously described (Kim, B-H et al., 2015). Briefly, cells (1.0×10^5 cells/300 μL/well) were plated in 48-well plates for 24 h and then simultaneously treated with 6-OHDA (75 μM) and samples (0.16 – 20 μg/mL of CTE50, 0.2 – 25 μM of nine isolates) for 48 h. After washing twice with PBS, cells were lysed by freeze-thawing 3 times (between -70 ºC and 37 ºC, 5 min each) and scraped into PBS buffer. Supernatants were collected by centrifugation at 15,000 rpm (15 min, 4 ºC), and the total protein concentration was determined by the Bradford method (Bradford, 1976). The proteolytic activity of the proteasomes was evaluated with a 20S proteasome activity kit (APT 280;

Millipore, USA). In brief, supernatants (40 μg) were incubated for 2 h at 37 °C in the provided buffer with fluorophore-linked peptide substrates. Suc-LLVY-AMC (40 μM), Boc-LRR-AMC (40 μM), and Z-LLE-MCA (80 μM) were used as the substrates for chymotrypsin-, trypsin- and caspase-like protease activities, respectively. Reaction mixtures without cell lysates were used as negative controls, and aminomethylcoumarin (AMC) or methylcoumarylamide (MCA) fluorescence was measured at excitation/emission wavelengths of 380/460 and 380/440 nm, respectively, using a microplate reader (SpectraMax M5, Molecular Devices, USA).

2.9. Measurement of mRNA expression

After treatments, total RNA was isolated from SH-SY5Y cells by easy-BLUE® and cDNA was synthesized by using SuPrimeScript RT premix® according to the manufacturer's procedure. The synthesized cDNA was used for PCR and the primer pair sequence were listed as follows:

Chymotrypsin-like proteasome subunit (PSMB-8)

5-GTTCCAGCATGGAGTGATTG-3 (sense) and

5- TGTTCACCCGTAAGGCACTA-3 (antisense);

Trypsin-like proteasome subunit (PSMB-7)

5-ATGGCTGTACCACGAAACAA-3 (sense) and

5-AGGGATCCTTCAGTTTCTTCAGT-3 (antisense);

Caspase-like proteasome subunit (PSMB-6)

5-TCGATTTGATACCTTTGATAGCC-3 (sense) and

5-CCAGGGTCAATGGGTGAC-3 (antisense);

GAPDH

5-CTCTGCTCCTCCTGTTCGAC-3 (sense) and

5-ACGACCAAATCCGTTGACTC-3 (antisense). The cycle condition was as follow; 94℃ for 20s, 56℃ for 20s, 72℃ for 30s and 40 cycles. PCR were performed by using SYBRs HS Prime qPCR premix® in an ABI 7300 real-time PCR (Applied Bio systems, CA, USA). Ct (threshold cycle) values were obtained using the Sequence Detection Software version1.2.3 (Applied Bio systems, CA, USA). To evaluate quantification of the changes in target gene expression, we used the $2^{-\triangle\triangle Ct}$ method (Tucker and Munchus, 1998). Fold change=$2^{-\triangle\triangle Ct}$, $\triangle\triangle Ct = (Ct_{\text{target gene}} - Ct_{GAPDH}) - (Ct_{\text{control}} - Ct_{GAPDH})$

2.10. Measurement of protein expression

SH-SY5Y cells were plated at a density of 2×10^6 cells/4 mL in 60-mm dishes for 24 h. The cells were then simultaneously treated with 6-OHDA (75 μM) and samples (0.16 – 20 μg/mL of CTE50, 0.2 – 25 μM of three orobol

derivatives) for 48 h, washed three times with PBS, and lysed with a PRO-PREP protein extraction solution at -20 ºC for 20 min. After centrifugation at 13,000 rpm for 30 min, the supernatant was used as the total protein extract. Western blot analysis was accomplished as previously described (Ham et al., 2013). Briefly, protein extracts were separated by electrophoresis on a SDS-PAGE gel and then transferred to PVDF membranes. Then, the PVDF membranes were incubated overnight at 4 ºC with primary antibodies followed by a 1-h incubation at RT with the secondary antibody. The blots were developed using WEST-Queen® ECL solution and analysed using LAS4000 (GE Healthcare, UK)

2.11. Immunoprecipitation assay

Immunoprecipitation was performed as previously described with slight modifications (Chen et al., 2014). Briefly, SH-SY5Y cells were plated at a density of 2×10^6 cells/4 mL in 100-mm dishes for 24 h. The cells were then simultaneously treated with 6-OHDA (75 μM) and samples (0.8 – 20 μg/mL of CTE50, 1 – 25 μM of three orobol derivatives) for 48 h and washed three times with PBS. SH-SY5Y cells were homogenized and lysed in cold-lysis buffer (50 mM Tris, 1 mM PMSF, 150 mM NaCl, 50 mM NaF, 1% Nonidet P-40, 0.25% sodium deoxycholate, 10 mM sodium pyrophosphate) and

centrifuged at 14,000 × g (10 min, 4 °C), and the supernatant was transferred to a new ep-tube and incubated with 2 μg of α-synuclein or synphilin-1 antibody overnight at 4 °C. The next day, A/G plus agarose beads were added and incubated overnight at 4 °C followed by 3 washes in cold-lysis buffer. The loading samples were adjusted to total volume of 30 μL with lysis buffer, and the immune-complexes were eluted at 95 °C on a heating block for 5 min, vortexed, and spun down by centrifugation at 15,000 × g for 10 min.

2.12. Statistical analysis

All experimental data are expressed as the mean ± standard deviation. Statistical significance between multiple groups was determined by one-way ANOVA (PRISM Graph Pad, San Diego, CA, USA). When the ANOVA showed a significant difference, Bonferroni's multiple comparison *post hoc* tests were conducted. A *P* value less than 0.05 was considered statistically significant.

3. Results

3.1. Protective effects against 6-OHDA-induced neuronal cell death in SH-SY5Y cell

Ethanol is often used to extract bioactive compounds from plant materials, and the bioactivity of plant extracts depends on the ratio of water to ethanol used in the extraction process (Ganora, 2009). We evaluated the neuroprotective effects within non-cytotoxic concentration ranges from different CTE extracts (0, 30, 50, 70, and 100% ethanol) and nine isolates. As shown in Table 2, CTE50 showed the most potent protective effects with an EC_{50} value of 3.3 μg/mL. The constituents of CTE50 were identified using UPLC, and nine isolates were obtained (Figs. 17 and 18). Among the nine isolates, three orobol derivatives (OB, POB, and DPOB) significantly attenuated 6-OHDA-induced neurotoxicity with EC_{50} values of 6.4 μM, 4.5 μM, and 10.1 μM, respectively (Table. 2). As shown in Fig. 20, 6-OHDA-induced neuronal cell death was observed by the morphology of cells: 6-OHDA resulted in cellular morphological changes including cell shrinkage and rounding. However, treatment with CTE50 (20 μg/mL) or the three orobol derivatives (25 μM)

ameliorated the 6-OHDA-induced morphological changes to almost normal levels. As shown in Fig. 19, the 6-OHDA-induced group showed a significant decrease in cell viability compared to the vehicle-treated group. However, CTE50 (0.16 – 20 μg/mL) or the three orobol derivatives (0.2 – 25 μM) protected 6-OHDA-induced neuronal cell death in a concentration-dependent manner. Additionally, it was examined that the comparison of neuroprotective effect of CTE50 and three orobol derivatives against 6-OHDA-induced neurotoxicity by pre-, co-, and post treatment. Among three groups, co-treatment group exerted potent neuroprotective effects (Fig. 31).

Table 2. Inhibitory effects of ethanol extracts and isolates from the fruits of *C. tricuspidata* against 6-OHDA-induced cell death and ROS generation in SH-SY5Y cells

Extract / Compound	Neuroprotective effect against 6-OHDA-induced cell death (EC_{50} value)	Inhibitory effect against 6-OHDA-induced ROS generation (IC_{50} value)
0% ethanol extract of *C.tricuspidata* fruit	>20 μg/mL	>20 μg/mL
30% ethanol extract of *C.tricuspidata* fruit	5.4 ± 0.8 μg/mL	10.2 ± 1.2 μg/mL
50% ethanol extract of *C.tricuspidata* fruit	3.3 ± 0.3 μg/mL	6.7 ± 0.7 μg/mL
70% ethanol extract of *C.tricuspidata* fruit	7.8 ± 0.9 μg/mL	14.2± 1.1 μg/mL
100% ethanol extract of *C.tricuspidata* fruit	>20 μg/mL	>20 μg/mL
(**1**) orobol	6.4 ± 0.5 μM	7.2 ± 0.6 μM
(**2**) 6-prenylorobol	4.5 ± 0.3 μM	5.9 ± 0.4 μM
(**3**) 6,8-diprenylorobol	10.1 ± 0.8 μM	17.3 ± 1.0 μM
(**4**) millewanin H	15.2 ± 1.3 μM	19.2 ± 1.5 μM
(**5**) millewanin G	18.5 ± 2.1 μM	22.4 ± 2.4 μM
(**6**) alpinumisoflavone	>25 μM	>25 μM
(**7**) 4'-*O*-methylalpinumisoflavone	>25 μM	>25 μM
(**8**) erysenegalensein E	>25 μM	>25 μM
(**9**) 6,8-diprenylgenistein	>25 μM	>25 μM

The EC_{50} & IC_{50} values were determined in a semi-logarithmic graph with 4 different concentrations.
The values are presented as the mean ± standard deviation of three independent experiments

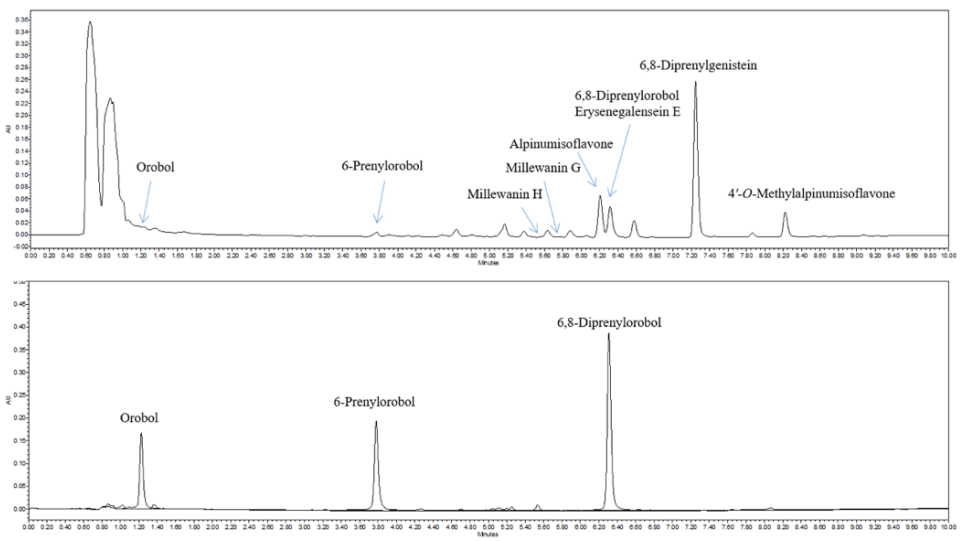

Figure 17. UPLC chromatograms and structures of isolates from CTE50.

UPLC chromatogram of CTE50 and isolates from CTE50. Nine compounds were isolated from CTE50. Among nine isolates, orobol, 6-prenylorobol, and 6,8-diprenylorobol were selected for further study. The selected three orobol derivatives were confirmed the elution time for identification.

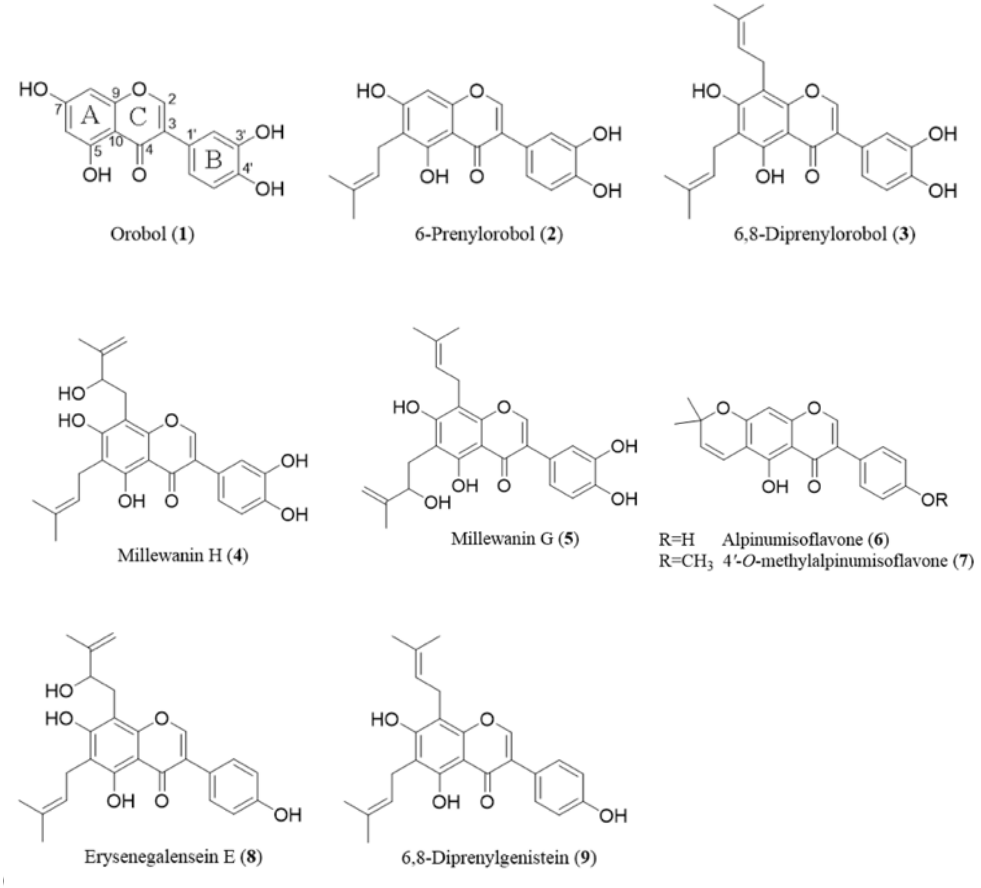

Figure 18. Chemical structures of the isolates from CTE50.

The isolated compounds are orobol (**1**), 6-prenylorobol (**2**), 6,8-diprenylorobol (**3**), millewanin H (**4**), millewanin G (**5**), alpinumisoflavone (**6**), 4′-O-methylalpinumisoflavone (**7**), erysenegalensein E (**8**), and 6,8-diprenylgenistein (**9**).

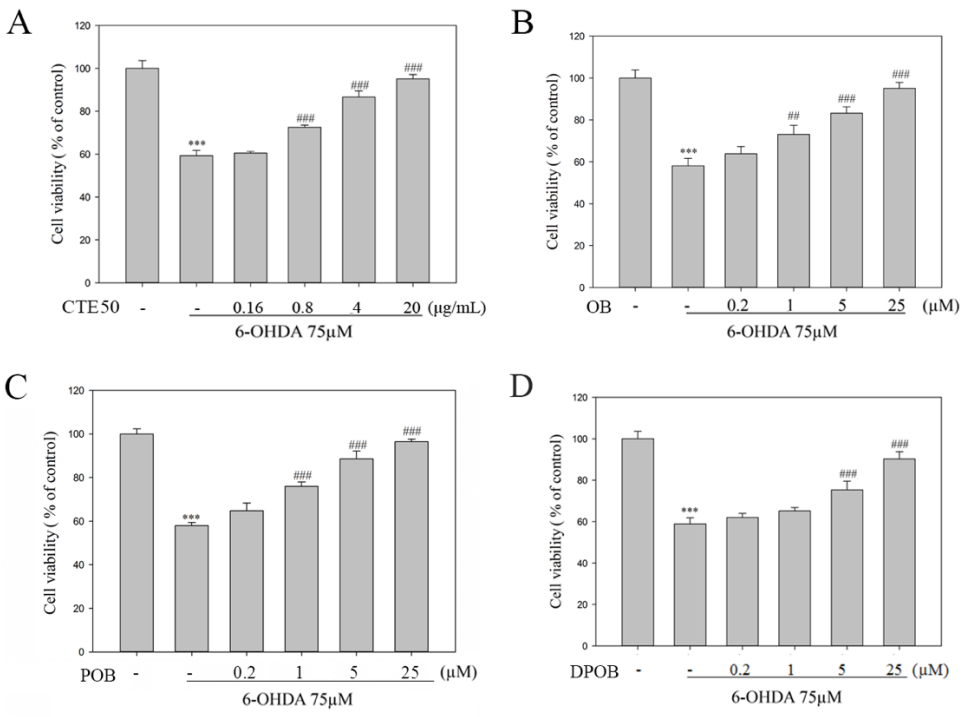

Figure 19. Inhibitory effects of CTE50 and three orobol derivatives (OB, POB, and DPOB) against 6-OHDA-induced neurotoxicity.

Cells were cultured in 96-well plate for 24 h, and CTE50 or orobol derivatives were simultaneously treated with 6-OHDA (75 μM) for 48 h. Cell viability were measured by MTT reduction assay (A – D). Data represent the mean ± SD of three independent experiments. (***$p<0.001$ versus control group, $^{\#\#}p<0.01$ and $^{\#\#\#}p<0.001$ versus 6-OHDA-induced group)

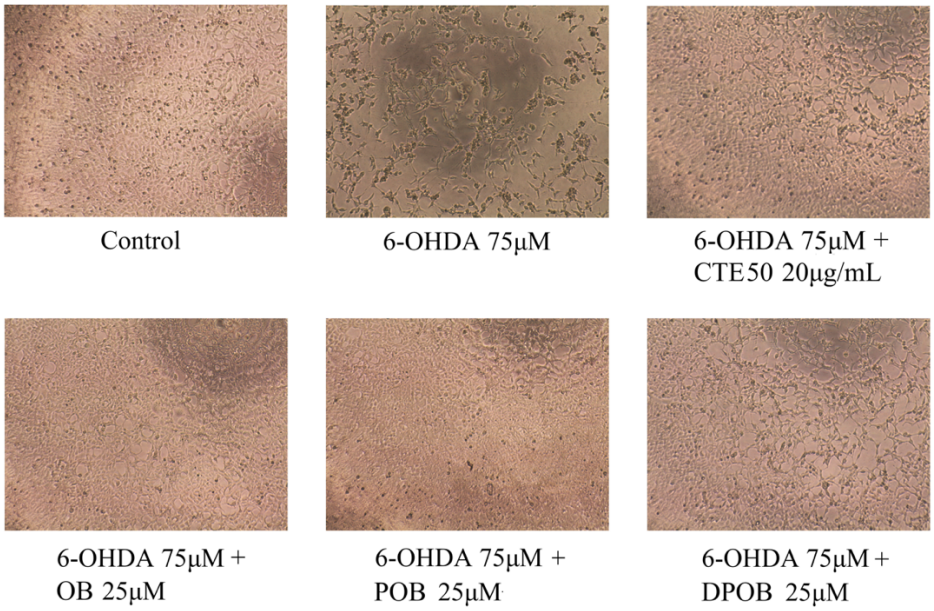

Figure 20. Neuroprotective effects of CTE50 and the three orobol derivatives (OB, POB, and DPOB) against 6-OHDA-induced neurotoxicity in SH-SY5Y cells.

Cells were cultured in 96-well plate for 24h, and CTE50 or three orobol derivatives were simultaneously treated with 6-OHDA (75 μM) for 48 h. The morphological change of cell was observed by inverted phase-contrast microscopy. Representative images were captured at 100× magnification.

3.2. Inhibition of 6-OHDA-induced intracellular ROS generation

Excessive intracellular ROS induce cellular stress and neuronal cell death, and it has been reported that ROS play important roles in the pathogenesis of neurodegenerative diseases. As shown in Table 2, CTE50 showed the most potent inhibition of 6-OHDA-induced ROS generation with an IC_{50} value of 6.7 μg/mL. Among the nine compounds derived from CTE50, the three orobol derivatives showed a significant inhibitory effect against 6-OHDA-induced intracellular ROS generation with IC_{50} values of 7.2 μM (OB), 5.9 μM (POB), and 17.3 μM (DPOB). As shown in Fig. 21 and 22, 6-OHDA-treated cells showed strong DCF fluorescence intensities compared to vehicle-treated cells. The amount of intracellular ROS was decreased in a concentration-dependent manner when cells were treated with CTE50 (0.8 – 20 μg/mL) or the three orobol derivatives (1 – 25 μM).

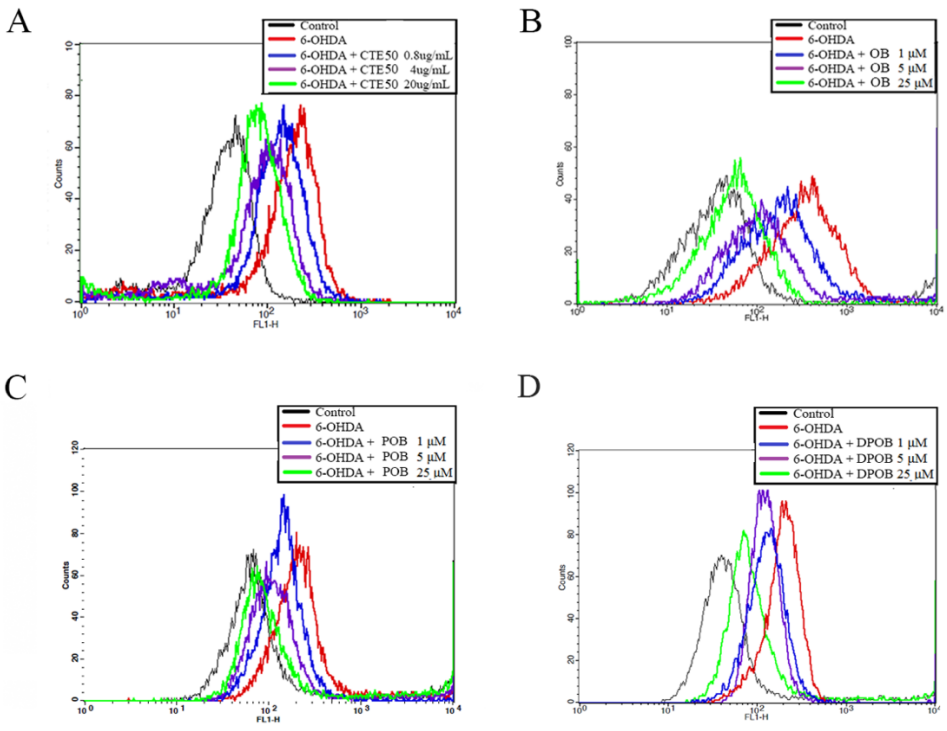

Figure 21. Inhibitory effects of CTE50 and three orobol derivatives (OB, POB, and DPOB) against 6-OHDA-induced ROS generation.

Cells were cultured in 12-well plate for 24h, and CTE50 or three orobol derivatives were simultaneously treated with 6-OHDA (75 μM) for 48 h (A – D). The cells were stained with DCFH-DA dyes for 30 min and determined by FACS analysis using FL-1 channel. The values of fluorescence intensity were obtained from histogram statistic of CellQuest software.

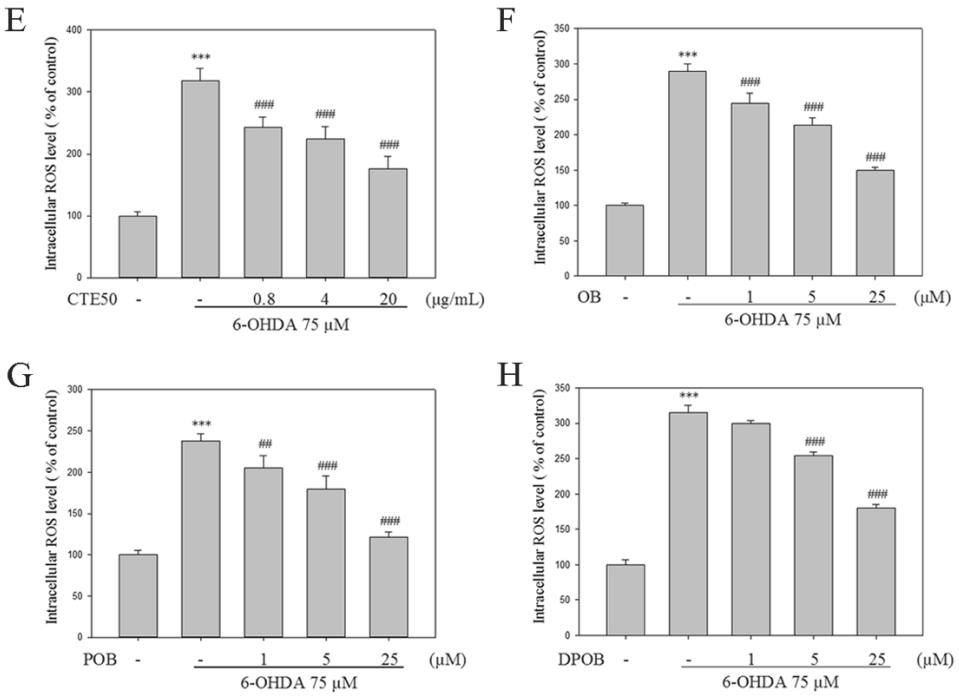

Figure 22. Inhibitory effects of CTE50 and three orobol derivatives (OB, POB, and DPOB) against 6-OHDA-induced ROS generation.

Cells were cultured in 96-well plate for 24h, and CTE50 or three orobol derivatives were simultaneously treated with 6-OHDA (75 μM) for 48 h (E – H). The cells were stained with DCFH-DA dyes for 30 min and fluorescence intensity was measured by multi-plate reader. Data represent the mean ± SD of three independent experiments. (***$p<0.001$ versus control group, $^{\#\#}p<0.01$ and $^{\#\#\#}p<0.001$ versus 6-OHDA-induced group)

3.3. Neuroprotective effects against 6-OHDA-induced apoptosis

It has been reported that 6-OHDA induces ROS-dependent apoptosis, which is characterized by the cleavage of caspase-9, caspase-3 and PARP**.** Excessive ROS accumulation results in the activation of the caspases (caspase-9 and caspase-3), and activated caspase-3 cleaves the DNA repair protein PARP**;** cleaved, activated PARP is final apoptotic marker. To investigate the inhibitory effects of CTE50 and three orobol derivatives on the levels of cleaved caspase-9, caspase-3, and PARP protein, we performed a western blot assay. As shown in Fig. 23, the cleavage levels of caspase-9, caspase-3, and PARP were increased when the SH-SY5Y cells were exposed to 6-OHDA. However, CTE50 (0.16 – 20 μg/mL) or the three orobol derivatives (0.2 – 25μM) inhibited the cleavage of caspase-9, caspase-3, and PARP protein in a concentration-dependent manner in 6-OHDA-induced SH-SY5Y cells.

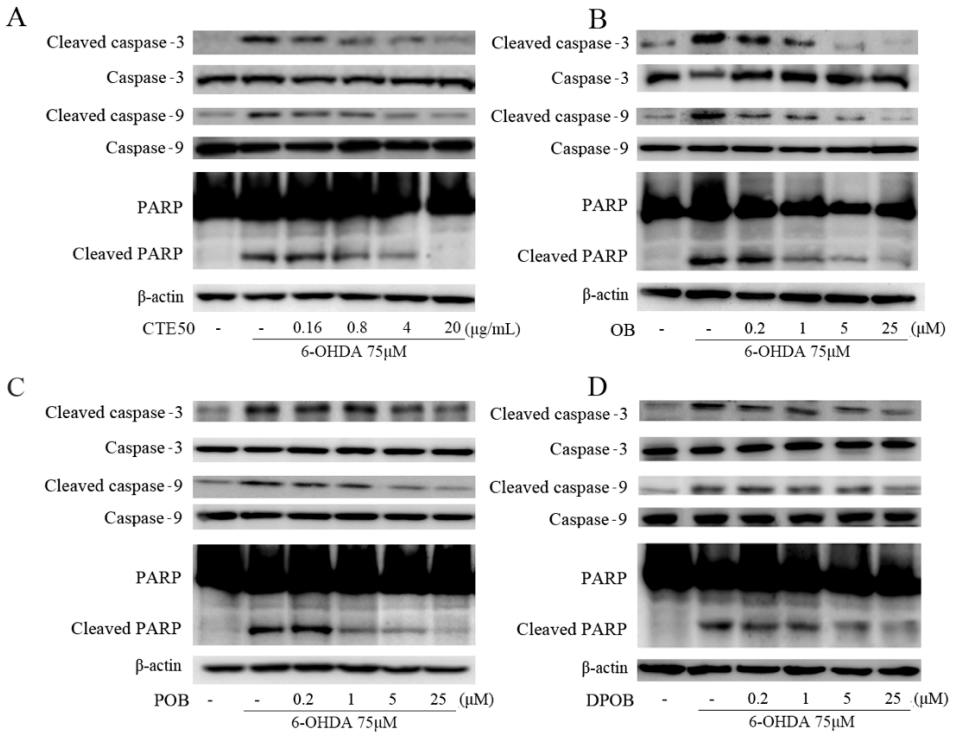

Figure 23. Inhibitory effects of CTE50 and three orobol derivatives against 6-OHDA-induced apoptotic markers.

Cells were simultaneously treated with 6-OHDA (75 μM) and (A) CTE50-or (B – D) three orobol derivatives for 48 h. The levels of cleaved caspase-9, caspase-3 and PARP were assessed by western blot; β-actin was used as a housekeeping protein. Representative data from three independent experiments are shown.

3.4. Protective effects against 6-OHDA-induced dysfunction of proteasome activity

Proteasome function is essential for cellular physiology and protein degradation. To evaluate the effects of CTE50 and the nine isolates against the dysfunction of proteasome activity induced by 6-OHDA in SH-SY5Y cells, we measured the activities of chymotrypsin-, trypsin- and caspase-like proteases. As shown in Table 3 and Fig. 24, 6-OHDA significantly inhibited all three different types of proteasome activities; however, CTE50 most potently attenuated the 6-OHDA-induced dysfunction of proteasome activities from extracts (0 – 100%) with an EC_{50} value of 1.2 μg/mL (chymotrypsin-like), 1.5 μg/mL (trypsin-like), and 6.7 μg/mL (caspase-like). The three orobol derivatives at the concentration of 25 μM prominently protected against 6-OHDA-induced dysfunction of the proteasome and almost restored the activities to normal levels. (Fig. 24B – 24D).

Table 3. The protective effects of ethanol extracts and isolates from the fruits of *C. tricuspidata* against 6-OHDA-induced proteasome dysfunction in SH-SY5Y cells

Extract / Compound	Protective effect against 6-OHDA-induced dysfunction of proteasome activities		
	Chymotrypsin-like (EC_{50} value)	Trypsin-like (EC_{50} value)	Caspase-like (EC_{50} value)
0% ethanol extract of *C.tricuspidata* fruit	>20 μg/mL	>20 μg/mL	>20 μg/mL
30% ethanol extract of *C.tricuspidata* fruit	5.4 ± 0.4 μg/mL	9.5 ± 0.6 μg/mL	18.5 ± 1.5 μg/mL
50% ethanol extract of *C.tricuspidata* fruit	1.2 ± 0.3 μg/mL	1.5 ± 0.4 μg/mL	6.7 ± 0.8 μg/mL
70% ethanol extract of *C.tricuspidata* fruit	7.8 ± 0.7 μg/mL	13.2 ± 1.2 μg/mL	>20 μg/mL
100% ethanol extract of *C.tricuspidata* fruit	>20 μg/mL	>20 μg/mL	>20 μg/mL
(1) orobol	7.4 ± 0.3 μM	3.7 ± 0.3 μM	2.9 ± 0.2 μM
(2) 6-prenylorobol	6.8 ± 0.7 μM	3.9 ± 0.4 μM	1.3 ± 0.2 μM
(3) 6,8-diprenylorobol	7.9 ± 0.4 μM	4.2 ± 0.4 μM	1.8 ± 0.1 μM
(4) millewanin H	22.1 ± 2.0 μM	24.4 ± 2.1 μM	6.8 ± 0.4 μM
(5) millewanin G	24.4 ± 1.5 μM	5.9 ± 0.3 μM	1.2 ± 0.3 μM
(6) alpinumisoflavone	>25 μM	>25 μM	>25 μM
(7) 4'-*O*-methylalpinumisoflavone	>25 μM	>25 μM	>25 μM
(8) erysenegalensein E	>25 μM	>25 μM	>25 μM
(9) 6,8-diprenylgenistein	>25 μM	>25 μM	>25 μM

The EC_{50} values were determined in a semi-logarithmic graph with 4 different concentrations.

The values are presented as the mean ± standard deviation of three independent experiments

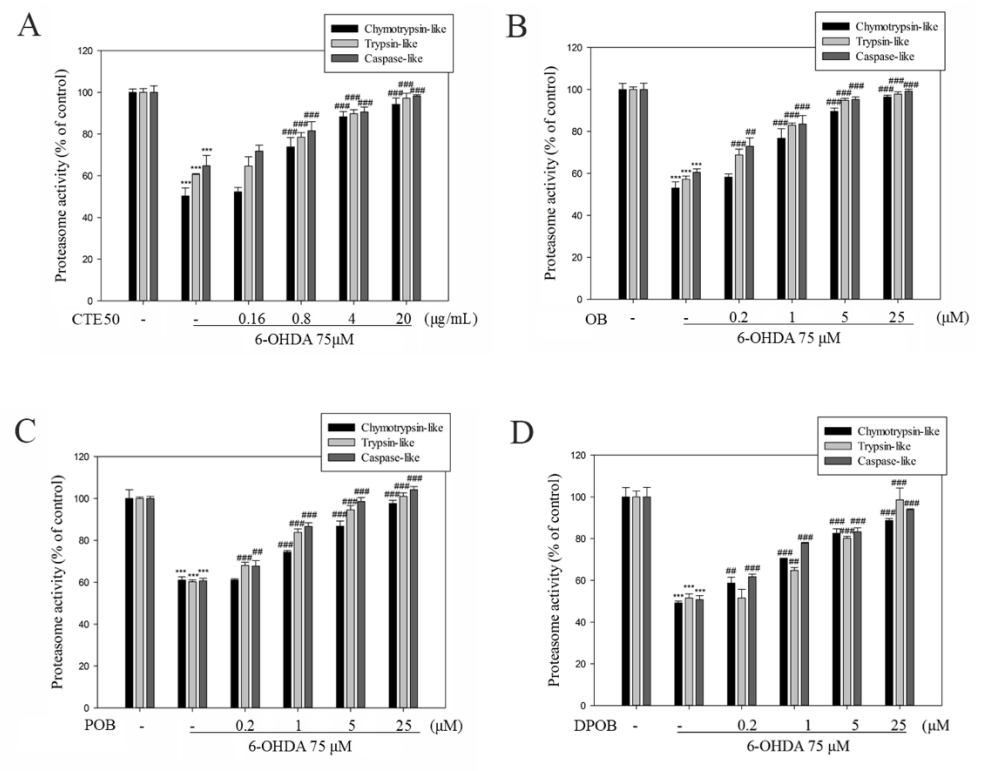

Figure 24. Protective effects of CTE50 and three orobol derivatives (OB, POB, and DPOB) against 6-OHDA-induced dysfunction of proteasome activities in SH-SY5Y cells.

Cells were cultured in 48-well plate for 24h, and (A) CTE50 or (B – D) three orobol derivatives were treated with 6-OHDA (75 μM) for 48 h. Chymotrypsin-, trypsin-, and caspase-like proteasome activities were measured by multiplate reader with fluorophore-linked peptide substrates. The relative fluorescence intensity was indicated. Data represent the mean ± SD

of three independent experiments. (***$p<0.001$ versus control group, $^{\#\#}p<0.01$ and $^{\#\#\#}p<0.001$ versus 6-OHDA-induced group)

3.5. Effects of CTE50 and three orobol derivatives on proteasome subunit mRNA expression

Proteasome function is essential for cellular physiology and protein degradation. Proteasome is composed of subunit and each subunit correlates chymotrypsin-like, trypsin-like, caspase-like proteasome activities. To evaluate the effects of CTE50 and three orobol derivatives on proteasome subunit mRNA expression, we measured the mRNA expression of chymotrypsin-, trypsin- and caspase-like proteases. As shown in Fig. 25, CTE50 significantly increase all three different types of proteasome subunit mRNA expressions; Also, three orobol derivatives increased three types of proteasome subunit mRNA expression at a concentration dependent manner. However, the increased mRNA expression of each proteasome subunits was not correlated the results about the protective effect of 6-OHDA-induced proteasome activities.

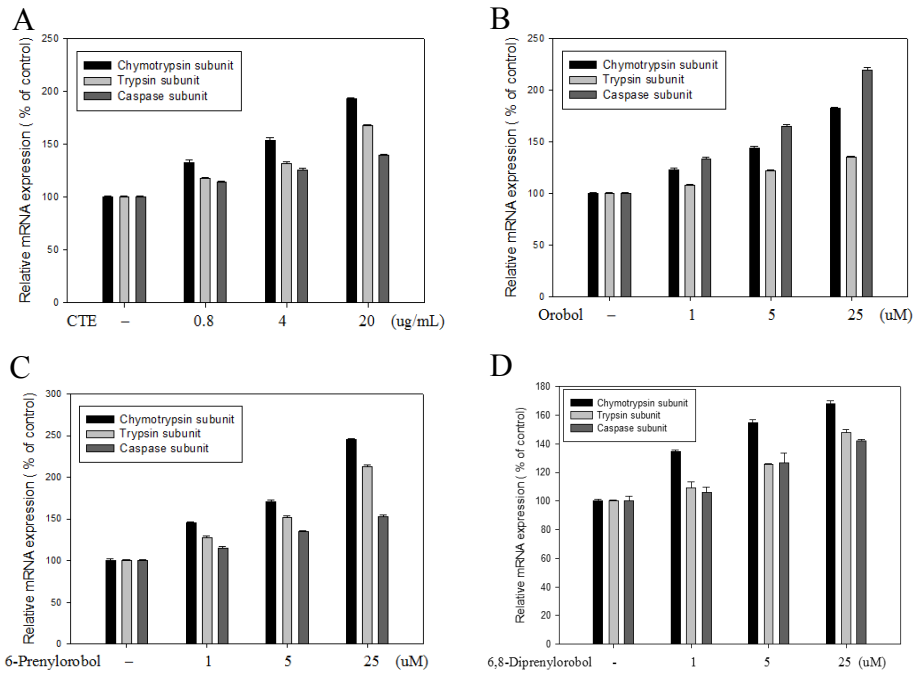

Figure 25. Effects of CTE50 and three orobol derivatives (OB, POB, and DPOB) on mRNA expression of proteasome subunits in SH-SY5Y cells.

Cells were cultured in 12-well plate for 24h, and (A) CTE50 or (B – D) three orobol derivatives were treated for 24 h. The mRNA expression of Chymotrypsin-, trypsin-, and caspase-like proteasome subunit were measured by qRT-PCR analysis. Data represent the mean ± SD of three independent experiments.

3.6. Inhibition of 6-OHDA-induced ubiquitin-conjugated proteins

Proteasome dysfunction causes a reduction in the degradation of misfolded proteins, consequently resulting in the accumulation of polyubiquitinated proteins. To investigate the inhibitory effects of CTE50 and the three orobol derivatives against 6-OHDA-induced ubiquitin conjugated-protein formation, we performed western blot analysis. As shown in Fig. 26, 6-OHDA increased the levels of high molecular ubiquitin-conjugated proteins. When cells were treated with different concentrations of CTE50 (0.16 – 20 μg/mL) (Fig. 26A) or the three orobol derivatives (0.2 – 25 μM) (Fig. 26B – 26D), the levels of ubiquitin-conjugated proteins were decreased to normal in a concentration-dependent manner. CTE50 (20 μg/mL) and the three orobol derivatives (25 μM) restored the ubiquitin-conjugated proteins to almost normal levels.

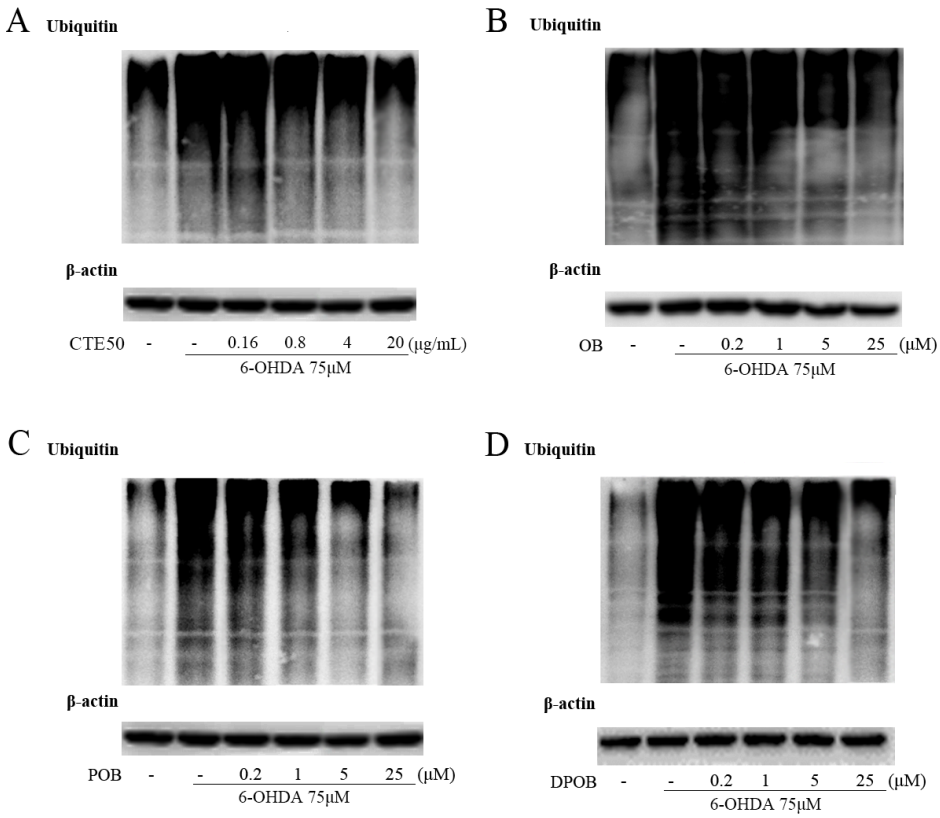

Figure 26. Inhibitory effects of CTE50 and three orobol derivatives against 6-OHDA-induced ubiquitin-conjugated proteins.

Cells were simultaneously treated with 6-OHDA (75 μM) and (A) CTE50 or (B – D) three orobol derivatives for 48 h. The levels of ubiquitin-conjugated proteins were determined by western blot; β-actin was used as a housekeeping protein. Representative data from three independent experiments are shown.

3.7. Inhibition of 6-OHDA-induced poly-ubiquitination of α-synuclein, and synphilin-1

Physiologically, polyubiquitinated proteins are normally rapidly degraded by the proteasome. However, dysfunction in proteasome activity increases the polyubiquitination of α-synuclein and synphilin-1, inducing neurotoxicity. As shown in Fig. 27, 6-OHDA increased the polyubiquitination of α-synuclein. When the cells were treated with different concentrations of CTE50 (0.8 – 20 μg/mL) or the three orobol derivatives (1 – 25 μM), the polyubiquitination of α-synuclein was restored to almost normal levels in a concentration-dependent manner (Fig. 27A – 27D). Additionally, as shown in Fig. 28, 6-OHDA increased the polyubiquitination of synphilin-1; however, CTE50 (0.8 – 20 μg/mL) and the three orobol derivatives (1 – 25 μM) reduced the polyubiquitinated synphilin-1 to almost normal levels in a concentration-dependent manner (Fig. 28E – 28H).

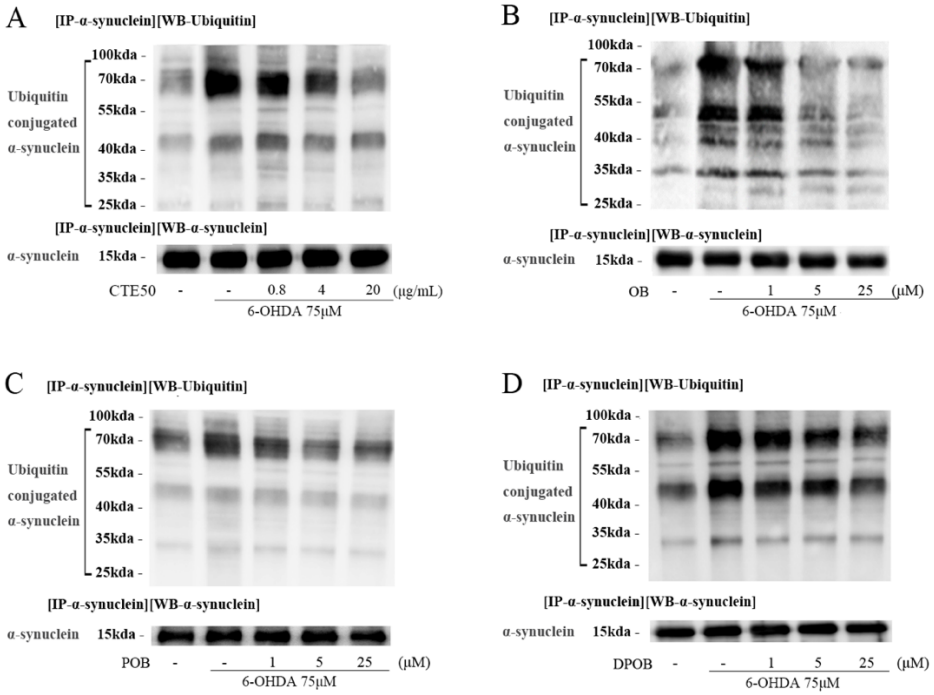

Figure 27. Inhibitory effects of CTE50 and three orobol derivatives against 6-OHDA-induced polyubiquitination of α-synuclein.

Cells were simultaneously treated with 6-OHDA (75 μM) and (A) CTE50 or (B – D) three orobol derivatives for 48 h. The polyubiquitination of α-synuclein was determined by immunoprecipitation and western blot analysis. Representative data from three independent experiments are shown.

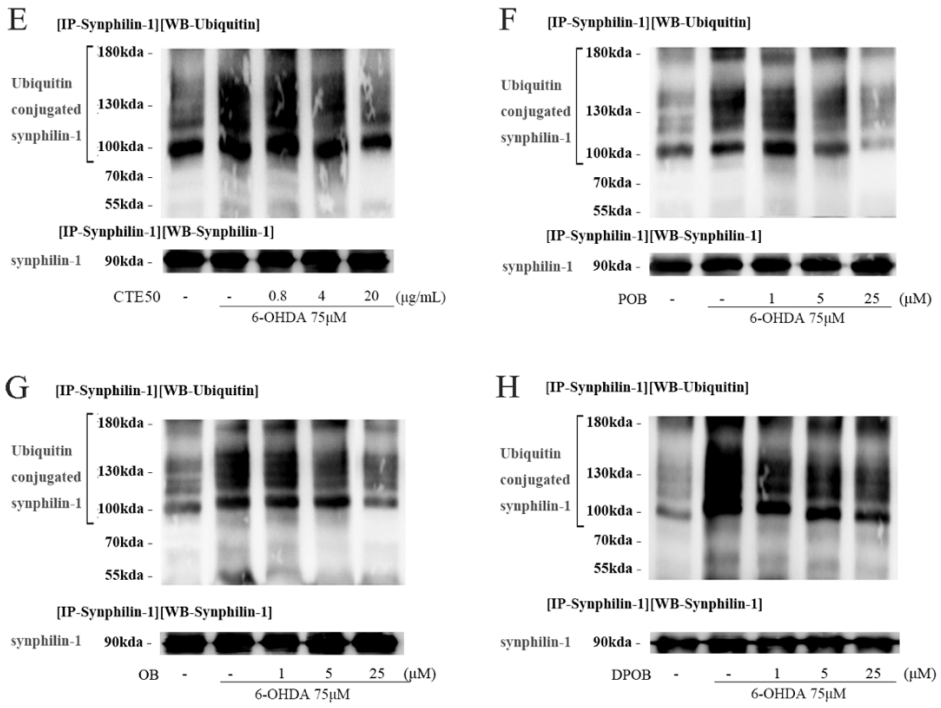

Figure 28. Inhibitory effects of CTE50 and three orobol derivatives against 6-OHDA-induced polyubiquitination of synphilin-1.

Cells were simultaneously treated with 6-OHDA (75 μM) and (E) CTE50 or (F – H) three orobol derivatives for 48 h. The polyubiquitination of synphilin-1 was determined by immunoprecipitation and western blot analysis. Representative data from three independent experiments are shown.

3.8. A proteasome inhibitor (MG-132) diminished the protective effects of CTE50 and the three orobol derivatives against 6-OHDA-induced neuronal cell death and proteasome dysfunction

It has been reported that proteasome inhibition induces dopaminergic neuronal cell degeneration and apoptosis (Park et al., 2011). In contrast, proteasome activation enhances survival in a neuronal model of neurodegenerative disease (Seo et al., 2007). To investigate whether the neuroprotective effects of CTE50 and the three orobol derivatives are due to the amelioration of proteasomal dysfunction, MG132, a proteasome inhibitor, was co-applied with the samples. As shown in Fig. 29, CTE50 (20 μg/mL) and three orobol derivatives (25 μM) protected against 6-OHDA-induced neuronal cell death; however, co-treatment with MG132 (1 μM, non-cytotoxic concentration) significantly blocked the protective effects of CTE50 and the three orobol derivatives against 6-OHDA-induced cell death. Additionally, MG132 (1 μM) blocked the recovery effects of CTE50 and the three orobol derivatives against 6-OHDA-induced proteasome dysfunction (Fig. 30).

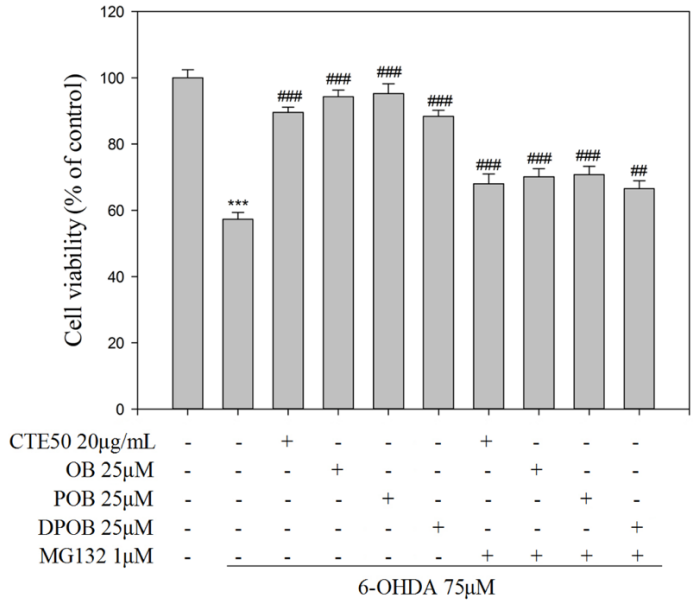

Figure 29. Inhibitory effects of MG132 on the protective effects of CTE50 and three orobol derivatives against 6-OHDA-induced neuronal cell death.

The protective effects of CTE50 and three orobol derivatives 6-OHDA-induced neuronal cell death were blocked by MG132. Cell viability was measured by the MTT reduction assay. (Data represent the mean ± SD of three independent experiments. (***$p<0.001$ versus control group, $^{\#}p<0.05$, $^{\#\#}p<0.01$, and $^{\#\#\#}p<0.001$ versus 6-OHDA-induced group)

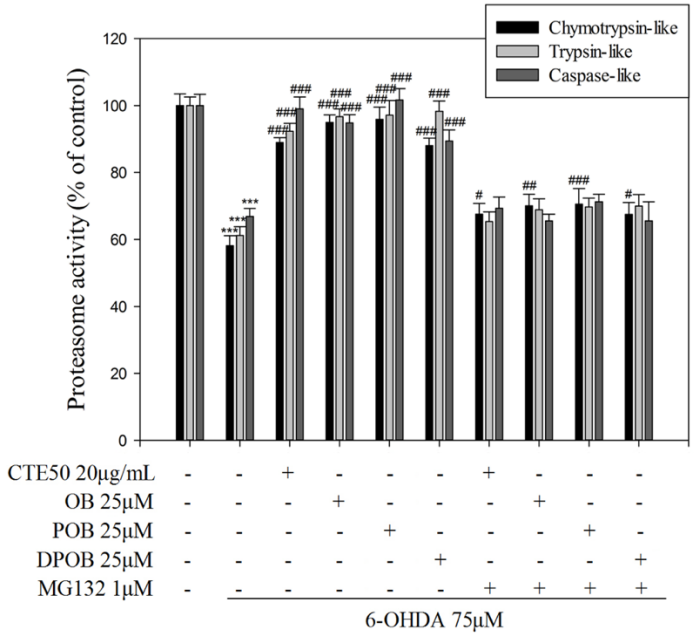

Figure 30. Inhibitory effects of MG132 on the protective effects of CTE50 and three orobol derivatives against 6-OHDA-induced proteasome dysfunction.

The protective effects of CTE50 and three orobol derivatives against 6-OHDA-induced proteasome dysfunction were blocked by MG132. Three types of proteasome activity were measured using a multi-plate reader with fluorophore-linked peptide substrates. Data represent the mean ± SD of three independent experiments. (***$p<0.001$ versus control group, $^{\#}p<0.05$, $^{\#\#}p<0.01$, and $^{\#\#\#}p<0.001$ versus 6-OHDA-induced group)

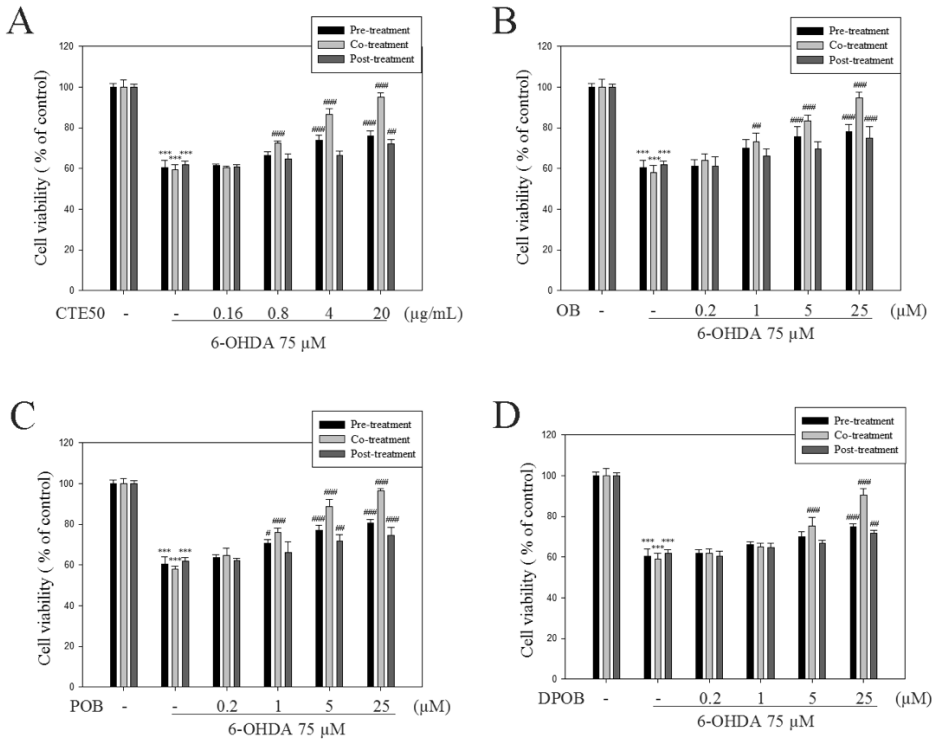

Figure 31. Comparison of neuroprotective effect of CTE50 and three orobol derivatives (OB, POB, and DPOB) against 6-OHDA-induced neurotoxicity by pre-, co-, and post treatment.

In pre-treatment group, cells were cultured in 96-well plate for 24 h, and CTE50 or orobol derivatives pre-treated for 48h. After 48h, medium was changed and cells were treated with 6-OHDA (75 μM) for 48 h. In co-treatment group, cells were cultured, and CTE50 or orobol derivatives were simultaneously treated with 6-OHDA for 48 h. In post-treatment group, cells were cultured, and treated with 6-OHDA for 48 h. After 48h, medium was

changed and cells were treated CTE50 or orobol derivatives for 48 h. Cell viability were measured by MTT reduction assay. Data represent the mean ± SD of three independent experiments. (***$p<0.001$ versus control group, $^{\#}p<0.05$, $^{\#\#}p<0.01$, and $^{\#\#\#}p<0.001$ versus 6-OHDA-induced group)

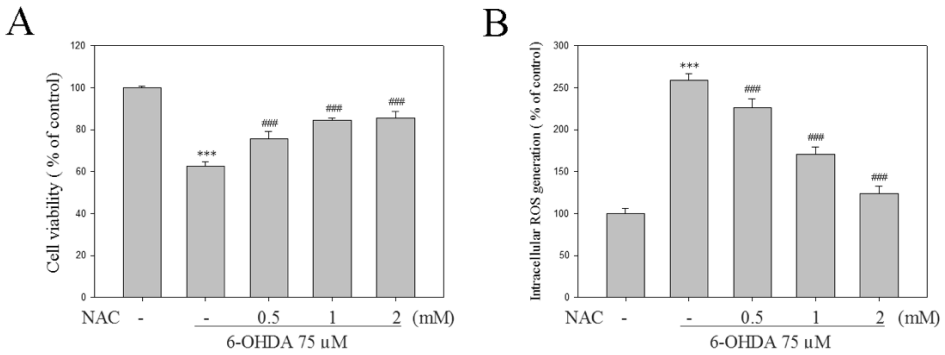

Figure 32. The effects of N-acetylcystein (NAC) against 6-OHDA-induced neurotoxicity and ROS generation.

Cells were cultured in 96-well plate for 24 h, and NAC was simultaneously treated with 6-OHDA (75 μM) for 48 h. Cell viability were measured by MTT reduction assay (A). Cells were cultured in 12-well plate for 24h, and NAC were simultaneously treated with 6-OHDA (75 μM) for 48 h. The relative fluorescence intensities of total 10,000 events by FACs analysis with DCFH-DA dye were quantified (B). Data represent the mean ± SD of three independent experiments. (***$p<0.001$ versus control group, $^{###}p<0.001$ versus 6-OHDA-induced group)

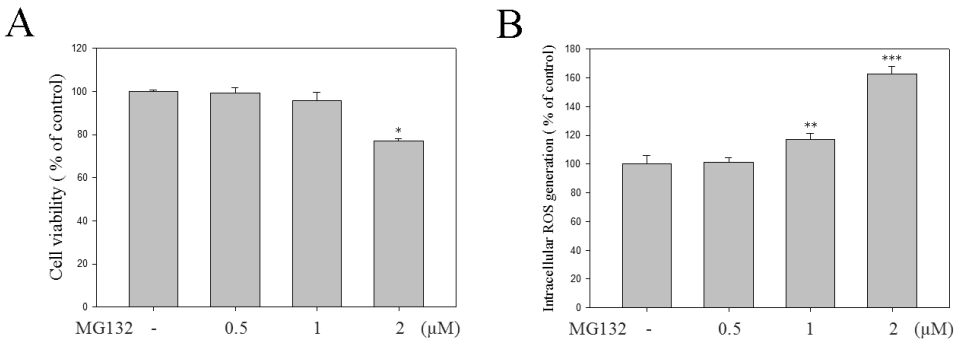

Figure 33. The effect of MG132 on neurotoxicity and ROS generation.

Cells were cultured in 96-well plate for 24 h, and MG132 was for 48 h. Cell viability were measured by MTT reduction assay (A). Cells were cultured in 12-well plate for 24h, and MG132 were for 48 h. The relative fluorescence intensities of total 10,000 events by FACS analysis with DCFH-DA dye were quantified (B). Data represent the mean ± SD of three independent experiments. (*$p<0.05$, **$p<0.01$, ***$p<0.001$ versus control group)

4. Discussion

As the world's population is rapidly ageing, the number of patients suffering from PD is increasing significantly. Although the cause of PD has not been definitively verified, recent research findings have suggested that oxidative stress and the impairment of the proteasome are major events in its pathogenesis (Ciechanover and Kwon, 2015). Oxidative stress has been implicated in ageing and neurodegenerative diseases such as PD. Oxidative stress induces the oxidation and aggregation of proteins in the brain (Butterfield and Kanski, 2001). In addition, excessive oxidative stress advances cellular apoptosis through the accumulation of oxidized proteins (Klovekorn and Munch, 1998). Many studies have reported that protein homeostasis is essential for cellular physiology and that the proteasome is responsible for selectively degrading targets including short-lived, damaged or misfolded protein, which comprise approximately 80% of all intracellular proteins. Hence, considerable interest has been paid to the importance of the role of the proteasome. The ubiquitination process is activated by ubiquitin-activating enzymes (E1), ubiquitin-conjugating enzymes (E2), and ubiquitin-transferring enzymes (E3). Through a sequential enzymatic reaction, proteins

are polyubiquitinated by E3 ligase. The polyubiquitin chain is recognized by the regulatory domain of the proteasome, in which the target protein is degraded by the catalytic core domain (Amm et al., 2014). Under normal conditions, polyubiquitinated proteins are rapidly degraded and do not accumulate. The accumulation of polyubiquitinated proteins is observed when excessive intracellular ROS, cellular stress, and diverse stress impair proteasome function (Elkon et al., 2004), and the accumulation of polyubiquitinated proteins induces neurotoxicity and neurodegeneration. Thus, the restoration of proteasome activity through the down-regulation of intracellular ROS is one of the primary mechanisms regulating ubiquitin-conjugated proteins, Lewy body-associated α-synuclein, and synphilin-1 proteins and the protection against neuronal cell death.

In the present study, 6-OHDA-induced ROS generation decreased in a concentration-dependent manner when cells were treated with different concentrations of CTE50 or the three orobol derivatives, and these compounds significantly elicited their neuroprotective effects against 6-OHDA-induced cell death and inhibited 6-OHDA-induced changes in cell morphology including shrinkage and rounding. In addition, we evaluated the inhibitory effects of CTE50 and the three orobol derivatives on the levels of cleaved caspase-9, caspase-3 and PARP, which are apoptosis signal factors; 6-OHDA

treatment increased the levels of cleaved caspase-9, caspase-3 and PARP protein; however, these increases were inhibited by co-treatment with CTE50 and the three orobol derivatives. A previous study demonstrated that the inhibitory effect of (-)-epigallocatechin-3-gallate (EGCG) on ROS generation led to a suppression of apoptosis (Ning et al., 2016). In our results, the inhibitory effects of CTE50 and three orobol derivatives on ROS generation are also concomitant with the protection against neuronal cell death and the activation of apoptosis signalling markers. Based on the neuroprotective effects of three orobol derivatives, we evaluated structure-bioactivity relationship (SAR). The compounds with two hydroxy groups at C-3′ and C-4′ in B-ring of flavonoid (**1** – **5**) exhibited neuroprotective effects, whereas the others with one hydroxy group at C-4' (**6** – **9**) did not. This suggested that the hydroxy group in the B-ring of flavonoid influences neuroprotective effects. The neuroprotective effect of prenyl-groups is not clear from 9 isolates to evaluate SAR. Therefore, further study will be necessary to evaluate SAR with prenylated flavonoids on neuroprotective activity.

A recent study emphasized the role of the proteasome in neurodegenerative disease and showed that proteasome inhibition induced neurotoxicity via the accumulation of polyubiquitinated proteins and protein aggregation (Canu et al., 2000). As neuronal cells are vulnerable to the accumulation of

polyubiquitinated proteins, several neurodegenerative diseases are related to the neurotoxicity resulting from protein accumulation. It has been shown that proteasome activity can gradually decrease with ageing and environmental stress, among other reasons, which results in a reduced ability to degrade misfolded proteins, contributing to the development of pathological protein aggregates (Ciechanover and Kwon, 2015). In cellular models, proteasome inhibition induced apoptosis and neuronal cell degeneration (Park et al., 2011; Sun et al., 2006), whereas proteasome activation enhanced neuronal cell survival (Seo et al., 2007). Thus, the protection against proteasome dysfunction could be a possible therapeutic strategy for neuroprotection. To investigate the mechanism underlying the protective effects of CTE50 and the three orobol derivatives against 6-OHDA-induced neuronal cell death, chymotrypsin-, trypsin-, and caspase-like proteasome activities were measured in SH-SY5Y cells. Our results showed that 6-OHDA significantly inhibited all three types of proteasome activities due to excessive ROS generation, and these results correlate with previously reported studies (Elkon et al., 2004). CTE50 and the three orobol derivatives at concentration of 20 μg/mL and 25 μM, respectively, attenuated 6-OHDA-induced dysfunction of the proteasome and nearly restored proteasome activities to normal levels. Additionally, we measured the levels of ubiquitin-conjugated proteins and

found an increase following 6-OHDA treatment. However, CTE50 (20 μg/mL) and the three orobol derivatives (25 μM) attenuated the 6-OHDA-induced increase in ubiquitin-conjugated protein levels to almost normal. These results suggested that 6-OHDA-induced proteasome dysfunction triggers the accumulation of ubiquitin-conjugated proteins, leading to neuronal cell death; however, CTE50 and the three orobol derivatives prevented the dysfunction of ubiquitin proteasome system (UPS) and protected against neuronal cell death. The impairment of UPS is involved in the formation of Lewy bodies, which is a characteristic hallmark of PD. Lewy bodies are composed of abnormal filamentous aggregates containing α-synuclein, and synphilin-1 has been found to colocalize with α-synuclein in Lewy bodies. It has been demonstrated that the overexpression of α-synuclein in *Drosophila* and *C. elegans* induced neuronal cell loss (Kontopoulos et al., 2006; Pesah et al., 2005). It has also been reported that α-synuclein filaments and oligomers themselves inhibited proteasome activities (Lindersson et al., 2004). Synphilin-1 has been reported to enhance the aggregation and neurotoxicity of α-synuclein (Buttner et al., 2010) and to promote inclusion formation under conditions of proteasome inhibition. Additionally, it has been reported that synphilin-1 inhibits the degradation of α-synuclein by the proteasome and thus increases the half-life of α-synuclein (Alvarez-Castelao and Castano, 2011).

Therefore, it has been suggested that the regulation of α-synuclein and synphilin-1 through UPS is important for neuroprotection (Sidhu et al., 2004). It was also previously reported that a relationship exists between proteasome dysfunction and neuronal cell death. Proteasome inhibition triggers a dramatic activation of the pro-apoptotic caspase-3,-9, PARP and DNA fragment (Sun et al., 2006; Yuan et al., 2008). The proteasome inhibitor MG132 induces dopaminergic neuronal cell degeneration and apoptosis (Park et al., 2011), and bortezomib, a proteasome inhibitor, induces caspase-dependent apoptosis. In contrast, a proteasome activator enhances the survival of neuronal cells (Seo et al., 2007), and betulinic acid and demethylsuberosin, reported to be proteasome activators, showed neuroprotective effects (Eksioglu-Demiralp et al., 2010; Kim, B-H et al., 2015). In our results, 6-OHDA-induced proteasome dysfunction resulted in the polyubiquitination of α-synuclein and synphilin-1 protein. However, CTE50 and the three orobol derivatives reduced the levels of 6-OHDA-induced polyubiquitination of α-synuclein and synphilin-1 protein in addition to ameliorating the dysfunction of proteasome activities. Furthermore, treatment with MG132, a proteasome inhibitor, significantly reduced the protective effects of CTE50 and the three orobol derivatives against 6-OHDA-induced neuronal cell death and proteasome dysfunction, suggesting that their neuronal cell protective effects are partly due to the

protection against proteasome dysfunction. In spite of the evidence for neuroprotection by orobol derivatives, there has been little research reported on the blood-brain barrier (BBB) permeability of orobol derivatives. However, some studies have demonstrated that isoflavones and several metabolites have been proven to transverse the BBB (Chandrasekharan and Aglin, 2013; Youdim et al., 2003). Therefore, BBB permeability of orobol and its derivatives should be studied to elucidate its potential for permeation across BBB in the further study.

5. Conclusion

In conclusion, this study demonstrated that CTE50 and three orobol derivatives protected against neuronal cell death and ROS generation, and attenuated proteasome dysfunction, the accumulation of ubiquitin-conjugated proteins, and the levels of polyubiquitinated α-synuclein and synphilin-1, the constituents of Lewy bodies. However, the neuroprotective effects of CTE50 and three orobol derivatives and the attenuation of proteasome dysfunction were significantly inhibited by MG132, suggesting their neuroprotective effects are partly due to the protection of the ubiquitin/proteasome-dependent degradation of α-synuclein and synphilin-1. Based on the results, it was suggested that CTE50 and the three orobol derivatives might be promising candidates for the therapy of neurodegenerative diseases such as PD.

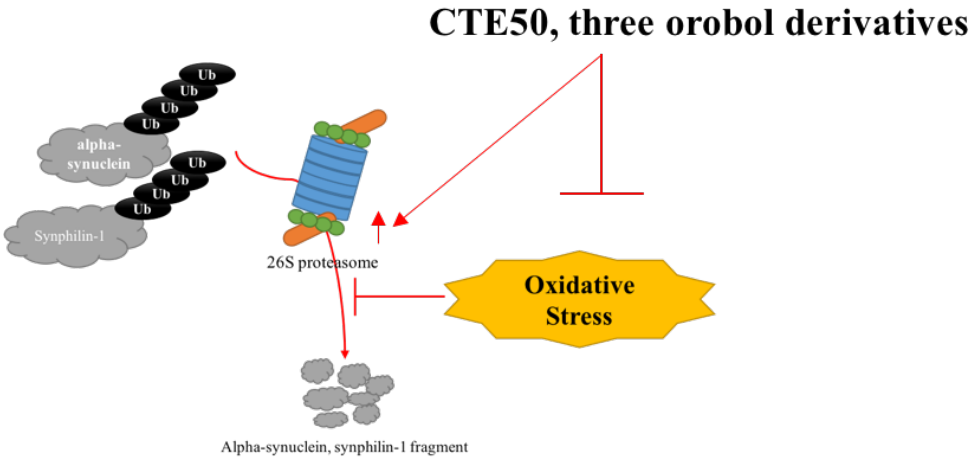

Figure 34. A scheme of protective effects of CTE50 and three orobol derivatives on 6-OHDA-induced neuronal cell death via enhancing proteasome activity and the ubiquitin/proteasome-dependent degradation of α-synuclein and synphilin-1.

CTE50 and three orobol derivatives protected against neuronal cell death, ROS generation, and accumulation of ubiquitin-conjugated proteins, polyubiquitinated α-synuclein and synphilin-1 via protecting proteasome dysfunction.

Chapter 3

Protective effects of TH3-125-4 (TH20) from the root barks of *Cudrania tricuspidata* on CCCP-induced neuronal cell death via the inhibition of USP30 deubiquitinating enzyme in Parkin knock down SH-SY5Y cells

1. Introduction

Mitophagy, a specialized autophagy pathway that mediates the clearance of damaged mitochondria by lysosomes, is important for mitochondrial quality control. Defective mitochondria, if left uncleared, can be a source of oxidative stress and compromise the health of the entire mitochondrial network. Parkinson's disease is characterized prominently, but not solely, by loss of dopaminergic neurons in the substantia nigra. Although the pathogenic mechanisms of Parkinson's disease are unclear, several lines of evidence propose that mitochondrial dysfunction is central to the disease. Most compellingly, familial Parkinson's disease can be caused by mutations in the ubiquitin ligase parkin and protein kinase PINK1 (Valente et al., 2004), both of which maintain healthy mitochondria via regulating mitochondrial dynamics and quality control (Narendra and Youle, 2011). Genetic studies established that PINK1 acts upstream of parkin (Park, J et al., 2006a). PINK1 recruits parkin from the cytoplasm to the surface of damaged mitochondria, leading to parkin-mediated ubiquitination of mitochondrial outer membrane proteins and deletion of damaged mitochondria by mitophagy (Narendra et al., 2010; Chan et al., 2011). Parkinson's disease-associated mutations in PINK1

or parkin impair parkin recruitment, mitochondrial ubiquitination, and/or mitophagy (Matsuda et al., 2010; Vives-Bauza et al., 2010). In the context of the inherently high mitochondrial oxidative stress in substantia nigra dopamine neurons, loss of parkin-mediated mitophagy could explain the greater susceptibility of substantia nigra neurons to neurodegeneration. Thus, promoting mitophagy and enhancing mitochondrial quality control could benefit dopaminergic neurons. Recent studies reported that deubiquitinating enzyme antagonizes the role of parkin e3 ligase. In culture of dopaminergic cells overexpressing parkin, Ubiquitin-specific protease (USP) 15, 30 blocks ubiquitination of mitochondrial proteins by parkin and inhibits lysosomal delivery of mitochondria and mitophagy (Nakamura and Hirose, 2008) . USP 30 can counteract parkin-mediated ubiquitination and degradation of mitochondrial Rho GTPase 1 (MIRO1) and translocase of outer mitochondrial membrane 20 (TOM20), two mitochondrial proteins, after mitochondrial damage. Also, USP30 can inhibit parkin-mediated ubiquitination of mitofusin 1, 2 (Mfn1,2), mitochondria fusion proteins. In cells transfected with green-fluorescent-protein-parkin (GFP-parkin) and expressing pathogenic parkin mutations, the mitophagy process is deficient. In this model, a knockdown of USP30 protein restores mitophagy, allowing cells to overcome parkin deficiency. Finally, using PINK1 or parkin mutant Drosophilia, the authors

demonstrated that USP30 suppression maintained mitochondrial health, improved climbing capability, and prevented dopamine depletion (Park, J et al., 2006b). Finally, in flies treated by paraquat, a mitochondrial toxin inducing parkinsonism, knockdown of USP30 rescued climbing ability, improved flies' survival, and prevented dopamine depletion (Tanner et al., 2011). All of these experiments show that USP30 plays a major role in dopaminergic cell dysfunction by altering mitophagy and that inhibiting this protein could represent a promising strategy for PD treatment. In this study, we evaluated the inhibitory effects of the isolated compounds from *C. tricuspidata* on USP15, 30. Also, the study investigated the potential effects on neuroprotection, parkin mediated mitophagy, mitochondrial membrane potential against CCCP-induced SH-SY5Y cells and parkin knock down SH-SY5Y cells.

2. Material and methods

2.1. Chemicals and reagents

Carbonyl cyanide 3-chlorophenylhydrazone (CCCP), JC-1, MG132, CCK-8, mitotracker, and PR-619 were purchased from Sigma-Aldrich (St. Louis, MO, USA). Dulbecco's modified Eagle's medium (DMEM) and fetal bovine serum (FBS) were purchased from Gibco BRL (Rockville, MD, USA). Hybond-polyvinylidene difluoride (PVDF) membranes were purchased from Amersham Pharmacia Biotechnology Inc. (Piscataway, NJ, USA). PRO-PREP protein extraction solution and WEST-Queen® ECL solution were purchased from iNtRON Biotech Inc. (Kyunggi, Korea). USP15, USP30, tetra ubiquitin peptides were purchased from Bio-Vision, Inc. (Milpitas, CA, USA) Parkin siRNA, scrambled siRNA, Mfn1, Mfn2, ubiquitin, USP15, USP30, OPA1, VDAC, alpha-tubulin, parkin, LC3-II first antibody, secondary antibody and FITC-conjugated secondary antibody were purchased from Santa Cruz Biotechnology, Inc. (Santa Cruz, CA, USA)

2.2. Preparation of TH3-125-4 (TH20)

Cudrania tricuspidata was stored at the Korea Forest Research Institute at Southern Forest Research Center (Jinju, Korea) in September 2008. A voucher specimen (accession number KH1-4-090814) was kept at the Department of Biosystems and Biotechnology at Korea University (Seoul, Korea). TH3-125-4 (TH20) was isolated from the roots of *Cudrania tricuspidata* and the structure of TH3-125-4 (TH20) was determined by spectroscopic methods, and the purity was more than 98% (Wei and Yu, 2008). TH3-125-4 (TH20) was dissolved in DMSO and diluted with PBS to obtain the proper concentration. Final concentration of DMSO was less than 0.1% and it didn't influence the performed assays.

2.3. Cell cultures

The human neuroblastoma cell line SH-SY5Y (ATCC No. CRL-2266) was purchased from the American Type Culture Collection (Manassas, VA, USA) and cultured in DMEM supplemented with 10 % heat-inactivated FBS and 1 % penicillin/streptomycin at 37 ºC in a humidified 5 % CO_2 atmosphere.

2.4. Measurement of cell viability

SH-SY5Y cells were seeded at a density of 1×10^5 cells/200 μL/well in 96-well plates for 24 h, and the cells were pre-treated with isolated compounds from *C. tricuspidata* for 24 h followed by subsequent treatment with CCCP (10 μM) for an additional 24 h. To evaluate the effect of parkin, cells were transfected with scrambled siRNA or parkin siRNA for 48 h and its final concentration was 100 nM. After transfected cells were treated with isolated compounds and CCCP (10 μM), cell viability was determined using a CCK-8 and measured by ELISA (Koo et al., 2011).

2.5. Measurement of mitochondrial membrane potential by JC-1 staining

SH-SY5Y cells were seeded at a density of 2×10^5 cells/2 mL/well in 6-well plates for 24 h, and the cells were pre-treated with isolated compounds for 24 h followed by subsequent treatment with CCCP (10 μM) for an additional 8 h. Mitochondrial membrane potential was determined using a JC-1 dyes. Briefly, the cells were washed with PBS, and then incubated with 10 μg/mL of JC-1 for 30 min at 37 ºC in the dark. The cells were then washed with PBS. The fluorescence intensities were measured by flow cytometry (BD FACSCalibur ™).

2.6. Measurement of intracellular ROS by Flow cytometry

ROS levels in cells were measured with the 2',7'-dichlorofluorescein diacetate (DCFH-DA) method (Munch et al., 1998a). Briefly, the cells were washed with PBS, and then incubated with 4 μM of DCFH-DA for 30 min at 37 ºC in the dark. The cells were then washed with PBS. The fluorescence intensities were measured by flow cytometry (BD FACSCalibur ^{TM}).

2.7. Mitochondrial and cytosolic fraction preparations

The mitochondrial and cytosolic proteins were extracted with a commercial kit (Mitochondria/Cytosol Fractionation Kit) according to the manufacturer's procedure (Bio-Vision, Milpitas, CA,). Briefly, the cells were incubated in cytosolic fraction buffer on ice for 15 min and homogenize cells in an ice-cold dounce tissue grinder. After homogenize, centrifuged for 10 min at 700 x g in a microcentrifuge at 4 ºC. Transfer the supernatant to a fresh 1.5-ml tube, and centrifuge at 10,000 x g in a microcentrifuge for 30 min at 4 ºC. Collect supernatant as a cytosolic fraction and mitochondrial pellet were washed with cold PBS, extracted completely with mitochondrial fraction buffer.

2.8. Parkin knock down via the transfection of small interfering RNA (siRNA)

The transfection with scrambled siRNA or parkin siRNA were progressed at final concentrations of 100 nM for 48 h by Lipofectamine 2000 (Invitrogen, Carlsbad, CA) prior to treatment with isolated compounds and CCCP (10 μM) as recommended by the manufacturer's guidelines.

2.9. Measurement of protein expression

The cells were collected, washed with PBS and lysed with a PRO-PREP protein extraction solution at -20 ºC for 20 min. After centrifugation at 13,000 x g for 30 min, the supernatant was used as the total protein extracts. Western blot analysis was accomplished as previously described method (Ham et al., 2013).

2.10. Immunoprecipitation assay

Immunoprecipitation was performed as previously described with slight modifications (Chen et al., 2014). After treatment, cells were washed three times with PBS and homogenized and lysed in cold-lysis buffer (50 mM Tris, 1 mM PMSF, 150 mM NaCl, 50 mM NaF, 1% Nonidet P-40, 0.25% sodium deoxycholate, 10 mM sodium pyrophosphate) and centrifuged at 14,000 × g (10 min, 4 °C), and the supernatant was transferred to a new ep-tube and incubated with 2 μg of Mfn1 or Mfn2 antibody overnight at 4 °C. The next

day, A/G plus agarose beads were added and incubated overnight at 4 °C followed by 3 washes in cold-lysis buffer. The loading samples were adjusted to total volume of 30 μL with lysis buffer, and the immune-complexes were eluted at 95 °C on a heating block for 5 min, vortexed, and spun down by centrifugation at 15,000 × g for 10 min.

2.11. Measurement of mitophagy by fluorescence microscope

The culture dish was coated with 0.2 % gelatin at 37 °C for 30 min and dried at RT on a clean bench. The SH-SY5Y cells were plated at a density of 5×10^4 cells/200 μL/well in coated dishes for 24 h and CCCP for 8 h. After treatment, the cells were washed with 1x PBS/Tween-20 buffer (pH 7.4) (PBST) once. The cells were fixed with 4 % paraformaldehyde for 30 min at room temperature (RT). After washing with PBST, the blocking steps were performed with 1 % BSA in PBST. Next, the cells were incubated with the primary antibody at 4 °C overnight. The next day, the cells were washed with PBST 3 times and incubated with FITC-conjugated secondary antibody for 1 h at RT. After 1 h, the cells were washed with PBST 3 times, and DAPI staining was performed for 5 min at RT. Lastly, the PBST washing and mounting steps were conducted.

2.12. Measurement of deubiquitinating enzyme activity

DUB assay buffer is composed of 20 mM HEPES at pH7.2, 100 mM NaCl, 0.05 % Tween 20, 0.1 mg/mL BSA, 1 mM DTT. Purified DUBs at optimal concentrations (USP 15, 50 nmol/L; USP30, 50 nmol/L) were incubated in DUB buffer containing isolated compounds (indicated concentration), vehicle alone (DMSO), or PR-619, (positive control for DUB inhibition) in a 100 μL reaction volume for 30 to 60 minutes at 37 °C. The reaction was initiated by the addition of 500 nmol/L Ub-AMC, and the release of AMC fluorescence was recorded at excitation/emission of 380/480 using a fluorometer.

2.13. Measurement of ubiquitin chain disassembly

In vitro disassembly of purified polyubiquitin chains (K48/K63 linked) was performed as described earlier (Dayal et al., 2009). USP30 (50 ng) prepared in DUB buffer was incubated with K48- or K63-linked chains (1 μg) and isolated compound for 15 min at 37 °C. The extent of chain disassembly was assessed by Western blotting.

2.14. Statistical analysis

All experimental data are expressed as mean value ± standard deviation. Statistical significance between multiple groups was determined by one-way

ANOVA (PRISM Graph Pad, San Diego, CA, USA). When ANOVA had a significant difference, *post hoc* Bonferroni's multiple comparison tests was conducted. *P* value less than 0.05 was regarded to be statistically significant.

3. Results

3.1. Inhibitory effect of TH3-125-4 (TH20) on deubiquitinating enzymes, USP15, USP30.

The isolated compounds from *C. tricuspidata* were evaluated to determine its inhibitory effects on deubiquitinating enzyme (DUB) activity. As shown in Table. 4, twelve isolated compounds inhibited USP15, USP30 activity. Among twelve isolated compounds, TH3-125-4 (TH20) showed potent inhibitory effects on USP30 with an IC_{50} values of 38.1 μM. TH20 inhibited USP30 enzyme activity concentration-dependently manner (Fig. 36). However, TH20 did not show inhibitory effect on USP15, total DUB enzyme activity. PR-619, a non-selective DUB inhibitor, significantly inhibited USP15, USP30, and total DUB enzyme activities, respectively (Fig. 37). The result of PR-619 was correlated with previous reports.

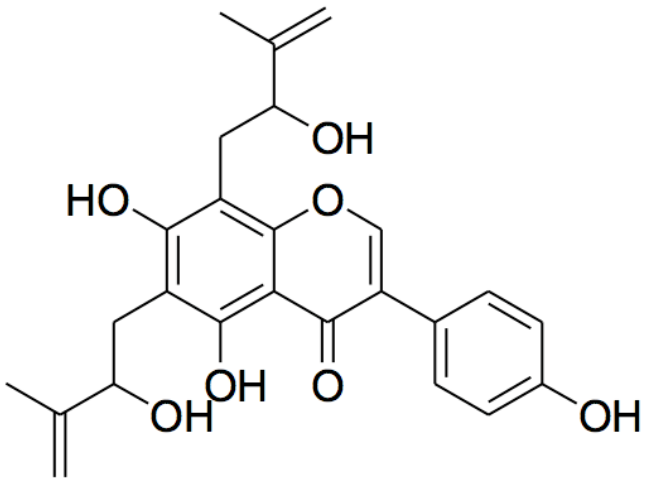

Figure 35. Chemical structures of TH3-125-4 (TH20)

Table 4. Inhibitory effect of isolated compounds from *C.tricuspidata* on deubiquitinating enzymes (USP15, USP30, Total DUB enzymes)

No.	Sample	USP15 inhibitory effect IC_{50} (μM)	USP30 inhibitory effect IC_{50} (μM)	Total DUB inhibitory effect IC_{50} (μM)
1	**TH3-125-4 (TH20)**	**>160**	**38.1**	**>160**
2	TH4-165-3K(TH49)	69.9	>160	>160
3	TH4-165-7 (TH50)	>160	60.5	>160
4	TH4-199-1K1 (TH59)	>160	82.3	>160
5	TH4-199-1K2 (TH60)	57.6	>160	>160
6	TH4-199-2K1 (TH61)	50.8	>160	>160
7	TH4-199-2K2 (TH62)	>160	83.7	>160

Table 4. Continued

No.	Sample	USP15 inhibitory effect IC_{50} (μM)	USP30 inhibitory effect IC_{50} (μM)	Total DUB inhibitory effect IC_{50} (μM)
8	TH5-17-5 (TH72)	>160	78.8	>160
9	JY1-154-2 (JY23)	150.7	>160	>160
10	JY1-164-4 (JY26)	132.2	>160	>160
11	JY1-190-1 (JY51)	130.8	>160	>160
12	JY1-191-3 (JY53)	155.2	>160	>160
…	…	…	…	…
129	JY1-134-5	>160	>160	>160
130	**PR619**	**4**	**6.7**	**8.5**

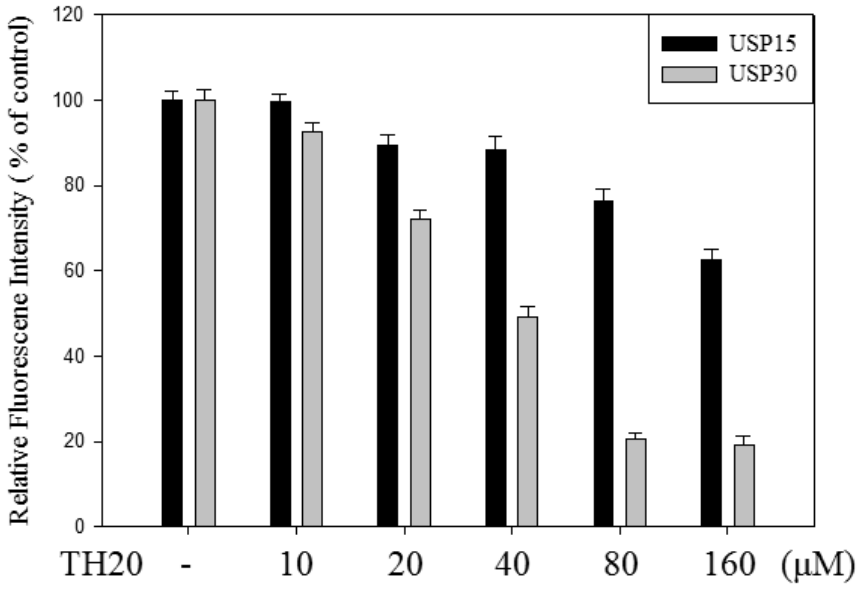

Figure 36. Inhibitory effects of TH3-125-4 (TH20) on USP15 and USP30 enzyme activities.

TH20 was incubated with 1 x DUB assay buffer for 30 min. DUB enzyme activities were measured by multiplate reader with fluorophore-linked Ub-AMC peptide substrates. The relative fluorescence intensity was indicated. Data represent the mean ± SD of three independent experiments.

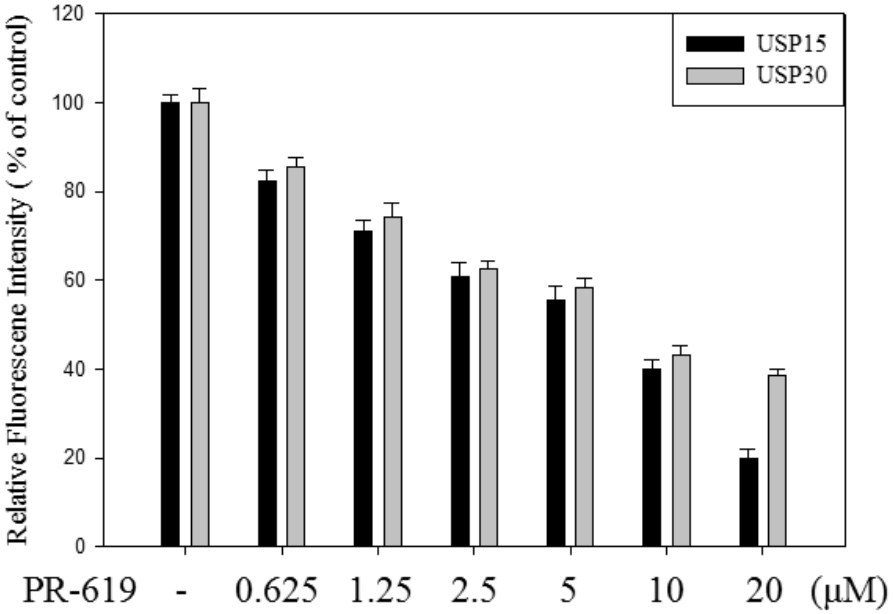

Figure 37. Inhibitory effects of PR-619 on USP15 and USP30 enzyme activities.

PR-619 was incubated with 1 x DUB assay buffer for 30 min. DUB enzyme activities were measured by multiplate reader with fluorophore-linked Ub-AMC peptide substrates. The relative fluorescence intensity was indicated. Data represent the mean ± SD of three independent experiments.

3.2. Effect of TH3-125-4 (TH20) on ubiquitin chain disassembly

The polyubiquitin chains (K48/K63 linked) are formed by e3 ligase like a parkin. The polyubiquitin chains are resolved by DUB. The incubation polyubiquitin chain with USP30 significantly induced disassembly of tetra ubiquitin. However, incubation with TH3-125-4 (TH20) inhibited disassembly of tetra ubiquitin at a concentration-dependent manner. The 80 μM of TH20 completely blocked the degradation of tetra ubiquitin. The results were correlated with inhibitory effects on USP30 activity in Fig. 38.

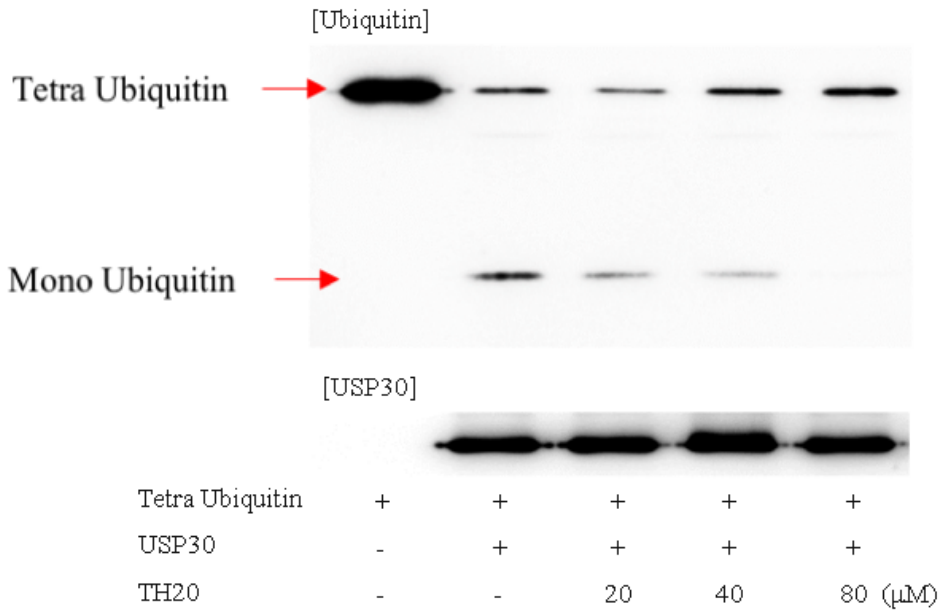

Figure 38. Inhibitory effects of TH3-125-4 (TH20) on USP30 enzyme mediated tetra ubiquitin disassembly.

TH20 was incubated with 1 x DUB assay buffer for 30 min. USP30 enzyme activities were measured by western blot assay with tetra ubiquitin peptide substrates. Representative data from three independent experiments are shown.

3.3. The protective effects of TH3-125-4 (TH20) against CCCP-induced neuronal cell death in parkin knock down SH-SY5Y cells.

The previous study revealed that parkin knock down cells were increased the vulnerability against CCCP neurotoxin. In the results, parkin siRNA transfected SH-SY5Y cells were more vulnerable to CCCP induce than scramble siRNA transfected SH-SY5Y cells. Also, USP15 or USP30 siRNA-transfected SH-SY5Y cells significantly protected the CCCP-induced cell death (Fig.39 and 40). Pre-treatment of TH20 protected CCCP-induced parkin knock down cell death at a concentration dependent manner. However, TH20 did not protect CCCP-induced scramble knock down cell death (Fig. 41).

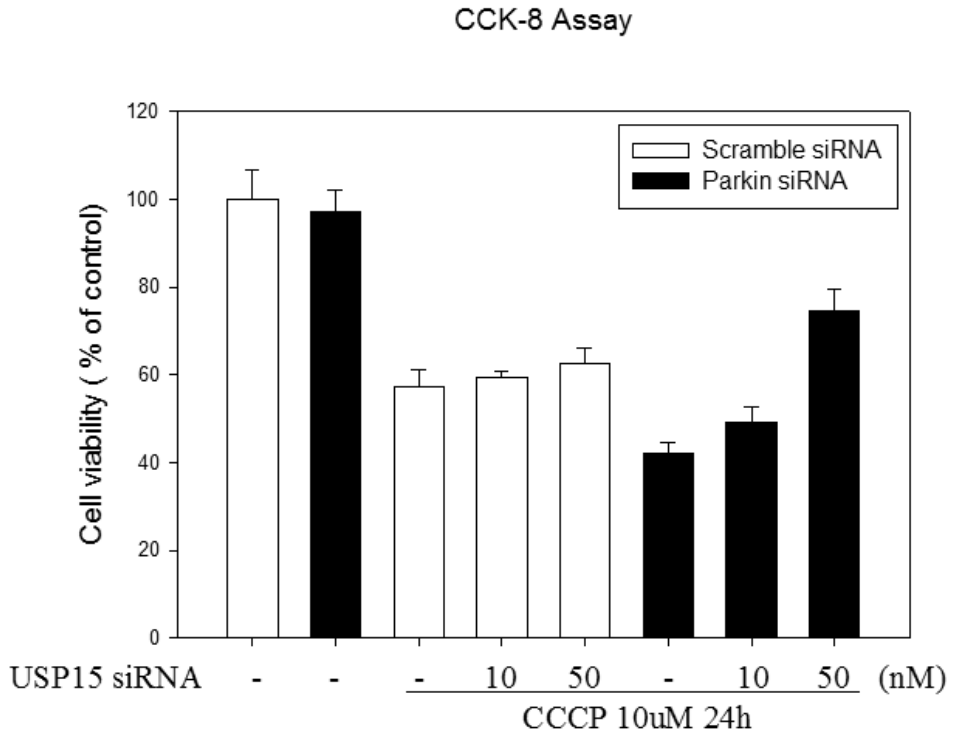

Figure 39. The protective effects of USP15 siRNA against CCCP-induced neuronal cell death in parkin knock down SH-SY5Y cells.

The cells were double-transfected with different concentrations of USP15 siRNA (10 - 50 nM) and Parkin siRNA or scramble siRNA (100 nM) for 48 h. After 24h, cells were subsequently treated with CCCP (10 μM) for another 24 h. The cell viability was determined by CCK-8 assay.

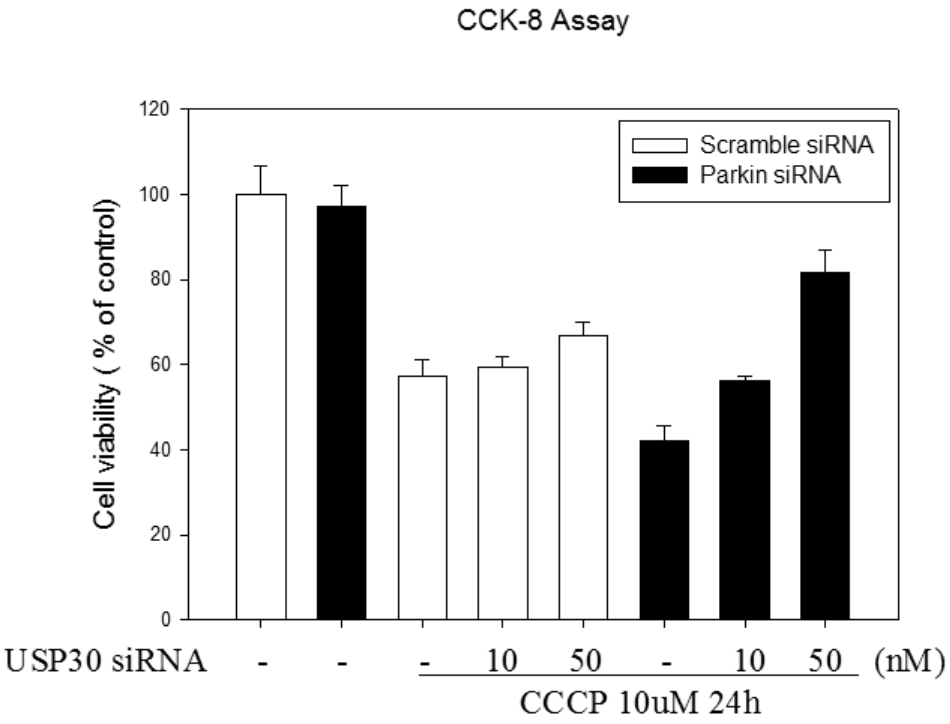

Figure 40. The protective effects of TH3-125-4 (TH20) against CCCP-induced neuronal cell death in parkin knock down SH-SY5Y cells.

The cells were double-transfected with different concentrations of USP30 siRNA (10 - 50 nM) and Parkin siRNA or scramble siRNA (100 nM) for 48 h. After 24h, cells were subsequently treated with CCCP (10 μM) for another 24 h. The cell viability was determined by CCK-8 assay.

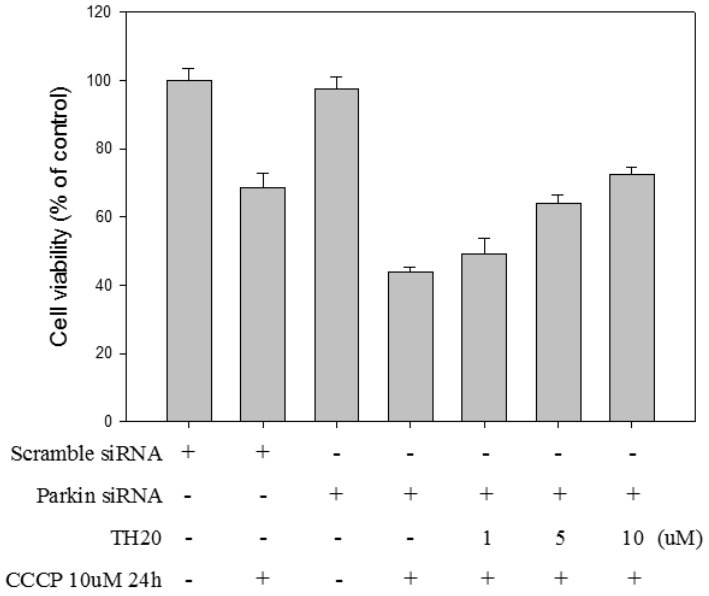

Figure 41. The protective effects of TH3-125-4 (TH20) against CCCP-induced neuronal cell death in parkin knock down SH-SY5Y cells.

The cells were pre-treated with different concentrations of TH20 (1 - 10 μM) for 24 h and subsequently treated with CCCP (10 μM) for another 24 h. The cells were transfected with Parkin siRNA or scramble siRNA (100 nM) for 48 h before the treatment with TH20. The cell viability was determined by CCK-8 assay.

3.4. Inhibitory effect of TH3-125-4 (TH20) on USP30 protein expression in SH-SY5Y cells.

We evaluated USP15, USP30 protein expression in SH-SY5Y cells. Among twelve isolated compounds, TH20 inhibited USP30 protein expression (Fig. 42). However, TH20 did not affect the protein expression of USP15. The protein expression of USP30 were gradually decreased by TH20 treatment at a concentration dependent manner. PR-619, a non-selective DUB inhibitor, did not affect the protein expression of USP15, USP30 (Fig. 43). The concentration of TH20 and PR-619 used in this experiment did not show cytotoxicity.

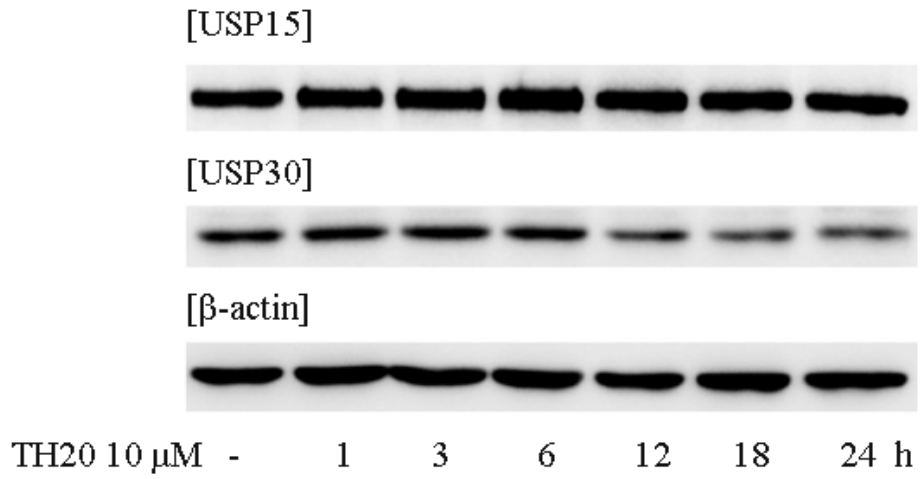

Figure 42. Inhibitory effect of TH3-125-4 (TH20) on USP30 protein expression in SH-SY5Y cells.

The cells were treated with TH20 (10 μM) for different durations (0 - 24 h). After treatment, the total protein was extracted and determined protein expression level by western blot assay. Representative data from three independent experiments are shown.

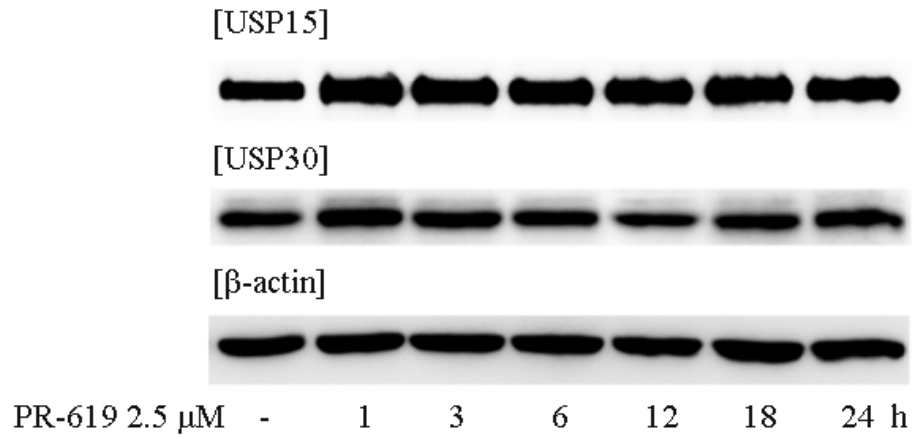

Figure 43. The protective effects of TH3-125-4 (TH20) against CCCP-induced neuronal cell death in parkin knock down SH-SY5Y cells.

The cells were treated with PR-619 (2.5 μM) for different durations (0 - 24 h). After treatment, the total protein was extracted and determined protein expression level by western blot assay. Representative data from three independent experiments are shown.

3.5. Effect of TH3-125-4 (TH20) on CCCP-induced disruption of mitochondrial membrane potential.

CCCP induces the rapid collapse of mitochondrial membrane potential (MMP) in SH-SY5Y cells. In our results, CCCP-induced collapse of MMP was peaked at 8 h. To evaluate the effect of TH20 on MMP, SH-SY5Y cell were pre-treated by TH20 for 24h. After then, MMP was disrupted by CCCP for 8h. TH20 did not protected CCCP-induced disruption of MMP (Fig. 44). The 10 μM of TH20 treatment slightly protected CCCP-induced collapse of MMP. However, the protective effect of TH20 was not significant result.

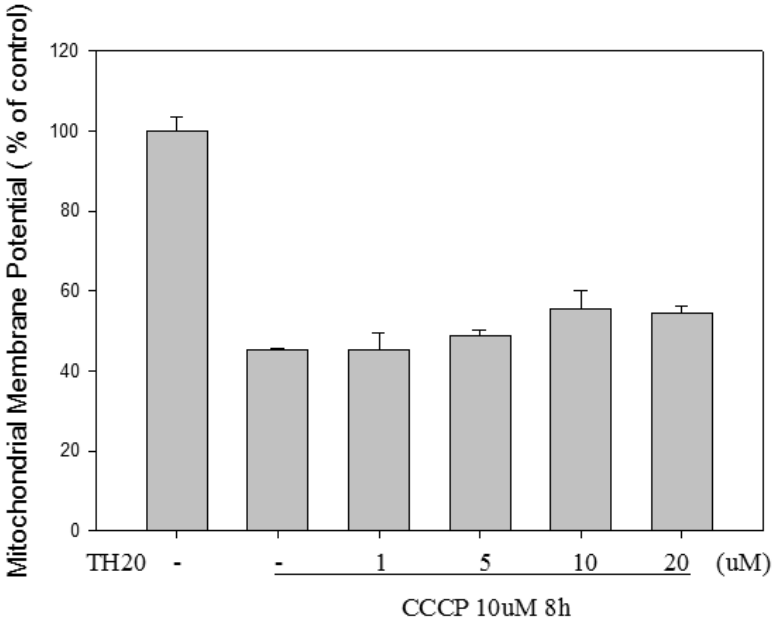

Figure 44. Effect of TH3-125-4 (TH20) on CCCP-induced disruption of mitochondrial membrane potential.

The cells were pre-treated with different concentrations of TH20 (1 - 10 μM) for 24 h and subsequently treated with CCCP (10 μM) for another 8 h. The cells were stained with JC-1 dyes for 30 min and determined by FACS analysis using FL-1 and FL-2 channel. The values of fluorescence intensity were obtained from histogram statistic of CellQuest software.

4. Discussion

Parkinson's disease is the most common neurodegenerative movement disorder. Although most cases are sporadic, several genes have been recently linked to familial PD, and loss-of-function mutations in Park2, the gene coding for the ubiquitin ligase Parkin, represent the most common recessive cause (Kitada et al., 1998). Parkin-null Drosophila melanogaster exhibit a severe phenotype, with the loss of dopaminergic neurons, disrupted spermatogenesis, and swollen and disordered mitochondria appearing before degeneration of their indirect flight muscles (Greene et al., 2003). The role of parkin in mitochondria phenotype was demonstrated. Parkin is selectively recruited to dysfunctional mitochondria in mammalian cells, and that after recruitment, Parkin mediates the engulfment of mitochondria by autophagosomes and their subsequent degradation. The results suggest that loss of Parkin activity may allow the accumulation of dysfunctional mitochondria, leading to neuron loss in PD, and that Parkin normally functions to survey mitochondrial activity and maintain mitochondrial fidelity by activating the autophagy of damaged organelles (Narendra et al., 2008). A recent proteomic study in human cells showed that Parkin ubiquitinates over

100 sites in more than 30 different MOM proteins, including Mfn1,2, in response to mitochondrial depolarization (Sarraf et al., 2013). In a recent research, deubiquitinating enzymes were reported that it can be an antagonist of parkin e3 ligase and inhibit parkin-mediated mitophagy. Among diverse DUBs, USP15 and USP30 were emerged as a major factor in opposing parkin e3 ligase activity. USP15, -30 deubiquitinates parkin-mediated mitochondrial fusion, fission proteins (Bingol et al., 2014; Cornelissen et al., 2014). Hence, the inhibition of USP15,-30 could be a therapeutic implication for familial PD.

In the current study, we identified a small natural compound, TH3-125-4 (TH20) derived from *C. tricuspidata*, which potently inhibits USP30 enzyme activity. However, TH20 did not significantly affect USP15 and total DUB enzyme activity. The inhibition of USP30 enzyme activity has a major role in PINK1-Parkin mediated mitophagy. It was reported that UPS30 physically interacts with Mfn1, 2 and decreases ubiquitination of Mfn1and Mfn2, whereas mutation of the active cysteine (C77) in the catalytic domain to serine abolishes its deubiquitinase activity, and thus the USP30-C77S mutant is unable to affect the ubiquitination of Mfns. Furthermore, it was demonstrated that inhibition of USP30 could lead to enhanced ubiquitination of Mfn1 or Mfn2, which promotes mitochondrial fusion (Yue et al., 2014). Hence, inhibitory effect of TH20 on USP30 enzyme activity could enhance PINK1-

Parkin mediated mitophagy. When the cells were transfected with Parkin siRNA, CCCP-induced neuronal cell death was increased comparing scramble siRNA treated SH-SY5Y. While TH20 treatment protected CCCP-induced neuronal cell death in Parkin K.D. SH-SY5Y cells, TH20 did not show protective effect against CCCP-induced neuronal cell death in scramble K.D. SH-SY5Y cells. Also, TH20 did not protect CCCP-induced disruption of MMP. The neuroprotective effect of TH20 in Parkin K.D. SH-SY5Y cells was predicted to be due to the DUB inhibitory effect, and the experiment for the DUB inhibitory effect was carried out. TH20 inhibited the enzymatic activity of USP30, while the inhibitory effect on USP15 and total DUB activity was weak. In addition, TH20 decreased the protein expression of USP30 in SH-SY5Y cells. Based on our results, we suggest that the protective effect of TH20 on CCCP-induced neuronal cell death in Parkin K.D. SH-SY5Y cells is mainly inhibition of USP30 enzyme activity. Further studies are needed to validate the hypothesis of the study, such as the effects of TH20 on Mfn1,2, OPA1, VDAC, LC3-beta, and p62 which are one of Parkin-mediated mitophagy factors. We are under investigating the effect of TH20 on Parkin-mediated mitophagy factors.

5. Conclusion

In conclusion, this study demonstrated that TH20 protected against CCCP-induced neuronal cell death in Parkin K.D. SH-SY5Y cells. Also, TH20 significantly inhibited USP30 enzyme activity and disassembly of polyubiquitin chain in *in vitro* assay. Our results showed that the protein expression of USP30 was decreased by treatment with TH20. Based on our results, we suggest that TH20 might be promising candidates for the therapy of familiar PD via restoring Parkin-mediated mitophagy.

References

Alfieri, A, Srivastava, S, Siow, RC, Modo, M, Fraser, PA, Mann, GE. 2011. Targeting the Nrf2-Keap1 antioxidant defence pathway for neurovascular protection in stroke. *The Journal of physiology* **589**(Pt 17): 4125-4136.

Alvarez-Castelao, B, Castano, JG. 2011. Synphilin-1 inhibits alpha-synuclein degradation by the proteasome. *Cell Mol Life Sci* **68**(15): 2643-2654.

Amm, I, Sommer, T, Wolf, DH. 2014. Protein quality control and elimination of protein waste: the role of the ubiquitin-proteasome system. *Biochim Biophys Acta* **1843**(1): 182-196.

Betarbet, R, Sherer, TB, Greenamyre, JT. 2005. Ubiquitin-proteasome system and Parkinson's diseases. *Exp Neurol* **191 Suppl 1**: S17-27.

Bingol, B, Tea, JS, Phu, L, Reichelt, M, Bakalarski, CE, Song, QH, et al. 2014. The mitochondrial deubiquitinase USP30 opposes parkin-mediated mitophagy. *Nature* **510**(7505): 370-+.

Bochkov, VN, Oskolkova, OV, Birukov, KG, Levonen, AL, Binder, CJ, Stockl, J. 2010. Generation and biological activities of oxidized phospholipids. *Antioxid Redox Signal* **12**(8): 1009-1059.

Bradford, MM. 1976. A rapid and sensitive method for the quantitation of microgram quantities of protein utilizing the principle of protein-dye binding. *Anal Biochem* **72**: 248-254.

Butterfield, DA, Kanski, J. 2001. Brain protein oxidation in age-related neurodegenerative disorders that are associated with aggregated proteins. *Mech Ageing Dev* **122**(9): 945-962.

Buttner, S, Delay, C, Franssens, V, Bammens, T, Ruli, D, Zaunschirm, S, et al. 2010. Synphilin-1 enhances alpha-synuclein aggregation in yeast and contributes to cellular stress and cell death in a Sir2-dependent manner. *PLoS One* **5**(10): e13700.

Canu, N, Barbato, C, Ciotti, MT, Serafino, A, Dus, L, Calissano, P. 2000. Proteasome involvement and accumulation of ubiquitinated proteins in cerebellar granule neurons undergoing apoptosis. *J Neurosci* **20**(2): 589-599.

Chan, NC, Salazar, AM, Pham, AH, Sweredoski, MJ, Kolawa, NJ, Graham, RLJ, et al. 2011. Broad activation of the ubiquitin-proteasome system by Parkin is critical for mitophagy. *Hum Mol Genet* **20**(9): 1726-1737.

Chandrasekharan, S, Aglin, A. 2013. Pharmacokinetics of dietary isoflavones. *Journal of Steroids & Hormonal Science* **2014**.

Chen, S, Zhu, P, Guo, HM, Solis, RS, Wang, YQ, Ma, YN, et al. 2014. Alpha1 catalytic subunit of AMPK modulates contractile function of cardiomyocytes through phosphorylation of troponin I. *Life Sciences* **98**(2): 75-82.

Chen, X, Guo, C, Kong, J. 2012. Oxidative stress in neurodegenerative diseases. *Neural Regen Res* **7**(5): 376-385.

Ciechanover, A, Kwon, YT. 2015. Degradation of misfolded proteins in neurodegenerative diseases: therapeutic targets and strategies. *Exp Mol Med* **47**: e147.

Cookson, MR. 2005. The biochemistry of Parkinson's disease*. *Annu. Rev. Biochem.* **74**: 29-52.

Cornelissen, T, Haddad, D, Wauters, F, Van Humbeeck, C, Mandemakers, W, Koentjoro, B, et al. 2014. The deubiquitinase USP15 antagonizes Parkin-mediated mitochondrial ubiquitination and mitophagy. *Hum Mol Genet* **23**(19): 5227-5242.

Dahlmann, B. 2007. Role of proteasomes in disease. *BMC Biochem* **8 Suppl 1**: S3.

Dayal, S, Sparks, A, Jacob, J, Allende-Vega, N, Lane, DP, Saville, MK. 2009. Suppression of the Deubiquitinating Enzyme USP5 Causes the

Accumulation of Unanchored Polyubiquitin and the Activation of p53. *Journal of Biological Chemistry* **284**(8): 5030-5041.

Dinkova-Kostova, AT, Talalay, P. 2010. NAD(P)H:quinone acceptor oxidoreductase 1 (NQO1), a multifunctional antioxidant enzyme and exceptionally versatile cytoprotector. *Arch Biochem Biophys* **501**(1): 116-123.

Dodel, RC, Du, Y, Bales, KR, Ling, Z, Carvey, PM, Paul, SM. 1999. Caspase-3-like proteases and 6-hydroxydopamine induced neuronal cell death. *Brain research. Molecular brain research* **64**(1): 141-148.

Doskeland, AP, Flatmark, T. 2002. Ubiquitination of soluble and membrane-bound tyrosine hydroxylase and degradation of the soluble form. *Eur J Biochem* **269**(5): 1561-1569.

Eksioglu-Demiralp, E, Kardas, ER, Ozgul, S, Yagci, T, Bilgin, H, Sehirli, O, et al. 2010. Betulinic acid protects against ischemia/reperfusion-induced renal damage and inhibits leukocyte apoptosis. *Phytother Res* **24**(3): 325-332.

Elkon, H, Melamed, E, Offen, D. 2004. Oxidative stress, induced by 6-hydroxydopamine, reduces proteasome activities in PC12 cells - Implications for the pathogenesis of Parkinson's disease. *Journal of Molecular Neuroscience* **24**(3): 387-400.

Espinosa-Diez, C, Miguel, V, Mennerich, D, Kietzmann, T, Sanchez-Perez, P, Cadenas, S, et al. 2015. Antioxidant responses and cellular adjustments to oxidative stress. *Redox Biol* **6**: 183-197.

Farooqui, T, Farooqui, AA. 2011. Lipid-mediated oxidative stress and inflammation in the pathogenesis of Parkinson's disease. *Parkinson's disease* **2011**: 247467.

Fraser, JA, Saunders, RD, McLellan, LI. 2002. Drosophila melanogaster glutamate-cysteine ligase activity is regulated by a modifier subunit with a mechanism of action similar to that of the mammalian form. *The Journal of biological chemistry* **277**(2): 1158-1165.

Fujimoto, T, Hano, Y, Nomura, T. 1984. Components of Root Bark of Cudrania tricuspidata l.1,2 Structures of Four New Isoprenylated Xanthones, Cudraxanthones A, B, C and D. *Planta Med* **50**(3): 218-221.

Ganora, L. 2009. Herbal constituents: Foundations of phytochemistry. *Lisa Ganora, Louisville, CO*.

Greene, JC, Whitworth, AJ, Kuo, I, Andrews, LA, Feany, MB, Pallanck, LJ. 2003. Mitochondrial pathology and apoptotic muscle degeneration in Drosophila parkin mutants. *P Natl Acad Sci USA* **100**(7): 4078-4083.

Ham, A, Kim, DW, Kim, KH, Lee, SJ, Oh, KB, Shin, J, et al. 2013. Reynosin protects against neuronal toxicity in dopamine-induced SH-SY5Y cells and 6-hydroxydopamine-lesioned rats as models of Parkinson's disease: Reciprocal up-regulation of E6-AP and down-regulation of alpha-synuclein. *Brain Res* **1524**: 54-61.

Hano, Y, Matsumoto, Y, Shinohara, K, Sun, JY, Nomura, T. 1991. Structures of Four New Isoprenylated Xanthones, Cudraxanthones L,

M, N, and O from Cudrania tricuspidata1,2. *Planta Med* **57**(2): 172-175.

Hiep, NT, Kwon, J, Kim, DW, Hwang, BY, Lee, HJ, Mar, W, et al. 2015. Isoflavones with neuroprotective activities from fruits of Cudrania tricuspidata. *Phytochemistry* **111**: 141-148.

Huang, Q, Figueiredo-Pereira, ME. 2010. Ubiquitin/proteasome pathway impairment in neurodegeneration: therapeutic implications. *Apoptosis* **15**(11): 1292-1311.

Jeong, CH, Choi, GN, Kim, JH, Kwak, JH, Jeong, HR, Kim, DO, et al. 2010. Protective Effects of Aqueous Extract from Cudrania tricuspidata on Oxidative Stress-induced Neurotoxicity. *Food Science and Biotechnology* **19**(4): 1113-1117.

Jeong, JY, Jo, YH, Lee, KY, Do, SG, Hwang, BY, Lee, MK. 2014. Optimization of pancreatic lipase inhibition by Cudrania tricuspidata fruits using response surface methodology. *Bioorg Med Chem Lett* **24**(10): 2329-2333.

Jung, T, Grune, T. 2013. The proteasome and the degradation of oxidized proteins: Part I-structure of proteasomes. *Redox Biol* **1**: 178-182.

Kang, DG, Hur, TY, Lee, GM, Oh, H, Kwon, TO, Sohn, EJ, et al. 2002. Effects of Cudrania tricuspidata water extract on blood pressure and renal functions in NO-dependent hypertension. *Life sciences* **70**(22): 2599-2609.

Kang, KW, Lee, SJ, Kim, SG. 2005. Molecular mechanism of nrf2 activation by oxidative stress. *Antioxidants & redox signaling* **7**(11-12): 1664-1673.

Kanthasamy, A, Jin, H, Mehrotra, S, Mishra, R, Kanthasamy, A, Rana, A. 2010. Novel cell death signaling pathways in neurotoxicity models of dopaminergic degeneration: relevance to oxidative stress and neuroinflammation in Parkinson's disease. *Neurotoxicology* **31**(5): 555-561.

Kaufmann, SH, Desnoyers, S, Ottaviano, Y, Davidson, NE, Poirier, GG. 1993. Specific proteolytic cleavage of poly(ADP-ribose) polymerase: an early marker of chemotherapy-induced apoptosis. *Cancer research* **53**(17): 3976-3985.

Kim, B-H, Kwon, J, Lee, D, Mar, W. 2015. Neuroprotective Effect of Demethylsuberosin, a Proteasome Activator, against MPP+-induced Cell Death in Human Neuroblastoma SH-SY5Y Cells. *Planta Medica Letters* **2**(01): e15-e18.

Kim, D-W, Lee, K-t, Kwon, J, Lee, HJ, Lee, D, Mar, W. 2015. Neuroprotection against 6-OHDA-induced oxidative stress and apoptosis in SH-SY5Y cells by 5, 7-Dihydroxychromone: Activation of the Nrf2/ARE pathway. *Life sciences* **130**: 25-30.

Kitada, T, Asakawa, S, Hattori, N, Matsumine, H, Yamamura, Y, Minoshima, S, et al. 1998. Mutations in the parkin gene cause autosomal recessive juvenile parkinsonism. *Nature* **392**(6676): 605-608.

Klovekorn, P, Munch, J. 1998. Variable optical delay line with diffraction-limited autoalignment. *Appl Opt* **37**(10): 1903-1904.

Kontopoulos, E, Parvin, JD, Feany, MB. 2006. Alpha-synuclein acts in the nucleus to inhibit histone acetylation and promote neurotoxicity. *Hum Mol Genet* **15**(20): 3012-3023.

Koo, U, Nam, KW, Ham, A, Lyu, D, Kim, B, Lee, SJ, et al. 2011. Neuroprotective effects of 3alpha-acetoxyeudesma-1,4(15),11(13)-trien-12,6alpha-olide against dopamine-induced apoptosis in the human neuroblastoma SH-SY5Y cell line. *Neurochem Res* **36**(11): 1991-2001.

Kuida, K, Haydar, TF, Kuan, CY, Gu, Y, Taya, C, Karasuyama, H, et al. 1998. Reduced apoptosis and cytochrome c-mediated caspase activation in mice lacking caspase 9. *Cell* **94**(3): 325-337.

Lee, Ha, H, Lee, JK, Seo, CS, Lee, NH, Jung, DY, et al. 2012. The fruits of Cudrania tricuspidata suppress development of atopic dermatitis in NC/Nga mice. *Phytother Res* **26**(4): 594-599.

Lee, IK, Kim, CJ, Song, KS, Kim, HM, Koshino, H, Uramoto, M, et al. 1996. Cytotoxic benzyl dihydroflavonols from Cudrania tricuspidata. *Phytochemistry* **41**(1): 213-216.

Lee, T, Kwon, J, Lee, D, Mar, W. 2015. Effects of Cudrania tricuspidata Fruit Extract and Its Active Compound, 5,7,3 ',4 '-Tetrahydroxy-6,8-diprenylisoflavone, on the High-Affinity IgE Receptor-Mediated Activation of Syk in Mast Cells. *Journal of Agricultural and Food Chemistry* **63**(22): 5459-5467.

Leutner, S, Czech, C, Schindowski, K, Touchet, N, Eckert, A, Muller, WE. 2000. Reduced antioxidant enzyme activity in brains of mice transgenic for human presenilin-1 with single or multiple mutations. *Neuroscience letters* **292**(2): 87-90.

Lim, JH, Kim, KM, Kim, SW, Hwang, O, Choi, HJ. 2008. Bromocriptine activates NQO1 via Nrf2-PI3K/Akt signaling: Novel cytoprotective mechanism against oxidative damage. *Pharmacol Res* **57**(5): 325-331.

Lindersson, E, Beedholm, R, Hojrup, P, Moos, T, Gai, W, Hendil, KB, et al. 2004. Proteasomal inhibition by alpha-synuclein filaments and oligomers. *J Biol Chem* **279**(13): 12924-12934.

Matsuda, N, Sato, S, Shiba, K, Okatsu, K, Saisho, K, Gautier, CA, et al. 2010. PINK1 stabilized by mitochondrial depolarization recruits Parkin to damaged mitochondria and activates latent Parkin for mitophagy. *J Cell Biol* **189**(2): 211-221.

McNaught, KS, Jenner, P. 2001. Proteasomal function is impaired in substantia nigra in Parkinson's disease. *Neurosci Lett* **297**(3): 191-194.

Meyer, T, Munch, C, Volkel, H, Booms, P, Ludolph, AC. 1998. The EAAT2 (GLT-1) gene in motor neuron disease: absence of mutations in amyotrophic lateral sclerosis and a point mutation in patients with hereditary spastic paraplegia. *Journal of neurology, neurosurgery, and psychiatry* **65**(4): 594-596.

Munch, G, Cunningham, AM, Riederer, P, Braak, E. 1998a. Advanced glycation endproducts are associated with Hirano bodies in Alzheimer's disease. *Brain research* **796**(1-2): 307-310.

Munch, G, Gerlach, M, Sian, J, Wong, A, Riederer, P. 1998b. Advanced glycation end products in neurodegeneration: more than early markers of oxidative stress? *Annals of neurology* **44**(3 Suppl 1): S85-88.

Nakamura, N, Hirose, S. 2008. Regulation of mitochondrial morphology by USP30, a deubiquitinating enzyme present in the mitochondrial outer membrane. *Mol Biol Cell* **19**(5): 1903-1911.

Narendra, D, Tanaka, A, Suen, DF, Youle, RJ. 2008. Parkin is recruited selectively to impaired mitochondria and promotes their autophagy. *J Cell Biol* **183**(5): 795-803.

Narendra, DP, Jin, SM, Tanaka, A, Suen, DF, Gautier, CA, Shen, J, et al. 2010. PINK1 Is Selectively Stabilized on Impaired Mitochondria to Activate Parkin. *Plos Biol* **8**(1).

Narendra, DP, Youle, RJ. 2011. Targeting Mitochondrial Dysfunction: Role for PINK1 and Parkin in Mitochondrial Quality Control. *Antioxid Redox Sign* **14**(10): 1929-1938.

Nguyen, T, Nioi, P, Pickett, CB. 2009. The Nrf2-antioxidant response element signaling pathway and its activation by oxidative stress. *J Biol Chem* **284**(20): 13291-13295.

Ning, W, Wang, S, Liu, D, Fu, L, Jin, R, Xu, A. 2016. Potent effects of peracetylated (-)-epigallocatechin-3-gallate against hydrogen peroxide-induced damage in human epidermal melanocytes via attenuation of oxidative stress and apoptosis. *Clin Exp Dermatol* **41**(6): 616-624.

Okamoto, Y, Suzuki, A, Ueda, K, Ito, C, Itoigawa, M, Furukawa, H, et al. 2006. Anti-estrogenic activity of prenylated isoflavones from Millettia pachycarpa: implications for pharmacophores and unique mechanisms. *Journal of health science* **52**(2): 186-191.

Park, HS, Jun do, Y, Han, CR, Woo, HJ, Kim, YH. 2011. Proteasome inhibitor MG132-induced apoptosis via ER stress-mediated apoptotic pathway and its potentiation by protein tyrosine kinase p56lck in human Jurkat T cells. *Biochem Pharmacol* **82**(9): 1110-1125.

Park, J, Lee, SB, Lee, S, Kim, Y, Song, S, Kim, S, et al. 2006a. Mitochondrial dysfunction in Drosophila PINK1 mutants is complemented by parkin. *Nature* **441**(7097): 1157-1161.

Park, J, Lee, SB, Lee, S, Kim, Y, Song, S, Kim, S, et al. 2006b. Mitochondrial dysfunction in Drosophila PINK1 mutants is complemented by parkin. *Nature* **441**(7097): 1157-1161.

Park, KH, Park, YD, Han, JM, Im, KR, Lee, BW, Jeong, IY, et al. 2006. Anti-atherosclerotic and anti-inflammatory activities of catecholic xanthones and flavonoids isolated from Cudrania tricuspidata. *Bioorg Med Chem Lett* **16**(21): 5580-5583.

Park, SH, Jang, JH, Chen, CY, Na, HK, Surh, YJ. 2010. A formulated red ginseng extract rescues PC12 cells from PCB-induced oxidative cell

death through Nrf2-mediated upregulation of heme oxygenase-1 and glutamate cysteine ligase. *Toxicology* **278**(1): 131-139.

Pesah, Y, Burgess, H, Middlebrooks, B, Ronningen, K, Prosser, J, Tirunagaru, V, et al. 2005. Whole-mount analysis reveals normal numbers of dopaminergic neurons following misexpression of alpha-Synuclein in Drosophila. *Genesis* **41**(4): 154-159.

Pompella, A, Visvikis, A, Paolicchi, A, De Tata, V, Casini, AF. 2003. The changing faces of glutathione, a cellular protagonist. *Biochem Pharmacol* **66**(8): 1499-1503.

Qiu, J, Chen, L, Zhu, Q, Wang, D, Wang, W, Sun, X, et al. 2012. Screening natural antioxidants in peanut shell using DPPH-HPLC-DAD-TOF/MS methods. *Food chemistry* **135**(4): 2366-2371.

Rahman, K. 2007. Studies on free radicals, antioxidants, and co-factors. *Clinical interventions in aging* **2**(2): 219-236.

Ramos-Gomez, M, Kwak, MK, Dolan, PM, Itoh, K, Yamamoto, M, Talalay, P, et al. 2001. Sensitivity to carcinogenesis is increased and chemoprotective efficacy of enzyme inducers is lost in nrf2 transcription factor-deficient mice. *Proceedings of the National Academy of Sciences of the United States of America* **98**(6): 3410-3415.

Rizzardini, M, Terao, M, Falciani, F, Cantoni, L. 1993. Cytokine induction of haem oxygenase mRNA in mouse liver. Interleukin 1 transcriptionally activates the haem oxygenase gene. *The Biochemical journal* **290 (Pt 2)**: 343-347.

Sarraf, SA, Raman, M, Guarani-Pereira, V, Sowa, ME, Huttlin, EL, Gygi, SP, et al. 2013. Landscape of the PARKIN-dependent ubiquitylome in response to mitochondrial depolarization. *Nature* **496**(7445): 372-+.

Seo, H, Sonntag, KC, Kim, W, Cattaneo, E, Isacson, O. 2007. Proteasome activator enhances survival of Huntington's disease neuronal model cells. *PLoS One* **2**(2): e238.

Seo, WG, Pae, HO, Oh, GS, Chai, KY, Yun, YG, Chung, HT, et al. 2001. Ethyl acetate extract of the stem bark of Cudrania tricuspidata induces apoptosis in human leukemia HL-60 cells. *Am J Chin Med* **29**(2): 313-320.

Shiotsuka, S, Isonishi, S. 2001. Differential sensitization by orobol in proliferating and quiescent human ovarian carcinoma cells. *Int J Oncol* **18**(2): 337-342.

Sidhu, A, Wersinger, C, MOUSSA, CEH, Vernier, P. 2004. The role of α-synuclein in both neuroprotection and neurodegeneration. *Annals of the New York Academy of Sciences* **1035**(1): 250-270.

Su, ZY, Shu, L, Khor, TO, Lee, JH, Fuentes, F, Kong, AN. 2013. A perspective on dietary phytochemicals and cancer chemoprevention: oxidative stress, nrf2, and epigenomics. *Topics in current chemistry* **329**: 133-162.

Sun, F, Anantharam, V, Zhang, D, Latchoumycandane, C, Kanthasamy, A, Kanthasamy, AG. 2006. Proteasome inhibitor MG-132 induces dopaminergic degeneration in cell culture and animal models. *Neurotoxicology* **27**(5): 807-815.

Sun, X, Huang, L, Zhang, M, Sun, S, Wu, Y. 2010. Insulin like growth factor-1 prevents 1-mentyl-4-phenylphyridinium-induced apoptosis in PC12 cells through activation of glycogen synthase kinase-3beta. *Toxicology* **271**(1-2): 5-12.

Tai, HC, Schuman, EM. 2008. Ubiquitin, the proteasome and protein degradation in neuronal function and dysfunction. *Nat Rev Neurosci* **9**(11): 826-838.

Tanner, CM, Kamel, F, Ross, GW, Hoppin, JA, Goldman, SM, Korell, M, et al. 2011. Rotenone, Paraquat, and Parkinson's Disease. *Environ Health Persp* **119**(6): 866-872.

Tucker, JL, 3rd, Munchus, GM, 3rd. 1998. The predictors of quality care. *Military medicine* **163**(11): 754-757.

Turkseven, S, Kruger, A, Mingone, CJ, Kaminski, P, Inaba, M, Rodella, LF, et al. 2005. Antioxidant mechanism of heme oxygenase-1 involves an increase in superoxide dismutase and catalase in experimental diabetes. *Am J Physiol Heart Circ Physiol* **289**(2): H701-707.

Uddin, GM, Jeon, JS, Kim, CY. 2011. Isolation of Prenylated Isoflavonoids from Cudrania tricuspidata Fruits that Inhibit A2E Photooxidation. *Natural Product Sciences* **17**(3): 206-211.

Uttara, B, Singh, AV, Zamboni, P, Mahajan, RT. 2009. Oxidative stress and neurodegenerative diseases: a review of upstream and downstream antioxidant therapeutic options. *Current neuropharmacology* **7**(1): 65-74.

Valente, EM, Abou-Sleiman, PM, Caputo, V, Muqit, MM, Harvey, K, Gispert, S, et al. 2004. Hereditary early-onset Parkinson's disease caused by mutations in PINK1. *Science* **304**(5674): 1158-1160.

Vives-Bauza, C, Zhou, C, Huang, Y, Cui, M, de Vries, RLA, Kim, J, et al. 2010. PINK1-dependent recruitment of Parkin to mitochondria in mitophagy. *P Natl Acad Sci USA* **107**(1): 378-383.

Wei, G, Yu, B. 2008. Isoflavone glycosides: Synthesis and evaluation as alpha-glucosidase inhibitors. *Eur J Org Chem*(18): 3156-3163.

Wojcik, C, DeMartino, GN. 2003. Intracellular localization of proteasomes. *Int J Biochem Cell Biol* **35**(5): 579-589.

Youdim, KA, Dobbie, MS, Kuhnle, G, Proteggente, AR, Abbott, NJ, Rice-Evans, C. 2003. Interaction between flavonoids and the blood–brain barrier: in vitro studies. *Journal of neurochemistry* **85**(1): 180-192.

Yuan, BZ, Chapman, JA, Reynolds, SH. 2008. Proteasome Inhibitor MG132 Induces Apoptosis and Inhibits Invasion of Human Malignant Pleural Mesothelioma Cells. *Transl Oncol* **1**(3): 129-140.

Yue, W, Chen, ZH, Liu, HY, Yan, C, Chen, M, Feng, D, et al. 2014. A small natural molecule promotes mitochondrial fusion through inhibition of the deubiquitinase USP30. *Cell Res* **24**(4): 482-496.

Zhang, M, An, C, Gao, Y, Leak, RK, Chen, J, Zhang, F. 2013. Emerging roles of Nrf2 and phase II antioxidant enzymes in neuroprotection. *Progress in neurobiology* **100**: 30-47.

Zuo, Y, Xiang, B, Yang, J, Sun, X, Wang, Y, Cang, H, et al. 2009. Oxidative modification of caspase-9 facilitates its activation via disulfide-mediated interaction with Apaf-1. *Cell research* **19**(4): 449-457.

국문초록

꾸지뽕나무로부터 분리한 유효성분물질의 파킨슨병 세포모델에서의 신경보호효과: Ubiquitin-proteasome system 및 Nrf2-ARE 관련 기전에 관한 효과연구

김 동 우

약학과 천연물과학 전공

서울대학교 약학대학 대학원

파킨슨 병은 운동 장애, 기억 상실, 운동 부조 및 도파민 신경의 손실등의 특징을 보이는 퇴행성 뇌질환이다. 파킨슨 병의 원인은 명확하게 특정되지 않았지만 산화적 스트레스, 유비퀴틴 – 프로테아좀 기능저하, mitophagy 기능이상은 세포 기능 장애 및 과도한 독성단백질의 축적 및 미토콘드리아 장애를 초래하며 주요 병인으로 간주되고있다. 신경독성으로 알려진 6-OHDA, CCCP 는 라디칼과 같은 과도한 활성산소종을 유도하거나 미토콘드리아의 기능이상을 유도함으로써 도파민 뉴런을 파괴하고 단백질 산화 및

신경 세포 사멸을 일으킨다. 산화적스트레스는 다양한 분자병리학적 기전을 통해 세포사멸을 유발하며, 유비퀴틴 – 프로테아좀 기능저하는 독성 단백질의 과다축적을 유도하고 이로인해 신경 세포사를 초래한다. Mitophagy 의 기능이상은 제거해야할 미토콘드리아의 과축적을 유발하여 신경 세포사를 초래한다. 현재 개발중인 새로운 치료법은 도파민 뉴런을 보호하는 것을 목적으로 하고 있다. 본 연구에서 파킨슨 병의 치료제제로써 가능성 있는 선도 화합물을 발견하기 위해 SH-SY5Y 신경아종 세포에서 6-OHDA, CCCP 로 유도한 뇌세포 사멸 보호효과 및 관련 기전에 대하여 연구하였다.

첫번째로, 꾸지뽕나무 뿌리로부터 분리한 5,7-Dihydroxychromone (DHC)의 Nrf2/ARE 기전 활성화를 통한 6-OHDA 로 유도한 뇌세포사멸 보호효과를 연구하고자 하였다. 6-OHDA 로 유도한 SH-SY5Y 뇌세포 사멸은 DHC 처리에 의해 농도의존적으로 감소하는 결과를 보였으며, 세포내 활성산소종 역시 DHC 처리에 의해 감소하는 결과를 확인하였다. 이에 DHC 의 뇌세포사멸 보호효과의 기전을 확인하고자, DHC 의 Nrf2 nuclear translocation 에 대해

연구하였고, DHC 처리에 의해 Nrf2 의 핵안으로 이동이 증가함을 확인하였다. 이어진 연구에 의해 핵안으로 이동한 Nrf2 가 ARE 와 binding 하는 것을 확인할 수 있었으며, 이로인해 phase 2 antioxidant enzyme 의 발현량이 증가하는 결과를 확인하였다. 이어진 실험에서 Nrf2 knock down 시킨 세포주에서 DHC 의 뇌세포사멸 보호효과는 현저히 감소되는 결과를 확인하였다. 즉, DHC 의 6-OHDA 로 유도한 뇌세포사멸의 보호효과가 Nrf2/ARE 기전을 통한 phase 2 antioxidant enzyme 의 활성화를 통한것임을 증명할 수 있었다. 최종적으로 Nrf2/ARE 기전의 활성화를 통한 퇴행성뇌질환 예방 및 치료제 선도물질로써 가능성을 제시할 수 있다.

두번째로, 꾸지뽕나무 열매로부터 분리한 Orobol 유도체 및 에탄올 추출물을 이용하여 6-OHDA 로 유도한 뇌세포 사멸 및 ubiquitin-proteasome system 에 대한 효과를 연구 하였다. 꾸지뽕나무 열매 50% 에탄올 추출물 및 orobol, 6-prenylorobol, 6,8-diprenylorobol 이 6-OHDA 로 유도한 SH-SY5Y 뇌세포사멸 보호효과가 가장 우수하였다. 또한, 50% 에탄올 추출물 및 orobol 유도체는 6-OHDA 로 유도한 proteasome dysfunction 을 효과적으로

보호하는 결과를 보였다. Proteasome 보호효과를 통해 파킨슨 질환의 주요 독성 단백질 중 하나인 a-synuclein, synphilin-1 의 제거를 효과적으로 유도하였다. 하지만 proteasome inhibitor 인 MG132 를 처리함에 따라 50% 에탄올 추출물 및 orobol 유도체의 세포사멸 보호효과 및 proteasome 보호효과가 현저히 저하되는 결과를 보였다. 즉, 꾸지뽕나무 열매 50% 에탄올 추출물 및 orobol 유도체는 ubiquituin-proteasome system 의 정상화를 통해 a-synuclein, synphilin-1 의 제거를 유도하고, apoptosis, 활성산소종 생성을 억제하며 뇌세포를 효과적으로 보호함을 증명할 수 있었다. 최종적으로 proteasome 보호효과를 통한 퇴행성 뇌질환 예방 및 치료제의 선도물질로써의 가능성을 제시할 수 있다.

마지막으로, 꾸지뽕나무로부터 분리한 유효물질이 deubiquitinating 효소에 미치는 영향을 연구 하였다. 꾸지뽕나무 뿌리로부터 분리된 TH3-125-4 (TH20)는 Parkin K.D. SH-SY5Y 세포주에서 CCCP 로 유도한 신경 세포 사멸을 보호하였다. TH20 은 deubiquitinating 효소로 알려진 USP30 의 활성을 효과적으로 억제하였으며, USP30 의 polyubiquitin 분해활성 역시 억제하는 효과를 보였다. 또한, TH20 은

USP30 의 단백질 발현을 감소시켰다. 연구 결과에 따르면 TH20 은 Parkin 매개 mitophagy 를 정상적으로 회복하여 유전형 파킨슨 병의 치료제 선도물질로써의 가능성을 보였다.

주요어: 꾸지뽕나무, 산화적 스트레스, 6-OHDA, 뇌세포사멸 보호, 5,7-Dihydroxychromone, Nrf2/ARE pathway, orobol 유도체, 프로테아좀 활성, ubiquitination, deubiquitinating 효소, PINK1, Parkin, mitophagy

학번: 2012-21566

First-Author publications

Journal of Functional Foods 29 (2017) 104–114

Contents lists available at ScienceDirect

Journal of Functional Foods

journal homepage: www.elsevier.com/locate/jff

Orobol derivatives and extracts from *Cudrania tricuspidata* fruits protect against 6-hydroxydomamine-induced neuronal cell death by enhancing proteasome activity and the ubiquitin/proteasome-dependent degradation of α-synuclein and synphilin-1

Dong-Woo Kim [a], Jaeyoung Kwon [b], Su Jin Sim [c], Dongho Lee [d,**], Woongchon Mar [a,*]

[a] Natural Products Research Institute, College of Pharmacy, Seoul National University, Seoul 08826, Republic of Korea
[b] Natural Constituents Research Center, Korea Institute of Science and Technology (KIST) Gangneung Institute, Gangneung 25451, Republic of Korea
[c] Forest Medicinal Resources Research Center, National Institute of Forest Science, Yeongju 36040, Republic of Korea
[d] Department of Biosystems and Biotechnology, Korea University, Seoul 02841, Republic of Korea

ARTICLE INFO

Article history:
Received 8 September 2016
Received in revised form 21 November 2016
Accepted 9 December 2016

Keywords:
Cudrania tricuspidata
Orobol derivatives
Proteasome activity
Polyubiquitination
Neuroprotection
6-OHDA

ABSTRACT

We investigated the neuroprotective effects of orobol derivatives and ethanol extracts from *Cudrania tricuspidata* fruits. Among the nine isolates from a 50% ethanol extract from *Cudrania tricuspidata* fruits (CTE50), orobol (OB), 6-prenylorobol (POB), and 6,8-diprenylorobol (DPOB) showed neuroprotective effects in 6-OHDA-induced SH-SY5Y cell death. In addition, CTE50 and the three orobol derivatives (OB, POB, and DPOB) attenuated the cleavage of caspase-3, caspase-9, and PARP and inhibited the excessive generation of ROS. Furthermore, it enhanced the 6-OHDA-induced dysfunction of proteasome activity and reduced the accumulation of ubiquitin conjugated-proteins and the polyubiquitination of α-synuclein and synphilin-1. The proteasome inhibitor MG132 blocked the neuroprotective effects and the enhanced proteasome activity produced by CTE50 and the three orobol derivatives. These results demonstrate that CTE50 and three orobol derivatives protect against 6-OHDA-induced neurotoxicity by enhancing the ubiquitin/proteasome-dependent degradation of α-synuclein and synphilin-1, suggesting that they might be possible candidates for the treatment of neurodegenerative diseases.

1. Introduction

Cudrania tricuspidata (Moraceae) is a subtropical tree that is widely distributed in Korea, China, and Japan. The fruits of *C. tricuspidata* are used in jams, juices, and a fermented alcoholic beverage with sugar, and they are commercially produced as food in Korea. In addition, the root, stem, leaf, and fruits of this plant have been reported to have anti-atherosclerotic, anti-inflammatory and antioxidant activities (Jeong et al., 2010; Lee et al., 2012; Park et al., 2006). Recent studies have demonstrated that the fruit of *C. tricuspidata* inhibited pancreatic lipase (Jeong et al., 2014), protected neuronal cells against oxidative stress-induced toxicity (Jeong et al., 2010), and inhibited IgE-mediated allergic and inflammatory responses (Lee, Kwon, Lee, & Mar, 2015). The compounds isolated from *C. tricuspidata* are primarily xanthones and flavones in addition to some alkaloids, lignins, coumarins, polysaccharides, and chromones (Fujimoto, Hano, & Nomura, 1984; Hano, Matsumoto, Shinohara, Sun, & Nomura, 1991; Hiep et al., 2015; Lee et al., 1996; Seo et al., 2001). The isoflavones from the fruits of *C. tricuspidata* have been reported to exert protective effects against 6-hydroxydopamine (6-OHDA)-induced neurotoxicity (Hiep et al., 2015) and to have inhibitory effects against IgE-mediated allergic and inflammatory responses (Lee et al., 2015). Orobol (OB), 6-prenylorobol (POB) and 6,8-diprenylorobol (DPOB) are prenylated isoflavones. It was reported that OB increases cisplatin sensitivity in human ovarian carcinoma (Shiotsuka & Isonishi, 2001) and that DPOB shows anti-estrogenic activity (Okamoto et al., 2006) and inhibits lipofuscin fluorophore-mediated photo oxidation (Uddin, Jeon, & Kim, 2011).

Abbreviations: 6-OHDA, 6-hydroxydomamine; PD, Parkinson's disease; PARP, poly (ADP-ribose) polymerase; ROS, reactive oxygen species; UPP, ubiquitin-proteasome pathway; UPS, ubiquitin-proteasome system; CTE50, 50% ethanol extract from *Cudrania tricuspidata* fruits; OB, orobol; POB, 6-prenylorobol; DPOB, 6,8-diprenylorobol.

* Corresponding author.
** Corresponding author.
E-mail addresses: dongholee@korea.ac.kr (D. Lee), mars@snu.ac.kr (W. Mar).

http://dx.doi.org/10.1016/j.jff.2016.12.017
1756-4646/

Parkinson's disease (PD) is characterized by severe motor deficits, cogwheel rigidity, bradykinesia, and the loss of dopaminergic neurons. The aetiology of PD has not been clearly identified; however, oxidative stress is thought to be a common factor that leads to cellular dysfunction and neurodegeneration. Reactive oxygen species (ROS) are mainly produced as a by-product of cellular metabolism and oxidative phosphorylation. Non-neutralized ROS produce oxidative stress in cellular organisms and lead to abnormal molecular activities (Bochkov et al., 2010). In particular, the pathological events that occur in PD have been suggested to be linked to protein oxidation caused by oxidative stress (Butterfield & Kanski, 2001), and excessive intracellular ROS induce apoptosis that is characterized by the cleavage of caspase-3, caspase-9 and poly ADP-ribose polymerase (PARP) (Klovekorn & Munch, 1998). The neurotoxin 6-OHDA destroys dopaminergic and noradrenergic neurons in the brain by inducing excessive ROS such as superoxide radicals, which leads to protein oxidation and neuronal cell death (Kanthasamy et al., 2010).

The proteasome plays a key role in the selective degradation of oxidized proteins via ubiquitin-mediated processes, and its role is essential for cellular protein maintenance (Jung & Grune, 2013; Tai & Schuman, 2008). The diversity in E3 ubiquitin ligases confers specificity in selecting substrate proteins, and ubiquitin-tagged proteins are targeted by the proteasome for selective ubiquitin-dependent protein degradation. The catalytic domain of the proteasome contains chymotrypsin, trypsin, and caspases type, and each type has a different role in protein degradation (Huang & Figueiredo-Pereira, 2010). In general, high levels of ubiquitinated proteins do not accumulate in normal cells because they are rapidly degraded by the ubiquitin-proteasome pathway (UPP). However, dysfunctions in the ubiquitination machinery or in the proteolytic activities of the proteasome are associated with multiple pathological conditions, such as excessive intracellular ROS, cellular stress, and diverse stress. These factors impair the normal states of the ubiquitin-proteasome system (UPS) and induce the accumulation of polyubiquitinated misfolded proteins and oxidized proteins, thus leading to dysfunction in the ubiquitin-proteasome system. Subsequently, this induces protein aggregation, further inhibits proteasome activity, generates additional cellular stress, and ultimately leads to cell death (Dahlmann, 2007). Recent research has suggested that oxidative stress-induced proteasome dysfunction might play a key role in neurodegenerative diseases and that rescuing the decrease in proteasome activity could be a new therapeutic strategy (Seo, Sonntag, Kim, Cattaneo, & Isacson, 2007). Additionally, dysfunction in proteasome activity was observed in the substantia nigra of PD patients, suggesting that the impairment of the UPS is involved in the formation of Lewy bodies and in dopaminergic neuronal cell death in PD (McNaught & Jenner, 2001). Lewy bodies are characteristic hallmarks of PD and are composed of primarily α-synuclein and synphilin-1 along with ubiquitin and other fibrils. α-synuclein, a small acidic protein composed of 140 amino acids, is abundant in the human brain; is also found in the heart, muscles, and other tissues; and is a naturally unfolded protein with the ability to self-aggregate. The aggregation process of α-synuclein results in potential cell damage, leading to dopaminergic neuronal loss in Parkinson's disease (Cookson, 2005). α-synuclein also associates with other protein partners in the cell, including a significant interaction with synphilin-1. It has been reported that synphilin-1 is a presynaptic protein that could be a modulator of UPS, and the overexpression of synphilin-1 promotes the formation of inclusions under conditions of proteasome inhibition. Additionally, synphilin-1 inhibits the degradation of α-synuclein by the proteasome, thus increasing its half-life (Alvarez-Castelao & Castano, 2011). Therefore, it is possible that the inhibition Lewy body-associated protein accumulation through the protection against proteasome dysfunction could be a key aspect of PD treatment.

In our previous reports, we investigated the neuroprotective effect of different extracts (0–100% ethanol ratio) containing isoflavones from *C. tricuspidata* fruits (Hiep et al., 2015). Here, nine isolates obtained from 50% ethanol extract from *C. tricuspidata* fruits (CTE50) were evaluated for their neuroprotective potential against 6-OHDA-induced cell death in SH-SY5Y human neuroblastoma cells. We focused on the potential effects on apoptosis, intracellular ROS generation, proteasome activities, polyubiquitination of Lewy body-associated α-synuclein and synthilin-1 against 6-OHDA-induced SH-SY5Y cells.

2. Materials and methods

2.1. Reagents

6-Hydroxydopamine (6-OHDA), and 2′,7′-dichlorfluorescein-diacetate (DCFH-DA) were purchased from Sigma-Aldrich (St. Louis, MO, USA). MG132 was purchased from Enzo Life Sciences (Farmingdale, NY, USA). Dulbecco's modified Eagle's medium (DMEM) and foetal bovine serum (FBS) were purchased from Hyclone™ Thermo Scientific (Wyman Street Waltham, MA, USA). Hybond®-Polyvinylidene difluoride (PVDF) membranes were purchased from Amersham Pharmacia Biotechnology Inc. (Piscataway, NJ, USA). PRO-PREP protein extraction solution and WEST-ZOL® ECL solution were purchased from iNtRON Biotech Inc. (Kyunggi, Korea). Antibodies against ubiquitin, α-synuclein, synphilin-1, β-actin, caspase-3, cleaved caspase-3, caspase-9, cleaved caspase-9, PARP, and A/G Plus-Agarose and secondary antibodies were purchased from Santa Cruz Biotechnology, Inc. (CA, USA)

2.2. Preparation of ethanol extracts from C. tricuspidata fruits

The fruits of *C. tricuspidata* were collected from the Korea Forest Research Institute, Southern Forest Research Center (Jinju, Korea). A voucher specimen (accession no. KH1-5-090904) was deposited at the Department of Biosystems and Biotechnology, Korea University (Seoul, Korea). The dry fruit of *C. tricuspidata* (3.4 kg) was ground into powder form and sifted through a 120-mesh sieve. The dry powder (7 g) was refluxed three times for 1 h each by means of a heating mantle with 250 mL of 0%, 30%, 50%, 70%, or 100% ethanol in round 500-mL flasks. The combined extracts were filtered and concentrated in vacuo to yield 2.85 g, 2.71 g, 2.57 g, 2.67 g, and 2.1 g, respectively.

2.3. Isolation and identification of compounds from CTE50

Nine isoflavones, namely, orobol (**1**, 0.0021%), 6-prenylorobol (**2**, 0.0100%), 6,8-diprenylorobol (**3**, 0.0015%), millewanins H and G (**4** and **5**, 0.0029 and 0.0045%), alpinumisoflavone (**6**, 0.0762%), 4′-*O*-methylalpinumisoflavone (**7**, 0.0046%), erysenegalensein E (**8**, 0.0181%), and 6,8-diprenylgenistein (**9**, 0.0055%), were isolated from the fruits of *C. tricuspidata*. The chemical structures were determined by interpretation of spectroscopic data, including MS and NMR spectra, as compared to the previously reported literature (supplementary data 1). The detailed isolation procedures are included in the supplementary materials and methods. The purity of each compound was more than 95%.

2.4. Ultra-Performance Liquid Chromatography (UPLC) analysis

The CTE50 was analysed using an Acquity UPLC system (Waters, Millford, MA, USA) with an Acquity UPLC BEH C18 column (1.7 μm, 2.1 × 150 mm i.d.). The mobile phase consisted of solvent A (0.05% formic acid in water) and solvent B (acetonitrile), which flowed at rate of 0.3 mL/min. The starting eluent was 40% B at 0 min, and the

proportion of B was increased linearly to 100% from 0 to 10 min, held constant at 100% for 11.5 min, and then returned to the initial condition over the course of 1.5 min to re-equilibrate the column. The sample injection volume was 4 μL for extract and 2 μL for compounds (CTE50: 3 mg/mL, OB, POB, and DPOB: 0.2 mg/mL). The column and sample managers were maintained at 35 and 15 °C, respectively, and the UV detection wavelength was monitored at 265 nm.

2.5. SH-SY5Y cell culture

The human neuroblastoma cell line SH-SY5Y (ATCC No. CRL-2266) was purchased from the American Type Culture Collection (Manassas, VA, USA) and cultured in DMEM supplemented with 10% heat-inactivated FBS and 1% penicillin/streptomycin at 37 °C in a humidified 5% CO_2 atmosphere. Test samples were dissolved in 10% DMSO, and the cells were treated within non-cytotoxic concentration ranges of test samples at a final concentration of 0.1% DMSO.

2.6. Measurement of cell viability

SH-SY5Y cells were plated at a density of 1×10^5 cells/200 μL/well in 96-well plates for 24 h, and the cells were simultaneously treated with 6-OHDA and test samples (0.16–20 μg/mL of 0–100% CTE; 0.2–25 μM of nine isolates) for 48 h. After treatment, cell viability was evaluated using the MTT assay as previously described (Koo et al., 2011). Briefly, the medium was removed, and the cells were incubated with fresh medium containing 0.5 mg/mL MTT for 4 h at 37 °C, after which the medium was gently removed. Formazan crystals were dissolved in 100 μL DMSO, and absorbance was measured at 540 nm using a microplate reader (SpectraMax M5, Molecular Devices, USA).

2.7. Measurement of intracellular ROS by flow cytometry

Intracellular ROS levels were measured by the 2′,7′-dichloro fluorescein diacetate (DCFH-DA) method as described previously (Kim et al., 2015). Briefly, SH-SY5Y cells were plated at a density of 1×10^6 cells/1 mL/well in 12-well plates for 24 h, simultaneously treated with 6-OHDA (75 μM) and test samples (0.16–20 μg/mL of 0–100% CTE, 0.2–25 μM of isolates) for 48 h, and washed three times with PBS. DCFH-DA (4 μM/mL in PBS) was then added, and afterwards, the cells were incubated for 30 min at 37 °C in the dark. The cells were then washed 3 times with PBS, and the fluorescence intensities of a total of 10,000 events were measured by the FL-1 channel of a flow cytometer (BD FACS Calibur™).

2.8. Measurement of proteasome activity in 6-OHDA-induced SH-SY5Y cells

Proteasome activity was determined using SH-SY5Y cells as previously described (Kim, Kwon, Lee, & Mar, 2015). Briefly, cells (1.0×10^5 cells/300 μL/well) were plated in 48-well plates for 24 h and then simultaneously treated with 6-OHDA (75 μM) and samples (0.16–20 μg/mL of CTE50, 0.2–25 μM of nine isolates) for 48 h. After washing twice with PBS, cells were lysed by freeze-thawing 3 times (between −70 °C and 37 °C, 5 min each) and scraped into PBS buffer. Supernatants were collected by centrifugation at 15,000 rpm (15 min, 4 °C), and the total protein concentration was determined by the Bradford method (Bradford, 1976). The proteolytic activity of the proteasomes was evaluated with a 20S proteasome activity kit (APT 280; Millipore, USA). In brief, supernatants (40 μg) were incubated for 2 h at 37 °C in the provided buffer with fluorophore-linked peptide substrates. Suc-LLVY-AMC (40 μM), Boc-LRR-AMC (40 μM), and Z-LLE-MCA (80 μM) were used as the substrates for chymotrypsin-, trypsin- and caspase-like protease activities, respectively. Reaction mixtures without cell lysates were used as negative controls, and aminomethylcoumarin (AMC) or methylcoumarylamide (MCA) fluorescence was measured at excitation/emission wavelengths of 380/460 and 380/440 nm, respectively, using a microplate reader (SpectraMax M5, Molecular Devices, USA).

2.9. Immunoprecipitation assay

Immunoprecipitation was performed as previously described with slight modifications (Chen et al., 2014). Briefly, SH-SY5Y cells were plated at a density of 2×10^6 cells/4 mL in 100-mm dishes for 24 h. The cells were then simultaneously treated with 6-OHDA (75 μM) and samples (0.8–20 μg/mL of CTE50, 1–25 μM of three orobol derivatives) for 48 h and washed three times with PBS. SH-SY5Y cells were homogenized and lysed in cold-lysis buffer (50 mM Tris, 1 mM PMSF, 150 mM NaCl, 50 mM NaF, 1% Nonidet P-40, 0.25% sodium deoxycholate, 10 mM sodium pyrophosphate) and centrifuged at 14,000g (10 min, 4 °C), and the supernatant was transferred to a new ep-tube and incubated with 2 μg of α-synuclein or synphilin-1 antibody overnight at 4 °C. The next day, A/G plus agarose beads were added and incubated overnight at 4 °C followed by 3 washes in cold-lysis buffer. The loading samples were adjusted to total volume of 30 μL with lysis buffer, and the immune-complexes were eluted at 95 °C on a heating block for 5 min, vortexed, and spun down by centrifugation at 15,000g for 10 min.

2.10. Western blot analysis

SH-SY5Y cells were plated at a density of 2×10^6 cells/4 mL in 60-mm dishes for 24 h. The cells were then simultaneously treated with 6-OHDA (75 μM) and samples (0.16–20 μg/mL of CTE50, 0.2–25 μM of three orobol derivatives) for 48 h, washed three times with PBS, and lysed with a PRO-PREP protein extraction solution at −20 °C for 20 min. After centrifugation at 13,000 rpm for 30 min, the supernatant was used as the total protein extract. Western blot analysis was accomplished as previously described (Ham et al., 2013). Briefly, protein extracts were separated by electrophoresis on a SDS-PAGE gel and then transferred to PVDF membranes. Then, the PVDF membranes were incubated overnight at 4 °C with primary antibodies followed by a 1-h incubation at RT with the secondary antibody. The blots were developed using WEST-Queen® ECL solution and analysed using LAS4000 (GE Healthcare, UK)

2.11. Statistical analysis

All experimental data are expressed as the mean ± standard deviation. Statistical significance between multiple groups was determined by one-way ANOVA (PRISM Graph Pad, San Diego, CA, USA). When the ANOVA showed a significant difference, Bonferroni's multiple comparison *post hoc* tests were conducted. A P value less than 0.05 was considered statistically significant.

3. Results

3.1. Protective effects against 6-OHDA-induced neuronal cell death in SH-SY5Y cells

Ethanol is often used to extract bioactive compounds from plant materials, and the bioactivity of plant extracts depends on the ratio of water to ethanol used in the extraction process (Ganora, 2009). We evaluated the neuroprotective effects within non-cytotoxic

Table 1
Inhibitory effects of ethanol extracts and isolates from the fruits of *C. tricuspidata* against 6-OHDA-induced cell death and ROS generation in SH-SY5Y cells.

Extract/Compound	Neuroprotective effect against 6-OHDA-induced cell death (EC_{50} value)	Inhibitory effect against 6-OHDA-induced ROS generation (IC_{50} value)
0% ethanol extract of *C. tricuspidata* fruit	>20 μg/mL	>20 μg/mL
30% ethanol extract of *C. tricuspidata* fruit	5.4 ± 0.8 μg/mL	10.2 ± 1.2 μg/mL
50% ethanol extract of *C. tricuspidata* fruit	3.3 ± 0.3 μg/mL	6.7 ± 0.7 μg/mL
70% ethanol extract of *C. tricuspidata* fruit	7.8 ± 0.9 μg/mL	14.2 ± 1.1 μg/mL
100% ethanol extract of *C. tricuspidata* fruit	>20 μg/mL	>20 μg/mL
(**1**) orobol	6.4 ± 0.5 μM	7.2 ± 0.6 μM
(**2**) 6-prenylorobol	4.5 ± 0.3 μM	5.9 ± 0.4 μM
(**3**) 6,8-diprenylorobol	10.1 ± 0.8 μM	17.3 ± 1.0 μM
(**4**) millewanin H	15.2 ± 1.3 μM	19.2 ± 1.5 μM
(**5**) millewanin G	18.5 ± 2.1 μM	22.4 ± 2.4 μM
(**6**) alpinumisoflavone	>25 μM	>25 μM
(**7**) 4′-O-methylalpinumisoflavone	>25 μM	>25 μM
(**8**) erysenegalensein E	>25 μM	>25 μM
(**9**) 6,8-diprenylgenistein	>25 μM	>25 μM

The EC_{50} & IC_{50} values were determined in a semi-logarithmic graph with 4 different concentrations. The values are presented as the mean ± standard deviation of three independent experiments.

concentration ranges from different CTE extracts (0%, 30%, 50%, 70%, and 100% ethanol) and nine isolates. As shown in Table 1, CTE50 showed the most potent protective effects with an EC_{50} value of 3.3 μg/mL. The constituents of CTE50 were identified using UPLC, and nine isolates were obtained (Fig. 1). Among the nine isolates, three orobol derivatives (OB, POB, and DPOB) significantly attenuated 6-OHDA-induced neurotoxicity with EC_{50} values of 6.4 μM, 4.5 μM, and 10.1 μM, respectively (Table. 1). As shown in Fig. S1, 6-OHDA-induced neuronal cell death was observed by the morphology of cells: 6-OHDA resulted in cellular morphological changes including cell shrinkage and rounding. However, treatment with CTE50 (20 μg/mL) or the three orobol derivatives (25 μM) ameliorated the 6-OHDA-induced morphological changes to almost normal levels. As shown in Fig. 2, the 6-OHDA-induced group showed a significant decrease in cell viability compared to the vehicle-treated group. However, CTE50 (0.16–20 μg/mL) or the three orobol derivatives (0.2–25 μM) protected 6-OHDA-induced neuronal cell death in a concentration-dependent manner. Additionally, we examined the comparison of neuroprotective effect of CTE50 and three orobol derivatives against 6-OHDA-induced neurotoxicity by pre-, co-, and post treatment. Among three groups, co-treatment group exerted potent neuroprotective effects (Fig. S5).

3.2. Inhibition of 6-OHDA-induced intracellular ROS generation

Excessive intracellular ROS induce cellular stress and neuronal cell death, and it has been reported that ROS play important roles in the pathogenesis of neurodegenerative diseases. As shown in Table 1, CTE50 showed the most potent inhibition of 6-OHDA-induced ROS generation with an IC_{50} value of 6.7 μg/mL. Among the nine compounds derived from CTE50, the three orobol derivatives showed a significant inhibitory effect against 6-OHDA-induced intracellular ROS generation with IC_{50} values of 7.2 μM (OB), 5.9 μM (POB), and 17.3 μM (DPOB). As shown in Figs. 2, 6-OHDA-treated cells showed strong DCF fluorescence intensities compared to vehicle-treated cells. The amount of intracellular ROS was decreased in a concentration-dependent manner when cells were treated with CTE50 (0.8–20 μg/mL) or the three orobol derivatives (1–25 μM).

3.3. Neuroprotective effects against 6-OHDA-induced apoptosis

It has been reported that 6-OHDA induces ROS-dependent apoptosis, which is characterized by the cleavage of caspase-9, caspase-3 and PARP. Excessive ROS accumulation results in the activation of the caspases (caspase-9 and caspase-3), and activated caspase-3 cleaves the DNA repair protein PARP; cleaved, activated PARP is final apoptotic marker. To investigate the inhibitory effects of CTE50 and three orobol derivatives on the levels of cleaved caspase-9, caspase-3, and PARP protein, we performed a western blot assay. As shown in Fig. 3, the cleavage levels of caspase-9, caspase-3, and PARP were increased when the SH-SY5Y cells were exposed to 6-OHDA. However, CTE50 (0.16–20 μg/mL) or the three orobol derivatives (0.2–25 μM) inhibited the cleavage of caspase-9, caspase-3, and PARP protein in a concentration-dependent manner in 6-OHDA-induced SH-SY5Y cells.

3.4. Protective effects against 6-OHDA-induced dysfunction of proteasome activity

Proteasome function is essential for cellular physiology and protein degradation. To evaluate the effects of CTE50 and the nine isolates against the dysfunction of proteasome activity induced by 6-OHDA in SH-SY5Y cells, we measured the activities of chymotrypsin-, trypsin- and caspase-like proteases. As shown in Table 2 and Fig. S3A, 6-OHDA significantly inhibited all three different types of proteasome activities; however, CTE50 most potently attenuated the 6-OHDA-induced dysfunction of proteasome activities from extracts (0–100%) with an EC_{50} value of 1.2 μg/mL (chymotrypsin-like), 1.5 μg/mL (trypsin-like), and 6.7 μg/mL (caspase-like). The three orobol derivatives at the concentration of 25 μM prominently protected against 6-OHDA-induced dysfunction of the proteasome and almost restored the activities to normal levels. (Fig. S3B–D).

3.5. Inhibition of 6-OHDA-induced ubiquitin-conjugated proteins

Proteasome dysfunction causes a reduction in the degradation of misfolded proteins, consequently resulting in the accumulation of polyubiquitinated proteins. To investigate the inhibitory effects of CTE50 and the three orobol derivatives against 6-OHDA-induced ubiquitin conjugated-protein formation, we performed western blot analysis. As shown in Figs. 3, 6-OHDA increased the levels of high molecular ubiquitin-conjugated proteins. When cells were treated with different concentrations of CTE50 (0.16–20 μg/mL) (Fig. 4A) or the three orobol derivatives (0.2–25 μM) (Fig. 4B–D), the levels of ubiquitin-conjugated proteins were decreased to normal in a concentration-dependent manner. CTE50 (20 μg/mL) and

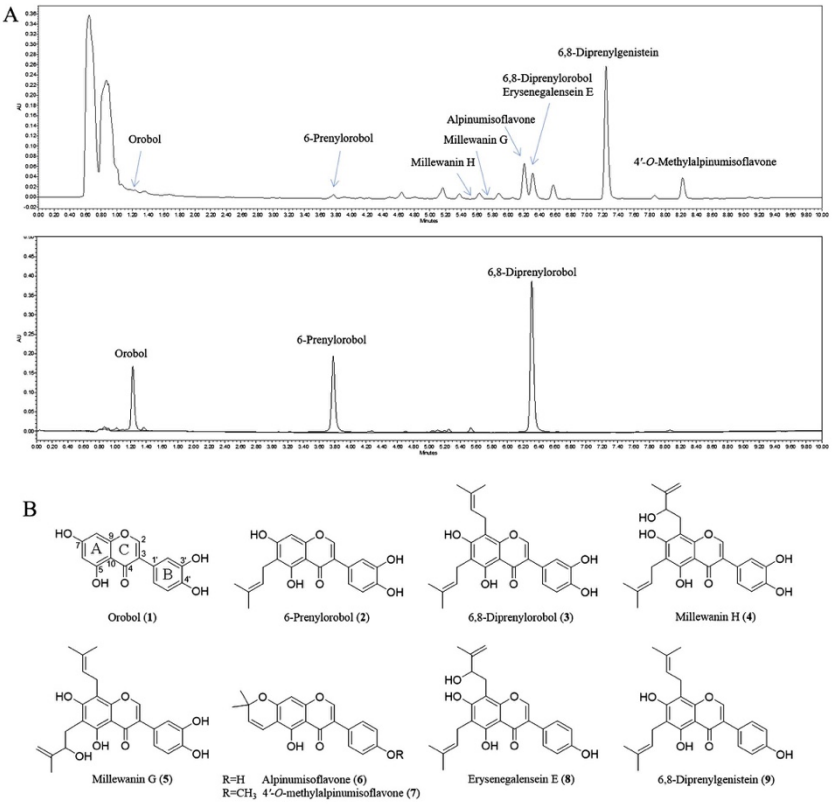

Fig. 1. UPLC chromatograms and structures of isolates from CTE50. (A) UPLC chromatogram of CTE50 and isolates from CTE50. Nine compounds were isolated from CTE50. Among nine isolates, orobol, 6-prenylorobol, and 6,8-diprenylorobol were selected for further study. The selected three orobol derivatives were confirmed the elution time for identification (B) Chemical structures of the isolates. The isolated compounds are orobol (**1**), 6-prenylorobol (**2**), 6,8-diprenylorobol (**3**), millewanin H (**4**), millewanin G (**5**), alpinumisoflavone (**6**), 4′-O-methylalpinumisoflavone (**7**), erysenegalensein E (**8**), and 6,8-diprenylgenistein (**9**).

the three orobol derivatives (25 μM) restored the ubiquitin-conjugated proteins to almost normal levels.

3.6. Inhibition of 6-OHDA-induced poly-ubiquitination of α-synuclein, and synphilin-1

Physiologically, polyubiquitinated proteins are normally rapidly degraded by the proteasome. However, dysfunction in proteasome activity increases the polyubiquitination of α-synuclein and synphilin-1, inducing neurotoxicity. As shown in Figs. 5, 6-OHDA increased the polyubiquitination of α-synuclein. When the cells were treated with different concentrations of CTE50 (0.8–20 μg/mL) or the three orobol derivatives (1–25 μM), the polyubiquitination of α-synuclein was restored to almost normal levels in a concentration-dependent manner (Fig. 5A–D). Additionally, as shown in Figs. 5, 6-OHDA increased the polyubiquitination of synphilin-1; however, CTE50 (0.8–20 μg/mL) and the three orobol derivatives (1–25 μM) reduced the polyubiquitinated synphilin-1 to almost normal levels in a concentration-dependent manner (Fig. 5E–H).

3.7. A proteasome inhibitor (MG-132) diminished the protective effects of CTE50 and the three orobol derivatives against 6-OHDA-induced neuronal cell death and proteasome dysfunction

It has been reported that proteasome inhibition induces dopaminergic neuronal cell degeneration and apoptosis (Park, Jun do, Han, Woo, & Kim, 2011). In contrast, proteasome activation

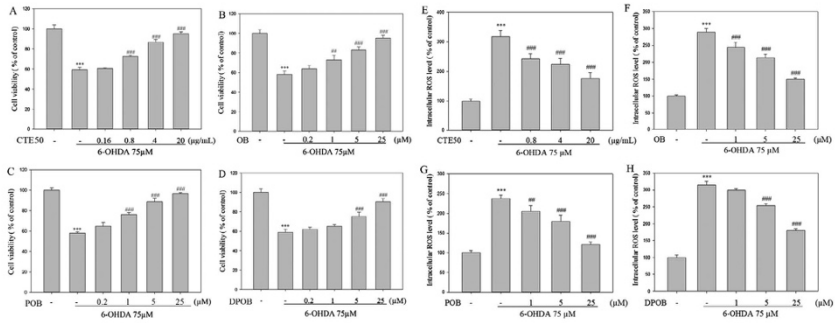

Fig. 2. Inhibitory effects of CTE50 and three orobol derivatives (OB, POB, and DPOB) against 6-OHDA-induced neurotoxicity and ROS generation. (A–D) Cells were cultured in 96-well plate for 24 h, and CTE50 or orobol derivatives were simultaneously treated with 6-OHDA (75 μM) for 48 h. Cell viability were measured by MTT reduction assay. (E–H) Cells were cultured in 12-well plate for 24 h, and CTE50 or three orobol derivatives were simultaneously treated with 6-OHDA (75 μM) for 48 h. The relative fluorescence intensities of total 10,000 events by FACs analysis were quantified. Data represent the mean ± SD of three independent experiments. (*** $p < 0.001$ versus control group, ## $p < 0.01$ and ### $p < 0.001$ versus 6-OHDA-induced group.)

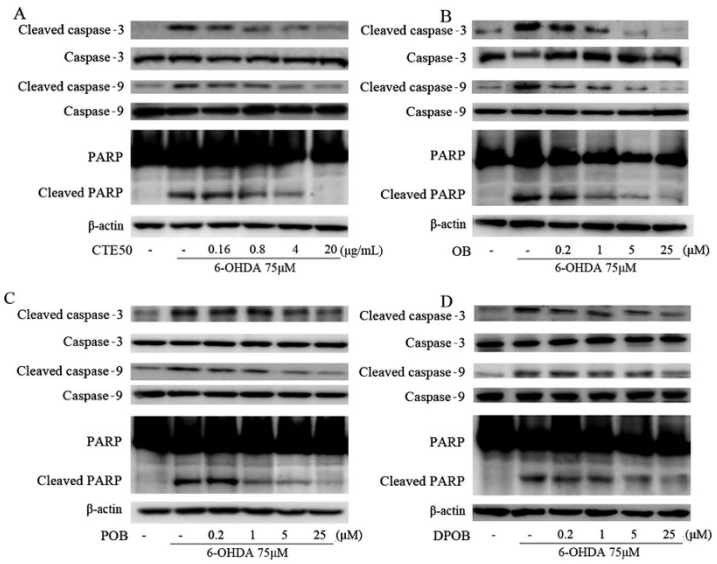

Fig. 3. Inhibitory effects of CTE50 and three orobol derivatives against 6-OHDA-induced apoptotic markers. Cells were simultaneously treated with 6-OHDA (75 μM) and (A) CTE50 or (B – D) three orobol derivatives for 48 h. The levels of cleaved caspase-9, caspase-3 and PARP were assessed by western blot; β-actin was used as a housekeeping protein. Representative data from three independent experiments are shown.

enhances survival in a neuronal model of neurodegenerative disease (Seo et al., 2007). To investigate whether the neuroprotective effects of CTE50 and the three orobol derivatives are due to the amelioration of proteasomal dysfunction, MG132, a proteasome inhibitor, was co-applied with the samples. As shown in Fig. 6A, CTE50 (20 μg/mL) and three orobol derivatives (25 μM) protected against 6-OHDA-induced neuronal cell death; however, co-treatment with MG132 (1 μM, non-cytotoxic concentration)

Table 2
The protective effects of ethanol extracts and isolates from the fruits of *C. tricuspidata* against 6-OHDA-induced proteasome dysfunction in SH-SY5Y cells.

Extract/Compound	Protective effect against 6-OHDA-induced dysfunction of proteasome activities		
	Chymotrypsin-like (EC_{50} value)	Trypsin-like (EC_{50} value)	Caspase-like (EC_{50} value)
0% ethanol extract of *C. tricuspidata* fruit	>20 μg/mL	>20 μg/mL	>20 μg/mL
30% ethanol extract of *C. tricuspidata* fruit	5.4 ± 0.4 μg/mL	9.5 ± 0.6 μg/mL	18.5 ± 1.5 μg/mL
50% ethanol extract of *C. tricuspidata* fruit	1.2 ± 0.3 μg/mL	1.5 ± 0.4 μg/mL	6.7 ± 0.8 μg/mL
70% ethanol extract of *C. tricuspidata* fruit	7.8 ± 0.7 μg/mL	13.2 ± 1.2 μg/mL	>20 μg/mL
100% ethanol extract of *C. tricuspidata* fruit	>20 μg/mL	>20 μg/mL	>20 μg/mL
(**1**) orobol	7.4 ± 0.3 μM	3.7 ± 0.3 μM	2.9 ± 0.2 μM
(**2**) 6-prenylorobol	6.8 ± 0.7 μM	3.9 ± 0.4 μM	1.3 ± 0.2 μM
(**3**) 6,8-diprenylorobol	7.9 ± 0.4 μM	4.2 ± 0.4 μM	1.8 ± 0.1 μM
(**4**) millewanin H	22.1 ± 2.0 μM	24.4 ± 2.1 μM	6.8 ± 0.4 μM
(**5**) millewanin G	24.4 ± 1.5 μM	5.9 ± 0.3 μM	1.2 ± 0.3 μM
(**6**) alpinumisoflavone	>25 μM	>25 μM	>25 μM
(**7**) 4′-O-methylalpinumisoflavone	>25 μM	>25 μM	>25 μM
(**8**) erysenegalensein E	>25 μM	>25 μM	>25 μM
(**9**) 6,8-diprenylgenistein	>25 μM	>25 μM	>25 μM

The EC_{50} values were determined in a semi-logarithmic graph with 4 different concentrations. The values are presented as the mean ± standard deviation of three independent experiments.

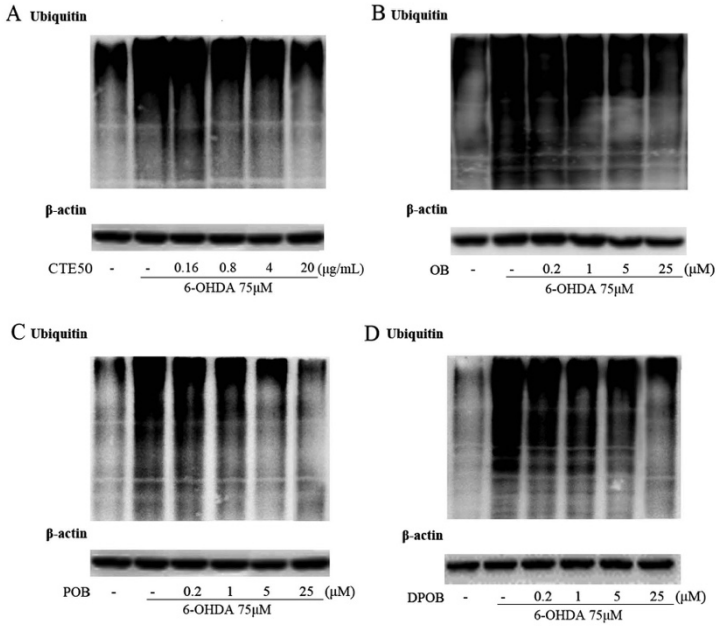

Fig. 4. Inhibitory effects of CTE50 and three orobol derivatives against 6-OHDA-induced ubiquitin-conjugated proteins. Cells were simultaneously treated with 6-OHDA (75 μM) and (A) CTE50 or (B–D) three orobol derivatives for 48 h. The levels of ubiquitin-conjugated proteins were determined by western blot; β-actin was used as a housekeeping protein. Representative data from three independent experiments are shown.

significantly blocked the protective effects of CTE50 and the three orobol derivatives against 6-OHDA-induced cell death. Additionally, MG132 (1 μM) blocked the recovery effects of CTE50 and the three orobol derivatives against 6-OHDA-induced proteasome dysfunction (Fig. 6B).

4. Discussion

As the world's population is rapidly ageing, the number of patients suffering from PD is increasing significantly. Although the cause of PD has not been definitively verified, recent research

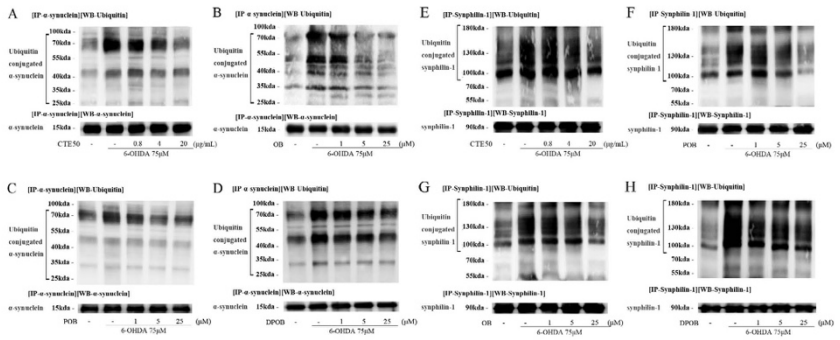

Fig. 5. Inhibitory effects of CTE50 and three orobol derivatives against 6-OHDA-induced polyubiquitination of α-synuclein and synphilin-1. Cells were simultaneously treated with 6-OHDA (75 μM) and (A, E) CTE50 or (B–D, F–H) three orobol derivatives for 48 h. The polyubiquitination of α-synuclein and synphilin-1 was determined by immunoprecipitation and western blot analysis. Representative data from three independent experiments are shown.

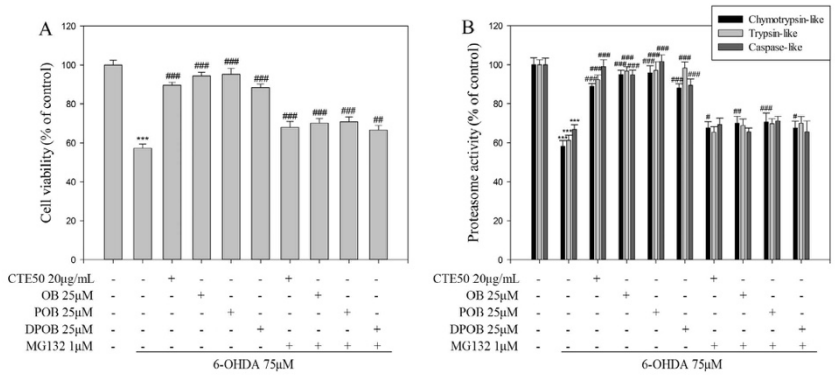

Fig. 6. Inhibitory effects of MG132 on the protective effects of CTE50 and three orobol derivatives against 6-OHDA-induced neuronal cell death and proteasome dysfunction. (A) The protective effects of CTE50 and three orobol derivatives 6-OHDA-induced neuronal cell death were blocked by MG132. Cell viability was measured by the MTT reduction assay. (B) The protective effects of CTE50 and three orobol derivatives against 6-OHDA-induced proteasome dysfunction were blocked by MG132. Three types of proteasome activity were measured using a multi-plate reader with fluorophore-linked peptide substrates. Data represent the mean ± SD of three independent experiments. (*** $p < 0.001$ versus control group, # $p < 0.05$, ## $p < 0.01$, and ### $p < 0.001$ versus 6-OHDA-induced group.)

findings have suggested that oxidative stress and the impairment of the proteasome are major events in its pathogenesis (Ciechanover & Kwon, 2015). Oxidative stress has been implicated in ageing and neurodegenerative diseases such as PD. Oxidative stress induces the oxidation and aggregation of proteins in the brain (Butterfield & Kanski, 2001). In addition, excessive oxidative stress advances cellular apoptosis through the accumulation of oxidized proteins (Klovekorn & Munch, 1998). Many studies have reported that protein homeostasis is essential for cellular physiology and that the proteasome is responsible for selectively degrading targets including short-lived, damaged or misfolded protein, which comprise approximately 80% of all intracellular proteins. Hence, considerable interest has been paid to the importance of the role of the proteasome. The ubiquitination process is activated by ubiquitin-activating enzymes (E1), ubiquitin-conjugating enzymes (E2), and ubiquitin-transferring enzymes (E3). Through a sequential enzymatic reaction, proteins are polyubiquitinated by E3 ligase. The polyubiquitin chain is recognized by the regulatory domain of the proteasome, in which the target protein is degraded by the catalytic core domain (Amm, Sommer, & Wolf, 2014). Under normal conditions, polyubiquitinated proteins are rapidly degraded and do not accumulate. The accumulation of polyubiquitinated proteins is observed when excessive intracellular ROS, cellular stress, and diverse stress impair proteasome function (Elkon, Melamed, & Offen, 2004), and the accumulation of polyubiquitinated proteins induces neurotoxicity and neurodegeneration. Thus, the restoration of proteasome activity through the down-regulation of intracellular ROS is one of the primary

mechanisms regulating ubiquitin-conjugated proteins, Lewy body-associated α-synuclein, and synphilin-1 proteins and the protection against neuronal cell death.

In the present study, 6-OHDA-induced ROS generation decreased in a concentration-dependent manner when cells were treated with different concentrations of CTE50 or the three orobol derivatives, and these compounds significantly elicited their neuroprotective effects against 6-OHDA-induced cell death and inhibited 6-OHDA-induced changes in cell morphology including shrinkage and rounding. In addition, we evaluated the inhibitory effects of CTE50 and the three orobol derivatives on the levels of cleaved caspase-9, caspase-3 and PARP, which are apoptosis signal factors; 6-OHDA treatment increased the levels of cleaved caspase-9, caspase-3 and PARP protein; however, these increases were inhibited by co-treatment with CTE50 and the three orobol derivatives. A previous study demonstrated that the inhibitory effect of (−)-epigallocatechin-3-gallate (EGCG) on ROS generation led to a suppression of apoptosis (Ning et al., 2016). In our results, the inhibitory effects of CTE50 and three orobol derivatives on ROS generation are also concomitant with the protection against neuronal cell death and the activation of apoptosis signalling markers. Based on the neuroprotective effects of three orobol derivatives, we evaluated structure-bioactivity relationship (SAR). The compounds with two hydroxy groups at C-3′ and C-4′ in B-ring of flavonoid (**1–5**) exhibited neuroprotective effects, whereas the others with one hydroxy group at C-4′ (**6–9**) did not. This suggested that the hydroxy group in the B-ring of flavonoid influences neuroprotective effects. The neuroprotective effect of preny groups is not clear from 9 isolates to evaluate SAR. Therefore, further study will be necessary to evaluate SAR with prenylated flavonoids on neuroprotective activity.

A recent study emphasized the role of the proteasome in neurodegenerative disease and showed that proteasome inhibition induced neurotoxicity via the accumulation of polyubiquitinated proteins and protein aggregation (Canu et al., 2000). As neuronal cells are vulnerable to the accumulation of polyubiquitinated proteins, several neurodegenerative diseases are related to the neurotoxicity resulting from protein accumulation. It has been shown that proteasome activity can gradually decrease with ageing and environmental stress, among other reasons, which results in a reduced ability to degrade misfolded proteins, contributing to the development of pathological protein aggregates (Ciechanover & Kwon, 2015). In cellular models, proteasome inhibition induced apoptosis and neuronal cell degeneration (Park et al., 2011; Sun et al., 2006), whereas proteasome activation enhanced neuronal cell survival (Seo et al., 2007). Thus, the protection against proteasome dysfunction could be a possible therapeutic strategy for neuroprotection. To investigate the mechanism underlying the protective effects of CTE50 and the three orobol derivatives against 6-OHDA-induced neuronal cell death, chymotrypsin-, trypsin-, and caspase-like proteasome activities were measured in SH-SY5Y cells. Our results showed that 6-OHDA significantly inhibited all three types of proteasome activities due to excessive ROS generation, and these results correlate with previously reported studies (Elkon et al., 2004). CTE50 and the three orobol derivatives at concentration of 20 μg/mL and 25 μM, respectively, attenuated 6-OHDA-induced dysfunction of the proteasome and nearly restored proteasome activities to normal levels. Additionally, we measured the levels of ubiquitin-conjugated proteins and found an increase following 6-OHDA treatment. However, CTE50 (20 μg/mL) and the three orobol derivatives (25 μM) attenuated the 6-OHDA-induced increase in ubiquitin-conjugated protein levels to almost normal. These results suggested that 6-OHDA-induced proteasome dysfunction triggers the accumulation of ubiquitin-conjugated proteins, leading to neuronal cell death; however, CTE50 and the three orobol derivatives prevented the dysfunction of ubiquitin proteasome system (UPS) and protected against neuronal cell death. The impairment of UPS is involved in the formation of Lewy bodies, which is a characteristic hallmark of PD. Lewy bodies are composed of abnormal filamentous aggregates containing α-synuclein, and synphilin-1 has been found to colocalize with α-synuclein in Lewy bodies. It has been demonstrated that the overexpression of α-synuclein in *Drosophila* and *C. elegans* induced neuronal cell loss (Kontopoulos, Parvin, & Feany, 2006; Pesah et al., 2005). It has also been reported that α-synuclein filaments and oligomers themselves inhibited proteasome activities (Lindersson et al., 2004). Synphilin-1 has been reported to enhance the aggregation and neurotoxicity of α-synuclein (Buttner et al., 2010) and to promote inclusion formation under conditions of proteasome inhibition. Additionally, it has been reported that synphilin-1 inhibits the degradation of α-synuclein by the proteasome and thus increases the half-life of α-synuclein (Alvarez-Castelao & Castano, 2011). Therefore, it has been suggested that the regulation of α-synuclein and synphilin-1 through UPS is important for neuroprotection (Sidhu, Wersinger, Moussa, & Vernier, 2004). It was also previously reported that a relationship exists between proteasome dysfunction and neuronal cell death. Proteasome inhibition triggers a dramatic activation of the pro-apoptotic caspase-3,-9, PARP and DNA fragment (Sun et al., 2006; Yuan, Chapman, & Reynolds, 2008). The proteasome inhibitor MG132 induces dopaminergic neuronal cell degeneration and apoptosis (Park et al., 2011), and bortezomib, a proteasome inhibitor, induces caspase-dependent apoptosis. In contrast, a proteasome activator enhances the survival of neuronal cells (Seo et al., 2007), and betulinic acid and demethylsuberosin, reported to be proteasome activators, showed neuroprotective effects (Eksioglu-Demiralp et al., 2010; Kim, Kwon et al., 2015). In our results, 6-OHDA-induced proteasome dysfunction resulted in the polyubiquitination of α-synuclein and synphilin-1 protein. However, CTE50 and the three orobol derivatives reduced the levels of 6-OHDA-induced polyubiquitination of α-synuclein and synphilin-1 protein in addition to ameliorating the dysfunction of proteasome activities. Furthermore, treatment with MG132, a proteasome inhibitor, significantly reduced the protective effects of CTE50 and the three orobol derivatives against 6-OHDA-induced neuronal cell death and proteasome dysfunction, suggesting that their neuronal cell protective effects are partly due to the protection against proteasome dysfunction. In spite of the evidence for neuroprotection by orobol derivatives, there has been little research reported on the blood-brain barrier (BBB) permeability of orobol derivatives. However, some studies have demonstrated that isoflavones and several metabolites have been proven to transverse the BBB (Chandrasekharan & Aglin, 2013; Youdim et al., 2003). Therfore, BBB permeability of orobol and its derivatives should be studied to elucidate its potential for permeation across BBB in the further study.

In conclusion, this study demonstrated that CTE50 and three orobol derivatives protected against neuronal cell death and ROS generation, and attenuated proteasome dysfunction, the accumulation of ubiquitin-conjugated proteins, and the levels of polyubiquitinated α-synuclein and synphilin-1, the constituents of Lewy bodies. However, the neuroprotective effects of CTE50 and three orobol derivatives and the attenuation of proteasome dysfunction were significantly inhibited by MG132, suggesting their neuroprotective effects are partly due to the protection of the ubiquitin/proteasome-dependent degradation of α-synuclein and synphilin-1. Based on our results, we suggest that CTE50 and the three orobol derivatives might be promising candidates for the therapy of neurodegenerative diseases such as PD.

Conflict of interest

The authors have declared that there are no conflicts of interest.

Acknowledgements

This work was supported by the Basic Science Research Program through the National Research Foundation of Korea (NRF) (Grant No. NRF-2013R1A1A2008111) and the BK21 Plus Program through the National Research Foundation (NRF) funded by the Ministry of Education of Korea.

Appendix A. Supplementary material

Supplementary data associated with this article can be found, in the online version, at http://dx.doi.org/10.1016/j.jff.2016.12.017.

References

Alvarez-Castelao, B., & Castano, J. G. (2011). Synphilin-1 inhibits alpha-synuclein degradation by the proteasome. *Cellular and Molecular Life Sciences, 68*(15), 2643–2654. http://dx.doi.org/10.1007/s00018-010-0592-3.

Amm, I., Sommer, T., & Wolf, D. H. (2014). Protein quality control and elimination of protein waste: the role of the ubiquitin-proteasome system. *Biochimica et Biophysica Acta, 1843*(1), 182–196. http://dx.doi.org/10.1016/j.bbamcr.2013.06.031.

Bochkov, V. N., Oskolkova, O. V., Birukov, K. G., Levonen, A. L., Binder, C. J., & Stockl, J. (2010). Generation and biological activities of oxidized phospholipids. *Antioxidants & Redox Signaling, 12*(8), 1009–1059. http://dx.doi.org/10.1089/ars.2009.2597.

Bradford, M. M. (1976). A rapid and sensitive method for the quantitation of microgram quantities of protein utilizing the principle of protein-dye binding. *Analytical Biochemistry, 72*, 248–254.

Butterfield, D. A., & Kanski, J. (2001). Brain protein oxidation in age-related neurodegenerative disorders that are associated with aggregated proteins. *Mechanisms of Ageing and Development, 122*(9), 945–962.

Buttner, S., Delay, C., Franssens, V., Bammens, T., Ruli, D., Zaunschirm, S., ... Winderickx, J. (2010). Synphilin-1 enhances alpha-synuclein aggregation in yeast and contributes to cellular stress and cell death in a Sir2-dependent manner. *PLoS One, 5*(10), e13700. http://dx.doi.org/10.1371/journal.pone.0013700.

Canu, N., Barbato, C., Ciotti, M. T., Serafino, A., Dus, L., & Calissano, P. (2000). Proteasome involvement and accumulation of ubiquitinated proteins in cerebellar granule neurons undergoing apoptosis. *Journal of Neuroscience, 20*(2), 589–599.

Chandrasekharan, S., & Aglin, A. (2013). Pharmacokinetics of dietary isoflavones. *Journal of Steroids & Hormonal Science, 2014*.

Chen, S., Zhu, P., Guo, H. M., Solis, R. S., Wang, Y. Q., Ma, Y. N., ... Li, J. (2014). Alpha1 catalytic subunit of AMPK modulates contractile function of cardiomyocytes through phosphorylation of troponin I. *Life Sciences, 98*(2), 75–82. http://dx.doi.org/10.1016/j.lfs.2014.01.006.

Ciechanover, A., & Kwon, Y. T. (2015). Degradation of misfolded proteins in neurodegenerative diseases: therapeutic targets and strategies. *Experimental & Molecular Medicine, 47*, e147. http://dx.doi.org/10.1038/emm.2014.117.

Cookson, M. R. (2005). The biochemistry of Parkinson's disease». *Annual Review of Biochemistry, 74*, 29–52.

Dahlmann, B. (2007). Role of proteasomes in disease. *BMC Biochemistry, 8*(Suppl 1), S3. http://dx.doi.org/10.1186/1471-2091-8-S1-S3.

Eksioglu-Demiralp, E., Kardas, E. R., Ozgul, S., Yagci, T., Bilgin, H., Sehirli, O., ... Sener, G. (2010). Betulinic acid protects against ischemia/reperfusion-induced renal damage and inhibits leukocyte apoptosis. *Phytotherapy Research, 24*(3), 325–332. http://dx.doi.org/10.1002/ptr.2929.

Elkon, H., Melamed, E., & Offen, D. (2004). Oxidative stress, induced by 6-hydroxydopamine, reduces proteasome activities in PC12 cells - Implications for the pathogenesis of Parkinson's disease. *Journal of Molecular Neuroscience, 24*(3), 387–400. http://dx.doi.org/10.1385/jmn:24:3:387.

Fujimoto, T., Hano, Y., & Nomura, T. (1984). Components of root bark of cudrania tricuspidata 11,2 structures of four new isoprenylated xanthones, cudraxanthones A, B, C and D. *Planta Medica, 50*(3), 218–221. http://dx.doi.org/10.1055/s-2007-969682.

Ganora, L. (2009). *Herbal constituents: Foundations of phytochemistry*. Louisville CO: Lisa Ganora.

Ham, A., Kim, D. W., Kim, K. H., Lee, S. J., Oh, K. B., Shin, J., & Mar, W. (2013). Reynosin protects against neuronal toxicity in dopamine-induced SH-SY5Y cells and 6-hydroxydopamine-lesioned rats as models of Parkinson's disease: Reciprocal up-regulation of E6-AP and down-regulation of alpha-synuclein. *Brain Research, 1524*, 54–61. http://dx.doi.org/10.1016/j.brainres.2013.05.036.

Hano, Y., Matsumoto, Y., Shinohara, K., Sun, J. Y., & Nomura, T. (1991). Structures of four new isoprenylated xanthones, cudraxanthones L, M, N, and O from cudrania tricuspidata1,2. *Planta Medica, 57*(2), 172–175. http://dx.doi.org/10.1055/s-2006-960059.

Hiep, N. T., Kwon, J., Kim, D. W., Hwang, B. Y., Lee, H. J., Mar, W., & Lee, D. (2015). Isoflavones with neuroprotective activities from fruits of *Cudrania tricuspidata*. *Phytochemistry, 111*, 141–148. http://dx.doi.org/10.1016/j.phytochem.2014.10.021.

Huang, Q., & Figueiredo-Pereira, M. E. (2010). Ubiquitin/proteasome pathway impairment in neurodegeneration: therapeutic implications. *Apoptosis, 15*(11), 1292–1311. http://dx.doi.org/10.1007/s10495-010-0466-z.

Jeong, C. H., Choi, G. N., Kim, J. H., Kwak, J. H., Jeong, H. R., Kim, D. O., & Heo, H. J. (2010). Protective effects of aqueous extract from cudrania tricuspidata on oxidative stress-induced neurotoxicity. *Food Science and Biotechnology, 19*(4), 1113–1117. http://dx.doi.org/10.1007/s10068-010-0158-z.

Jeong, J. Y., Jo, Y. H., Lee, K. Y., Do, S. G., Hwang, B. Y., & Lee, M. K. (2014). Optimization of pancreatic lipase inhibition by *Cudrania tricuspidata* fruits using response surface methodology. *Bioorganic & Medicinal Chemistry Letters, 24*(10), 2329–2333. http://dx.doi.org/10.1016/j.bmcl.2014.03.067.

Jung, T., & Grune, T. (2013). The proteasome and the degradation of oxidized proteins: Part I-structure of proteasomes. *Redox Biology, 1*, 178–182. http://dx.doi.org/10.1016/j.redox.2013.01.004.

Kanthasamy, A., Jin, H., Mehrotra, S., Mishra, R., Kanthasamy, A., & Rana, A. (2010). Novel cell death signaling pathways in neurotoxicity models of dopaminergic degeneration: Relevance to oxidative stress and neuroinflammation in Parkinson's disease. *Neurotoxicology, 31*(5), 555–561. http://dx.doi.org/10.1016/j.neuro.2009.12.003.

Kim, B.-H., Kwon, J., Lee, D., & Mar, W. (2015). Neuroprotective effect of demethylsuberosin, a proteasome activator, against MPP+-induced Cell death in human neuroblastoma SH-SY5Y cells. *Planta Medica Letters, 2*(01), e15–e18.

Kim, D.-W., Lee, K.-T., Kwon, J., Lee, H. J., Lee, D., & Mar, W. (2015). Neuroprotection against 6-OHDA-induced oxidative stress and apoptosis in SH-SY5Y cells by 5, 7-dihydroxychromone: Activation of the Nrf2/ARE pathway. *Life Sciences, 130*, 25–30.

Klovekorn, P., & Munch, J. (1998). Variable optical delay line with diffraction-limited autoalignment. *Applied Optics, 37*(10), 1903–1904.

Kontopoulos, E., Parvin, J. D., & Feany, M. B. (2006). Alpha-synuclein acts in the nucleus to inhibit histone acetylation and promote neurotoxicity. *Human Molecular Genetics, 15*(20), 3012–3023. http://dx.doi.org/10.1093/hmg/ddl243.

Koo, U., Nam, K. W., Ham, A., Lyu, D., Kim, B., Lee, S. J., ... Shin, J. (2011). Neuroprotective effects of 3alpha-acetoxyeudesma-1,4(15),11(13)-trien-12,6alpha-olide against dopamine-induced apoptosis in the human neuroblastoma SH-SY5Y cell line. *Neurochemical Research, 36*(11), 1991–2001. http://dx.doi.org/10.1007/s11064-011-0523-1.

Lee Ha, H., Lee, J. K., Seo, C. S., Lee, N. H., Jung, D. Y., ... Shin, H. K. (2012). The fruits of *Cudrania tricuspidata* suppress development of atopic dermatitis in NC/Nga mice. *Phytotherapy Research, 26*(4), 594–599. http://dx.doi.org/10.1002/ptr.3577.

Lee, I. K., Kim, C. J., Song, K. S., Kim, H. M., Koshino, H., Uramoto, M., & Yoo, I. D. (1996). Cytotoxic benzyl dihydroflavonols from *Cudrania tricuspidata*. *Phytochemistry, 41*(1), 213–216.

Lee, T., Kwon, J., Lee, D., & Mar, W. (2015). Effects of *Cudrania tricuspidata* fruit extract and its active compound, 5,7,3',4'-Tetrahydroxy-6,8-diprenylisoflavone, on the high-affinity IgE receptor-mediated activation of syk in mast cells. *Journal of Agricultural and Food Chemistry, 63*(22), 5459–5467. http://dx.doi.org/10.1021/acs.jafc.5b00903.

Lindersson, E., Beedholm, R., Hojrup, P., Moos, T., Gai, W., Hendil, K. B., & Jensen, P. H. (2004). Proteasomal inhibition by alpha-synuclein filaments and oligomers. *Journal of Biological Chemistry, 279*(13), 12924–12934. http://dx.doi.org/10.1074/jbc.M306390200.

McNaught, K. S., & Jenner, P. (2001). Proteasomal function is impaired in substantia nigra in Parkinson's disease. *Neuroscience Letters, 297*(3), 191–194.

Ning, W., Wang, S., Liu, D., Fu, L., Jin, R., & Xu, A. (2016). Potent effects of peracetylated (−)-epigallocatechin-3-gallate against hydrogen peroxide-induced damage in human epidermal melanocytes via attenuation of oxidative stress and apoptosis. *Clinical and Experimental Dermatology, 41*(6), 616–624. http://dx.doi.org/10.1111/ced.12855.

Okamoto, Y., Suzuki, A., Ueda, K., Ito, C., Itoigawa, M., Furukawa, H., ... Kojima, N. (2006). Anti-estrogenic activity of prenylated isoflavones from Millettia pachycarpa: Implications for pharmacophores and unique mechanisms. *Journal of Health Science, 52*(2), 186–191.

Park, H. S., Jun do, Y., Han, C. R., Woo, H. J., & Kim, Y. H. (2011). Proteasome inhibitor MG132-induced apoptosis via ER stress-mediated apoptotic pathway and its potentiation by protein tyrosine kinase p56lck in human Jurkat T cells. *Biochemical Pharmacology, 82*(9), 1110–1125. http://dx.doi.org/10.1016/j.bcp.2011.07.085.

Park, K. H., Park, Y. D., Han, J. M., Im, K. R., Lee, B. W., Jeong, I. Y., ... Lee, W. S. (2006). Anti-atherosclerotic and anti-inflammatory activities of catecholic xanthones and flavonoids isolated from *Cudrania tricuspidata*. *Bioorganic & Medicinal Chemistry Letters, 16*(21), 5580–5583. http://dx.doi.org/10.1016/j.bmcl.2006.08.032.

Pesah, Y., Burgess, H., Middlebrooks, B., Ronningen, K., Prosser, J., Tirunagaru, V., ... Mardon, G. (2005). Whole-mount analysis reveals normal numbers of dopaminergic neurons following misexpression of alpha-Synuclein in Drosophila. *Genesis, 41*(4), 154–159. http://dx.doi.org/10.1002/gene.20106.

Seo, W. G., Pae, H. O., Oh, G. S., Chai, K. Y., Yun, Y. G., Chung, H. T., ... Kwon, T. O. (2001). Ethyl acetate extract of the stem bark of Cudrania tricuspidata induces apoptosis in human leukemia HL-60 cells. *American Journal of Chinese Medicine, 29*(2), 313–320. http://dx.doi.org/10.1142/S0192415X01000332.

Seo, H., Sonntag, K. C., Kim, W., Cattaneo, E., & Isacson, O. (2007). Proteasome activator enhances survival of Huntington's disease neuronal model cells. *PLoS One, 2*(2), e238. http://dx.doi.org/10.1371/journal.pone.0000238.

Shiotsuka, S., & Isonishi, S. (2001). Differential sensitization by orobol in proliferating and quiescent human ovarian carcinoma cells. *International Journal of Oncology, 18*(2), 337–342.

Sidhu, A., Wersinger, C., Moussa, C. E. H., & Vernier, P. (2004). The role of α-synuclein in both neuroprotection and neurodegeneration. *Annals of the New York Academy of Sciences, 1035*(1), 250–270.

Sun, F., Anantharam, V., Zhang, D., Latchoumycandane, C., Kanthasamy, A., & Kanthasamy, A. G. (2006). Proteasome inhibitor MG-132 induces dopaminergic degeneration in cell culture and animal models. *Neurotoxicology, 27*(5), 807–815. http://dx.doi.org/10.1016/j.neuro.2006.06.006.

Tai, H. C., & Schuman, E. M. (2008). Ubiquitin, the proteasome and protein degradation in neuronal function and dysfunction. *Nature Reviews Neuroscience, 9*(11), 826–838. http://dx.doi.org/10.1038/nrn2499.

Uddin, G. M., Jeon, J. S., & Kim, C. Y. (2011). Isolation of prenylated isoflavonoids from *Cudrania tricuspidata* fruits that inhibit A2E photooxidation. *Natural Product Sciences, 17*(3), 206–211.

Youdim, K. A., Dobbie, M. S., Kuhnle, G., Proteggente, A. R., Abbott, N. J., & Rice-Evans, C. (2003). Interaction between flavonoids and the blood–brain barrier: in vitro studies. *Journal of Neurochemistry, 85*(1), 180–192.

Yuan, B. Z., Chapman, J. A., & Reynolds, S. H. (2008). Proteasome inhibitor MG132 induces apoptosis and inhibits invasion of human malignant pleural mesothelioma cells. *Transl Oncol, 1*(3), 129–140.

Life Sciences 130 (2015) 25–30

Contents lists available at ScienceDirect

Life Sciences

journal homepage: www.elsevier.com/locate/lifescie

Neuroprotection against 6-OHDA-induced oxidative stress and apoptosis in SH-SY5Y cells by 5,7-Dihydroxychromone: Activation of the Nrf2/ARE pathway ☆

Dong-Woo Kim [a], Kyoung-tae Lee [b], Jaeyoung Kwon [c], Hak Ju Lee [b], Dongho Lee [c,*], Woongchon Mar [a,**]

[a] Natural Products Research Institute, College of Pharmacy, Seoul National University, Seoul 151-742, Republic of Korea
[b] Division of Wood Chemistry & Microbiology, Department of Forest Products, Korea Forest Research Institute, Seoul 130-712, Republic of Korea
[c] Department of Biosystems and Biotechnology, Korea University, Seoul 136-713, Republic of Korea

ARTICLE INFO

Article history:
Received 31 October 2014
Received in revised form 3 February 2015
Accepted 28 February 2015
Available online 26 March 2015

Keywords:
5,7-Dihydroxychromone
Oxidative stress
6-OHDA
Nrf2/ARE pathway
Neuroprotection
Cudrania tricuspidata

ABSTRACT

Aims: The aim of this study was to prove the neuroprotective effect of 5,7-Dihydroxychromone (DHC) through the Nrf2/ARE signaling pathway. To elucidate the mechanism, we investigated whether 6-hydroxydopamine (6-OHDA)-induced neurotoxicity in SH-SY5Y cells could be attenuated by DHC via activating the Nrf2/ARE signal and whether DHC could down-regulate 6-OHDA-induced excessive ROS generation

Main methods: To evaluate the neuroprotective effect of DHC against 6-OHDA-induced apoptosis, FACS analysis was performed using PI staining. The inhibitory effect of DHC against 6-OHDA-induced ROS generation was evaluated by DCFH-DA staining assay. Additionally, translocation of Nrf2 to the nucleus and increased Nrf2/ARE binding activity, which subsequently resulted in the up-regulation of the Nrf2-dependent antioxidant gene expressions including HO-1, NQO1, and GCLc, were evaluated by Western blotting and EMSA.

Key findings: Pre-treatment of DHC, one of the constituents of *Cudrania tricuspidata*, significantly protects 6-OHDA-induced neuronal cell death and ROS generation. Also, DHC inhibited the expression of activated caspase-3 and caspase-9 and cleaved PARP in 6-OHDA-induced SH-SY5Y cells. DHC induced the translocation of Nrf2 to the nucleus and increased Nrf2/ARE binding activity which results in the up-regulation of the expression of Nrf2-dependent antioxidant genes, including HO-1, NQO1, and GCLc. The addition of Nrf2 siRNA abolished the neuroprotective effect of DHC against 6-OHDA-induced neurotoxicity and the expression of Nrf2-mediated antioxidant genes.

Significance: Activation of Nrf2/ARE signal by DHC exerted neuroprotective effects against 6-OHDA-induced oxidative stress and apoptosis. This finding will give an insight that activating Nrf2/ARE signal could be a new potential therapeutic strategy for neurodegenerative disease.

1. Introduction

The incidence of neurodegenerative diseases is increasing with the continuous growth of the elderly population. Although the causes of neurodegenerative diseases have not been clearly elucidated, recent studies have demonstrated that reactive oxygen species (ROS) might be one of the important factors in neurotoxicity that occurs in neurodegenerative diseases [3]. Increased ROS production causes impairment to cell organelles. Many studies have confirmed the benefits of antioxidants in reducing oxidative stress in neurons and protecting against neurodegenerative diseases [1].

In response to excessive ROS, the cellular expressions and bioactivity of numerous antioxidant enzymes are changed via initiating the upstream factor NF-E2-related factor 2 (Nrf2)/antioxidant response element (ARE) complex [12]. The Nrf2/ARE signal has an important effect on the induction of antioxidant gene expression, and it has been reported that the activation of Nrf2 is an important signal which can neutralize oxidative stress [24]. Under normal state, Nrf2 is localized in the cytoplasm and is subject to ubiquitination and proteasomal degradation. However, antioxidant agents block the elimination of Nrf2 from the cytosolic Nrf2 complex, which induces nuclear translocation of Nrf2 and subsequently makes the Nrf2/ARE complex mediate the induction of many antioxidant enzyme genes, such as heme oxygenase 1 (HO-1), NAD(P)H:quinone oxidoreductase (NQO1), and glutamate–cysteine ligase catalytic (GCLc) subunit [27]. Numerous research results reported that Nrf2 and Nrf2 dependent antioxidant genes are potent factors for developing the therapy of neurodegenerative diseases due to its ability to regulate the excessive oxidative stress and inflammation.

☆ English language in this manuscript was edited and revised by a professional editorial service, Elsevier Language Editing (Kidlington, UK. http://webshop.elsevier.com).

* Corresponding author. Tel.: +82 2 3290 3017; fax: +82 2 953 0737.
** Corresponding author. Tel.: +82 2 880 2473; fax: +82 2 888 9122.
E-mail address: dongholee@korea.ac.kr (D. Lee), mars@snu.ac.kr (W. Mar).

http://dx.doi.org/10.1016/j.lfs.2015.02.026
0024-3205/

A recent study demonstrated that the extracts of *Cudrania tricuspidata* protect neurons against oxidative stress-induced cytotoxicity [6] and have inhibitory effects on nitric oxide synthase (NOS) [7]. It was also reported that 5,7-Dihydroxychromone (DHC), from *C. tricuspidata*, has an antioxidant activity [19]. However, the neuroprotective effects of DHC and the related mechanisms of neuroprotection were poorly elucidated.

In this study, we demonstrated that the neuroprotective effects of DHC against 6-OHDA-induced neurotoxicity via the induction of the Nrf2/ARE-mediated signal.

2. Materials and methods

2.1. Materials

Propidium iodide (PI), 6-hydroxydopamine (6-OHDA), and 2′,7′-dichlorofluorescein-diacetate (DCFH-DA) were purchased from Sigma-Aldrich (St. Louis, MO, USA). Dulbecco's modified Eagle's medium (DMEM) and fetal bovine serum (FBS) were purchased from Gibco BRL (Rockville, MD, USA). Hybond-polyvinylidene difluoride (PVDF) membranes were purchased from Amersham Pharmacia Biotechnology Inc. (Piscataway, NJ, USA). Easy-Blue® total RNA extraction solution, PRO-PREP protein extraction solution and WEST-ZOL® ECL solution were purchased from iNtRON Biotech Inc. (Kyunggi, Korea). SuPrimeScript RT premix®, and SYBR HS Prime qPCR premix® were purchased from Genet Bio (Daejeon, Korea). Nrf2 siRNA, scrambled siRNA, Nrf2, HO-1, NQO1, GCLc, LaminB1, α-tubulin, β-actin, caspase-3, caspase-9, PARP, secondary antibody and FITC-conjugated secondary antibody were purchased from Santa Cruz Biotechnology, Inc. (Santa Cruz, CA, USA).

2.2. Preparation of DHC

C. tricuspidata was stored at the Korea Forest Research Institute at the Southern Forest Research Center (Jinju, Korea) in September 2008. A voucher specimen (accession number KH1-4-090814) was kept at the Department of Biosystems and Biotechnology at Korea University (Seoul, Korea). 5,7-Dihydroxychromone (DHC) was isolated from the roots of *C. tricuspidata* and the structure of DHC was determined by spectroscopic methods, and the purity was more than 98.5% [26]. DHC was dissolved in DMSO and diluted with PBS to obtain the proper concentration of DHC. The final concentration of DMSO was less than 0.1% and it didn't influence the performed assays.

2.3. SH-SY5Y cell culture

The human neuroblastoma cell line SH-SY5Y (ATCC No. CRL-2266) was purchased from the American Type Culture Collection (Manassas, VA, USA) and cultured in DMEM supplemented with 10% heat-inactivated FBS and 1% penicillin/streptomycin at 37 °C in a humidified 5% CO_2 atmosphere.

2.4. Measurement of cell viability

SH-SY5Y cells were seeded at a density of 2×10^5 cells/2 mL/well in 6-well plates for 24 h, and the cells were pre-treated with DHC (0.4, 2, or 10 μM) for 24 h followed by subsequent treatment with 6-OHDA (100 μM) for an additional 24 h. To evaluate the effect of Nrf2, cells were transfected with scrambled siRNA or Nrf2 siRNA for 48 h and its final concentration was 50 nM. After transfected cells were treated with DHC (10 μM) and 6-OHDA (100 μM), cell viability was determined using a propidium iodide (PI) staining and measured by flow cytometry (BD FACSCalibur™). Also, cell viability was evaluated using MTT assay as previously described [10].

2.5. Measurement of intracellular ROS by flow cytometry

ROS levels in cells were measured with the 2′,7′-dichlorofluorescein diacetate (DCFH-DA) method [15]. Briefly, the cells were washed with PBS, and then incubated with 4 μM of DCFH-DA for 30 min at 37 °C in the dark. The cells were then washed with PBS. The fluorescence intensities were measured by flow cytometry (BD FACSCalibur™).

2.6. Nuclear and cytosolic lysate preparations

The nuclear and cytosolic proteins were extracted with a commercial kit (Nuclear Extract Kit) according to the manufacturer's procedure (Active Motif, Carlsbad, CA). Briefly, the cells were incubated in hypotonic buffer on ice for 15 min, homogenized with detergent, and centrifuged for 30 s at 14,000 ×*g* in a microcentrifuge at 4 °C. The supernatant was used as the cytosolic proteins. The nuclear pellets were washed with cold PBS, extracted completely with lysis buffer for 30 min on ice and centrifuged for 10 min at 14,000 ×*g* in a microcentrifuge at 4 °C. The supernatant was used as the nuclear proteins.

2.7. Electrophoretic mobility shift assay (EMSA)

To determine the Nrf2–ARE binding activity, an electrophoretic mobility shift assay (EMSA) was accomplished as previously described [14]. Briefly, the nuclear proteins from the SH-SY5Y cells were reacted with ^{32}P-end-labeled 22-mer double-stranded oligonucleotide containing the Nrf2 sequence for 30 min at 37 °C. The DNA–protein complexes were electrophoresed and gels were dried. The binding signals were visualized by BAS-1500 (Fuji, Tokyo, Japan).

2.8. Nrf2 knockout via the transfection of small interfering RNA (siRNA)

The transfection with scrambled siRNA or Nrf2 siRNA were progressed at the final concentrations of 50 nM for 48 h by Lipofectamine 2000 (Invitrogen, Carlsbad, CA) prior to treatment with DHC (10 μM) and 6-OHDA (100 μM) as recommended by the manufacturer's guidelines.

2.9. Western blot analysis

The SH-SY5Y cells were collected, washed with PBS and lysed with a PRO-PREP protein extraction solution at − 20 °C for 20 min. After centrifugation at 13,000 ×*g* for 30 min, the supernatant was used as the total protein extracts. Western blot analysis was accomplished as in previously described method [5].

2.10. Immunocytochemical staining

The culture dish was coated with 0.2% gelatin at 37 °C for 30 min and dried at RT on a clean bench. The SH-SY5Y cells were plated at a density of 5×10^4 cells/200 μL/well in coated dishes for 24 h and incubated with DHC (0.4, 2, or 10 μM) for 6 h. After treatment with DHC, the cells were washed with 1× PBS/Tween-20 buffer (pH 7.4) (PBST) once. The cells were fixed with 4% paraformaldehyde for 30 min at room temperature (RT). After washing with PBST, the blocking steps were performed with 1% BSA in PBST. Next, the cells were incubated with the primary antibody at 4 °C overnight. The next day, the cells were washed with PBST 3 times and incubated with FITC-conjugated secondary antibody for 1 h at RT. After 1 h, the cells were washed with PBST 3 times, and DAPI staining was performed for 5 min at RT. Lastly, the PBST washing and mounting steps were conducted.

2.11. Statistical analysis

All experimental data are expressed as mean value ± standard deviation. Statistical significance between multiple groups was determined

by one-way ANOVA (PRISM Graph Pad, San Diego, CA, USA). When ANOVA had a significant difference, post-hoc Bonferroni multiple comparison tests was conducted. A p value less than 0.05 was regarded to be statistically significant.

3. Results

3.1. Protective effect of DHC against 6-OHDA-induced neuronal cell death

The protective effects of DHC (Fig. 1A) on SH-SY5Y cells were evaluated to determine the non-cytotoxic dose range (data not shown). The percentage of cell necrosis was evaluated with PI staining. As shown in Fig. 1C, the percentage of PI-stained dead cells induced by 6-OHDA increased to 44.5% compared to the vehicle-treated group (8.7%). In contrast, 6-OHDA-induced cell death was dose-dependently prevented by DHC treatments at concentrations of 0.4, 2 and 10 μM within the non-toxic dose range. DHC (10 μM) treatment elicited its neuroprotective effects against 6-OHDA by decreasing the percentage of PI-positive cells to 13.8%, whereas treatment with Nrf2 siRNA and DHC (10 μM) reduced the neuroprotective effect by increasing the percentage of PI-positive cells to 50.1%. Also, the neuroprotective effect of DHC was evaluated by MTT assay (Fig. 1B). The result of the MTT assay was correlated with the PI staining assay.

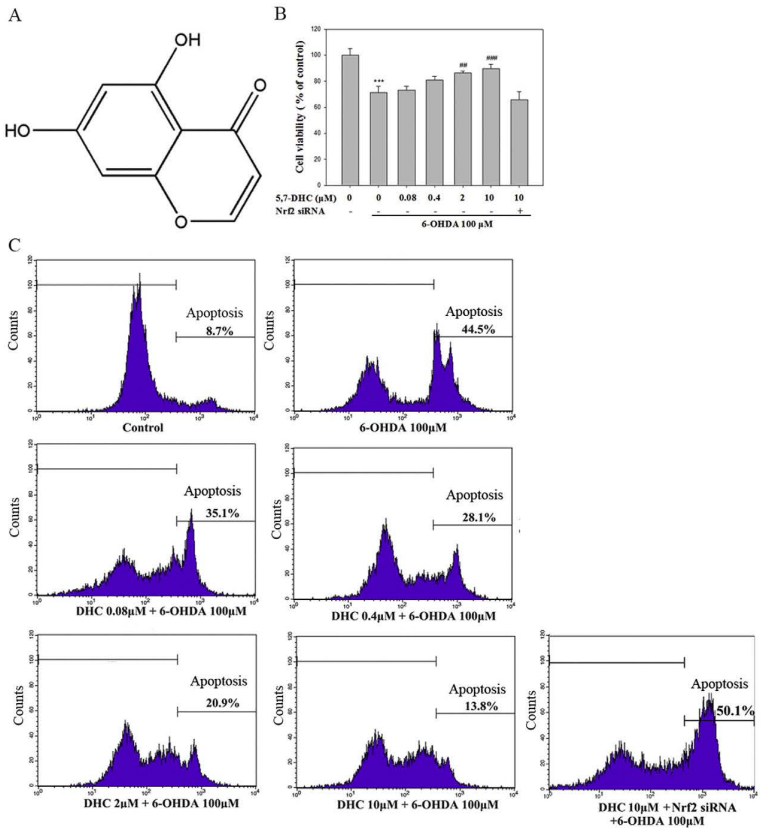

Fig. 1. (A) Chemical structure of 5,7-Dihydroxychromone (DHC). (B) Effects of DHC against 6-OHDA-induced cell death in SH-SY5Y cells were measured by MTT reduction assay and (C) illustrated by PI staining and FACS analysis using the FL-2 channel. The cells were pre-treated with different concentrations of DHC (0.4–10 μM) for 24 h and subsequently treated with 6-OHDA (100 μM) for another 24 h. The cells were transfected with Nrf2 siRNA (50 nM) for 48 h before the treatment with DHC (10 μM). (***$p < 0.001$ versus control group, ##$p < 0.01$ and ###$p < 0.001$ versus 6-OHDA-induced group).

3.2. Inhibitory effect of DHC against 6-OHDA-induced intracellular ROS generation

Intracellular ROS were detected by a DCFH-DA dye, which can be diffused to the cell membrane and deacetylated by esterase to the 2′,7′-dichlorodihydrofluorescein (DCFH), which is swiftly converted into the dichlorofluorescein (DCF) emitting fluorescence by ROS. As shown in Fig. 2, the 6-OHDA-induced cells exhibited higher DCF fluorescence intensities than the vehicle-treated cells. The amount of ROS generation was decreased in a dose-dependent manner when the 6-OHDA-induced cells were treated with different concentrations of DHC (0.4–10 μM). The 6-OHDA-induced group generated an approximately 5-fold greater amount of ROS than that of the vehicle-treated group. When the DHC (10 μM)-treated cells were treated with 6-OHDA, the ROS level was approximately 2-fold greater than that of the vehicle-treated group. However, the inhibitory effect of DHC (10 μM) on intracellular ROS generation disappeared upon treatment with Nrf2 siRNA, and the combined treatment with Nrf2 siRNA and DHC (10 μM) produced a similar ROS generation compared to the 6-OHDA-treated group.

3.3. Effects of DHC on induction of the nuclear Nrf2 and binding affinity of Nrf2/ARE in SH-SY5Y cells

Nrf2 in nucleus has a binding affinity to the ARE region and the Nrf2/ARE complex induces the transcription of ARE-mediated antioxidant genes. DHC increased the induction of nuclear Nrf2 with a peak effect that occurred at 6 h. As shown in Fig. 3A, the nuclear Nrf2 was dose-dependently increased by DHC treatment (0.08–10 μM) at 6 h (Fig. 3B). The increase of nuclear Nrf2 by DHC was visualized by immunocytochemistry in Fig. 3C. To elucidate the binding activity between Nrf2 and ARE, an electrophoretic mobility gel-shift assay (EMSA) was performed. As shown in Fig. 4, DHC (2 μM) drastically increased the Nrf2–ARE binding activity and the maximum binding activity was observed at 12 h.

3.4. Effects of DHC on HO-1, NQO1 and GCLc protein expression in SH-SY5Y cells

The protein levels of HO-1, NQO1, and GCLc, which are reported as major phase II antioxidant enzymes that are transcribed upon Nrf2/ARE binding, were measured in the SH-SY5Y cells. As shown in Fig. 5A and B, HO-1, NQO1, and GCLc protein expression levels were increased in a time- and dose-dependent manner by DHC treatment. As shown in Fig. 5B, HO-1, NQO1, and GCLc protein expression levels at 24 h were gradually increased by DHC treatment (0.08–10 μM). Upon Nrf2 siRNA treatment, the increased protein expression levels of HO-1, NQO1, and GCLc induced by DHC treatment (10 μM) were drastically reduced to a near-baseline level (Fig. 5C). These results revealed that Nrf2/ARE binding is a key step in the transcriptions of HO-1, NQO1, and GCLc proteins.

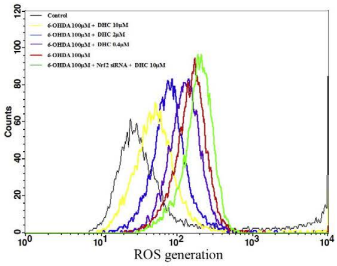

Fig. 2. Effects of DHC against 6-OHDA-induced intracellular ROS generation in SH-SY5Y cells illustrated by DCFH-DA staining and FACS analysis using the FL-1 channel. The cells were pre-treated with different concentrations of DHC (0.4–10 μM) for 24 h and subsequently treated with 6-OHDA (100 μM) for another 24 h. The cells were transfected with Nrf2 siRNA (50 nM) for 48 h before treatment with DHC (10 μM).

3.5. The inhibitory effects of DHC on the 6-OHDA-induced apoptotic signal

The inhibitory effects of DHC on the expressions of cleaved caspase-9, caspase-3, and PARP during the process of apoptosis were evaluated. ROS accumulation is known to activate caspase-9 and caspase-3, and activated caspase-3 cleaves PARP. As shown in Fig. 6, the cleaved caspase-9, caspase-3, and PARP were over-expressed when the SH-SY5Y cells were induced by 6-OHDA. However, the over-expression of these cleaved proteins was dose-dependently inhibited by DHC treatment (0.08–10 μM).

4. Discussion

Neurodegenerative diseases may occur without obvious causes or be the result of numerous circumstances that cause the impairment of cellular performance in neuron and ultimately cell death. Due to the rapid aging of the populations of societies across the world, the number of patients suffering from the neurodegenerative disease is also increasing. Although the causes of these diseases have not been clearly elucidated, recent studies have revealed that ROS is composed of their pathogenesis [3]. Because of their abundant iron contents and relatively deficient antioxidant defense system, neuronal cells are vulnerable to excessive ROS and electrophile related stress. It has been suggested that ROS is highly involved in the neurotoxicity of neurodegenerative disease [16]. Over the past decade, many studies of antioxidant enzymes have resulted in progress in the treatment and prevention of diseases [20]. In this context, it has been suggested that the coordinated expression of phase II antioxidant enzymes via the induction of nuclear Nrf2 could be a promising strategy for protection against oxidative stress-related neurodegenerative diseases.

The effects of DHC (Fig. 1A) have not been thoroughly examined, particularly in relation to protection against neuronal cell death. In this report, DHC was found to protect against neuronal cell death and the ROS generation in 6-OHDA-induced SH-SY5Y cells. It was reported that caspase-9 could be cleaved by ROS generation [28]. Cleaved caspase-9 induces activation of caspase-3 by making a cleaved form of caspase-3, which is the important caspase involved in the apoptotic process and neuronal cell death caused by 6-OHDA [2,11]. PARP is cleaved by an active form of caspase-3, and this cleaved PARP loses the ability to participate in DNA repair, which results in apoptosis. PARP cleavage by the active form of caspase-3 is a reliable indicator of apoptosis [9]. In our results, DHC prevented the 6-OHDA-induced cleavages of caspase-3, caspase-9, and PARP, which inhibited the activation of the apoptotic cascade in the SH-SY5Y cells. Moreover, DHC down-regulated the ROS level, which was increased by treatment with 6-OHDA. Based on its results, we suggest that this anti-apoptotic effect of DHC is associated with the down-regulation of ROS.

The effects of the Nrf2/ARE signaling pathway on ROS generation were also evaluated. Our results revealed that treatment with DHC inhibited the generation of 6-OHDA-induced ROS, which affect the early and late stages of apoptosis. The ability of DHC to inhibit ROS generation seems to be an important factor in neuronal cell protection. DHC also increased the induction of nuclear Nrf2, which has a binding affinity to ARE and activates ARE-driven phase II antioxidant enzymes; NQO1, HO-1, and GCLc. Nrf2 is regarded as a key regulator of antioxidant defensive responses and a sensor of cellular redox status [8]. Many lines of research have proven the importance of Nrf2-related antioxidant enzymes in neuroprotection [17]. It has been also reported that the levels of antioxidant genes are considerably decreased in Nrf2-K.O. mice and the expression levels of antioxidant enzymes were eliminated

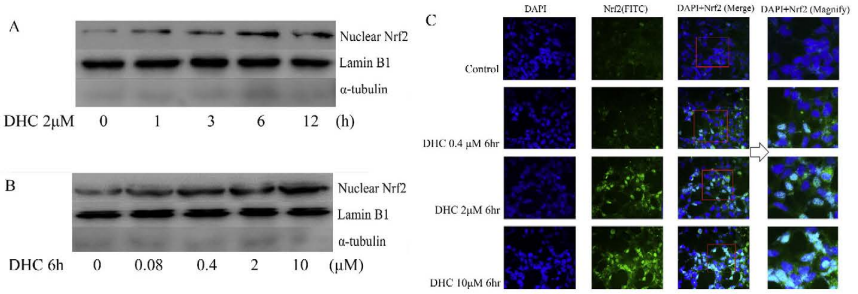

Fig. 3. Effects of DHC on the nuclear translocation of Nrf2 in SH-SY5Y cells illustrated by Western blot analysis and immunocytochemistry. (A) The cells were treated with DHC (2 μM) for different durations (0–12 h). (B) The cells were treated with different concentrations of DHC (0.4–10 μM) for 6 h. Representative data from three independent experiments are shown. (C) The cells were treated with DHC (0.4–10 μM) for 6 h, and the nuclei were visualized with DAPI staining. Nrf2 was detected with FITC-conjugated antibodies. Cellular morphologies were visualized with a fluorescence microscope (400×). Representative images from three independent experiments are shown.

by Nrf2-siRNA in in vitro models [21]. NQO1, HO-1, and GCLc are representative antioxidant enzymes whose expressions are increased by diverse environmental stimulus including ROS and thiol-reactive substances [4,22,23]. NQO1 has been reported to be a potentially attractive therapeutic target for protecting cells from oxidative damage because it makes a stable form of hydroquinone by catalyzing quinone [13]. Moreover, it has been reported that HO-1 catalyzes heme to carbon monoxide, biliverdin and iron, which exerts potent antioxidant effects [3]. GCLc participates in glutathione synthesis and prevents the impairment of cellular function from excessive ROS [18]. Many studies have shown that these antioxidant enzymes have powerful antioxidant effects, and it has been suggested that the regulation of antioxidant enzymes might be a key factor in the prevention of age-related diseases [25]. Our results revealed that DHC treatment induced the nuclear translocation of Nrf2, which resulted in the increases in NQO1, HO-1, and GCLc at the level of protein expression, suggesting that the neuroprotective effects of DHC against 6-OHDA-induced cell death are involved in the inhibition of ROS generation. Based on our research, we expect that one of the neuroprotective effects exerted by DHC is the increased induction of the Nrf2/ARE signal. When the cells were transfected with Nrf2 siRNA, the protective effects of DHC against 6-OHDA-induced neurotoxicity and ROS generation were inhibited. Moreover, the increased protein expression levels of NQO1, HO-1, and GCLc by DHC treatment (10 μM) were also drastically reduced to basal levels by treatment with Nrf2 siRNA. Our results showed that the neuroprotective effects of DHC are due to the activation of the Nrf2/ARE signaling pathways and the subsequent inhibition of ROS generation.

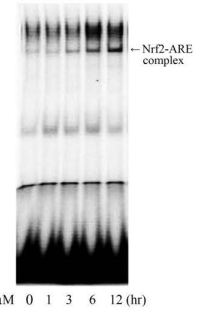

Fig. 4. Effects of DHC on the binding activity of Nrf2–ARE. The cells were treated with DHC (2 μM) for different durations (0–12 h), and the nuclear extracts were incubated with [γ-^{32}P]-labeled oligonucleotides harboring an ARE consensus sequence. Nrf2–ARE binding activity was measured via an electrophoretic mobility gel-shift assay (EMSA).

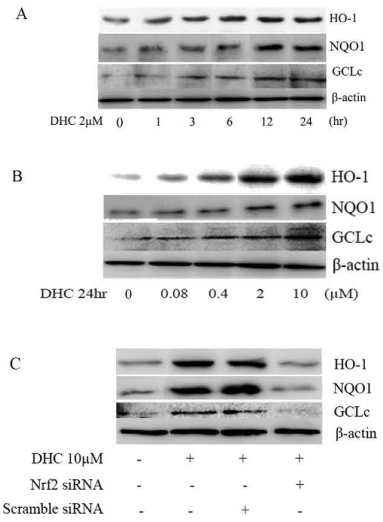

Fig. 5. Effects of DHC on the expressions of the HO-1, NQO1, and GCLc proteins in the SH-SY5Y cells illustrated by Western blot analysis. (A) The cells were treated with DHC (2 μM) for different durations (0–24 h). (B) The cells were treated with different concentrations of DHC (0.08–10 μM) for 24 h. (C) The cells were transfected with Nrf2 siRNA (50 nM) or scrambled siRNA (50 nM) prior to treatment with DHC (10 μM) for 48 h. Representative data from three independent experiments are shown.

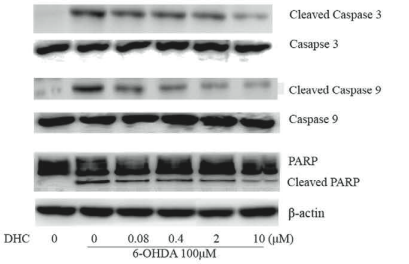

Fig. 6. Inhibitory effects of DHC on the expressions of cleaved caspase-9, caspase-3 and PARP illustrated by Western blot analysis. The cells were pre-treated with different concentrations of DHC (0.4–10 μM) for 24 h and subsequently treated with 6-OHDA (100 μM) for another 24 h. Representative data from three independent experiments are shown.

5. Conclusion

The present study demonstrated that DHC prevented 6-OHDA-induced neurotoxicity via the induction of the Nrf2/ARE signal, which subsequently led to the overexpression of antioxidant enzymes, including NQO1, HO-1, and GCLc. As a result of these effects, DHC inhibited the generation of ROS and neuronal cell death in 6-OHDA-induced SH-SY5Y cells. Our study suggests that DHC can be a promising neuroprotective candidate in the therapy of neurodegenerative diseases such as Parkinson's disease.

Conflict of interest statement

The authors declare that there are no conflicts of interest.

Acknowledgments

This work was supported by the Basic Science Research Program through the National Research Foundation (NRF) of Korea (Grant no. NRF-2013R1A1A2008111) and the BK21 plus program in 2015 through the National Research Foundation (NRF) funded by the Ministry of Education of Korea. The author appreciates Korea University and the Korea Forest Research Institute for supporting the plant materials.

References

[1] A. Alfieri, S. Srivastava, R.C. Siow, M. Modo, P.A. Fraser, G.E. Mann, Targeting the Nrf2–Keap1 antioxidant defence pathway for neurovascular protection in stroke, J. Physiol. 589 (2011) 4125–4136.
[2] R.C. Dodel, Y. Du, K.R. Bales, Z. Ling, P.M. Carvey, S.M. Paul, Caspase-3-like proteases and 6-hydroxydopamine induced neuronal cell death, Brain Res. Mol. Brain Res. 64 (1999) 141–148.
[3] T. Farooqui, A.A. Farooqui, Lipid-mediated oxidative stress and inflammation in the pathogenesis of Parkinson's disease, Park. Dis. 2011 (2011) 247467.
[4] J.A. Fraser, R.D. Saunders, I.I. McLellan, *Drosophila melanogaster* glutamate–cysteine ligase activity is regulated by a modifier subunit with a mechanism of action similar to that of the mammalian form, J. Biol. Chem. 277 (2002) 1158–1165.
[5] A. Ham, D.W. Kim, K.H. Kim, S.J. Lee, K.B. Oh, J. Shin, W. Mar, Reynosin protects against neuronal toxicity in dopamine-induced SH-SY5Y cells and 6-hydroxydopamine-lesioned rats as models of Parkinson's disease: reciprocal up-regulation of E6-AP and down-regulation of alpha-synuclein, Brain Res. 1524 (2013) 54–61.
[6] C.H. Jeong, G.N. Choi, J.H. Kim, J.H. Kwak, H.R. Jeong, D.O. Kim, H.J. Heo, Protective effects of aqueous extract from *Cudrania tricuspidata* on oxidative stress-induced neurotoxicity, Food Sci. Biotechnol. 19 (2010) 1113–1117.
[7] D.G. Kang, T.Y. Hur, G.M. Lee, H. Oh, T.O. Kwon, E.J. Sohn, H.S. Lee, Effects of *Cudrania tricuspidata* water extract on blood pressure and renal functions in NO-dependent hypertension, Life Sci. 70 (2002) 2599–2609.
[8] K.W. Kang, S.J. Lee, S.G. Kim, Molecular mechanism of nrf2 activation by oxidative stress, Antioxid. Redox Signal. 7 (2005) 1664–1673.
[9] S.H. Kaufmann, S. Desnoyers, Y. Ottaviano, N.E. Davidson, G.G. Poirier, Specific proteolytic cleavage of poly(ADP-ribose) polymerase: an early marker of chemotherapy-induced apoptosis, Cancer Res. 53 (1993) 3976–3985.
[10] U. Koo, K.W. Nam, A. Ham, D. Lyu, B. Kim, S.J. Lee, K.H. Kim, K.B. Oh, W. Mar, J. Shin, Neuroprotective effects of 3alpha-acetoxyeudesma-1,4(15),11(13)-trien-12,6alpha-olide against dopamine-induced apoptosis in the human neuroblastoma SH-SY5Y cell line, Neurochem. Res. 36 (2011) 1991–2001.
[11] K. Kuida, T.F. Haydar, C.Y. Kuan, Y. Gu, C. Taya, H. Karasuyama, M.S. Su, P. Rakic, R.A. Flavell, Reduced apoptosis and cytochrome c-mediated caspase activation in mice lacking caspase 9, Cell 94 (1998) 325–337.
[12] S. Leutner, C. Czech, K. Schindowski, N. Touchet, A. Eckert, W.E. Muller, Reduced antioxidant enzyme activity in brains of mice transgenic for human presenilin-1 with single or multiple mutations, Neurosci. Lett. 292 (2000) 87–90.
[13] J.H. Lim, K.M. Kim, S.W. Kim, O. Hwang, H.J. Choi, Bromocriptine activates NQO1 via Nrf2-PI3K/Akt signaling: novel cytoprotective mechanism against oxidative damage, Pharmacol. Res. 57 (2008) 325–331.
[14] T. Meyer, C. Munch, H. Volkel, P. Booms, A.C. Ludolph, The EAAT2 (GLT^{-1}) gene in motor neuron disease: absence of mutations in amyotrophic lateral sclerosis and a point mutation in patients with hereditary spastic paraplegia, J. Neurol. Neurosurg. Psychiatry 65 (1998) 594–596.
[15] G. Munch, A.M. Cunningham, P. Riederer, E. Braak, Advanced glycation endproducts are associated with Hirano bodies in Alzheimer's disease, Brain Res. 796 (1998) 307–310.
[16] G. Munch, M. Gerlach, J. Sian, A. Wong, P. Riederer, Advanced glycation end products in neurodegeneration: more than early markers of oxidative stress? Ann. Neurol. 44 (1998) S85–S88.
[17] S.H. Park, J.H. Jang, C.Y. Chen, H.K. Na, Y.J. Surh, A formulated red ginseng extract rescues PC12 cells from PCB-induced oxidative cell death through Nrf2-mediated upregulation of heme oxygenase-1 and glutamate cysteine ligase, Toxicology 278 (2010) 131–139.
[18] A. Pompella, A. Visvikis, A. Paolicchi, V. De Tata, A.F. Casini, The changing faces of glutathione, a cellular protagonist, Biochem. Pharmacol. 66 (2003) 1499–1503.
[19] J. Qiu, L. Chen, Q. Zhu, D. Wang, W. Wang, X. Sun, X. Liu, F. Du, Screening natural antioxidants in peanut shell using DPPH–HPLC–DAD–TOF/MS methods, Food Chem. 135 (2012) 2366–2371.
[20] K. Rahman, Studies on free radicals, antioxidants, and co-factors, Clin. Interv. Aging 2 (2007) 219–236.
[21] M. Ramos-Gomez, M.K. Kwak, P.M. Dolan, K. Itoh, M. Yamamoto, P. Talalay, T.W. Kensler, Sensitivity to carcinogenesis is increased and chemoprotective efficacy of enzyme inducers is lost in nrf2 transcription factor-deficient mice, Proc. Natl. Acad. Sci. U. S. A. 98 (2001) 3410–3415.
[22] M. Rizzardini, M. Terao, F. Falciani, L. Cantoni, Cytokine induction of haem oxygenase mRNA in mouse liver. Interleukin 1 transcriptionally activates the haem oxygenase gene, Biochem. J. 290 (Pt 2) (1993) 343–347.
[23] Z.Y. Su, L. Shu, T.O. Khor, J.H. Lee, F. Fuentes, A.N. Kong, A perspective on dietary phytochemicals and cancer chemoprevention: oxidative stress, nrf2, and epigenomics, Top. Curr. Chem. 329 (2013) 133–162.
[24] X. Sun, L. Huang, M. Zhang, S. Sun, Y. Wu, Insulin like growth factor-1 prevents 1-mentyl-4-phenylphyridinium-induced apoptosis in PC12 cells through activation of glycogen synthase kinase-3beta, Toxicology 271 (2010) 5–12.
[25] B. Uttara, A.V. Singh, P. Zamboni, R.T. Mahajan, Oxidative stress and neurodegenerative diseases: a review of upstream and downstream antioxidant therapeutic options, Curr. Neuropharmacol. 7 (2009) 65–74.
[26] G. Wei, B. Yu, Isoflavone glycosides: synthesis and evaluation as alpha-glucosidase inhibitors, Eur. J. Org. Chem. 3156-3163 (2008).
[27] M. Zhang, C. An, Y. Gao, R.K. Leak, J. Chen, F. Zhang, Emerging roles of Nrf2 and phase II antioxidant enzymes in neuroprotection, Prog. Neurobiol. 100 (2013) 30–47.
[28] Y. Zuo, B. Xiang, J. Yang, X. Sun, Y. Wang, H. Cang, J. Yi, Oxidative modification of caspase-9 facilitates its activation via disulfide-mediated interaction with Apaf-1, Cell Res. 19 (2009) 449–457.

BRAIN RESEARCH ▮ (▮▮▮▮) ▮▮▮–▮▮▮

Available online at www.sciencedirect.com

SciVerse ScienceDirect

www.elsevier.com/locate/brainres

Research Report

Reynosin protects against neuronal toxicity in dopamine-induced SH-SY5Y cells and 6-hydroxydopamine-lesioned rats as models of Parkinson's disease: Reciprocal up-regulation of E6-AP and down-regulation of α-synuclein

Ahrom Ham[a,1], Dong-Woo Kim[a,1], Kyeong Ho Kim[b], Sung-Jin Lee[c], Ki-Bong Oh[d], Jongheon Shin[a,*], Woongchon Mar[a,**]

[a]Natural Products Research Institute, College of Pharmacy, Seoul National University, 599 Gwanak-ro, Gwanak-gu, Seoul 151-742, Republic of Korea
[b]College of Pharmacy, Kangwon National University, Chuncheon 200-701, Republic of Korea
[c]Department of Animal Biotechnology, Kangwon National University, Chuncheon 200-701, Republic of Korea
[d]School of Agricultural Biotechnology, Seoul National University, 599 Gwanak-ro, Gwanak-gu, Seoul 151-742, Republic of Korea

ARTICLE INFO

Article history:
Accepted 22 May 2013

Keywords:
Reynosin
α-Synuclein
E6-associated protein
Neuroprotection
6-OHDA lesion
Parkinson's disease

ABSTRACT

Aggregation of α-synuclein (ASYN) is considered a major determinant of neuronal loss in Parkinson's disease (PD). E6-associated protein (E6-AP), an E3 ubiquitin protein ligase, has been known to promote the degradation of α-synuclein. The aim of this study was to assess the effects of the sesquiterpene lactone reynosin on dopamine (DA)-induced neuronal toxicity and regulation of E6-associated protein and α-synuclein proteins in both in vitro and in vivo models of Parkinson's disease. Usi"ng flow cytometry and western blot analysis, we determined that reynosin significantly protected both against cell death from dopamine-induced toxicity in human neuroblastoma SH-SY5Y cells and against the loss of tyrosine hydroxylase (TH)-positive cells in 6-hydroxydopamine (6-OHDA)-lesioned rats (a rodent Parkinson's disease model system). In addition, reynosin made up-regulation of E6-associated protein expression and down-regulation of the over-expression of α-synuclein protein in both dopamine-treated SH-SY5Y cells and 6-hydroxydopamine-lesioned rats. These results suggest that the protective effect of reynosin against dopamine-induced neuronal cell death may be due to the reciprocal up-regulation of E6-associated protein and down-regulation of α-synuclein protein expression.

*Corresponding author. Fax: +82 2 762 8322.
**Corresponding author. Fax: +82 2 880 2474.
E-mail addresses: shinj@snu.ac.kr (J. Shin), mars@snu.ac.kr (W. Mar).
[1]These authors contributed equally to this work.

0006-8993/$ - see front matter © 2013 Elsevier B.V. All rights reserved.
http://dx.doi.org/10.1016/j.brainres.2013.05.036

Please cite this article as: Ham, A., et al., Reynosin protects against neuronal toxicity in dopamine-induced SH-SY5Y cells and 6-hydroxydopamine-lesioned rats as models of Parkinson's disease: Reciprocal up-regulation of E6-AP and down-regulation of α-synuclein. Brain Research (2013), http://dx.doi.org/10.1016/j.brainres.2013.05.036

1. Introduction

Parkinson's disease (PD) is the second most common neurodegenerative disorder after Alzheimer's disease and is neuropathologically characterized by severe motor deficits caused by neuronal cell death (Golde, 2009). PD is neuropathologically characterized by a selective loss of nigrostriatal dopaminergic neurons (Nicotra and Parvez, 2002) and the presence of brainstem-type Lewy bodies, a hallmark of idiopathic PD composed of an abnormal aggregation of α-synuclein (ASYN), inside neurons (Dedov et al., 2001).

The presence of ASYN as a main component of Lewy bodies suggests that the aggregation of this protein is a key pathogenic event in PD; moreover, patients with PD exhibit the accumulation of ASYN in the substantia nigra. Phosphorylation of ASYN has been suggested to an important factor both for the cytoplasmic inclusion formation (Chu and Kordower, 2007; Smith et al., 2005) and the conformational changes. It induced the abnormal aggregation of ASYN that are considered to lead to neuronal cell loss (Chu et al., 2006). Over-expression of ASYN also caused its aggregation in the brain and induced neurodegeneration in an animal model (Feany and Bender, 2000; Kirik et al., 2002). Recently, it was reported that E6-associated protein (E6-AP), an E3 ubiquitin-protein ligase with a limited role in protein folding, promotes the degradation of polyglutamine proteins mediated by the ubiquitin–proteasome pathway; in addition, E6-AP possibly functions as a cellular quality control ubiquitin ligase (Mishra et al., 2009). Moreover, E6-AP is recruited to juxtanuclear aggregates of ASYN, which may play a critical regulatory role in the degradation of ASYN (Mulherkar et al., 2009).

It has been suggested that an imbalance between cytoplasmic and vesicular dopamine (DA) may cause neuronal degeneration (Barzilai et al., 2001), and this degeneration may be a factor in the dopaminergic damage observed in PD. In this study, neurotoxicity elicited by DA in SH-SY5Y cells was used as an in vitro model of PD (Asanuma et al., 2003; Gomez-Santos et al., 2003; Miyazaki and Asanuma, 2008), and 6-hydroxydopamine (6-OHDA)-lesioned rats were used as an in vivo model of PD (Foyet et al., 2011) to evaluate the neuroprotective effects of reynosin.

Reynosin, a sesquiterpene lactone isolated from the leaves of *Laurus nobilis* L. (Lauraceae), has been reported to have pharmacological actions such as the reduction of ethanol concentration in rat blood and nitric oxide production (Yoshikawa et al., 2000). In a previous study, we reported that spirafolide, another sesquiterpene lactone from *Laurus nobilis* L. (Lauraceae), has neuroprotective effects in human SH-SY5Y cells (Ham et al., 2010).

The aim of this study was to determine whether reynosin protects neuronal cells against DA toxicity through the regulation of E6-AP and ASYN protein expression in human dopaminergic cells and 6-OHDA-induced lesioned rat, as in vitro and in vivo models of PD, respectively. To our knowledge, this is the first report demonstrating the neuroprotective effects of reynosin in the context of the regulation of E6-AP and ASYN protein expression. These results suggest the therapeutic potential of reynosin in neurodegenerative diseases such as PD.

2. Results

2.1. Protection from DA-induced cell death by reynosin

SH-SY5Y cells were treated with reynosin to evaluate possible toxic effects at concentrations ranging from 0.08 μM to 50 μM (final 0.5% DMSO, v/v) for 48 h (data not shown). The neuroprotective effect of reynosin against DA-induced cell death was evaluated within the non-toxic dose range. As shown in Fig. 1B, treatment of SH-SY5Y cells with DA (600 μM) for 24 h resulted in important changes in cellular morphology; specifically, a reduction in the amount of cytoplasm and decrease in cell adherence were observed. However, cells reverted to normal shape, when pre-treated with reynosin (2 μM) for 24 h before DA treatment (24 h). In addition, treatment of cells with DA for 24 h (600 μM) reduced the viability to 29.2% ($p<0.001$) compared to vehicle-treated cells (control group), whereas DA-induced cell death was significantly prevented by reynosin pre-treatment for 24 h at concentrations of 0.08, 0.4, and 2 μM in a dose-dependent manner. The viability was 31.8%, 41.5% ($p<0.01$), and 76.8% ($p<0.001$), respectively (EC_{50}, 3.6 μM) as compared to the control group (Fig. 1C and D). Apomorphine (APO) was used as a positive control compound. APO is a non-selective dopamine agonist which activates both D_1-like and D_2-like receptors and used in the treatment of PD (Millan et al., 2002). The protective effect of reynosin against DA-induced cell death was approximately 5 times more potent than that of APO (a positive control compound) (EC_{50}, 18.2 μM).

2.2. Effects of reynosin on E6-AP and ASYN protein expression in SH-SY5Y cells

The protein expression levels of E6-AP and ASYN were detected by western blot analysis in SH-SY5Y cells. In DA-treated cells, E6-AP protein expression decreased but ASYN protein expression increased in a time-dependent manner. In particular, a dramatic increase in ASYN protein expression was observed after 15 h of DA treatment, whereas the E6-AP levels were reduced gradually. On the basis of these results, DA treatment for 15 h was used in subsequent experiments.

The level of E6-AP protein expression in the DA treatment group was reduced to 0.5-fold ($p<0.01$) compared with the control group, whereas, after pre-treatment with reynosin (0.08, 0.4, and 2 μM) for 24 h, E6-AP protein expression was dose-dependently increased to 0.6-, 0.7-, and 0.9-fold ($p<0.01$) compared with the control group, respectively. Interestingly, treatment with APO (2 μM) resulted in E6-AP protein expression that was only 0.6-fold that of the control group, indicating that reynosin is 1.5-fold more potent than APO at a concentration of 2 μM (Fig. 2C).

In addition, DA-treatment increased ASYN expression to 2.6-fold ($p<0.001$) compare with the control group, whereas pre-treatment with reynosin (0.08, 0.4, and 2 μM) for 24 h reduced ASYN expression in a dose-dependent manner to 1.8-, 1.3- ($p<0.01$), and 1.1-fold ($p<0.001$) compare with the control group, respectively (Fig. 2D). Interestingly, APO did not affect DA-induced over-expression of the ASYN protein at the concentration tested (2 μM) (Fig. 2D). In conclusion,

Please cite this article as: Ham, A., et al., Reynosin protects against neuronal toxicity in dopamine-induced SH-SY5Y cells and 6-hydroxydopamine-lesioned rats as models of Parkinson's disease: Reciprocal up-regulation of E6-AP and down-regulation of α-synuclein. Brain Research (2013), http://dx.doi.org/10.1016/j.brainres.2013.05.036

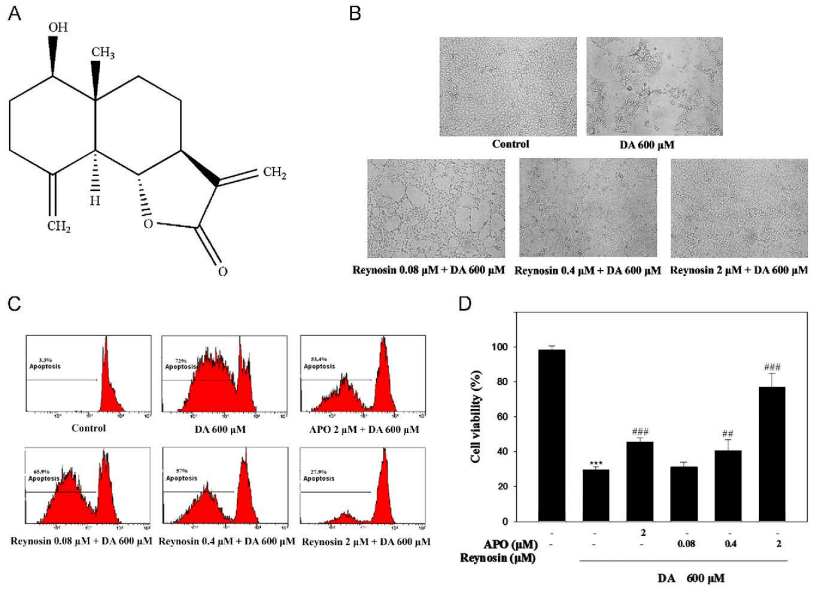

Fig. 1 – Reynosin protects against DA induced neuronal cell death in SH-SY5Y cells. (A) Chemical structure of reynosin. (B) Cellular morphological changes. Cells were pre-treated with reynosin (0.08, 0.4, and 2 μM) for 24 h, followed by DA treatment (600 μM) for an additional 24 h. (C) Effects on DA-induced cell death as observed by PI staining and FACS analysis. (D) Histograms show the proportion of dead cells relative to total cells. APO was used as a positive control compound. Plots were calculated from the flow cytometry histogram distributions (mean ± SD, $n \geq 5$) (‾$p < 0.001$ versus control group, $^{\#\#}p < 0.01$ and $^{\#\#\#}p < 0.001$ versus DA-treated group).

reynosin treatment reversed the concomitant down-regulation of E6-AP and up-regulation of ASYN proteins by DA.

2.3. *Effects of reynosin on TH-positive dopaminergic neurons in the substantia nigra in 6-OHDA-lesioned rats*

TH, the rate limiting enzyme in DA synthesis, was used as a marker for dopaminergic neurons in the substantia nigra (Masliah et al., 2000). TH-positive neurons in the substantia nigra were detected by immunohistochemistry (Fig. 3A). The effect of the various treatments on dopaminergic neurons was quantified by calculating the ratio of TH-positive neurons in the substantia nigra from the ipsilateral hemisphere to those from the contralateral hemisphere (I/C ratio). In the 6-OHDA-lesioned group, a significant loss of TH-positive neurons was observed. The I/C ratio of the sham group was 0.9 and that of the 6-OHDA lesion group was 0.3 ($p < 0.001$). The I/C ratio of reynosin treatment in 6-OHDA-lesioned rats was 0.4, 0.5 ($p < 0.001$), and 0.8 ($p < 0.001$) at doses of 0.2, 1, and 5 mg/kg, respectively, whereas treatment with APO, at 5 mg/kg, resulted in an I/C ratio of 0.7 ($p < 0.001$) (Fig. 3B).

2.4. *Effects of reynosin on E6-AP and ASYN protein expression in 6-OHDA-lesioned rats*

The effects of reynosin on the expression of E6-AP and ASYN proteins were determined in the rat model of PD. In the substantia nigra of 6-OHDA-lesioned rats, E6-AP protein expression was reduced to 0.39-fold ($p < 0.001$) compared with sham group, and the ASYN protein expression was increased to 2.3-fold ($p < 0.001$). However, treatment with reynosin (0.2, 1, and 5 mg/kg) in a lesioned rat increased the E6-AP protein expression to 0.44-, 0.52-, and 0.69-fold ($p < 0.05$) compare with the sham group and concomitantly decreased the ASYN protein expression to 2.1-, 1.5- ($p < 0.01$), and 1.3-fold ($p < 0.001$), respectively (Fig. 4). Interestingly, APO (5 mg/kg) reduced the E6-AP protein expression to 0.66-fold to that of sham group, which is similar to the effect caused by reynosin

Please cite this article as: Ham, A., et al., Reynosin protects against neuronal toxicity in dopamine-induced SH-SY5Y cells and 6-hydroxydopamine-lesioned rats as models of Parkinson's disease: Reciprocal up-regulation of E6-AP and down-regulation of α-synuclein. Brain Research (2013), http://dx.doi.org/10.1016/j.brainres.2013.05.036

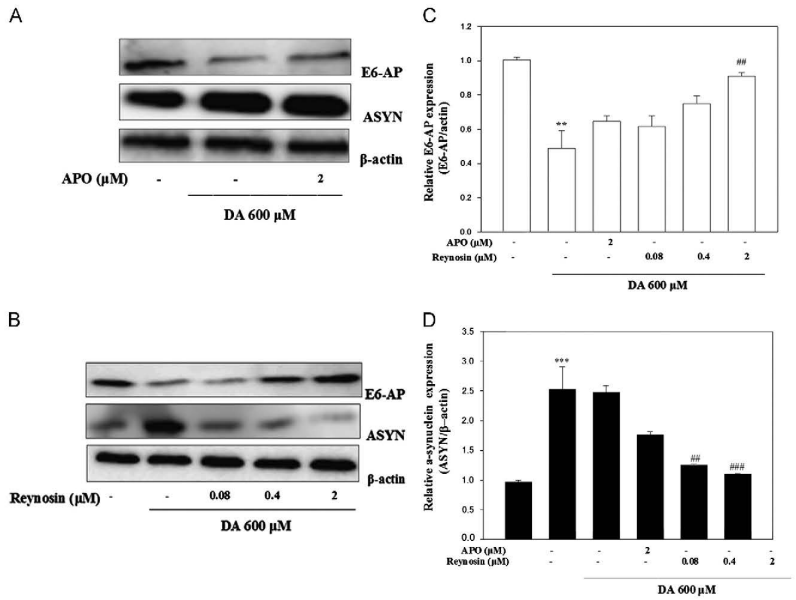

Fig. 2 – The effects of reynosin on the levels of ASYN and E6-AP protein expression were demonstrated by western blot analysis in SH-SY5Y cells treated with DA. (A and B) SH-SY5Y cells were pre-treated for 24 h with different concentrations of reynosin (0.08, 0.4, and 2 μM) or APO (2 μM) followed by treatment with DA (600 μM) for 15 h. Representative western blots using ASYN and E6-AP antibodies are presented. (C and D) Relative protein expression levels were normalized to β-actin expression. Data obtained from at least 5 independent experiments are shown and presented as the mean ± SD ($^{**}p<0.01$ and $^{***}p<0.001$ versus control group, $^{\#\#}p<0.01$ and $^{\#\#\#}p<0.001$ versus DA-treated group).

(5 mg/kg). However, APO did not affect the over-expression of the ASYN protein in lesioned rats. These results are consistent with the in vitro results obtained from SH-SY5Y cells.

3. Discussion

In this study, reynosin isolated from *Laurus nobilis* L. (Lauraceae) extract was evaluated for its neuroprotective effects in SH-SY5Y cells (Fig. 1) and in 6-OHDA-lesioned rats (Fig. 3) as in vitro and in vivo PD models, respectively. It has been reported that infusion of 6-OHDA causes a rapid and consistent loss of TH immunoreactivity in the substantia nigra (Masliah et al., 2000). In the present study, a significant loss of TH-positive neurons was observed in the substantia nigra of rats at 7 days after 6-OHDA lesion, and the number of TH-positive neurons in each group was illustrated in the representative photomicrographs, and quantified by image analysis (Fig. 3). Treatment with reynosin (i.p., once, 1 h after 6-OHDA lesion) significantly protected against the loss of TH-positive neurons from 6-OHDA-induced toxicity in the substantia nigra in a dose-dependent manner. This protective effect of reynosin was 1.2 times more potent than that of the APO, positive control compound, (Watanabe et al., 2004) at doses of 5 mg/kg.

It has been reported that many patients with PD have mutations in specific genes such as ASYN, and over-expression and mutation of ASYN are two of the most important pathogenic events in PD (Hughes et al., 1993). It has been reported that cells expressing mutant ASYN were more vulnerable to oxidative stress (Kanda et al., 2000). It also has been reported that Lewy bodies, abnormal protein inclusions, are the most common pathological hallmark of PD, and the main component of Lewy bodies is ASYN; thus, aggregation of this protein is believed to be a key pathogenic event in PD. In addition, aggregation of insoluble ASYN may remove soluble ASYN protofibrils, and this action is thought to induce greater toxicity of ASYN (Conway et al., 2001) and further aggregation of ASYN. Aggregation of ASYN is potentiated by exposure to a variety of stimuli such as mitochondrial inhibition and oxidative stress that are observed in PD pathology (Bennett, 2005). Extracellular DA is a stressor agent

Please cite this article as: Ham, A., et al., Reynosin protects against neuronal toxicity in dopamine-induced SH-SY5Y cells and 6-hydroxydopamine-lesioned rats as models of Parkinson's disease: Reciprocal up-regulation of E6-AP and down-regulation of α-synuclein. Brain Research (2013), http://dx.doi.org/10.1016/j.brainres.2013.05.036

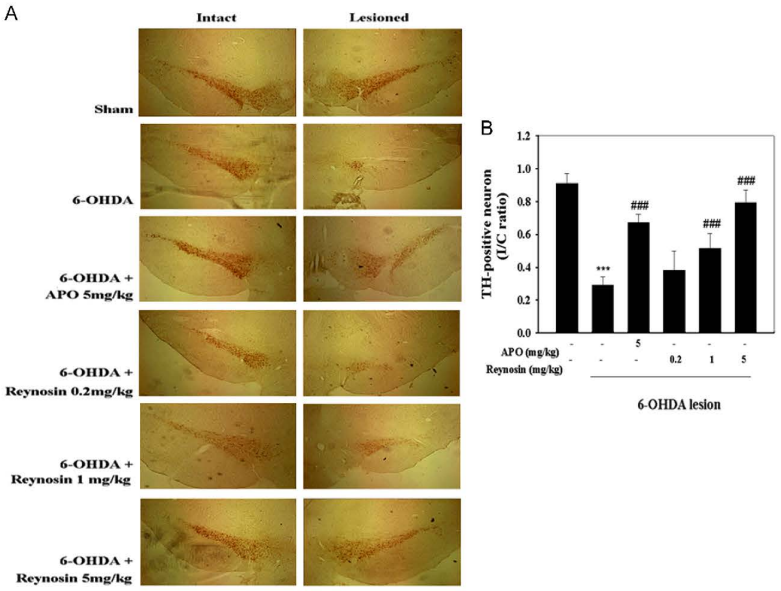

Fig. 3 – Neuroprotective effects of reynosin on TH-positive neurons in the substantia nigra in 6-OHDA-lesioned rats. (A) Photomicrograph of TH-positive neurons in both ipsilateral and contralateral hemispheres. Rats were divided into 4 groups; sham, 6-OHDA-lesioned, APO treatment (5 mg/kg), and reynosin treatment (0.2, 1, and 5 mg/kg) groups. (B) The effect of treatment on dopaminergic neurons was quantified by calculating the ratio of TH-positive neurons in the substantia nigra from the ipsilateral hemisphere to those from the contralateral hemisphere (*i*/C ratio). Each group represents the data from more than 9 rats, and mean values obtained from 5 sections from each rat were used ($^{***}p<0.001$ versus sham group, $^{###}p<0.001$ versus 6-OHDA-lesioned group).

that promotes ASYN over-expression (Gomez-Santos et al., 2003), and it has been reported that ASYN expression was significantly increased between 6 and 24 h after treatment with DA (Gomez-Santos et al., 2005). Our results demonstrated that DA-induced ASYN over-expression was significantly down-regulated by pre-treatment with reynosin in a dose-dependent manner in SH-SY5Y cells. However, pre-treatment with APO did not affect ASYN protein expression levels at the concentration tested (Fig. 2).

There are some disorders have been identified due to the malfunction of E3 ligases, including autosomal recessive juvenile PD (Jiang and Beaudet, 2004). Cell survival ultimately depends on the shift in equilibrium between the formation and clearance of improperly folded proteins. E6-AP, which plays a critical role in preventing the misfolding and the aggregation of proteins, is likely to control ubiquitin ligase activity, and it was presumed that E6-AP plays an important role in protein misfolding-related neurodegenerative disorders such as PD (Mishra et al., 2008). E6-AP has been shown to interact with Hsp70/Hsc70 chaperones and promotes the degradation of aggregate proteins (Mishra et al., 2009). The role of E6-AP is not limited polyglutamine or ASYN but misfolded proteins in general and E6-AP might act as a cellular quality control ligase. E6-AP has been shown to be located in Lewy bodies of the PD brain, and the endogenous E6-AP co-localizes with ASYN in intracellular inclusions in neuroblastoma cells. Over-expression of E6-AP enhances degradation of wild-type as well as mutant forms of ASYN by ubiquitination, indicating that E6-AP plays critical regulatory role in the degradation of AYN (Mulherkar et al., 2009). In addition, E6-AP regulates cell proliferation by proteasomal degradation of p53, tumor suppressor protein (Scheffner, 1998). It also promotes cell growth and proliferation by regulating the PI3K–AKT pathway (Srinivasan and Nawaz, 2011). E6-AP promotes SOD1 aggresomes degradation and suppresses cell toxicity along with heat shock protein 70 (Mishra et al., 2013). In the present study, decreased E6-AP protein expression level by DA was rescued by treatment with reynosin in both SH-SY5Y cells and 6-OHDA-lesioned rats (Fig. 2). Furthermore, treatment with reynosin

Please cite this article as: Ham, A., et al., Reynosin protects against neuronal toxicity in dopamine-induced SH-SY5Y cells and 6-hydroxydopamine-lesioned rats as models of Parkinson's disease: Reciprocal up-regulation of E6-AP and down-regulation of α-synuclein. Brain Research (2013), http://dx.doi.org/10.1016/j.brainres.2013.05.036

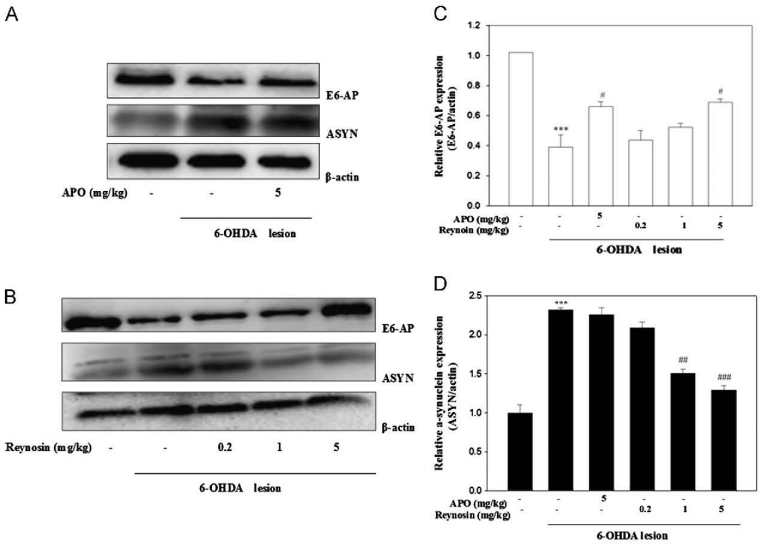

Fig. 4 – Effects of reynosin on the levels of ASYN and E6-AP protein expression in 6-OHDA-lesioned rats. (A and B) Rats were i. p. injected once with 0.2, 1, and 5 mg/kg of reynosin or 5 mg/kg of APO at 1 h after 6-OHDA lesion. The representative expression levels of ASYN and E6-AP protein are presented. (C and D) The mean values of ASYN and E6-AP were normalized to β-actin expression ($^{\sim}p<0.001$ versus sham group, $^{\#}p<0.05$, $^{\#\#}p<0.01$, and $^{\#\#\#}p<0.001$ versus 6-OHDA-lesioned group).

in 6-OHDA-lesioned rats down-regulated the over-expression of ASYN and simultaneously led to recovery of the down-regulated E6-AP protein expression (Fig. 4), consistent with the in vitro results.

In conclusion, our findings suggest that reynosin protects against DA-induced cell death and the resultant decrease in TH-positive neuronal loss in 6-OHDA-lesioned rats through the down-regulation of ASYN concomitant with the up-regulation of E6-AP protein expression. Our result, the reciprocal up-regulation of E6-AP and down-regulation of ASYN by reynosin, is the first reports about the neuroprotective effects of reynosin on in vitro and in vivo PD models, suggesting that reynosin might be a potential candidate for treatment of neurodegenerative diseases such as PD.

4. Experimental procedures

4.1. Reagents

Reynosin (98.2% purity) was provided by Prof. Jongheon Shin (Seoul National University, Korea). Dopamine (DA), apomorphine (APO), 6-OHDA, and propidium iodide (PI) were purchased from Sigma-Aldrich (St Louis, MO, USA). Dulbecco's modified Eagle's medium (DMEM) and fetal bovine serum (FBS) were purchased from Gibco BRL (Rockville, MD, USA). Hybond-polyvinylidene difluoride (PVDF) membrane was purchased from Amersham Pharmacia Biotechnology Inc. (Piscataway, NJ, USA). Protein extraction solution was purchased from iNtRON Biotech Inc. (Seoul, Korea).

4.2. Cell culture and neuronal cell protection test

Human neuroblastoma SH-SY5Y cells (ATCC no. CRL-2266) were cultured in DMEM supplemented with 10% heat-inactivated FBS and 1% penicillin/streptomycin (Meiji Seika, Tokyo, Japan), at 37 °C in a humidified 5% CO2 atmosphere. SH-SY5Y cells were cultured for 24 h and then treated with reynosin (0.08, 0.4, and 2 μM) or 2 μM of APO (a positive control compound) (Hara et al., 2006) for 24 h, followed by subsequent treatment with DA (600 μM) for an additional 24 h. Cell viability was analyzed by flow cytometry (FACS) (Calibur, Becton Dickinson, USA) using PI staining (Yang et al., 2009).

4.3. Animal

Male Sprague-Dawley rats were purchased from Samtako Bio Korea (Osan, Korea) and housed in groups (2–3 rats/cage) at room temperature for 1 week prior to the experiments in a humidity-controlled environment with a 12/12-light-dark cycle and unlimited access to food and water. All animal experiments were performed with the approval of the Institutional

Please cite this article as: Ham, A., et al., Reynosin protects against neuronal toxicity in dopamine-induced SH-SY5Y cells and 6-hydroxydopamine-lesioned rats as models of Parkinson's disease: Reciprocal up-regulation of E6-AP and down-regulation of α-synuclein. Brain Research (2013), http://dx.doi.org/10.1016/j.brainres.2013.05.036

Animal Care and Use Committee of Seoul National University, and in accordance with the requirements of European Directive 2010/63/EU. All efforts were made to minimize the number of animals used and their suffering. After experiments, all of the animals were sacrificed by overdose of anesthetics.

4.4. 6-OHDA lesion and APO/reynosin treatment

Injection of 6-OHDA into the rat substantia nigra was used as an animal model of PD (Ungerstedt, 1968). Rats weighing approximately 250 g were randomly divided into 4 groups: the sham group (vehicle solution, $n \geq 9$), the 6-OHDA-lesioned group (6-OHDA, $n \geq 9$), the APO treatment group (6-OHDA +APO, $n \geq 9$), and the reynosin treatment group (6-OHDA +reynosin, $n \geq 9$). The sham and 6-OHDA groups were intraperitoneally (i.p.) injected with the vehicle solution (1% EtOH/saline). The treatment groups were intraperitoneally injected with reynosin (0.2, 1, and 5 mg/kg, dissolved in 1% EtOH/saline) or APO (5 mg/kg, dissolved in 1% EtOH/saline) 1 h after 6-OHDA injection into the left substantia nigra. APO has been reported to have neuroprotective effects against 6-OHDA-lesioned nigrostriatal damage in the rat (Yuan et al., 2006) and was used as a positive control compound. At the beginning of the experiment, rats were anesthetized with ketamine (80 mg/kg, i.p.; Ketaset®; Fort Dodge, IA, USA) followed by xylazine (10 mg/kg, i.p.; Rompun®, Bayer, UK), and placed in a stereotaxic frame (Dae-Jong Instrument Industry Co., Seoul, Korea). 6-OHDA dissolved at a concentration of 5 μg/μl in saline containing 0.1% ascorbic acid was injected at a final dose of 20 μg into the substania nigra 4.8 mm posterior, 1.8 mm lateral and 7.8 mm ventral to the bregma and dura at a rate of 1 μl/min, using a Hamilton 10-μl syringe, according to the previously described procedure (Paxinos and Watson, 1998). After the 4 min of 6-OHDA injection at a rate of 1 μl/ml, the needle was kept in place for another 5 min to allow complete diffusion of 6-OHDA and then slowly removed at a rate of 1 mm/min. In the sham group, vehicle solution was injected instead of 6-OHDA. Next, the bone hole was sealed with restorative cement (GC Co., Tokyo, Japan) and then clipped. After 6-OHDA lesions, the animals were returned to their cages for 1 week.

4.5. Immunohistochemistry

TH-positive neurons were detected using the anti-TH antibody (Chemicon International, Temecula, CA, USA) and the Vectastain Elite ABC kit (Vector Laboratories, Burlingame, CA, USA) (Iancu et al., 2005). In brief, sections were incubated in PBS mixed with 3% goat serum and 0.2% Triton X-100 for 12 h, followed by an anti-mouse TH antibody at a dilution of 1:333 at 4 °C for another 24 h. The sections were then washed in 0.01 M PBS 3 times, incubated with secondary anti-mouse HRP-conjugated IgG antibody (1:1000; Santa Cruz Biotechnology, Inc., CA, USA) at room temperature for 1 h, and an avidin/biotin/peroxidase complex solution for another 1 h. The sections were subsequently stained with a diaminobenzidine immunohistochemistry kit (Vector Laboratories, CA, USA) and then mounted using cover slips and mounting fluid.

4.6. Image capture and analysis

Image analysis was performed using an optical microscope connected to a computerized image analysis system equipped with dedicated software (Viewfinder Lite software, Olympus, Japan). The average signal intensity of TH-positive neurons was determined. The effects on dopaminergic neurons were quantified by calculating the ratio of TH-positive neurons in the substantia nigra from the ipsilateral hemisphere to those from the contralateral hemisphere (I/C ratio) (Armentero et al., 2006; Blandini et al., 2004). For each animal, 4 or 5 sections were evaluated and pooled to provide the mean intensity value used to calculate the ratio ($n \geq 9$).

4.7. Western blot analysis

SH-SY5Y cells were cultured for 24 h and pre-treated within non-cytotoxic dose ranges of reynosin (0.08, 0.4, and 2 μM) or 2 μM of APO for 24 h, with a subsequent DA treatment for an additional 15 h. Proteins were extracted with a PRO-PREP protein extraction solution.

For animal-based (in vivo) western blotting, the rats were sacrificed and their brain tissues were rapidly obtained. The striatum from individual rats were dissected out and homogenized in 1% sodium dodecyl sulfate (SDS) TBST buffer, followed by boiling and centrifugation. Proteins from the brain tissue were prepared with a PRO-PREP protein extraction solution.

For western blotting analyses, equal amounts of protein were loaded onto each lane, separated by SDS-PAGE on a 10% gel, and transferred to a PVDF membrane. The membranes were incubated overnight at 4 °C with the anti-rabbit primary antibody for ASYN (1: 1000; Immuno-Biological Laboratories Co. Ltd., Gunma, Japan) and E6-AP (1:1000; Santa Cruz, CA, USA), followed by incubation for 1 h at room temperature with the secondary antibody (1:5000; anti-rabbit HRP-conjugated IgG, Santa Cruz, USA). Bands were analyzed using the LAS1000 (Fuji, Japan) image analyzer. After the blot was stripped and reprobed with anti-β-actin mouse antibody (1:5000; Santa Cruz, CA, USA), it was used as an internal control.

4.8. Statistical analysis

All experimental data are presented as the mean value ± standard deviation. Statistical significance between multiple groups was analyzed by one-way ANOVA (PRISM GraphPad, San Diego, CA, USA). When ANOVA showed a significant difference, post hoc Bonferroni's multiple comparison tests were performed. P values less than 0.05 were considered to be statistically significant.

Acknowledgments

This work was supported by the Basic Science Research Program through the National Research Foundation of Korea (NRF) funded by the Ministry of Education, Science and Technology (Grant no. 2010-0028078).

Please cite this article as: Ham, A., et al., Reynosin protects against neuronal toxicity in dopamine-induced SH-SY5Y cells and 6-hydroxydopamine-lesioned rats as models of Parkinson's disease: Reciprocal up-regulation of E6-AP and down-regulation of α-synuclein. Brain Research (2013), http://dx.doi.org/10.1016/j.brainres.2013.05.036

Appendix A. Supporting information

Supplementary data associated with this article can be found in the online version at http://dx.doi.org/10.1016/j.brainres.2013.05.036.

REFERENCES

Armentero, M.T., et al., 2006. Prolonged blockade of NMDA or mGluR5 glutamate receptors reduces nigrostriatal degeneration while inducing selective metabolic changes in the basal ganglia circuitry in a rodent model of Parkinson's disease. Neurobiol. Dis. 22, 1–9.

Asanuma, M., Miyazaki, I., Ogawa, N., 2003. Dopamine- or L-DOPA-induced neurotoxicity: the role of dopamine quinone formation and tyrosinase in a model of Parkinson's disease. Neurotoxic. Res. 5, 165–176.

Barzilai, A., Melamed, E., Shirvan, A., 2001. Is there a rationale for neuroprotection against dopamine toxicity in Parkinson's disease?. Cell Mol. Neurobiol. 21, 215–235.

Bennett, M.C., 2005. The role of alpha-synuclein in neurodegenerative diseases. Pharmacol. Ther. 105, 311–331.

Blandini, F., et al., 2004. Neuroprotective effect of rasagiline in a rodent model of Parkinson's disease. Exp. Neurol. 187, 455–459.

Chu, Y., et al., 2006. Nurr1 in Parkinson's disease and related disorders. J. Comp. Neurol. 494, 495–514.

Chu, Y., Kordower, J.H., 2007. Age-associated increases of alpha-synuclein in monkeys and humans are associated with nigrostriatal dopamine depletion: is this the target for Parkinson's disease?. Neurobiol. Dis. 25, 134–149.

Conway, K.A., et al., 2001. Kinetic stabilization of the alpha-synuclein protofibril by a dopamine-alpha-synuclein adduct. Science 294, 1346–1349.

Dedov, V.N., Cox, G.C., Roufogalis, B.D., 2001. Visualisation of mitochondria in living neurons with single- and two-photon fluorescence laser microscopy. Micron 32, 653–660.

Feany, M.B., Bender, W.W., 2000. A drosophila model of Parkinson's disease. Nature 404, 394–398.

Foyet, H.S., et al., 2011. Methanolic extract of Hibiscus asper leaves improves spatial memory deficits in the 6-hydroxydopamine-lesion rodent model of Parkinson's disease. J. Ethnopharmacol. 133, 773–779.

Golde, T.E., 2009. The therapeutic importance of understanding mechanisms of neuronal cell death in neurodegenerative disease. Mol. Neurodegener. 4, 8.

Gomez-Santos, C., et al., 2003. Dopamine induces autophagic cell death and alpha-synuclein increase in human neuroblastoma SH-SY5Y cells. J. Neurosci. Res. 73, 341–350.

Gomez-Santos, C., et al., 2005. Induction of C/EBP beta and GADD153 expression by dopamine in human neuroblastoma cells. Relationship with alpha-synuclein increase and cell damage. Brain Res. Bull. 65, 87–95.

Ham, A., et al., 2010. Spirafolide from bay leaf (*Laurus nobilis*) prevents dopamine-induced apoptosis by decreasing reactive oxygen species production in human neuroblastoma SH-SY5Y cells. Arch. Pharm. Res. 33, 1953–1958.

Hara, H., Ohta, M., Adachi, T., 2006. Apomorphine protects against 6-hydroxydopamine-induced neuronal cell death through activation of the Nrf2-ARE pathway. J. Neurosci. Res. 84, 860–866.

Hughes, A.J., et al., 1993. Subcutaneous apomorphine in Parkinson's disease: response to chronic administration for up to five years. Mov. Disord. 8, 165–170.

Iancu, R., et al., 2005. Behavioral characterization of a unilateral 6-OHDA-lesion model of Parkinson's disease in mice. Behav. Brain Res. 162, 1–10.

Jiang, Y.H., Beaudet, A.L., 2004. Human disorders of ubiquitination and proteasomal degradation. Curr. Opin. Pediatr. 16, 419–426.

Kanda, S., et al., 2000. Enhanced vulnerability to oxidative stress by alpha-synuclein mutations and C-terminal truncation. Neuroscience 97, 279–284.

Kirik, D., et al., 2002. Parkinson-like neurodegeneration induced by targeted overexpression of alpha-synuclein in the nigrostriatal system. J. Neurosci. 22, 2780–2791.

Masliah, E., et al., 2000. Dopaminergic loss and inclusion body formation in alpha-synuclein mice: implications for neurodegenerative disorders. Science 287, 1265–1269.

Millan, M.J., et al., 2002. Differential actions of antiparkinson agents at multiple classes of monoaminergic receptor. I. A multivariate analysis of the binding profiles of 14 drugs at 21 native and cloned human receptor subtypes. J. Pharmacol. Exp. Ther. 303, 791–804.

Mishra, A., et al., 2008. E6-AP promotes misfolded polyglutamine proteins for proteasomal degradation and suppresses polyglutamine protein aggregation and toxicity. J. Biol. Chem. 283, 7648–7656.

Mishra, A., et al., 2009. The ubiquitin ligase E6-AP is induced and recruited to aggresomes in response to proteasome inhibition and may be involved in the ubiquitination of Hsp70-bound misfolded proteins. J. Biol. Chem. 284, 10537–10545.

Mishra, A., et al., 2013. E6-AP association promotes SOD1 aggresomes degradation and suppresses toxicity. Neurobiol. Aging 34(4) (1310), e11–e23.

Miyazaki, I., Asanuma, M., 2008. Dopaminergic neuron-specific oxidative stress caused by dopamine itself. Acta Med. Okayama 62, 141–150.

Mulherkar, S.A., Sharma, J., Jana, N.R., 2009. The ubiquitin ligase E6-AP promotes degradation of alpha-synuclein. J. Neurochem. 110, 1955–1964.

Nicotra, A., Parvez, S., 2002. Apoptotic molecules and MPTP-induced cell death. Neurotoxicol. Teratol. 24, 599–605.

Paxinos, G., Watson, C., 1998. The Rat Brain in Stereotaxic Coordinates. Academic Press, San Diego.

Scheffner, M., 1998. Ubiquitin, E6-AP, and their role in p53 inactivation. Pharmacol. Ther. 78, 129–139.

Smith, W.W., et al., 2005. Alpha-synuclein phosphorylation enhances eosinophilic cytoplasmic inclusion formation in SH-SY5Y cells. J. Neurosci. 25, 5544–5552.

Srinivasan, S., Nawaz, Z., 2011. E3 ubiquitin protein ligase, E6-associated protein (E6-AP) regulates PI3K–Akt signaling and prostate cell growth. Biochim. Biophys. Acta 1809, 119–127.

Ungerstedt, U., 1968. 6-Hydroxy-dopamine induced degeneration of central monoamine neurons. Eur. J. Pharmacol. 5, 107–110.

Watanabe, H., et al., 2004. Protective effects of neuronal nitric oxide synthase inhibitor in mouse brain against MPTP neurotoxicity: an immunohistological study. Eur. Neuropsychopharmacol. 14, 93–104.

Yang, F., et al., 2009. Role of autophagy and proteasome degradation pathways in apoptosis of PC12 cells overexpressing human alpha-synuclein. Neurosci. Lett. 454, 203–208.

Yoshikawa, M., et al., 2000. Alcohol absorption inhibitors from bay leaf (Laurus nobilis): structure-requirements of sesquiterpenes for the activity. Bioorg. Med. Chem. 8, 2071–2077.

Yuan, H., et al., 2006. R-apomorphine protects against 6-hydroxydopamine-induced nigrostriatal damage in rat. Neurosci. Bull. 22, 331–338.

Please cite this article as: Ham, A., et al., Reynosin protects against neuronal toxicity in dopamine-induced SH-SY5Y cells and 6-hydroxydopamine-lesioned rats as models of Parkinson's disease: Reciprocal up-regulation of E6-AP and down-regulation of α-synuclein. Brain Research (2013), http://dx.doi.org/10.1016/j.brainres.2013.05.036